TRANSCRIPTIONAL REGULATION OF GENE NETWORKS

THOMAS R. BURKARD

DOCTORAL THESIS

Graz, University of Technology

Institute for Genomics and Bioinformatics

Petersgasse 14, 8010 Graz

and

Vienna, Research Institute of Molecular Pathology

Eisenhaber Group

Dr. Bohrgasse 7, 1030 Vienna

Vienna, May 2007

Abstract

Background: cDNA microarray studies result in a huge amount of expression data. The main focus lies often on revealing new components which end in long lists without understanding the global networks described by them. This doctoral thesis asks to which extent theoretical analyses can reveal gene networks, molecular mechanisms and new hypotheses in microarray expression data. For this purpose, gene expression profiles were generated using microarrays and a cell model for fat cell development.

Results: A novel adipogenic atlas was constructed using microarray expression data of fat cell development. In total, 659 gene products were subjected to *de novo* annotation and extensive literature curation. The resulting gene networks delineate phenotypic observations, such as clonal expansion, up-rounding of the cells and fat accumulation. Based on this global analysis, seven targets were selected for experimental follow up studies. Further, 26 transcription factors are suggested by promoter analysis to regulate co-expressed genes. 27 of 36 investigated pathways are preferentially controlled at rate-limiting enzymes on the transcriptional level. Additionally, the first set of 391 universal proteins that are known to be rate-determining was selected. This dataset was hand-curated from >15,000 PubMed abstracts and contains 126 rate-limiting proteins from curated databases with increased reliability. Two thirds of the rate-determining enzymes are oxidoreductases or transferases. The rate-limiting enzymes are dispersed throughout the metabolic network with the exception of citrate cycle. The knockout of the rate-limiting adipose triglyceride lipase responds in transcriptional down-regulation of the whole oxidative phosphorylation and specific control of many rate-limiting enzymes in brown fat tissue. Finally, it was shown that selective transcriptional regulation of rate-limiting enzymes is a widely applied mechanism for the control of metabolic networks.

Conclusion: This thesis demonstrates that large-scale transcription profiling in combination with sophisticated bioinformatics analyses can provide not only a list of novel players in a particular setting, but also a global view on biological processes and molecular networks.

Publications

This thesis is based on the following publications as well as upon unpublished observations.

Papers:

Hackl* H, Burkard* TR, Sturn A, Rubio R, Schleiffer A, Tian S, Quackenbush J, Eisenhaber F and Trajanoski Z (*contributed equally): **Molecular processes during fat cell development revealed by gene expression profiling and functional annotation.** *Genome Biol.* 2005; 6(13):R108

Burkard T, Trajanoski Z, Novatchkova M, Hackl H, Eisenhaber F: **Identification of New Targets Using Expression Profiles.** In: Antiangiogenic Cancer Therapy, Editors: Abbruzzese JL, Davis DW, Herbst RS; *CRC Press (in press)*

Hartler J, Thallinger GG, Stocker G, Sturn A, Burkard TR, Körner E, Scheucher A, Rader R, Schmidt A, Mechtler K, Trajanoski Z: **MASPECTRAS: a platform for management and analysis of proteomic LC-MS/MS data.** *BMC Bioinformatics.* (submitted)

Conference proceedings and poster presentations:

Hartler, J.; Thallinger, G.; Stocker, G.; Sturn, A.; Burkard, T.; Körner, E.; Mechtler, K.; Trajanoski, Z.: **Management and Analysis of Proteomics LC-MS/MS Data**. *Fourth International Symposium of the Austrian Proteomics Platform*. (2007), Seefeld in Tirol, Austria

Hackl, H.; Burkard, T.; Sturn, A.; Rubio, R.; Schleiffer, A.; Tian, S.; Quackenbush, J.; Eisenhaber, F.; Trajanoski, Z.: **Molecular processes during fat cell development revealed**

by large scale expression analysis and functional annotation. *1st Symposium on Lipid and Membrane Biology*. (2006), page. 12 – 12

Hartler, J.; Thallinger, G.; Stocker, G.; Sturn, A.; Burkard, T.; Körner, E.; Fuchs, T.; Mechtler, K.; Trajanoski, Z.: **MASPECTRAS:Web-based System for Storage, Retrieval, Quantification and Analysis of Proteomic LC MS/MS Data**. *Third International Symposium of the Austrian Proteomics Platform*. (2006), Seefeld in Tirol

Hartler, J.; Thallinger, G.; Sturn, A.; Burkard, T.; Körner, E.; Fuchs, T.; Mechtler, K.; Trajanoski, Z.: **MASPECTRAS:** ***Web-basiertes Datenbanksystem zur Verwaltung von Proteomik-Daten***. *Österreichische Akademie der Wissenschaften* (2005)

Hackl, H.; Burkard, T.; Paar, C.; Fiedler, R.; Sturn, A.; Stocker, G.; Rubio, R.; Schleiffer, A.; Quackenbush, J.; Eisenhaber, F.; Trajanoski, Z.: **Large Scale Expression Profiling and Functional Annotation of Adipocyte Differentiation**. *Keystone Symposia: Molecular Control of Adipogenesis and Obesity*. (2004), S. 193 - 193

Hackl, H.; Burkard, T.; Paar, C.; Fiedler, R.; Sturn, A.; Stocker, G.; Rubio, R.; Quackenbush, J.; Schleiffer, A.; Eisenhaber, F.; Trajanoski, Z.: **Large Scale Expression Profiling and Functional Annotation of Adipocyte Differentiation**. -*First Internatrional Symposium of the Austrian Proteomics Platform*. (2004), Seefeld, Austra

Hartler, J.; Thallinger, G.; Stocker, G.; Sturn, A.; Burkard, T.; Körner, E.; Fuchs, T.; Mechtler, K.; Trajanoski, Z.: **MASPECTRAS:Web-based System for Storage, Retrieval, and Analysis of Proteomic LC MS/MS Data**. *HUPO 4th Annual World Congress*. (2004) Munich

Hackl, H.; Burkard, T.; Rubio, R.; Quackenbush, J.; Trajanoski, Z.: **Gene expression analysis during adipocyte differentiation**. *High-Level Scientific Conferences: Molecular Mechanisms in Metabolic Diseases*. (2003), S. 9 – 9

Index of contents

1. Introduction

cDNA microarray studies result in a large amount of expression data. Long lists of genes, which are regulated in a specific process, are often published without any in-depth analysis of the regulated features. In contrast, this work asks, to which extent gene networks describing molecular processes can be revealed with expression profiling. Therefore, this doctoral thesis investigates microarray data of fat cell differentiation with a broad spectrum of analytic tools with the aim to delineate all aspects of the complex adipogenic transcriptional scenario. In follow-up studies, the thesis explores the question if general transcriptional control mechanisms of metabolic pathways exist. In the next chapters, the biological system of fat cell differentiation and the methods used to address the objectives of this thesis are introduced.

1.1. Fat cell differentiation

Obesity, the excess deposition of adipose tissue, is an epidemic health risk. Over one billion adults worldwide suffer from overweight, with more than 300 million clinical cases [1]. Therefore, this field attracts considerable attention in the scientific community. Pharmaceutical companies and noncommercial institutes are spending great efforts in elucidating novel molecular mechanism of fat cell development and medical treatment. The cause for obesity prevalence in industrial and developing countries are diverse and range from psychosocial imbalance over wrong nutrition behavior to genetic malfunctions. Two main mechanisms for weight gain have been identified on the physiological level: On the one hand, deregulation of the metabolism leads to raised incorporation of fat in mature adipose tissue. On the other hand, development of new fat cells, known as adipogenesis, increases the number of storage depots. Fat cell development as one fundament of obesity is addressed in this study by analyzing microarray expression data of 3T3-L1 differentiation (see also appendix B-1, [2]), which is an over 30 years investigated *in vitro* model system of fat cell development.

3T3-L1 cell line – A model system to investigate adipogenesis

In the early 60ies, the mammalian 3T3 cell line, isolated from disaggregated mouse embryos, has become a useful tool for investigating growth control and oncogenic viruses [3]. In resting cultures of these cells the incorporation of lipid droplets was frequently observed. In the year 1974, the 3T3-L1 sub-cell line was cloned based on the tendency to differentiate to adipose cells and to accumulate fat [4]. Since then the 3T3-L1 preadipocyte cells were extensively studied and evolved to a well established adipogenic model system.

The complex process of adipogenesis is incompletely understood

To identify new components involved in fat cell development, several studies have used early Affymetrix technologies [5-11] or filter-based expression technologies [12] in the past. Those outdated platforms may have missed many genes important for the development of a fat cell. The problem of a potentially incomplete coverage of the developmental transcriptome by early chip technology has been demonstrated in a expressed sequence tag (EST) project. For the embryonic system, the EST project revealed a significant fraction of embryonic factors not represented in the collections of genes previously available [13]. The advantage of the modern chip design resulted in an expanded number of differentially expressed genes in the present study. Furthermore, in contrast to previous studies [6-11,14], the focus was mainly directed towards understanding the global mechanism of adipogenesis and less towards the discovery of individual genes for further functional analysis.

Adipogenesis is primarily regulated at the transcriptional level

Fat cell differentiation is induced in 3T3-L1 cells after exposure to an appropriate adipogenic cocktail containing dexamethasone, isobutylmethylxanthine, insulin, biotin and fetal bovine serum. Thereupon, 3T3-L1 confluent preadipocytes differentiate into mature adipocytes [15]. Chronic treatment with hyperphysiological concentrations of insulin accelerates the speed and efficiency of the adipose conversion in 3T3-L1 cell lines [16,17]. Two mechanisms are suggested for the need of this high insulin concentration: first, the involvement of cell

surface receptors for type I insulin-like growth factor have lower affinity for insulin and second, insulin shows a high degradation in the culture medium [18]. Newly synthesized fatty acids are the major part of accumulated triglycerides [16]. Therefore, the accumulation of lipids is inhibited if the medium contains no biotin, even in the presence of exogenous lipids and elevated cellular LPL activity [19]. The phosphodiesterase inhibitor isobutylmetyhlxanthin stimulates the conversion to adipocytes, which suggests a role for cyclic nucleotides in the control of differentiation [20]. The glucocorticoid dexamethasone also induces the adipocyte differentiation efficiently.

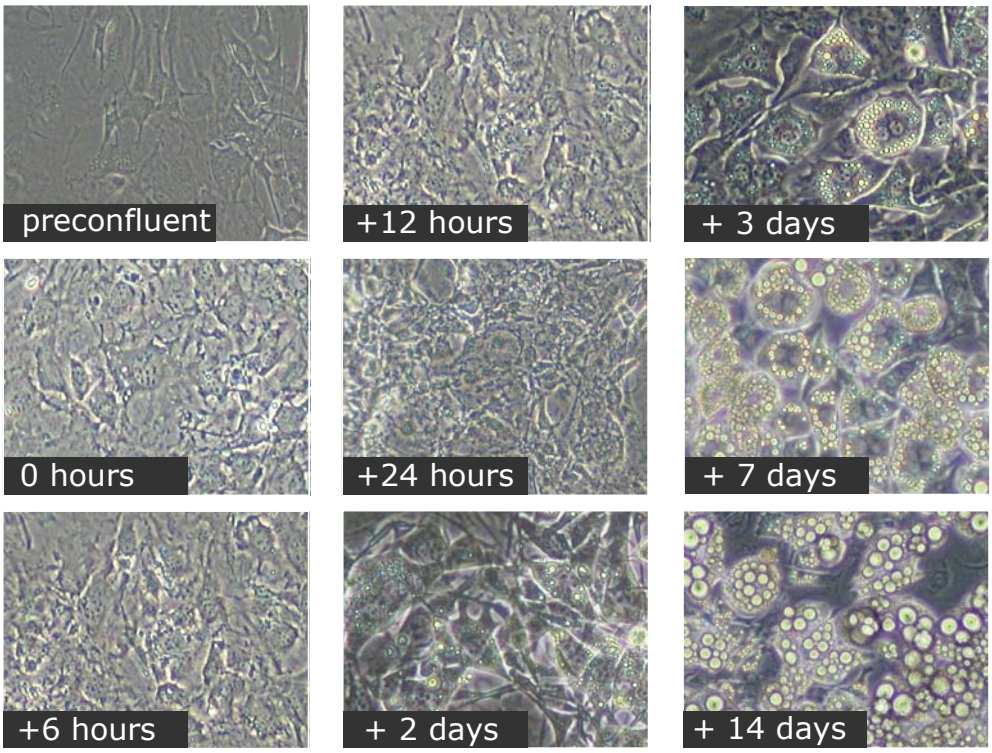

Figure 1 *Microscope images of the underlying fat cell differentiation study of 3T3-L1 cells. The preconfluent dividing cells were grown till contact inhibition occurred. After induction (0h), the cell density increased again at clonal expansion (12h/24h). Thereafter, the cells up-rounded and began to accumulate fat droplets. Mature adipocytes were fully differentiated at 14 days after induction.*

The differentiation can be characterized by three different states: growth arrest, clonal expansion and terminal differentiation (Figure 1). The fibroblast-like preconfluent 3T3-L1

cells grow up to the stage of confluence. Contact inhibition initiates growth arrest, which is essential for differentiation. 12h to 24h after induction with an appropriate cocktail, the density of the cells increases significantly, which is the result of one or two rounds of clonal expansion. Thereafter, the cells begin to remodel cytoskeleton and extra-cellular matrix resulting into an up-rounded phenotype. During terminal differentiation, the cells incorporate newly synthesize fatty acids, which can be observed by large fat droplets inside the cells. Finally, cells that are phenotypically similar to mature adipocytes evolve (14d after induction). The whole process is controlled by chronological reprogramming of the transcriptional machinery. It is also reflected by the expression of early, intermediate and late mRNA/protein markers and lipid accumulation [21]. The regulation and the changes occur primarily at the transcriptional level, although posttranscriptional regulation is known for some genes [22,23]. This characteristic makes 3T3-L1 differentiation an ideal candidate for expression profiling.

Expression profiling of 3T3-L1 differentiation to adipocytes

In this study, expression data of the 3T3-L1 adipogenic model system was used to characterize the networks involved in fat cell development. The preceding biochemical experiments were divided in two categories: cell culture differentiation and expression profiling (appendix B-1, [2]).

Three independent cell culture experiments were performed. Cells were harvested and the total RNA was isolated at the pre-confluent stage and at 8 time points (0h, 6h, 12h, 24h, 3d, 4d, 7d, 14d) after induction. For each independent experiment, RNA was pooled from three different culture dishes for each time point and from 24 dishes at the preconfluent stage used as reference.

The microarray technology is well suited to measure the complex changes during adipogenesis, as the process is known to be tightly regulated on the transcriptional level. A recently developed cDNA microarray with 27.648 ESTs [24] of which 15.000 are developmental ESTs representing 78% novel and 22% known genes, was used [25]. Relative measurement methods were used since the production of spotted microarrays is not as

accurate as *in situ* synthesized chips. Therefore, hybridization of Cy3/Cy5 labeled sample and reference was needed. During direct Cy3/Cy5 labeling, the two fluorescents incorporate with a different rate. To resolve this issue, amino-allyl modified nucleotides were incorporated in the first reverse transcription step followed by a coupling of the dyes to the reactive amino groups of the cDNA [26]. The remaining persistent dye-bias was addressed by the dye-swapping technique. For a comprehensive review of expression profiling consult appendix B-2.

Identification of the molecular role of the gene products[1]

Essentially, the basic element of expression data has a composite structure: On the one hand, it comprises a vector of n real numbers describing the expression status for n conditions/experiments/time points. On the other hand, a sequence tag is associated with the vector of expression values. Without the knowledge of the identity of the gene represented by the expressed sequence tag and the biological function of the respective gene, interpretation of the expression data in terms of biological mechanisms and processes is impossible. It should be noted that protein function requires a hierarchical description with molecular function, cellular function and phenotypic function [27].

The first step in EST chip analysis is to allocate all spotted ESTs to their corresponding genes if available. With the knowledge of complete genomes, sequence comparisons can identify genes from sufficiently long sequence tags. For instance, rounds of Megablast searches [28] against various nucleotide databases of decreasing trust-levels (in the order of RefSeq [29,30], FANTOM [31], UniGene [32], nr GenBank, and TIGR Mouse Gene Index [33] or other organism-specific databases) can be applied initially. For nucleic sequences that could not be assigned, the routine should be repeated with blastn [34] and finally against the genome of the whole organism. Long stretches (>100) of non-specific nucleotides have to be excluded. For the genes obtained, the respective gene product can be retrieved: This is either a protein sequence if the expressed RNA is translated to a protein or a functional RNA species (microRNA, etc.).

[1] Adapted from appendix B-2 for a better understanding of the main body

The molecular and cellular role of novel protein targets derived from an expression study is of special interest. A first insight of the processes involved can be obtained from Gene Ontology (GO) terms [35]. With GenPept/RefSeq accession numbers, GO numbers for molecular function, biological process, and cellular component can be derived from the gene ontology database (Gene Ontology Consortium). If considered in context with the expression cluster identity, it is possible to observe groups of co-regulated proteins, which are part of a unique process or share a molecular function. Such groups of genes can be visualized with Genesis [36].

Detailed *de novo* function prediction for the target proteins can reveal new aspects of their molecular and cellular function. This analysis step is especially important for sequences that entered the databases after large-scale sequencing efforts and that have remained experimentally uncharacterized. Furthermore, it is not possible to determine how the functional annotation of any given protein has been acquired in public databases. Thus, the possibility of chains of misannotation arises, a process termed 'error percolation' [37]. To address those aspects, a large variety of different sequence analysis tools are commonly applied. Full-length close homology is one established method of inferring functions for novel proteins [34].

In-depth protein sequence analysis follows a three-step procedure. This approach is based on the assumption that proteins consist of linear sequence modules that have their own structural and functional characteristics. The function of the whole protein is a superposition of the segments' functions. The sequence modules can represent globular domains or non-globular segments such as fibrillar segments with secondary structure, transmembrane helical segments or polar, flexible regions without inherent structural preferences.

The first step involves the detection of the non-globular part of the protein sequence, which houses many membrane-embedded segments, localization and posttranslational modifications sequence signals. Typically, non-globular segments are characterized by some type of amino acid compositional bias. Therefore, the principle procedure is to begin with analyses of compositional biases. They are found as low complexity regions with SEG [38] and compositional biased stretches with SAPS [39], XNU, Cast [40] and GlobPlot 1.2 [41]. N-terminal localization signals can be studied with SignalP [42] and Sigcleave [43], the C-

terminal PTS1 signal for peroxisomal targeting via the PEX5 mechanism is checked for with the predictor of Neuberger *et al*. [44-46]. A number of quite accurate predictors test the capacity of the query protein for lipid posttranslational modifications such as GPI lipid anchors [47-49], myristoyl [50] or prenyl (farnesyl or geranylgeranyl) [51] anchors. Membrane-embedded regions are recognized via the occurrence of strongly hydrophobic stretches. Standard predictors such as HMMTOP [52], TOPPRED, DAS-TMfilter [53] and SAPS [39] find transmembrane helical regions. Generally, several transmembrane recognition methods should map to the same position to obtain reliable predictions. Secondary structure prediction methods (COILS [54], SSCP [55,56], Predator [57]) can generate information about structure elements in non-globular parts of proteins.

The second step involves comparisons of the query sequence with libraries of known domains. Since domain definitions of even the same domain type do slightly differ among authors, it is necessary to compare the query sequence with all available definitions. Known sequence domains of the repositories Pfam and SMART [58] are characterized by hidden Markov models (HMM), which can be searched with a sequence using HMMER both in a global and local search mode. Further domain prediction method and databases are RPS-BLAST (CDD) [59], IMPALA [60] and PROSITE [61].

The third, the last step involves analysis of query protein segments (at least 50 amino acid residues long) that are not covered by hits produced by any of the prediction tools for non-globular regions and known domains. Most likely, these sequence segments represent not yet characterized globular domains. It is necessary to collect protein sequence segments that are significantly similar to the respective part of the query. This can be done with tools from the BLAST/PSI-BLAST suite [62-64], HMMsearch or SAM [65,66]. There are several strategies to collect as complete as possible sequence families; for example, each identified homologous protein can be resubmitted to an additional PSI-BLAST in an attempt to find more homologues. Through multiple alignments of the conserved residue stretches, sequence analysis of the found proteins and extensive literature search, a new functional domain can be characterized.

Finally, the different sequence-analytic findings for the various query segments need to be synthesized for a description of the function of the whole protein. Overlaps of predicted

features have to be resolved by assessing significances of hits, the amino acid compositional status of the respective segment and expected false-positive prediction rates of algorithms. With the entirety of sequence-analytic methods, some functional conclusion, at least in very general terms, is possible for most sequences. All these academic prediction tools for *de novo* sequence prediction are integrated in the user-friendly ANNOTATOR/NAVIGATOR environment, a novel protein sequence analysis system, which is in development at the IMP Bioinformatics group.

Gene networks are the basis for testing new hypothesis in fat cell development

In this thesis, genes of the 780 strongest transcriptionally regulated expressed sequence tags (ESTs) during adipogenesis and the corresponding protein products passed through in-depth computational analysis. As a result, a comprehensive molecular atlas of fat cell development was created. With its aid, it is possible to dive into the wealth of detailed gene networks of the underlying processes and use the in-depth view to test new hypothesis. Comparison to *in vivo* expression of adipose tissue revealed the importance of the study also for medical applications.

Several hypotheses were investigated using the global adipogenic atlas. Phenotypic changes were shown to be traceable in the expression networks. The hot topic, if co-expression corresponds to co-regulation, was investigated by prediction of all transcription factor binding sites. Finally, exhaustive analysis of enzymatic networks during adipogenesis uncovered two major control principles of metabolic circuits on the transcriptional level:

1. Whole pathways can be switched on or off by expressing each member similarly
2. Alternatively, rate-limiting enzymes, which control the flux through a pathway, can be regulated specifically

In this doctoral thesis, it is shown that careful *de novo* annotation and in-depth computational analysis of expression data can result in the construction of a detailed gene map reflecting the underlying molecular processes. This global atlas can be successfully used to test up-coming hypothesis and to find new candidate genes for further research. In case of adipogenesis, phenotypic changes such as clonal expansion, extra-cellular matrix remodeling and cytoskeleton reorganization can be elucidated on the basis of the gene network. With this comprehensive approach, we show that key loci of transcriptional regulation are often enzymes that control the rate-limiting steps of metabolic pathways.

1.2. Transcriptional control of metabolic fluxes

A tight regulation of the metabolic fluxes through cells is necessary to maintain their healthy and viable state. Deregulation can lead to severe health problems of an organism. An obvious example is the disturbance of the energy balance between intake and expenditure, which can result (besides adipogenesis) in obesity or anorexia. The storage of energy as triglyceride in adipose tissue, are determined by complex interaction between genetic, metabolic, environmental, and psychosocial factors (Figure 2).

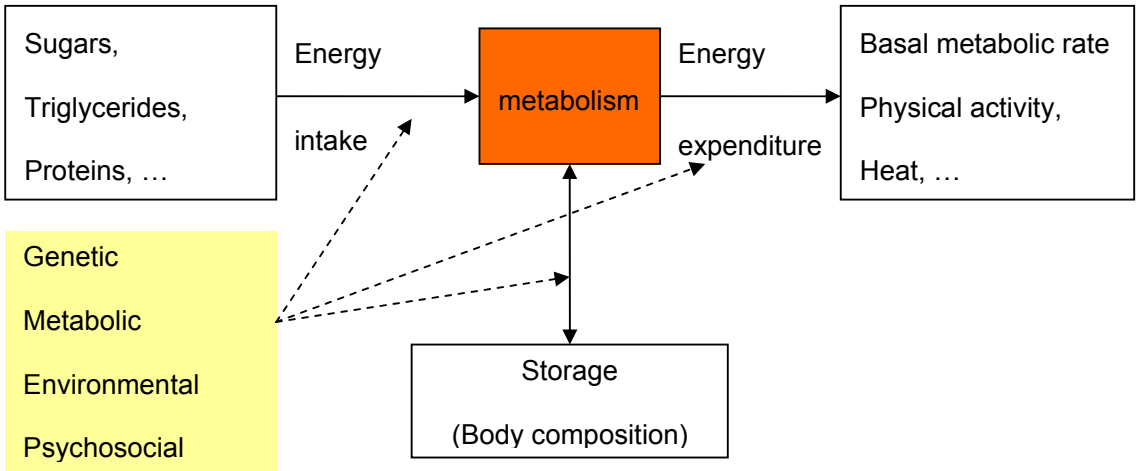

Figure 2 *Energy equilibrium:* Distortion of metabolic networks involved in energy intake and expenditure can lead to obesity or anorexia. Genetic, metabolic, environmental and psychosocial influences can facilitate those changes in the cells (adapted from [67]).

On the genetic tier, two mechanisms of transcriptional control became evident by in-depth analysis of the global gene networks during fat cell development [2]. On the one hand, all enzymes of a whole pathway shared similar mRNA regulation. An outstanding example was the synchronous expression of the cholesterol pathway. On the other hand specific key points, mainly the rate-limiting enzymes, of a pathway, were regulated, which might dictate metabolic fluxes to its remaining pathway members. 27 out of 36 pathways were identified to be regulated transcriptionally at the rate-determining enzyme during adipogenesis. The later finding raised the question, if this might be a general principle.

Previously, it was argued that the control of metabolic pathways only at one rate—determining step is unlikely. Since the total amount of the proteins within a cell occupies 15-35% of the cell volume, which is the maximum compatible with cell function, it might be evolutionary preferable to minimize protein levels by controlling pathways as a whole [68] and not only at one key locus. Nevertheless, strong transcriptional regulation of rate-limiting enzymes was shown in the special case of fat cell development. The control of the key steps within the pathway might be more energy efficient than synthesizing many enzymes of a pathway and the response to stimuli during differentiation might be faster. Resulting from this special case, a more general importance of transcriptional key step regulation was addressed.

With the objective to proof the concept of transcriptional control of rate-determining enzymes in developmental processes, all available definitions of the term rate-limiting were revisited. Blackman was the first to describe the phenomenon of rate-limitation in biology. He wrote in the year 1905 - "When a process is conditioned as to its rapidity by a number of separate factors, the rate of the process is limited by the pace of the slowest factor“. The IUPAC goes a little bit further and defines a rate-controlling (rate-determining or rate-limiting) step in a reaction occurring by a composite reaction sequence as an elementary reaction the rate constant for which exerts a strong effect — stronger than that of any other rate constant — on the overall rate [69] (Figure 3). However, scientists publishing in all kinds of journals are not that strict with the definition. Rate-limiting steps have been described previously as the step which is slower then the other members of the pathway, as the thermodynamically unfavorable step or as the step that is catalyzed by regulated

enzymes. In the current study, all above definitions are considered as valid and it is trusted in the expert judgment of the authors to specify a component as “rate-limiting”. Therefore, a rate-limiting step has somehow to exert a strong effect on the overall flux of a metabolic pathway.

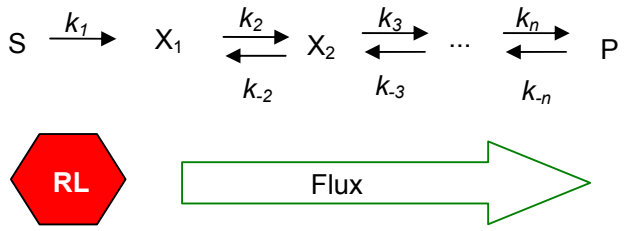

Figure 3 *A rate-limiting (RL) step exerts a strong effect on the overall flux.*

For the first time, this doctoral thesis has generated a comprehensive list of 391 rate-limiting proteins available from literature. A highly accurate subset of 126 proteins was compiled from curated biological databases. Computational analysis revealed that the molecular function of rate-limiting proteins is primarily involved in oxidoreductase and transferase processes. The rate-determining key loci were mainly dispersed throughout the metabolic networks. One prominent exception was the central citrate cycle. Disruption of the recently described rate-limiting enzyme, adipose triglyceride lipase, showed that it exerts major changes on the gene networks of brown adipose tissue. 31% of the transcriptionally influenced enzymes are themselves rate limiting. Finally, it was shown that approximately one third of an enzymatic gene network was transcriptionally controlled at rate-limiting steps. This general concept was found in 5 selected developmental processes.

2. Results

2.1. Fat cell development

The following chapter gives a review of the results, which are achieved in the main part of the doctoral thesis. It is attempted to reflect parts of the data from a slightly different point of view than in the available publication (see Appendix B-1, [2]). Contrary to the publication [2], this chapter presents in part new, yet not well documented aspects of the data. The approach tries by no means to reproduce the data again comprehensively. For an exhaustive view consult the publication in the appendix B-1 [2] and the additional material at the web-site http://genome.tugraz.at/fatcell.

The basis for understanding large scale data is the precise description of the proteins involved in the process of interest. Therefore, the chapter starts with mapping and *de novo* annotation results for the whole microarray of this study. The expression data is shown to be measured correctly and compared to tissue specific and other differentiation expression data. While the publication emphasizes the significant new impact of this data compared to other chip studies, this chapter focuses on the *in vivo* relevance of the underlying study for medical research. Further, large scale expression data is of extreme complex nature, which makes it necessary to focus on specific pattern identified by clustering procedures. These time profiles are assigned to corresponding biological functions. The simplified biological patterns are the perfect basis to extend the complexity again by investigating each gene product of the cluster extensively. This results in a comprehensive global molecular atlas describing the processes of adipogenesis. The detailed knowledge of the complex network allows the finding of substantial coherences like the preferential transcriptional regulation of rate-limiting genes. The global view highlights especially interesting research targets for in-depth analysis and medical treatment. Finally, two mechanism of regulating the enzymatic network on the transcriptional level are identified.

Annotation of expressed sequence tags is the basis for the comprehensive analysis of expression profiles

The basic requirement of large scale in-depth analysis is the comprehensive knowledge of the players involved in a study. Therefore, a mousechip database was constructed. This database is a small lightweight information retrieval platform for the in-house expressed sequence tag (EST) mouse chip of the Institute for Genomics and Bioinformatics (IGB, University of Technology, Graz). The resource provides EST mapping information and access to *de novo* sequence annotation and third party information of 22,850 proteins, which are associated with the ESTs. The relational database is implemented in PostgreSQL (www.postgresql.org). The database management system (DBMS) is implemented in Perl. The web-based retrieval front-end can be accessed through http://mendel.imp.ac.at/IGBmousechip/index.xhtml.

27,645 spots of the IGB mousechip were represented by 23,311 expressed sequence tags, which contain no long stretches of low complexity regions. In total 22,850 (91%) protein sequences were assigned to the corresponding ESTs of the mouse microarray. The reliability of the used homology search methods Megablast (with parameters: w=70; p=95), discontinuous Megablast (with parameters: w=11; p=95) and blastx/blastn (with parameter: E-value<1e-9) and the accuracy of the nucleotide databases RefSeq, FANTOM, Ensembl, EnsemblTranscript, UniGene, Trest, Entrez and the protein database IPI varied strongly. Table 1 lists the number of contributing sequences in decreasing reliability of the method - database combination. More than two third of the mapped proteins (15,705) were, therefore, of the most trusted level.

Table 1 *Protein sequences associated with the ESTs of the IGB mouse chip. The name of the mapping method is a combination of the species, database and homology search method which were performed (see Text).*

Mapping method	Contributing sequences	% of Chip-ESTs
MouseRefSeqMegablast	15706	63.6%
MouseFantomMegablast	931	3.7%
MouseEnsemblMegablast	338	1.3%
MouseEnsemblTranscriptMegablast	2297	9.2%
MouseUnigeneMegablast	162	0.6%
MouseTrestMegablast	1009	4.0%
MouseRefSeqMegablastDisc	1294	5.2%
MouseFantomMegablastDisc	118	0.5%
MouseEnsemblMegablastDisc	37	0.1%
MouseEnsemblTranscriptMegablastDisc	427	1.7%
MouseUnigeneMegablastDisc	19	0.1%
MouseTrestMegablastDisc	126	0.5%
MouseIPIBlastx	15	0.1%
MouseEntrez	1	0.0%
MouseRefSeqBlastn	247	1.0%
MouseFantomBlastn	33	0.1%
MouseEnsemblBlastn	15	0.1%
MouseEnsemblTranscriptBlastn	54	0.2%
MouseUnigeneBlastn	4	0.0%
MouseTrestBlastn	17	0.1%
Total	22850	92.1%

The IGB MouseChip database is like the microarray itself EST-centric. Therefore, the database provides an EST search form as a starting point (Figure 4). It is possible to show the results in a frame, which provides a comfortable way to navigate through the different third party sources. Additionally, it is possible to choose from a selected list of experiments, which have used the chip for expression analysis. This option leads to a predefined list of the ESTs with additional clustering (if provided) and gene name information.

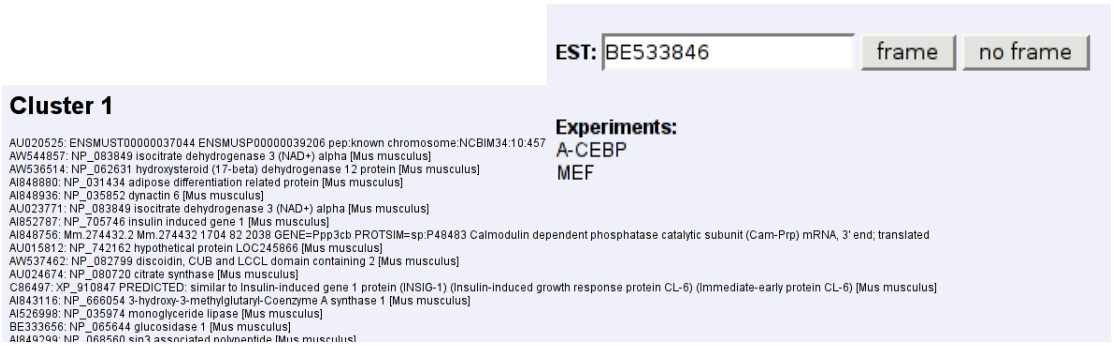

Figure 4 *Two possibilities are available to access the EST information. On the one hand an EST search can be performed, on the other hand an EST can be selected from predefined experiments.*

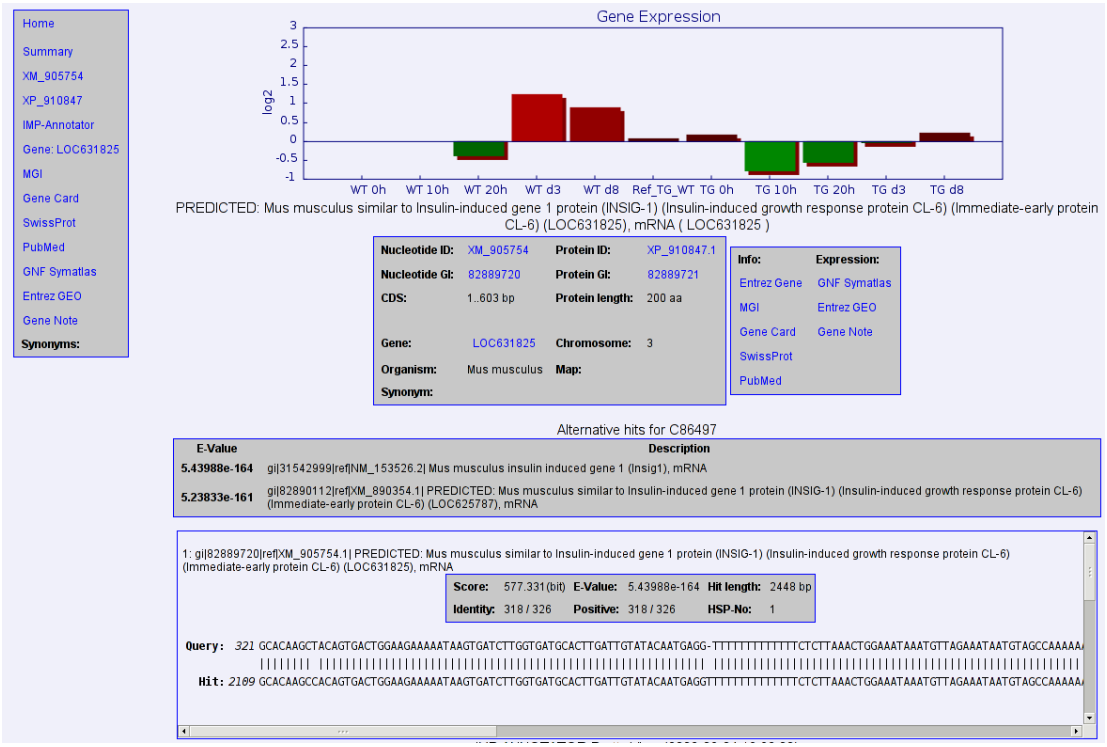

Figure 5 *The main view of the IGB mousechip database. It shows on the left side a navigation menu. Expression data of a predefined experiment are visible on the right side, as well as protein information and details of the mapping procedure.*

The main view of a specific EST provides basic data of the mapping procedure at the top (Figure 5). This includes the nucleotide and protein identifier, the mapping method and the statistical parameters of the first best hit. If the EST is selected from an experiment list, the corresponding expression profile is visualized. To verify the EST assignment, it is possible to view all alignments of the mapping method.

The corresponding nucleotide and protein of the first best hit is described in more detail including abbreviations of all synonyms. Detailed 3rd party information is available through links to the databases Entrez Gene [70,71], Mouse Genome Informatics (MGI) [72], GeneCard [73,74], SwissProt [75] and Pubmed. Published expression data is available through links to GNF symatlas [76], Entrez Gene Expression Omnibus [77,78] and GeneNotes [79].

The integrity of molecular functions in literature as well as yet uncharacterized features of the protein can be checked via the IMP ANNOTATOR pretty view. The IMP ANNOTATOR combines the results of more than 40 academic sequence analysis tools [80]. To access the protein sequence architecture a login and password is needed, due to restrictions of the ANNOTATOR user management (login: mousechip; password: expression).

The valid expression data is relevant for in vivo applications

Assessment of the *in vivo* relevance of the adipogenic model system is especially important for the development of medical applications treating obesity. Morphological arguments and the occurrence of a few biomarkers have substantiated the usage of the 3T3-L_1 model for adipocyte development. Here, three lines of arguments supporting the relevance of this expression profiling study in 3T3-L1 cells for *in vivo* adipogenesis are presented. First, RT-PCR experiments proof that the gene expression changes are sufficiently correctly measured with the microarray. Second, the expression profile of the 3T3-L_1 cell culture moves towards that of the native adipose tissue during the differentiation process. Third, known proteins characteristic for adipocytes are increasingly expressed at terminal differentiation stages.

The validity of the microarray data was tested with quantitative RT-PCR as an alternative method. Results showed a high correlation the RT-PCR assays and the microarray (r=0.93 for 7 genes at different time points). Statistical analyses of the independent chip experiments showed that the reproducibility of the generated data is very high. The Pearson correlation coefficient between the replicates was between 0.73 and 0.97 at different time points. The mean coefficient of variation across all genes at each time point was between 0.11 and 0.27.

The comparison between the adipogenesis experiment and the gene atlas V2 mouse data for adipose tissue [81] showed that the consistence of the two datasets increases with the differentiation state (http://genome.tugraz.at/fatcell/tissues/tissues.html). Among the 382 transcriptionally modulated genes common in both datasets, 67% were regulated in the same direction at time point zero (confluent pre-adipocyte cell culture). The similarity declined during the clonal expansion (55%), which was marked by regulation of cell division genes. At the final stage of differentiation, the correlation increased up to 72%. If the Gene Atlas expression data was restricted to strongly regulated genes (at least 2- and 4-fold change respectively), the consistency in mature adipocytes rises up to 82% (135 genes) and 93% (42 genes). Out of all 60 tissues in the Gene Atlas V2 mouse, the adipose tissue described the differentiated state of the 3T3-L_1 cells best. Brown fat tissue was the second best hit to the differentiated adipocytes (69% of the 382 genes), followed by adrenal gland (66%), kidney (65%) and heart (64%) and the worst correlation had embryo day 8.5 (32%). Interestingly, the similarity with the expression profile at the time points of clonal expansion did not depend much on tissue type (between 45% and 55% of all 382 genes).

For a group of 153 genes, comparison to a previous adipocyte model expression profiling experiment from Soukas *et al.* [82] was possible. The same up- or down-regulation was found for 72% to 89% (depending on time point) of all genes. Highest identity was found for the stage terminally differentiated 3T3-L1 cells, where the profile was less dependent on the exact extraction time. If the comparison was restricted to expression values, which were highly regulated in both experiments (at least two-fold change), the coincidence in every time point was higher than 90%. Comparison to further studies [6,9,83] showed that 326 genes were not shown previously to be regulated. This suggests that the current picture of fat cell development is far from complete.

A number of known genes for adipocyte function *in vivo* with a possible role in the pathogenesis of obesity and insulin resistance were highly expressed during the present study. Adipose triglyceride lipase, a patatin domain-containing triglyceride lipase that catalyzes the initial step in triglyceride hydrolysis [84], was increasingly up-regulated towards the terminal differentiation phase (up to ~20 fold). Another example was Visfatin, which is identical to the pre-B cell colony-enhancing factor (PBEF), a 52 kD cytokine, and has enzymatic and signaling function in adipocytes [85-87]. Mest (mesoderm-specific transcript)/ Peg1 (paternally expressed gene 1) was up-regulated in late differentiation and apparently constitutes a positive regulator of adipocyte size [88]. Kruppel-like factor 5 was expressed in early stages of adipocyte differentiation (it is induced by C/EBPß and δ and, in turn activates the PPARγ2 promoter) and down-regulated at the terminal adipocyte differentiation after 48h [89]. Several further markers are discussed below.

It is concluded that the expression profiles are measured significantly accurate with chip analysis. RT-PCR and comparison between replicates validate the expression data, which is substantiated by comparison to previous expression studies of fat cell differentiation. Even though, this study shares with those experiment many similar regulated genes, several hundreds of yet unidentified ESTs are revealed with the current study. Furthermore, the endpoint correspondence to adipose tissue and the resemblance of the expression profiles with many known *in vivo* biomarkers fosters the accuracy of the data. The latter two observations support the notion that the 3T3-L1 model system is also relevant for *in vivo*.

Biological functions can be assigned to dominant co-expression patterns

A generally accepted procedure is to reduce the intrinsic complexity of large scale expression studies by finding few common co-expression patterns. The present study of fat cell development yielded 1,327,104 data points (48 chips x 27.648 spots). After normalization and averaging over the replicates 14,368 ESTs with signals at all time points were detected. 780 genes with a complete profile over all time points showed dramatic transcriptional regulation (more than 2 fold up- or down-regulated in at least 4 time points). The expression profiles were parsimoniously clustered into 12 temporally distinct patterns, each containing between 23 and 143 genes (for figures see appendix B-1, [2]). Genes in 4

clusters were mostly up-regulated, and genes in 8 clusters were mostly down-regulated during adipogenesis.

The large number of transcriptionally modulated genes and the intricate cluster structure of even only the most extremely regulated genes suggested that the regulation of adipogenesis might be more complex than previously assumed [82]. To understand the major molecular process associated with each cluster, the genes were categorized by scanning the genes and assigning gene ontology (GO) terms for molecular function, cellular component, and biological process.

Reentry into the cell cycle of growth arrested preadipocytes is known as the clonal expansion phase and considered to be a requisite for terminal differentiation in 3T3-L1 adipocytes [90]. Genes in cluster 5 and 8 showed a steady down-regulation through the whole differentiation process and sharp up-regulation at 12h/24h. Typically, these genes in cluster 5 were annotated as cell cycle involved and proteins encoded by them reside in the nucleus.

Genes grouped in cluster 2 were highly expressed from 6h (onset of clonal expansion) to 3d (beginning appearance of adipocyte morphology) but only modestly expressed at the terminal adipocyte differentiation stage. They often carry GO terms indicating signaling molecules. Key transcription factors SREBP1c and PPARγ were highly expressed at the late time points when lipid droplets and rounding of cells, the typical adipocyte phenotype, appear (3d, 7d, 14d; cluster 6 and 9). As a tendency, the expression of known marker genes of the differentiated adipocyte was increased in parallel with these factors. These included genes from clusters 3, 6 and 9, which are targets of either of these factors such as lipoprotein lipase (LPL), c-Cbl-associated proteins (CAP), stearoyl-CoA desaturase 1 (SCD1), carnitine palmitoyltransferase II (CPT II), Acyl-CoA oxidase. Other genes in cluster 6 were known players in lipid metabolism and mitochondrial fatty acid metabolism. Genes in clusters 4 and 7 were also increasingly expressed towards the terminal differentiation stage, although from different starting values. Cluster 4 could be associated with cholesterol biosynthesis and cluster 7 was related to the extra-cellular space or matrix as indicated by GO terms. Contrary, cytoskeleton proteins were mainly down-regulated in cluster 10. Cluster 1, 11 and 12 had no obvious common molecular function.

The overwhelming amount of expression data was reduced to a dozen manageable expression patterns, which correspond to specific biological functions. This is the point, where many expression studies stop their analysis and publish long lists of genes. Unfortunately, the real value of a detailed global view was missed in those studies.

The following result sections focus around two objectives: First, arguments are presented that the observed expression profile is accurate and relevant for the development of adipocytes *in vivo*. Second, it is attempted to understand the full complex nature of the molecular processes underlying adipogenesis by the analysis of function of proteins involved as revealed by this expression profiling study. For this purpose, each protein was subjected to in-depth sequence analytic procedures and the structure and function was annotated on a sequence segment/domain-wise basis as indicated previously. If possible, the targets were mapped onto known pathways, possible cellular roles and sub-cellular location.

A global molecular atlas describes complex changes during adipogenesis

The valid and *in vivo* relevant expression data was simplified to 12 time patterns, which were assigned to major biological functions. These understandable features were the basis for a new gain of complexity by reconsidering all cluster members including their known molecular context. Of the 780 ESTs differentially expressed during adipogenesis, it was possible to derive 659 protein sequences that were all subjected to in-depth sequence analytic procedures. The protein sequences were annotated *de novo* using more than 40 academic prediction tools integrated in the ANNOTATOR sequence analysis system [80]. The structure and function was annotated on a sequence segment/domain-wise basis (see database above). After extensive literature search and curation using the sequence architecture, 345 gene products were mapped onto known pathways, possible cellular roles and sub-cellular localizations. This molecular atlas of fat cell development provides the first global view of the underlying biomolecular networks and represents a unique resource for deriving testable hypotheses for future studies on individual genes. Gene networks of cell cycle, metabolism, signal transduction, extra-cellular matrix changes and cytoskeleton remodeling are available in several figures. A detailed assembly drawing and comprehensive discussion is delineated in the appendix B-1 [2].

Clonal expansion is reflected in adipogenic gene networks

Three major phenotypic changes are visible in the microscope images (see Figure 1): clonal expansion, up-rounding of the cells and inclusion of fat droplets. As an example, the first is described in greater detail (for the others see appendix B-1, [2]). Clonal expansion can clearly be associated with cluster 5 and 8. The genes are not repressed between 12 and 24 hours after induction. The time resolution is not high enough to verify if one or two divisions occur during this phase. The genes are annotated for cell cycle involvement and proteins encoded by them reside in the nucleus. An interaction network of 68 genes derived from literature data can be found in Figure 6 and Figure 7.

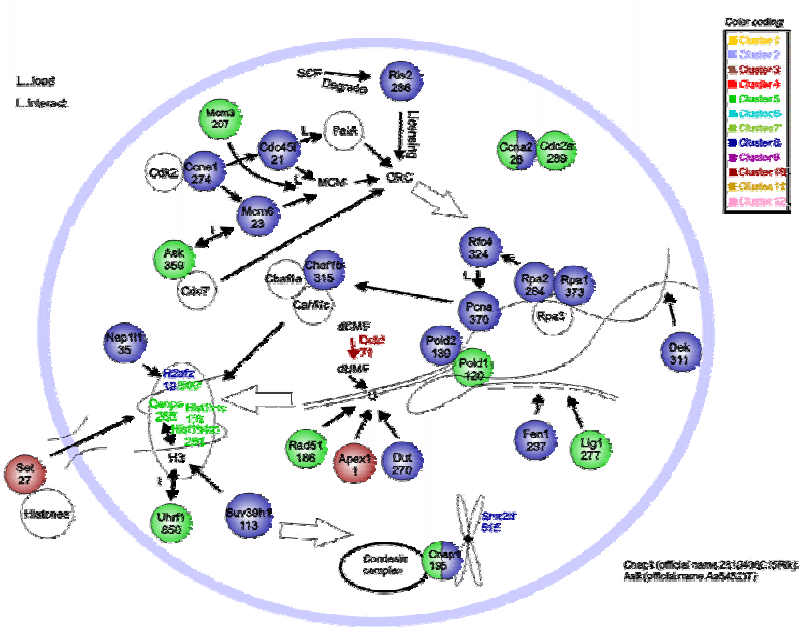

Figure 6 *Schema of DNA replication during clonal expansion. The gene network consists mainly of ESTs in cluster 5 and 8, which are not repressed between 12h and 24h after induction. Many important components of initiation, duplication and chromatin assembly are shown (following the arrows from upper left). Detailed information is found in the text.*

The duplication of the chromosomes is represented by many genes (Figure 6). The minichromosome maintainance (Mcm) complex is assembled at initiation of replication. The

heterogenic complex of Mcm4/6/7 acts as helicase while Mcm2/3/5 most likely regulates its activity [91]. Retroviral integration site 2 (Ris2 now Cdt1) is involved in binding of the MCM to the origin recognition complex and licenses one single replication of the chromosome [92]. The replication protein A (RPA) complex (Rpa1, Rpa2) stabilizes ssDNA at the replication fork and facilitates nascent strand synthesis by the replicative DNA polymerase [93]. The proliferating cell nuclear antigen (Pcna), is loaded by replication factor C (Rfc4) in the presence of RPA. Pcna promotes a switch to processive synthesis by DNA polymerase [94]. The lagging strand is synthesized from the Okazaki fragments by the flap structure specific endonuclease 1 (Fen1) and ligated by ligase I, DNA, ATP-dependent (Lig1) [95,96]. The mammalian recombinase Rad51 plays important roles in homologous recombination and DNA repair [97]. Deoxyuridine triphosphatase (Dut) and apurinic/apyrimidinic endonuclease 1 (Apex1) are further components, which participate in higher fidelity of replication and repair. Finally, components of DNA packaging are not repressed between 12h and 24h after induction. Several members of the histone family (Hist1h1c, Hist1h4m, H2afz) are part of the nucleosomes. Histone 3 is substituted by centromere autoantigen A (Cenpa). This crucial event is needed to recruit several factors of the kinetochore [98]. Finally, ubiquitine-like, containing PHD and RING finger domains, 1 (Uhrf1, also known as Np95) and suppressor of variegation 3-9 homolog 1 (Suv39h1) introduce essential post-translational modifications into the histones.

Beside the DNA replication, components of cytokinesis and regulatory network of cell cycle are found in great detail in the expression data (Figure 7). Karyopherin (importin) alpha 2 (Kpna2) imports proteins with a nuclear localization signal (NLS). In the nucleus, the Ras-like, family 2 locus 9 (Ran), releases the imported protein from Kpna2 [99]. The Ran-Kpna2 interaction prevents Tpx2, microtubule-associated protein homolog (Tpx2), which is involved in mitotic spindle assembly, binding to importin. In turn, Tpx2 binds to aurora A (Aurka), which is activated and recruited to the microtubules [100]. Further, ajuba (Jub) is essential in Aurka activation [101]. Several tubulins (Tubg1, Tubb5, Tuba4, Tubb6) and other components of the spindle apparatus (e.g. Kntc2, Cdca1, Kif22, Tacc3)) are co-expressed in parallel. Further important players of cell cycle signaling are not repressed between 12h to 24h hours after induction. Those include protein regulator of cytokinesis (Pcr1), checkpoint kinases (Chek1), regulators of the anaphase promoting complex (Bub1, Mad2l1, Cdc20) and several cyclins and cyclin kinases.

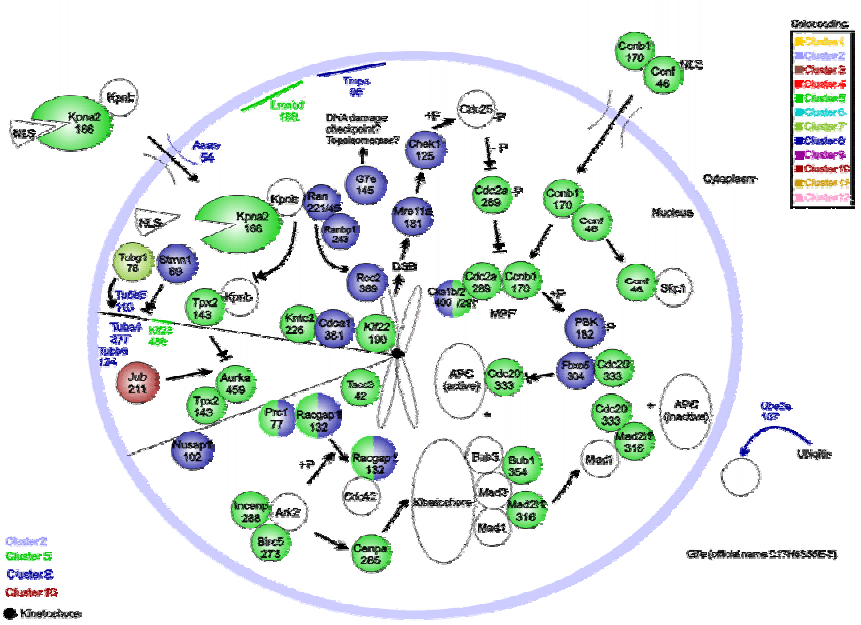

Figure 7 *Gene networks during cell cycle. The left half mainly delineates the mechanism of nuclear import and spindle microtubules assembly. The remaining networks illustrate transcriptionally regulated signaling cascades of clonal expansion. Checkpoint kinases, regulators of the anaphase promoting complex (ACP) and several cyclins and cyclin kinases are not repressed between 12h to 24h after induction.*

Altogether, the clonal expansion, which can be observed under the microscope, is clearly visible on the molecular level in the expression pattern of adipogenesis. Several further phenomena are described by means of the molecular atlas of fat cell development (see appendix B-1, [2]). Therefore, this resource provides the first global view of the underlying biomolecular networks and represents a unique resource for deriving testable hypotheses. The gene networks are also used for target identification. 7 promising research targets are shown in the following paragraphs.

Target identification powered by the global adipogenic atlas[2]

The detailed investigation of sequence architecture and gene function in combination with network interactions eased the identification of targets for further research significantly. The definition of a good target depends on the application of interest. A well suited target for fundamental research is in this context required to have direct or indirect regulatory potential on differentiation and to be not already assigned to a critical role in adipogenesis. A list of the seven top most favorites can be found in Table 2.

Table 2 *Seven promising targets for fundamental research are potentially involved in regulation of adipogenesis.*

RefSeq Id	EST Id on the mousechip	Cluster	Name
NM_010444	BE533846	2	nuclear receptor subfamily 4 group A member 1 (Nr4a1)
NM_026439	AI838653/AW552006/AW552313	3	Ssg1, Urb ('Riken cDNA 2610001E17 (steroid sensitive protein 1))
NM_008590	AI848227/BE377797/AI834945	6	mesoderm specific transcript PEG1/MEST
NM_177229	BE376542	6	RIP 13, NCoR ('RIKEN cDNA 5720405M06)
NM_007951	AI847976	7	Mer ('enhancer of rudimentary homolog)
NM_007833	AI838312/AW556372	7	Decorin
NM_007680	AU041627	9	Eph receptor B6

Nuclear receptor subfamily 4 group A (Nr4a1) has a large (233aa) N-terminal low complexity region, which is composed of more than 28% small polar amino acids. This sequence biased segment is followed by a region called 'C4 zinc finger in nuclear hormone receptors' (SM00399, E-value = 4.3e-40) and the 'Ligand binding domain of hormone

[2] Also contributing: Anne-Margrethe Krogsdam and Zlatko Trajanoski

receptors' (SM00430, E-value = 8.4e-34). The polar region might be responsible for putative dimerization, while the zinc finger recognizes and binds specific DNA motifs. The ligand binding domain has the capability to bind yet unknown effectors. This orphan nuclear receptor is up-regulated during the whole differentiation but markedly before and after clonal expansion. Nr4a1 has been implicated in cell proliferation, differentiation, and apoptosis [102]. Nr4a1 was experimentally investigated in further detail. It was shown that the transcription factor is important for very early differentiation. On the contrary, artificially prolonged expression (transduction) abrogates adipogenesis, which depends on the DNA binding feature[3].

The so called "**Coiled-coil domain containing 80 (Ccdc80)**" gene encodes a protein known as 'steroid sensitive protein 1'. Ccdc80 is predicted to be an extra-cellular protein due to its N-terminal signal peptide. Interestingly, there is no coiled-coil predicted with the ANNOTATOR. A closer look at the raw results shows that the region between 554 to 587 amino acids has some potential to be a coiled-coil segment. However, the coiled-coil motif of the hydrophilic segment is a putative false prediction due to the absence of heptad periodicity, which is addressed with the COIL parameters (window length 21, the 1995 matrix-based profile and down-weighting for polar residues [103]).

The protein contains three internal repeats (IR1, IR2, IR3) with approximately 200 amino acids and an amino acid composition similar to common globular domains. In the multiple alignment of the repeats, a distinct pattern is visible. Therefore, the segments (100-300; 570-770, 749-949) were applied to a fan like PSI-BLAST familysearch with an E-value cut-off of 0.005. 43 hits (all from first PSI-BLAST) were found.

All three internal repeats (IR) of the original protein can be found with following E-values: IR1 (1e-104); IR2 (5e-06); IR3 (9e-05). The ortholog proteins of *Homo sapiens* (NP_840058.1) and *Gallus gallus* (BAC54279.1) can be found too with almost the same E-values for the three internal repeats as in *Mus musculus*. Furthermore, many Sushi-repeat containing proteins of various species are found, as well as many hypothetical proteins. Very interesting is also the hit to ZP_00127997.1 (COG1530: Ribonuclease G and E;

[3] Anne-Magrethe Krogsdam personal communication

Pseudomonas syringae pv syringae B728a; from 298 to 425; E=4e-07). Therefore, it was investigated if a ribonuclease activity can be assigned to the internal repeats.

Unfortunately, there are several hints that this segment has no ribonuclease activity and RNA binding domain.

1. The COG1530 domain (RNase G and E) matches to amino acids 17-135 of the pseudomonas protein but the IRs of the steroid sensitive protein 1 matches to amino acids 298-425 of the pseudomonas protein.
2. In a NCBI-BLAST search with the ribonuclease of the *Pseudomonas species*, homology to other ribonucleases is restricted to the first 135 amino acids (N-terminal). The C-terminal region is only homolog to two hypothetical proteins (NP_744544 and ZP_00087).
3. There is no fold similarity (bioinfo.pl) to any ribonuclease.

A multiple alignment was constructed from the family search results. A distinct pattern is observed but nevertheless all bacterial species (NP_762334.1, NP_800493.1, ZP_00004514.1, NP_744544.1, ZP_00127997.1, ZP_00087571.1 and ZP_00050117.1) align not so well as the eukaryote species. A HMM model was constructed out of this multiple alignment, which found all proteins of the initial family, but no further candidates.

The IR1 of *Mus musculus*, the IR2 (E=1e-05) of the ortholog *Gallus gallus* protein (BAC54279.1) and the consensus sequence of the HMM model were submitted to the structure meta-sever bioinfo.pl. The pdbblast of all four sequences give no significant hits. The internal repeats and the consensus sequence have all structural similarity to the SCOP c47.1 (Structural Classification of Proteins) under supervision of 3djury (IR1 *Mm*.: 201aa, 3djury score: 68.25, 1jfua; IR2 *Gg*.:155aa, 3djury score: 69.2, 1qmv_A; HMM consensus: 151aa, 3djury score: 88.88, 1qmv_A). SCOP c47.1 stands for the superfamily of Thioredoxin-like fold.

Ccdc80 is repressed during clonal expansion and highly up-regulated in terminal differentiation. Previously, it was suggested that it may have a unique function in the regulation of body weight and energy metabolism [104].

Mesoderm specific transcript (Mest) has a predicted signal peptide for extra-cellular localization and a globular domain of alpha/beta hydrolase fold (PF00561, 4e-11). A special biological role is indicated with the RPS-BLAST hit 'Soluble epoxide hydrolase [Lipid transport and metabolism]' (KOG4178, E-value = 7.0e-92). Mest is strongly up-regulated during fat cell differentiation except at 6h and 12h after induction. The gene is widely expressed during development [105]. The imprinted Mest gene is induced in adult tissue only from the paternal allele [106]. It is markedly enhanced in white adipose tissue of mice with diet-induced and genetically caused obesity and appears to enlarge adipocytes and could be a novel marker of the size of adipocytes. Ectopic expression of Mest in 3T3-L1 cells causes increased gene expression of adipose markers such as PPARgamma, CCAAT/enhancer binding protein (C/EBP)alpha [107].

Nuclear receptor co-repressor 1 is a very long protein with many low complexity regions and coiled-coil segments. Two "SANT SWI3, ADA2, N-CoR and TFIIIB" DNA-binding domains' (SM00717, E-value = 1e-16 to 1e-10) are predicted, which had sequence specific binding sites. It seems from the protein architecture that the protein is mainly involved in protein-protein and protein-DNA interaction. Ncor1 is up-regulated after clonal expansion, which indicates an important role for fat cell maturation.

Enhancer of rudimentary homolog (Mer) consists only of the highly conserved domain with same name as the protein. The function is unknown. Mer is very strongly up-regulated throughout differentiation. It is proposed that Mer is a cell type-specific transcriptional repressor, probably interfering with HNF1-dependent gene regulation via DCoH/PCD [108].

Decorin (Dcn) is an extra-cellular protein composed mainly of leucin rich repeats (LRR). LRRs fold into a horseshoe like shape and act as protein-protein interaction structures. Dcn is very strongly up-regulated during adipogenesis. It is proposed that decorin is a bidentate ligand attached to two parallel neighboring collagen molecules in the fibril, helping to stabilize fibrils and orient fibrillogenesis [109]. Beside the structural role, the protein core can bind TGF-beta [110]. It is shown that interaction between decorin and TGF-beta play an important role in myogenesis [111] and that decorin reverses the repressive effect of autocrine-produced TGF-beta on mouse macrophage activation [112]. All this observations

result in the assumption that the interaction between TGF-beta and decorin plays an important role also in adipogenesis [67].

Eph receptor B6 (Ephb6) contains an N-terminal signal peptide and is located with one transmembrane helix in the membrane. The extra-cellular N-terminal region contains an 'Ephrin receptor ligand binding domain' (SM00615, E-value = 7*e-104) followed by a low complexity region rich in small amino acids and two 'Fibronectin type 3 domain' (SM00060, E-value = 1e-6 to 1e-12). Therefore, the extra-cellular part of the receptor is composed of protein-protein interaction features. Intracellularly, the sequence is consisting of a 'Tyrosine kinase, catalytic domain' (SM00219, E-value = 1.1e-74) and a 'Sterile alpha motif' (SM00454, E-value = 2.9e-20). The kinase of Eph6 is an inactive pseudo kinase domain since it lacks all three important catalytic residues [113]. Sterile alpha motif is a protein interaction domain. Even without an active kinase domain, EphB6 can pass on signaling stimuli [114,115]. Because both receptors and ligands are membrane-bound, a direct cell–cell contact is necessary for ligand binding and activation of the signaling cascades. As a unique feature, bidirectional signaling is initialized in both the receptor and the ligand-bearing cell [116].

Enzymatic networks are regulated in an ordered manner

It can be hypothesized that enzymatic networks undergo a specific regulation on the transcriptional level to react efficiently to environmental or genetic changes. Two mechanisms can be proposed:

1. Co-regulation of whole pathways/pathway segments
2. Ordered regulation of specific points, while the rest is unaffected

It was tried to evaluate both hypothesis with the molecular atlas of fat cell development. Transcriptional co-regulation of a whole pathway/pathway segment was identified in the case of cholesterol anabolism. 11 out of 14 enzymes of the cholesterol pathway share similar expression profiles after isopentenylpyrophosphate synthesis. All enzymes except 7-dehydrocholesterol reductase (Dhcr7) group together in the hierarchical cluster 4 (see

appendix B-1, [2]). Nevertheless, the profile of Dhcr7 is very similar to cluster 4. Analysis of the promoters shows that the co-expression of the cholesterol genes corresponds also to the regulatory features of the 3'-UTR. Transcription factor binding sites for SREBP-1 (SRE and E-box motifs [117]) is represented in significantly more genes in cluster 4 than all other clusters (p-value of Fisher exact test 0.0484, Table 3). Similarly, a putative SREBP-1 regulatory region is significantly more frequent in the promoters of the genes in cluster 4 compared to all unique sequences in the PromoSer database (p-value < 0.0289; PromoSer contains 22549 promoters of 12493 unique sequences).

The mechanism of co-regulation is only identified for cholesterol anabolism, which leaves the lion's share of enzymes unassigned. The enzymes are dispersed over the whole cellular metabolism. This raises the question, if those regulated points share some common feature in the network. Therefore, the transcriptionally regulated genes were analyzed if they obey common criteria in the 36 different metabolic pathways observed in the expression profiles (appendix B-1, Table 1, [2]). Within each pathway, it was asked whether these transcriptionally regulated genes occupy key positions, i.e., a position at the pathway start, which is the typical rate-limiting step where the amount of enzyme is critical [118], or at some other point of regulation. With the adipogenic atlas it is found that such key positions are occupied by transcriptionally regulated targets in 27 pathways (for detail see appendix B-1, Table 1, [2]).

2.2. Transcriptional regulation of rate-limiting steps

In the previous chapter of fat cell differentiation, it was shown that, through a scrutiny of expression profile and all involved components, testable hypothesis can be derived. The hypothesis of preferred transcriptional regulation of rate-limiting step as an efficient way to influence metabolism was proven by the case of fat cell differentiation. In this chapter, the hypothesis is raised on a more general tier.

An accurate set of 126 rate-determining enzymes from curated databases

Rate-limiting enzymes are described in many protein and gene databases. Three established databases in biology are selected for rate-limiting data retrieval. Online Mendelian Inheritance in Man (OMIM) of the Johns Hopkins University is a catalogue of genes and genetic disorders with links to literature references, sequence records, maps, and related databases. OMIM originates from the print edition MIM, which was founded more than 40 years ago and matured to an excellent knowledgebase with more than 17,300 entries [119]. This resource is selected as a highly reliable and significant disease database. The investigation of the data revealed 55 proteins, which are known to play part in rate-limitation. Since the transcriptional expression of rate-limiting proteins is the research focus, the gene-centric GeneCard is selected as second repository, which is aimed at providing concise and integrated biomedical information from many different online databases [73,74]. The advantage of combining several different resources in GeneCard provides an addition of 25 rate-limiting genes. The last repository of choice is the BRaunschweig ENzyme Database (BRENDA) since most known rate-determining processes are involved in metabolism. The primary literature based knowledgebase characterizes more than 83,000 different enzymes (4,200 EC numbers) from 9,800 different organisms with valuable information about metabolites, activators/inhibitors, kinetic parameters, literature and many more [120,121]. Further 46 enzymes are identified within the specialized hand-curated enzyme resource. Thus, 126 highly reliable rate-limiting proteins are revealed within the three major biological databases. It is unlikely that further investigations of gene/protein based databases will lead to an additional huge amount of rate-determining proteins due to the tactical choice of the databases and the interwoven nature of the major biological online databases.

Table 3 *Cumulative contribution of curated databases to the amount of rate-limiting (RL) enzymes. The +-sign indicates the additional number of rate-limiting enzymes.*

Database	Number of RL enzymes/isoforms
OMIM	55
GeneCard	+25
Brenda	+46
Total	126

Comprehensive collection of known rate-limiting enzymes using PubMed

A small selection of 126 highly reliable rate-determining proteins is available through gene and protein databases. Screening of 1000 recently published PubMed entries with the key word "rate-limiting" quickly reveals that this protein collection is far from complete. A set, which is as comprehensive as possible, is needed for a global examination of the transcriptional regulation of key points within the metabolism. Therefore, more than 15,000 abstracts, which are available through NCBI PubMed, are reviewed for proteins, which are rate-limiting for metabolic pathways and cellular processes. Synonyms are combined mainly with the Entrez Gene database. 391 mammalian genes are defined in literature to be rate-limiting for a larger process. Additional 42 splice variants are known for those genes. The gene table of all 391 rate-limiting genes of *Mus musculus* can be found in appendix A. This set contain also the highly reliable set of 126 proteins, which were found in curated databases.

Molecular functions associated with rate-limitation

The rate-determining proteins of the model organism *Mus musculus* are analyzed regarding their molecular function in the cell. To avoid biases of the 391 rate-limiting enzymes with many isoforms, a set of 273 unique protein species is constructed. 218 of the unique proteins match a sequence of the mouse-specific KEGG database with stringent BLAST criteria (identity>95%; E<1e-50). KEGG provides information of the enzyme commission (EC) numbers [122]. The classification of the enzymes by their catalytic reaction shows that transferases (35%) and oxidoreductases (32%) are the major part of the rate-determining proteins, which are described in the literature. The remaining one-third is covered by hydrolases (12%), lyases (7%), ligases (5%) and isomerases (2%) (Figure 8).

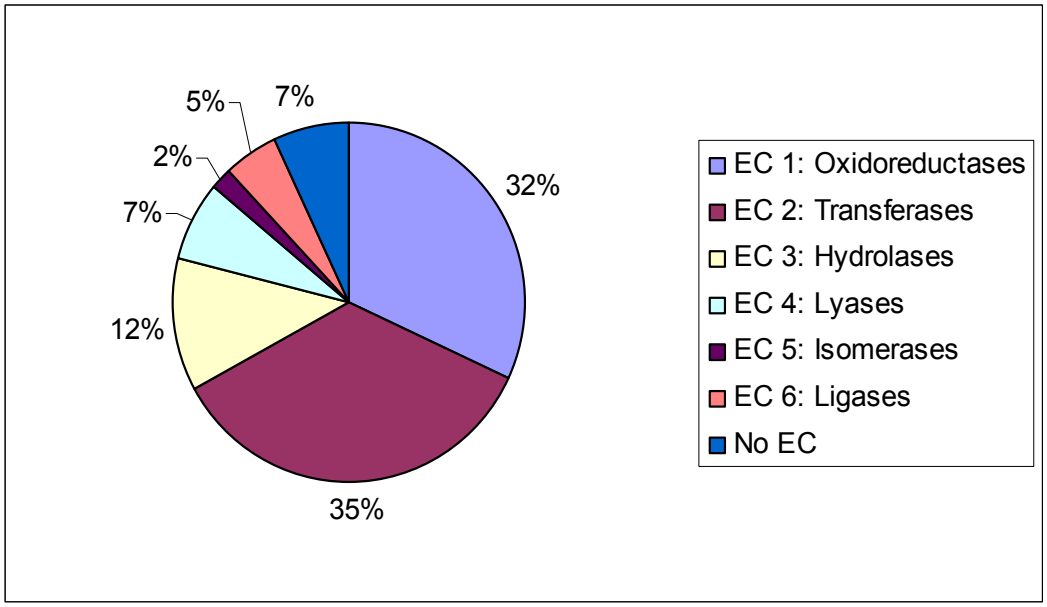

Figure 8 *Distribution of the rate-limiting enzyme classification defined by the enzyme commission. Rate-limiting enzymes are mainly oxidoreductases or transferases.*

An in-depth domain-wise analysis of the involved molecular functions is performed *de novo* with the IMP-ANNOTATOR [80]. In total, 516 sequence regions of the dataset are predicted to contain a Pfam domain. The ten top ranking domains, regarding the occurrence of unique proteins containing a domain (not domain occurrence), are part of 50 unique proteins. The Pfam domain cytochrome P450 (p450, PF00067) is the most frequent catalytic feature observed within the known rate-limiting proteins. 12 (4.4%) proteins contain this motif. Cytochromes P450 are haem-thiolate proteins involved mainly in oxidative degradation of various metabolites. Short chain dehydrogenase (adh_short, PF00106) family is representation with 5 members of known rate-limitation (1.8%). These proteins are known to be NAD- or NADP-dependent oxidoreductases. Also 5 (1.8%) sequences are identified to carry an Aminotransferase class I and II (aminotran_1_2, PF00155) domain. This huge clan combines many different nitrogenous group transferring Pfam-families, which share the ability to bind the prosthetic pyridoxal-phosphate group covalently to lysine. 7 different domain species are all represented in 4 proteins (1.5%), namely phosphoribosyl transferase domain (Pribosyltran, PF00156), FAD dependent oxidoreductase (DAO, PF01266), alpha/beta hydrolase fold (Abhydrolase_3, PF07859), pyridine nucleotide-disulphide

oxidoreductase (Pyr_redox, PF00070), pyridoxal-dependent decarboxylase conserved domain (Pyridoxal_dec), PF00282), trypsin (trypsin, PF00089) and fatty acid desaturase (FA_desaturase, PF00487).

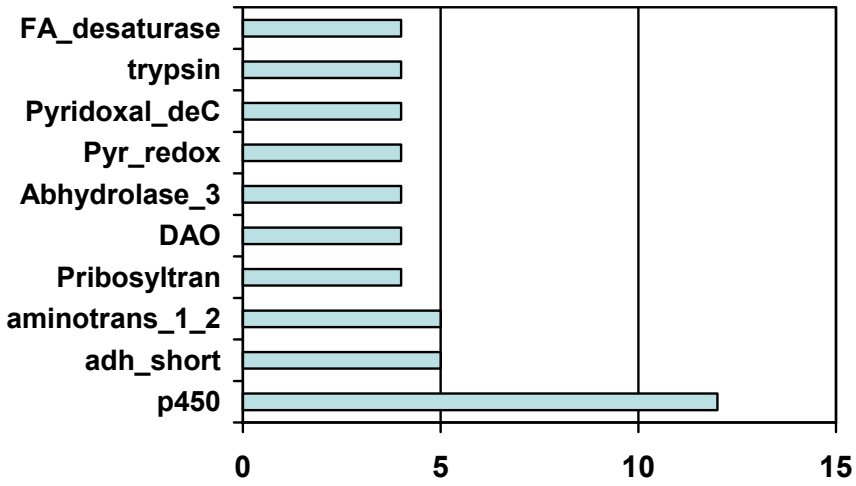

Figure 9 *Distribution of de novo predicted Pfam domains within a set of literature described rate-limiting proteins. The top six domains are associated with oxidoreductase or transferase activity. Abbreviations: Cytochrome P450 (p450), Short chain dehydrogenase (adh_shor); Aminotransferase class I and II (aminotran_1_2); Phosphoribosyl transferase domain (Pribosyltran); FAD dependent oxidoreductase (DAO); Alpha/beta hydrolase fold (Abhydrolase_3); Pyridine nucleotide-disulphide oxidoreductase (Pyr_redox); Pyridoxal-dependent decarboxylase conserved domain (Pyridoxal_dec); Trypsin (trypsin); Fatty acid desaturase (FA_desaturase)*

The remaining domain motifs are mainly very specific for one enzyme species and, therefore, do not cluster together. The rate-limiting proteins, which contain the top ranking domains, can be grouped in a more general way leading to a similar result than the analysis of the EC numbers. Altogether, this results in 29 oxidoreductases, 13 transferases and 8 hydrolases and no domain is classified to be specific for lyases, isomerases and ligases. The domain distribution shows a clear tendency towards oxidoreductases and transferases as the preferred molecular function within rate-determining proteins in literature.

Key loci are dispersed in the metabolic network

Mapping the rate-limiting proteins to the KEGG pathways showed that they are dispersed throughout the whole enzymatic network of the cell. They are mainly positioned before or after a node, where many pathways run together. There is one interesting exception. Nearly all eight enzymes of the citrate cycle are classified in literature as rate limiting (Figure 10). Only fumarase is not described as rate-limiting in literature. The Krebs cycle is the central hub of cellular anabolism and catabolism. The physiological free enthalpies of citrate synthase, isocitrate dehydrogenases and alpha-ketoglutarate-dehydrogenase complex are smaller than 0 [123]. Additionally, those enzymes and succinate dehydrogenase are listed to have specific activators and inhibitors. All steps but aconitase and fumarase are located before a metabolic central node.

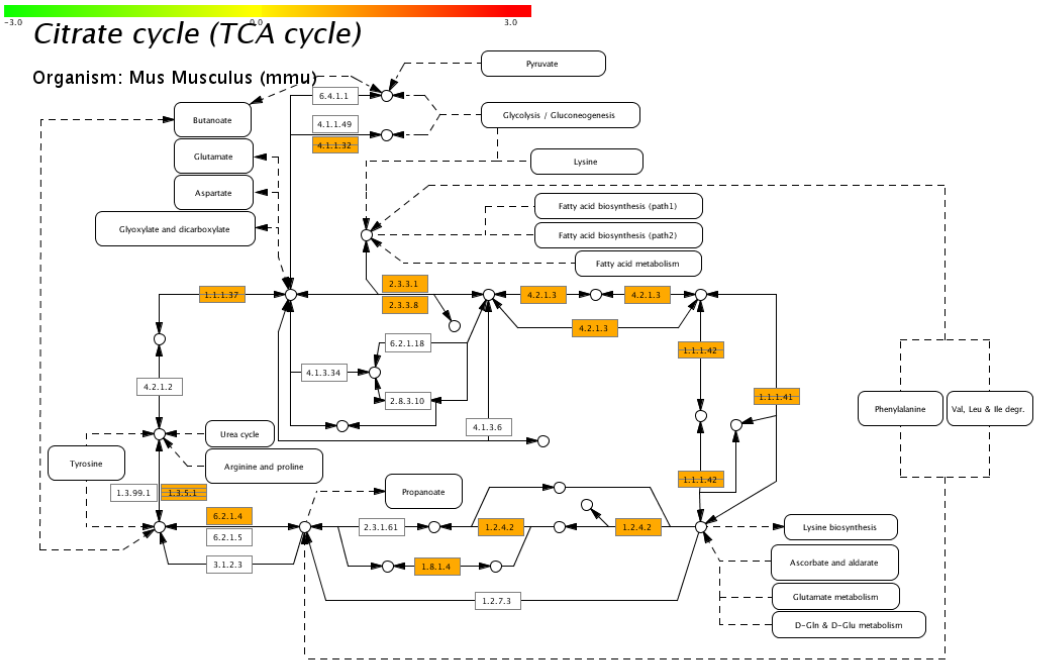

Figure 10 *All enzymes but one of the central citrate cycle are classified as rate-limiting*

Disturbance of the enzymatic network by knocking out a single rate-limiting enzyme

Adipose triglyceride lipase (ATGL) is a putative rate-limiting enzyme in the catabolism of fat depots [124]. Disturbances after knocking out a single metabolic rate-limiting factor ($ATGL^{-/-}$ mouse) were analyzed by means of microarray expression data[4]. Relative expression of knockout and wild-type situation was measured in 6 tissues/organs. Significant response to the $ATGL^{-/-}$ knockout was observed in brown adipose tissue (1110 ESTs) and cardiac muscle (382 ESTs) with at least 2-fold up- or down-regulation compared to wild type. Interestingly, it had nearly no effect on white adipose tissue (96 ESTs), liver (28 ESTs), kidney (5 ESTs) and smooth muscle (58 ESTs).

Brown adipose tissue (BAT) responded to the knockout of the rate-limiting enzyme most vigorously. The reason might be that triglyceride (TG) is the most important substrate for BAT, which is used in thermogenesis. The absence of ATGL diminishes or cancels totally the TG utilization in those cells. Therefore, the fat burning is completely down-regulated. Rate-limiting enzymes of fatty acid degradation (acyl-CoA dehydrogenases (Acad)), many citrate cycle enzymes and components of all electron transport and oxidative phosphorylation complexes have significant lower expression levels than in wild type mice. Contrary, adipose differentiation related protein (Adfp), which is responsible of lipid droplet formation, is up-regulated. Interestingly, the expression of fatty acid synthase (Fasn) is also stimulated. Steaoryl-CoA seems to be the predominant *de novo* fatty acid, since the post-processing stearoyl-CoA desaturase 1 (Scd1) and ELOVL family member 6, elongation of long chain fatty acids (Elovl6) are lower expressed than in wild type mice. Only desaturation by Scd2 might be an exception.

[4] Data provided by Montserrat Pinent Armengol, Hubert Hackl and Juliane Strauss (IGB, TU Graz) (publication in preparation)

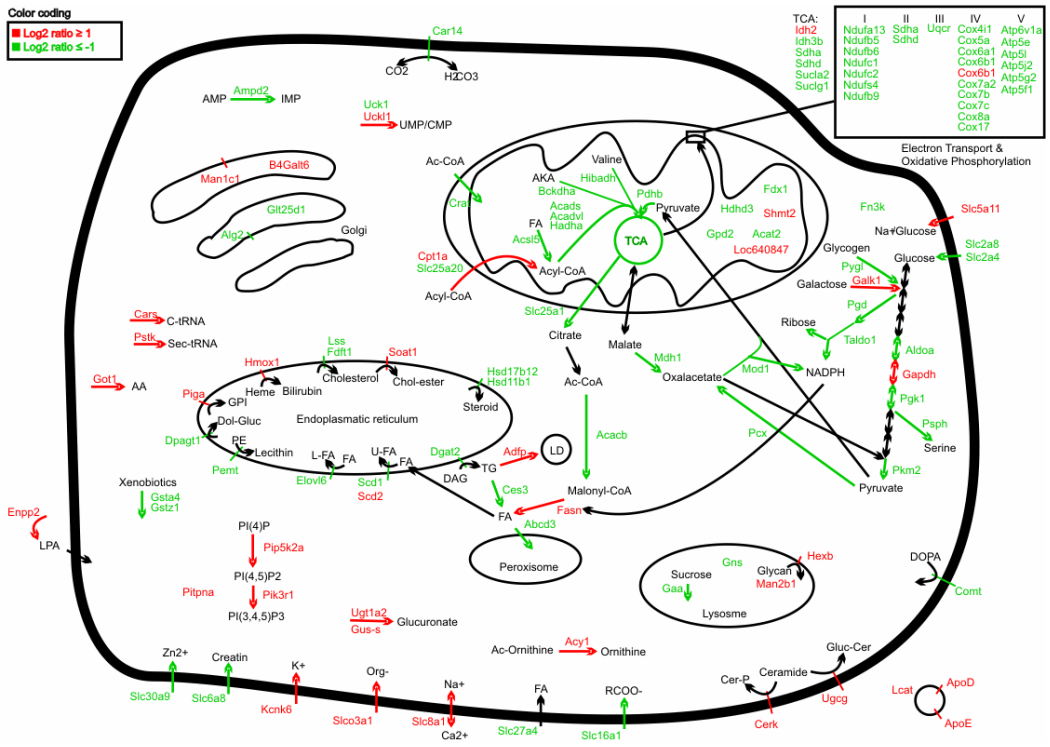

Figure 11 *The knockout of the rate-limiting adipose triglyceride lipase (ATGL) influences the metabolism of brown adipose tissue on the transcriptional level significantly. Especially fatty acid degradation, citrate cycle, electron transport and oxidative phosphorylation are down-regulated compared to the wild type mouse (for details see text).*

Beside the pathways, which are obviously influenced by the lack of TG degrading ATGL, also other substrate provider for the citrate cycle are shut down. This indirect influence is observed in catabolism of alpha-keto acids (AKA), valine and pyruvate, which is the main degradation product of the glycolysis. It might be that the accumulating degradation products induce a feedback inhibition of the rate-limiting enzymes on the transcriptional level since the citrate cycle is shut down.

Carbohydrate metabolism is the second major process influenced by ATGL knockout. Glucose/sodium symporter is induced (Slc5a11) while other important glucose importers (Slc2a8/Slc2a4) are down-regulated. Gycogen catabolism, which is a further substrate resource for glycolysis, seems also to be shut off. The glycolysis itself is mainly repressed at the transcriptional level. The absence of glycolysis metabolites might be the reason of the

down-regulation of pathways, which use the intermediates for anabolism like serine synthesis and the anaplerotic[5] oxalacetate production. Further the pentose phosphate shunt is repressed at different levels, which might turn of ribose and NADPH synthesis. The second possibility of NADPH supply through the enzyme called "malic enzyme, supernatant" (Mod1) shares the same repression. Beside those major changes, a noticeable number of transporters are transcriptionally influence. Additional components of cholesterol shuttling lipoproteins (ApoD, ApoE, Lcat) are up-regulated.

Altogether, the knockout of the rate-limiting ATGL enzyme exerts changes mainly on degradation as well as on energy supply and thermogenesis. Few pathways, which are not involved in those processes, are also influenced in different directions. As observed in the transcriptional regulation of enzyme networks during fat cell differentiation, pathway changes seem to be achieved in one of two ways. Either all pathway components are regulated simultaneously (e.g. electron transport) or, preferentially, individual rate-limiting steps are modified (e.g. fatty acid degradation). 31 rate-limiting metabolic proteins are differential regulated, which is 31% of the enzymes (98). If the co-expressed pathway of electron transport and oxidative phosphorylation is subtracted, the amount of strongly regulated enzymes rises to 39% (29 of 74).

Transcriptional regulation of rate-limiting enzymes during differentiation

Several expression profiling studies, which investigate differentiation processes, are analyzed with regard to the transcriptional regulation of rate-limiting enzymes. Fat cell differentiation from 3T3-L1 [2] and MEF cell lines (unpublished data) were performed with a cDNA microarray at 8 different time points. Significantly regulated genes were in at least 4 time points 2-fold up or down-regulated compared to the reference. 3T3-L1 contains 83 metabolic proteins in the KEGG database. 41% of those proteins were identified as rate-limiting. MEF differentiation yielded 147 enzymes in the metabolic part of KEGG, which contained 43 rate-limiting enzymes. Development of skeletal muscle was analyzed by

[5] replenish intermediates of the citrate cycle

Tomczak KK et. al [125]. The expression profile of differentiating C2C12 cells was measured with Affymetrix mouse MG_U74Av2 and MG_U74Cv2 oligonucleotide-based arrays for 12 days. 2895 probesets contain at least in one of the 7 time points a relative expression to the reference of at least 2-fold up or down regulation. 28% of the 189 enzymatic proteins, which are found in KEGG, are rate-determining. *In vitro* bile ductular differentiation of HBC-3 cells was performed by Ader T et. al [126]. The time course was profiled at 7 points with cDNA microarrays, which contain 27,400 sequence verified mouse clones. Statistical Significance Analysis for Microarray (SAM) was applied to get a set of significantly regulated genes. The set of annotated genes, contain 41% rate-limiting components. The global alterations in gene expression by studying A404 cells during smooth muscle cell (SMC) differentiation were transcriptionally profiled with oligonucleotide microarray from Agilent (Mouse Oligo Microarray G4120A platform), which consists of 20,371 60-mer oligonucleotides [127]. Significance analysis of microarrays (SAM) was performed and intersections of gene lists were obtained, providing expression patterns over the time course. Those intersections contain 8 of 30 rate-limiting metabolic proteins. Comparing to the expressed data sets, the total KEGG database itself contained 1411 proteins in metabolic pathways. 261 (19%) are described in literature as rate-limiting.

Table 4 *Involvement of transcriptional regulation of rate-limiting enzymes during differentiation. The numbers of transcriptionally regulated rate-limiting enzymes during differentiation and the total number of enzymes are shown. Enzymes are defined through involvement in metabolic KEGG pathways. For comparison rate-limiting and non-rate-determing enzymes of the total KEGG database are shown in the last row. The significant gene set was defined with different methods directly from the authors (indicated by stars).*

Differentiation experiment	Number of rate limiting metabolic KEGG proteins	Number of metabolic KEGG proteins	Percent of rate-limiting proteins
Adipogenesis (3T3-L1)*	34	83	41%
Adipogenesis (MEF)*	43	147	36%
Myogenesis**	53	189	28%
Bile duct***	20	51	41%
Smooth muscle cell***	8	30	27%
Total KEGG database	261	1411	19%

* At least 2-fold change in 4 of 8 timepoints;
** At least 2-fold change in 1 timepoint;
*** Significance analysis of microarrays (SAM)

3. Discussion

This thesis explores the question to which extent gene expression profiles can reveal molecular functions. Comprehensive bioinformatics analyses of microarray data from a cell model of fat cell development resulted in three novel biological insights. First, the analyses have resulted in comprehensive gene networks of fat cell differentiation for the first time. Second, the annotated adipogenic atlas puts many important biological processes in a common context and extends the view of previous microarray analyses in fat cells [6-11,128]. Third, continuative analysis of the gene networks revealed the preferential transcriptional regulation of rate-limiting enzymes as a mechanism to control the metabolism. This evaluation confirmed for five independently developmental processes that approximately one third of strongly transcriptionally regulated enzymes could be categorizes as rate limiting. These surveys were only possible after an extensive list of rate-limiting proteins was compiled from curated databases and literature. As no comparable effort has been previously reported, this selection is a very valuable contribution to the field of proteomics as it will allow set-consideration in a qualitatively new way. The three main achievements are discussed in the following.

First, in-depth analyses of expression profiles resulted in complex networks describing molecular processes after. Initially, a first glance into the wealth of the microarray data is possible by assigning GO terms to co-expression patterns. This strong simplification associated gene groups with cell cycle, extra-cellular matrix alteration, cytoskeleton remodeling and cholesterol biosynthesis. Nevertheless, more than 40 percent of the ESTs remained unassigned. Although the number of protein sequences to which a GO term can be matched is steadily increasing, specific and detailed annotation is only possible with in-depth bioinformatics analyses based on segment and domain predictions. Hence, *de novo* functional annotation of ESTs using integrated prediction tools and subsequent curation of the results based on the available literature is not only necessary to complete the annotation process, but also to reveal the actual biological processes and gene networks. Altogether, 345 gene products were mapped on known pathways, molecular processes and sub-cellular localizations. This molecular atlas of fat cell development provides the first global view of the underlying biomolecular networks.

Second, the novel adipogenic atlas enhances the understanding of fat cell differentiation significantly. On the one hand, 326 of the 780 ESTs were not shared with previous studies [6,9,129], suggesting that the comprehensive picture of this process is far from complete. On the other hand, a true novelity lies in the global view of the gene networks. The connected nature of the resource can be used to derive new hypothesis and test upcoming ones. Several phenotypic changes of adipose differentiation are particularly well characterized by the expression data. For example, clonal expansion, a prerequisite for terminal differentiation, is correlated with a network of 68 transcriptionally regulated gene products. Furthermore, a global view of the gene networks suggests that the reduced replenishment of the cytoskeleton with building blocks, the strong transcriptional up-regulation of modulating proteins and extra-cellular remodeling act in concert and cause the morphological up-rounding during adipogenesis. Most cytoskeleton gene products are co-expressed (cluster 10) and might have a common transcriptional regulatory mechanism (Appendix B-1, [2]). While most identified gene products are located at endpoints of regulation cascades and typically contribute highly abundant transcripts, this work could also identify complex changes of signal transduction and transcription factors with a role in adipogenesis (Appendix B-1, [2]).

Third, preferential control of rate-limiting enzymes and the synchronous regulation of whole pathway segments are two general principles, which regulate the metabolic networks on the transcriptional level. On the one hand, a whole pathway can be co-regulated, which is exemplified by SREBP mediated regulating of the cholesterol synthesis in case of fat cell differentiation (Appendix B-1, [2]). A further example is the shut down of oxidative phosphorylation and electron transport in the gene networks of brown adipose tissue as a response to knockout of adipose triglyceride lipase. On the other hand, 27 of 36 investigated pathways are preferentially transcriptionally regulated at rate-limiting steps in the context of adipogenesis. To investigate the generality of this observation, a comprehensive list of 391 rate-limiting proteins was compiled for the first time. It is supposed that the number of known rate-limiting proteins is far from complete, which is supported by the recent finding of the rate-limiting adipose triglyceride lipase. Nevertheless, it is shown in five different developmental processes that approximately one third of the significantly regulated genes are rate-determining.

Concluding, in-depth bioinformatics analysis can reveal a wealth of information in microarray expression data. In case of adipogenesis a novel molecular atlas, which contributes significantly to a better understanding of fat cell differentiation, is constructed using *de novo* annotation and extensive literature curation. The global view delineates many phenotypic changes and can be used to derive new testable hypothesis. This work determines co-regulation of whole pathway segments and preferential transcriptional regulation of rate-limiting enzymes as important mechanisms to control metabolism on the transcriptional tier.

3.1. Fat cell development

In addition to the previous section and the publication, the comparison to biomarkers and GNF SymAtlas suggests that the 3T3-L1 cell line and the gene networks are relevant for *in vivo* systems. This observation makes the global adipogenic atlas also a valuable resource for pharmaceutical industry to find promising medical targets and to estimate influences on the adipogenic networks. For fundamental research, seven promising candidate genes are proposed for further molecular investigation in the wet laboratories. Furthermore, analysis of predicted transcription factors regulating common features of the gene networks are of major concern for follow up studies. Finally, the annotation of the ESTs resulted in a convenient information retrieval system, which can help upcoming expression experiments to analyze the huge amount of chip data more efficiently. The importance of this work for future studies is reviewed in the following.

First, semi-quantitative comparison of the white adipose tissue (GNF SymAtlas) and the profile of known *in vivo* markers support the notion that the 3T3-L1 model system shows many features which are also found in *in vivo* adipogenesis. Many of the expression profiling results resemble the time course of expression changes during adipocyte development *in vivo* and, therefore, numerous transcriptionally regulated targets found in this study for the first time are potential candidates with important biological functions for medical application and *in vivo* fat cell differentiation. Without doubt, the error margin of microarray-based expression profiling is considerable and, typically, leads to semi-quantitative evaluation of expression ratios. But the observation of transcriptional regulation gains additional

significance when the known or predicted function of protein targets and their involvement in specific pathways make sense in the context of adipocyte development.

Second, several targets can be proposed as promising subjects for further fundamental research. Seven candidate genes are selected by examining the position in the gene networks and the sequence architecture. One success story is the investigation of the Nuclear receptor subfamily 4 group A (Nr4a1, formerly Nur77). Biologists at the Institute for Genomics and Bioinformatics (IGB) could confirm experimentally that the orphan receptor is indeed important for very early differentiation and its prolonged expression abrogates adipogenesis. This function of Nr4a1 was shown to depend on the DNA binding feature. Additionally, several other candidate genes that were not detected in the expression study are proposed by promoter analysis (appendix B-1, [2]) to be important for regulation of fat cell development. Possibly the differential expression of those targets was not identified because microarray technology was not sensitive enough for the low abundant factors [130]. However, 26 binding motifs of transcription factors are recognized as over-represented in a cluster potentially implicated in the regulation of co-expressed genes. One experimentally proven example for a functional transcription factor binding site is SREBP-1 in Cluster 4 [131]. Surprisingly, binding sites for other known key regulators for adipogenesis, PPAR and C/EBP are not significantly overrepresented in any of the promoters of the co-expressed genes. This demonstrates either that much more sophisticated methods must be developed, or that there are many cases where the current methods fail as they cannot consider biologically important aspects like chromatin structure at the recognition site.

Third, the EST annotation of the in-house *Mus musculus* chip of the Institute for Genomics and Bioinformatics (IGB, TUGraz) performed in the course of this work was stored in a relational database. This database helps to analyze upcoming expression studies more efficiently. The only requested input parameter for information retrieval is the EST accession number of interest. Mapping of the EST to nucleotides and proteins are presented upon query submission. One of the most important features is availability of the full mapping results. This is crucial, since the first best hit, which is sorted by the E-value, is sometimes not the correct hit. A short look at the Megablast sequence alignments is often enough to verify the mapping results.

In addition, the annotation database links RefSeq proteins with the most important 3rd party resources that give insight on the cellular function. Furthermore, all gene synonyms are linked to NCBI PubMed, which allows a fast screening of the important literature. Expression data of different sources are also well connected to the RefSeq entries. It is also possible to show the own expression profile in the user interface. Finally, for each protein a *de novo* sequence analysis is available through an integrated frame to the IMP ANNOTATOR suite. This feature needs authentification (username: mousechip; password: expression). The pretty view provides user friendly sequence architecture information, which is the result of over 40 academic sequence analysis algorithms. For proteins already described in literature, knowledge of the protein architecture can verify or extend the molecular function annotation. For proteins of unknown function it is possible to predict their molecular roles.

In summary, several target genes are proposed by directly investigating the gene networks and by indirect analysis of transcription factor binding motifs. Due to the correspondence of many expression profiles to *in vivo* observations, the data might also be a well suited resource for pharmaceutical target identification. Finally in the case of further expression experiment, the annotated ESTs stored in IGB mousechip database might save much time, since many bioinformatics analysis are pre-computed and accessed very fast. Especially, in the case of large datasets it helps to focus on the relevant biological insights, which are hidden in the expression data.

3.2. Rate-limitation

In addition to the first exhaustive list of 391 rate-determining enzymes from literature, a highly reliable subset from three different curated databases was constructed. Rate-limiting enzymes are found to act in biochemical processes mainly as oxidoreductases and transferases. Most of them are scattered in the metabolic networks. Rate-limiting enzymes and whole pathway segments are also transcriptionally regulated in response to the disruption of the gene networks by knocking out a rate-limiting enzyme. Furthermore, this

doctoral thesis shows that specific points of the metabolic network are regulated selectively during development.

First, 391 rate-limiting and hand-curated proteins are selected from more than 15,000 PubMed abstracts. Even though the exhaustive collection covers a broad band of the metabolic networks, it is likely that even more yet unknown key players exist. This became evident as the rate-determining adipose triglyceride lipase (ATGL) was discovered recently. Furthermore, the IUPAC definition of rate-limitation has been interpreted quite freely by scientists in daily usage. Hence, a subset of 126 proteins with improved reliability is constructed from three well established and curated databases. The advantage of using curated-databases is that the information is scrutinized several times from experienced scientist. OMIM, GeneCard and BRENDA were selected as primary resources. Therefore, the expertise incorporated in the retrieved set ranges from medical over gene-centric to enzyme specific information. Together the exhaustive and the reliable selection unfolds its true power depending on the context of the research.

Second, the molecular function of rate-limiting enzymes was found linked to oxidoreductases and transferases activity in two thirds of the studied proteins. A set of 273 rate-limiting proteins, which are not biased by a huge amount of isoforms, was subjected to in-depth analysis aiming at consolidation of the working definition of rate-limitation. KEGG and the enzyme nomenclature were used to classify the proteins. Approximately, one third of the enzymes are oxidoreductases and another third are transferases. The smallest portion is occupied by isomerases, which are mainly involved in reversible reactions. Cytochrome p450, NAD(P)H dependent short chain dehydrogenase and aminotransferase domains are the three domains most commonly found in the rate-limiting proteins. Those *de novo* sequence analytic observations confirm the conclusion of the KEGG analysis. To summarize, this work shows that the most suitable definition of a rate-limiting enzyme needs to include proteins, which are observed to be thermodynamically unfavorable, subjected to regulation or occupying the slowest step of a reaction. Their preferred molecular function in the cell is an oxidoreductase or transferase reaction. Maybe, the combination of the comprehensive selection of rate-limiting proteins with kinetic parameters will allow a more common and precise definition at a later date.

Third, mapping the set of 391 rate-limiting proteins on the enzymatic network shows that most of the enzymes are scattered. Often enzymes are found in vicinity to nodes, where many pathways come together. Therefore, they can influence the direction of the metabolic flux. One interesting exception is the citrate cycle. All components but one enzyme are described in literature in some context as rate-limiting. This mirrors the central role of the citrate cycle for the cell and reflects the tight regulation of most of its steps.

Fourth, knocking out one single rate-limiting factor can have significant effects on the transcriptional expression of the enzymatic network. Adipose triglyceride lipase $ATGL^{-/-}$ mutants influence the gene expression of brown adipose tissue (BAT) and cardiac muscle heavily, while there is nearly no change in white adipose tissue, kidney, liver. It seems that triglyceride degradation is not a crucial pathway of those compartments under tested conditions. However for BAT, triglyceride degradation is important for thermogenesis and energy production. The absence of ATGL dramatically down-regulates the citrate cycle, all parts of oxidative phosphorylation and electron transport. The observed effects might result from the absence of substrates. Interestingly, also other energy supplying pathways such as glycolysis are shut off. Since the BAT is not encapsulated by other tissues, it might be important that many transporter and lipoproteins are differentially regulated. Probably, this is a mechanism to allocate the excessive metabolites to other tissues. Additionally, the phenotypic observations of defective cold adaptation and fat accumulation in different tissues can be explained by means of the gene networks. Fat accumulates since the triglyceride and fatty acid metabolism is transcriptionally shut off at rate-limiting enzymes. Up-regulated transporting systems might distribute the excess fat in the whole body, which finally leads to cardiac dysfunction and premature death. In addition, large parts of oxidative phosphorylation are down-regulated in ATGL absence. This prohibits the build up of an H^+ gradient needed by uncoupling proteins to produce heat. Whereas lacking this function, the brown adipose tissue is not able to respond to cold environments.

Finally, this doctoral thesis shows that metabolic networks can be transcriptionally regulated at rate-limiting enzymes. Previously, it was argued that it is unlikely that a single protein regulates a whole pathway. The total amount of the proteins within a cell occupies 15-35% of the cell volume, which is the maximum compatible with cell function. Therefore it was

stated, that it is evolutionary preferable to minimize the pathway fluxes for minimal total protein level [132]. In the present study, it is dealt with expression levels of genes and not directly with protein levels. Hence, it cannot be totally excluded that post-transcriptional events prevent translation to the active genes but it is assumed that transcriptional levels in some way reflect the protein amount. Further, it also seems that the amount of enzymes is negligible in comparison to the huge amount of structural proteins during development. Especially during differentiation, it might be evolutionary preferable to react punctual and fast to stimuli. In the presence of heavy protein synthesis for matrix remodeling, this goal can be best achieved by maintaining the lion's share of the enzymatic networks, and by transcriptionally regulating only hotspots.

In-depth analysis of metabolic networks, which are involved in fat cell differentiation and the effects of ATGL deficiency, exposed that two mechanisms of transcriptional regulation coexist. On the one hand, whole pathway segments can be co-regulated (e.g. cholesterol metabolism, oxidative phosphorylation). On the other hand, rate-determining enzymes are selectively regulated. First this principle was observed in the case of adipogenesis. 27 metabolic pathways out of 36 were regulated at key points mainly the rate-limiting steps. Knocking out the rate-limiting protein ATGL resulted itself in transcriptional regulation of 31 rate-limiting metabolic enzymes (31%). If the co-expressed pathway of electron transport and oxidative phosphorylation is subtracted, the amount of strongly regulated enzymes rises even to 39% (29 of 74). Furthermore, five developmental expression studies were investigated. The experiments were carried out on different microarray platforms and the set of significantly relevant genes was determined with different methods. This selection minimizes biases by technologies and post-processing. Approximately, one third of the transcriptionally regulated enzymes are assigned to be rate-limiting. Considering that still unknown rate-limiting enzymes exist, the huge number substantiates, that selective regulation is an additional mechanism to efficiently control metabolic networks on the transcriptional level.

In summary, this doctoral thesis provides for the first time an exhaustive and reliable selection of known rate-limiting proteins. Many oxidoreductases and transferases are found in this selection. Absence of the rate-determining ATGL results in deregulation of those rate-

limiting hot spots in metabolic networks. In addition to regulation of whole pathway, the selective transcriptional regulation of rate-limiting enzymes is a valid mechanism in the control of metabolic networks.

4. Methods

4.1. Fat cell development

Nearly all methods regarding the fat cell development are available in appendix B-1 [2]. This include for example: cell culture experiments, labeling and hybridization, data preprocessing, data normalization, clustering, gene ontology classification, *de novo* annotation and promoter analysis. Please consult, therefore, the integral publication of the doctoral thesis.

EST mapping to genes and proteins

For each of the 23,311 expressed sequence tags (EST) (represent 27,645 spots) of the IGB mousechip, it was attempted to find the corresponding protein sequence. Megablast [133] searches (word length w=70, percent identity p=95%) against nucleotide databases (in the succession of RefSeq [134,135], FANTOM [136], Ensemble, UniGene [137] and Trest until a gene hit was found) were carried out. For the ESTs still remaining without gene assignment, discontigous megablast (word length w=11, percent identity p=95%) with the same succession as Megablast was performed. Blastx against the international protein index (IPI) was conducted with the remaining ESTs. If an EST was still left unassigned, the whole procedure was repeated with blastn [138]. In addition, a blastn (e-value cutoff e=1-9) search against the ENSEMBL mouse genome [139] was performed and ESTs with long stretches (>100 bp) of unspecified nucleotides (N) were excluded.

De novo annotation of the mapped proteins

The protein sequences of the first best hits in the mapping procedure have been annotated *de novo* with academic prediction tools that are integrated in the ANNOTATOR, a novel protein sequence analysis system [140]: Compositional bias (SAPS [141], Xnu, Cast [142]),

low complexity regions (SEG [143]), known sequence domains (Pfam [144], SMART [145], Prosite [146] and Prosite pattern [147] with HMMER (not Pfam), RPS-BLAST [148], IMPALA [149], PROSITE-Profile [150]), Transmembrane domains (HMMTOP 2.0 [151], TOPPRED [152], DAS-TMfilter [153], SAPS [154]), secondary structures (impCOIL written by Frank Eisenhaber following [155], Predator [156], SSCP [157,158]), targeting signals (SIGCLEAVE [159], SignalP-3.0 [160], PTS1 [161]), posttranslational modifications (big-PI [162], NMT [163], Prenylation) and a series of small sequence motifs (ELM, Prosite patterns [164], BioMotif-IMPlibrary), homology searches with NCBI blast [138].

Construction of an EST annotation database

The statistical parameters and the alignment of all ESTs (not only the first best hit) mapped to the sequences in the different databases were parsed from result files formatted as xml blast results. Nucleotide genbank XML files were parsed for RefSeq id, definition, gene identifier, organism, chromosome, chromosome map position, official gene abbreviation, synonyms, Entrey Gene is, mouse genome informatics id, gene onthology terms, product name, product information (definition, RefSeq, gi, length) and base pairs of open reading frame. All parsed information and the IMP annotator uniform resource names (URN) of the annotated proteins are stored in a relational PostGre database [165] which consists of the tables: alignment, annotator, est, gb_nucleotide and map_method. Parsing, database management system and user interface were implemented in the programming language Perl. The protein annotation data remains in the IMP ANNOTATOR and is linked by a specific URN.

4.2. Transcriptional regulation of rate-limiting enzymes

Compiling an accurate and comprehensive list of rate-limiting proteins

Rate-limiting enzymes of high quality were extracted from the curated database OMIM[119], the gene-centric hub GeneCard [73,74] and the enzyme database BRENDA [120,121] with the key word "rate-limiting" and "rate-determining". For a comprehensive data set, Pubmed was searched for the key word "rate-limitation". More than 15,000 entries were hand-curated on basis of the abstract. The rate limitation was addressed for a pathway or a macromolecular process. Entries were neglected in which a rate-limiting process of the enzyme mechanism itself was described. Entrez Gene was used to address the diffuse name space (synonyms).

Functional analysis of rate-limiting proteins

A set without isoenzymes was constructed to minimize different biases for functional distribution analysis. The rate-limiting proteins were subjected to blastp with conservative parameters (e-value = 1e-50, percent identity = 95%) to obtain only the identical protein in KEGG [122]. The EC distribution was based on the first digit, which corresponds to the six major enzyme classes. The detailed function analysis was carried out with the IMP ANNOTATOR suite [80]. Only HMMER (e-value cutoff = 0.01) with the Pfam library was used [166]. The integrated histogram was remodeled to count only the protein occurrences and not the Pfam hit incidences.

Position of rate-limiting proteins in the enzymatic network

The position in the enzymatic networks was analyzed with PathwayMapper [167] using the KEGG pathways. The whole set of literature based rate-limiting enzymes was used and mapped over the the RefSeq IDs.

ATGL knockout network analysis

Normalized gene expression data of a >27,000 EST mouse chip was provided by Montserrat Pinent Armengol, Hubert Hackl and Juliane Strauss (IGB, TU Graz) (publication in preparation). At least 2-fold up- or down-regulation compared to the wild type reference was needed to be considered as significantly regulated. The disturbances of the ATGL knockout mouse were analyzed with the IGB mousechip database (see above) which stores mapping information, and links to sequence architecture und valuable 3rd party resources.

Transcriptional regulation of rate-limiting proteins during differentiation

Datasets of significantly regulated genes (defined by the authors of the regarding study) from different developmental processes were analyzed: Fat cell differentiation (3T3-L1 cell line, >27,000 EST mouse chip, 2-fold change in at least 4 time points) [2]; Fat cell differentiation (MEF cell lines, >27,000 EST mouse chip 2-fold change in at least 4 time points) (unpublished data); Development of skeletal muscle (C2C12, Affymetrix mouse MG_U74Av2 and MG_U74Cv2 arrays, 2-fold change) [125]; Bile ductular differentiation (HBC-3; 27,400 EST mouse chip, Significance Analysis for Microarray [126]); Smooth muscle cell (A404 cells, Agilent G4120A Microarray, Significance analysis of microarrays) [127]. Only enzymes defined by metabolic KEGG pathways were further considered. The official gene symbols (one symbol includes all splice variants) were compared to the full comprehensive rate-limiting list of this study.

5. Bibliography

Reference List

1. Guilbert JJ: **The world health report 2.** *Educ Health (Abingdon)* 2003, **16:**230.

2. Hackl H, Burkard TR, Sturn A, Rubio R, Schleiffer A, Tian S, Quackenbush J, Eisenhaber F, Trajanoski Z: **Molecular processes during fat cell development revealed by gene expression profiling and functional annotation.** *Genome Biol* 2005, **6:**R108.

3. TODARO GJ, GREEN H: **Quantitative studies of the growth of mouse embryo cells in culture and their development into established lines.** *J Cell Biol* 1963, **17:**299-313.

4. GREEN H, Kehinde O: **Sublines of Mouse 3T3 Cells That Accumulate Lipid.** *Cell* 1974, **1:**113-116.

5. Soukas A, Socci ND, Saatkamp BD, Novelli S, Friedman JM: **Distinct transcriptional profiles of adipogenesis in vivo and in vitro.** *J Biol Chem* 2001, **276:**34167-34174.

6. Ross SE, Erickson RL, Gerin I, DeRose PM, Bajnok L, Longo KA, Misek DE, Kuick R, Hanash SM, Atkins KB et al.: **Microarray analyses during adipogenesis: understanding the effects of Wnt signaling on adipogenesis and the roles of liver X receptor alpha in adipocyte metabolism.** *Mol Cell Biol* 2002, **22:**5989-5999.

7. Burton GR, Guan Y, Nagarajan R, McGehee RE: **Microarray analysis of gene expression during early adipocyte differentiation.** *Gene* 2002, **293:**21-31.

8. Burton GR, McGehee REJ: **Identification of candidate genes involved in the regulation of adipocyte differentiation using microarray-based gene expression profiling.** *Nutrition* 2004, **20:**109-114.

9. Burton GR, Nagarajan R, Peterson CA, McGehee REJ: **Microarray analysis of differentiation-specific gene expression during 3T3-L1 adipogenesis.** *Gene* 2004, **329:**167-185.

10. Jessen BA, Stevens GJ: **Expression profiling during adipocyte differentiation of 3T3-L1 fibroblasts.** *Gene* 2002, **299:**95-100.

11. Gerhold DL, Liu F, Jiang G, Li Z, Xu J, Lu M, Sachs JR, Bagchi A, Fridman A, Holder DJ et al.: **Gene expression profile of adipocyte differentiation and its regulation by peroxisome proliferator-activated receptor-gamma agonists.** *Endocrinology* 2002, **143:**2106-2118.

12. Guo X, Liao K: **Analysis of gene expression profile during 3T3-L1 preadipocyte differentiation.** *Gene* 2000, **251:**45-53.

13. Ko MS, Kitchen JR, Wang X, Threat TA, Wang X, Hasegawa A, Sun T, Grahovac MJ, Kargul GJ, Lim MK et al.: **Large-scale cDNA analysis reveals phased gene expression patterns during preimplantation mouse development.** *Development* 2000, **127:**1737-1749.

14. Soukas A, Socci ND, Saatkamp BD, Novelli S, Friedman JM: **Distinct transcriptional profiles of adipogenesis in vivo and in vitro.** *J Biol Chem* 2001, **276:**34167-34174.

15. Macdougald OA, Lane MD: **Transcriptional regulation of gene expression during adipocyte differentiation.** *Annu Rev Biochem* 1995, **64:**345-373.

16. Wise LS, GREEN H: **Studies of lipoprotein lipase during the adipose conversion of 3T3 cells.** *Cell* 1978, **13:**233-242.

17. Hiragun A, Sato M, Mitsui H: **Establishment of a clonal cell line that differentiates into adipose cells in vitro.** *In Vitro* 1980, **16:**685-693.

18. Rubin CS, Hirsch A, Fung C, Rosen OM: **Development of hormone receptors and hormonal responsiveness in vitro. Insulin receptors and insulin sensitivity in the preadipocyte and adipocyte forms of 3T3-L1 cells.** *J Biol Chem* 1978, **253:**7570-7578.

19. Kuri-Harcuch W, GREEN H: **Adipose conversion of 3T3 cells depends on a serum factor.** *Proc Natl Acad Sci U S A* 1978, **75:**6107-6109.

20. Bjorntorp P, Karlsson M, Gustafsson L, Smith U, Sjostrom L, Cigolini M, Storck G, Pettersson P: **Quantitation of different cells in the epididymal fat pad of the rat.** *J Lipid Res* 1979, **20:**97-106.

21. Gregoire FM, Smas CM, Sul HS: **Understanding adipocyte differentiation.** *Physiol Rev* 1998, **78:**783-809.

22. Moustaid N, Sul HS: **Regulation of expression of the fatty acid synthase gene in 3T3-L1 cells by differentiation and triiodothyronine.** *J Biol Chem* 1991, **266:**18550-18554.

23. Wilkison WO, Min HY, Claffey KP, Satterberg BL, Spiegelman BM: **Control of the adipsin gene in adipocyte differentiation. Identification of distinct nuclear factors binding to single- and double-stranded DNA.** *J Biol Chem* 1990, **265:**477-482.

24. Larkin JE, Frank BC, Gaspard RM, Duka I, Gavras H, Quackenbush J: **Cardiac transcriptional response to acute and chronic angiotensin II treatments.** *Physiol Genomics* 2004, **18:**152-166.

25. Tanaka TS, Jaradat SA, Lim MK, Kargul GJ, Wang X, Grahovac MJ, Pantano S, Sano Y, Piao Y, Nagaraja R et al.: **Genome-wide expression profiling of mid-gestation placenta and embryo using a 15,000 mouse developmental cDNA microarray.** *Proc Natl Acad Sci U S A* 2000, **97:**9127-9132.

26. Richter A, Schwager C, Hentze S, Ansorge W, Hentze MW, Muckenthaler M: **Comparison of fluorescent tag DNA labeling methods used for expression analysis by DNA microarrays.** *Biotechniques* 2002, **33:**620-8, 630.

27. Bork P, Dandekar T, Diaz-Lazcoz Y, Eisenhaber F, Huynen M, Yuan Y: **Predicting function: from genes to genomes and back.** *J Mol Biol* 1998, **283:**707-725.

28. Zhang Z, Schwartz S, Wagner L, Miller W: **A greedy algorithm for aligning DNA sequences.** *J Comput Biol* 2000, **7:**203-14.

29. Pruitt KD, Katz KS, Sicotte H, Maglott DR: **Introducing RefSeq and LocusLink: curated human genome resources at the NCBI.** *Trends Genet* 2000, **16:**44-47.

30. Pruitt KD, Tatusova T, Maglott DR: **NCBI Reference Sequence (RefSeq): a curated non-redundant sequence database of genomes, transcripts and proteins.** *Nucleic Acids Res* 2005, **33 Database Issue:**D501-D504.

31. Okazaki Y, Furuno M, Kasukawa T, Adachi J, Bono H, Kondo S, Nikaido I, Osato N, Saito R, Suzuki H et al.: **Analysis of the mouse transcriptome based on functional annotation of 60,770 full-length cDNAs.** *Nature* 2002, **420:**563-573.

32. Schuler GD: **Pieces of the puzzle: expressed sequence tags and the catalog of human genes.** *J Mol Med* 1997, **75:**694-698.

33. Quackenbush J, Liang F, Holt I, Pertea G, Upton J: **The TIGR gene indices: reconstruction and representation of expressed gene sequences.** *Nucleic Acids Res* 2000, **28:**141-145.

34. Altschul SF, Gish W, Miller W, Myers EW, Lipman DJ: **Basic local alignment search tool.** *J Mol Biol* 1990, **215:**403-10.

35. Ashburner M, Ball CA, Blake JA, Botstein D, Butler H, Cherry JM, Davis AP, Dolinski K, Dwight SS, Eppig JT et al.: **Gene ontology: tool for the unification of biology. The Gene Ontology Consortium.** *Nat Genet* 2000, **25:**25-29.

36. Sturn A, Quackenbush J, Trajanoski Z: **Genesis: cluster analysis of microarray data.** *Bioinformatics* 2002, **18:**207-208.

37. Gilks WR, Audit B, De Angelis D, Tsoka S, Ouzounis CA: **Modeling the percolation of annotation errors in a database of protein sequences.** *Bioinformatics* 2002, **18:**1641-1649.

38. Wootton JC, Federhen S: **Analysis of compositionally biased regions in sequence databases.** *Methods Enzymol* 1996, **266:**554-71.

39. Brendel V, Bucher P, Nourbakhsh IR, Blaisdell BE, Karlin S: **Methods and algorithms for statistical analysis of protein sequences.** *Proc Natl Acad Sci U S A* 1992, **89:**2002-6.

40. Promponas VJ, Enright AJ, Tsoka S, Kreil DP, Leroy C, Hamodrakas S, Sander C, Ouzounis CA: **CAST: an iterative algorithm for the complexity analysis of sequence tracts. Complexity analysis of sequence tracts.** *Bioinformatics* 2000, **16:**915-22.

41. Linding R, Russell RB, Neduva V, Gibson TJ: **GlobPlot: Exploring protein sequences for globularity and disorder.** *Nucleic Acids Res* 2003, **31:**3701-8.

42. Bendtsen JD, Nielsen H, von Heijne G, Brunak S: **Improved prediction of signal peptides: SignalP 3.0.** *J Mol Biol* 2004, **340:**783-95.

43. von Heijne G: **A new method for predicting signal sequence cleavage sites.** *Nucleic Acids Res* 1986, **14:**4683-90.

44. Neuberger G, Kunze M, Eisenhaber F, Berger J, Hartig A, Brocard C: **Hidden localization motifs: naturally occurring peroxisomal targeting signals in non-peroxisomal proteins.** *Genome Biol* 2004, **5:**R97.

45. Neuberger G, Maurer-Stroh S, Eisenhaber B, Hartig A, Eisenhaber F: **Prediction of peroxisomal targeting signal 1 containing proteins from amino acid sequence.** *J Mol Biol* 2003, **328:**581-592.

46. Neuberger G, Maurer-Stroh S, Eisenhaber B, Hartig A, Eisenhaber F: **Motif refinement of the peroxisomal targeting signal 1 and evaluation of taxon-specific differences.** *J Mol Biol* 2003, **328:**567-579.

47. Eisenhaber B, Bork P, Eisenhaber F: **Prediction of potential GPI-modification sites in proprotein sequences.** *J Mol Biol* 1999, **292:**741-58.

48. Eisenhaber B, Wildpaner M, Schultz CJ, Borner GH, Dupree P, Eisenhaber F: **Glycosylphosphatidylinositol lipid anchoring of plant proteins. Sensitive prediction from sequence- and genome-wide studies for Arabidopsis and rice.** *Plant Physiol* 2003, **133:**1691-1701.

49. Eisenhaber B, Schneider G, Wildpaner M, Eisenhaber F: **A sensitive predictor for potential GPI lipid modification sites in fungal protein sequences and its application to genome-wide studies for Aspergillus nidulans, Candida albicans, Neurospora crassa, Saccharomyces cerevisiae and Schizosaccharomyces pombe.** *J Mol Biol* 2004, **337:**243-253.

50. Maurer-Stroh S, Eisenhaber B, Eisenhaber F: **N-terminal N-myristoylation of proteins: prediction of substrate proteins from amino acid sequence.** *J Mol Biol* 2002, **317:**541-57.

51. Maurer-Stroh S, Eisenhaber F: **Refinement and prediction of protein prenylation motifs.** *Genome Biology* 2005, **6:**R55.

52. Tusnady GE, Simon I: **Principles governing amino acid composition of integral membrane proteins: application to topology prediction.** *J Mol Biol* 1998, **283:**489-506.

53. Cserzo M, Eisenhaber F, Eisenhaber B, Simon I: **On filtering false positive transmembrane protein predictions.** *Protein Eng* 2002, **15:**745-52.

54. Lupas A, Van Dyke M, Stock J: **Predicting coiled coils from protein sequences.** *Science* 1991, **252:**1162-4.

55. Eisenhaber F, Imperiale F, Argos P, Frommel C: **Prediction of secondary structural content of proteins from their amino acid composition alone. I. New analytic vector decomposition methods.** *Proteins* 1996, **25:**157-68.

56. Eisenhaber F, Frommel C, Argos P: **Prediction of secondary structural content of proteins from their amino acid composition alone. II. The paradox with secondary structural class.** *Proteins* 1996, **25:**169-79.

57. Frishman D, Argos P: **Incorporation of non-local interactions in protein secondary structure prediction from the amino acid sequence.** *Protein Eng* 1996, **9:**133-42.

58. Letunic I, Copley RR, Schmidt S, Ciccarelli FD, Doerks T, Schultz J, Ponting CP, Bork P: **SMART 4.0: towards genomic data integration.** *Nucleic Acids Res* 2004, **32 Database issue:**142-4.

59. Marchler-Bauer A, Panchenko AR, Shoemaker BA, Thiessen PA, Geer LY, Bryant SH: **CDD: a database of conserved domain alignments with links to domain three-dimensional structure.** *Nucleic Acids Res* 2002, **30:**281-3.

60. Schaffer AA, Wolf YI, Ponting CP, Koonin EV, Aravind L, Altschul SF: **IMPALA: matching a protein sequence against a collection of PSI-BLAST-constructed position-specific score matrices.** *Bioinformatics* 1999, **15:**1000-11.

61. Sigrist CJ, Cerutti L, Hulo N, Gattiker A, Falquet L, Pagni M, Bairoch A, Bucher P: **PROSITE: a documented database using patterns and profiles as motif descriptors.** *Brief Bioinform* 2002, **3:**265-74.

62. Schaffer AA, Aravind L, Madden TL, Shavirin S, Spouge JL, Wolf YI, Koonin EV, Altschul SF: **Improving the accuracy of PSI-BLAST protein database searches with composition-based statistics and other refinements.** *Nucleic Acids Res* 2001, **29:**2994-3005.

63. Altschul SF, Koonin EV: **Iterated profile searches with PSI-BLAST--a tool for discovery in protein databases.** *Trends Biochem Sci* 1998, **23:**444-447.

64. Altschul SF, Madden TL, Schaffer AA, Zhang J, Zhang Z, Miller W, Lipman DJ: **Gapped BLAST and PSI-BLAST: a new generation of protein database search programs.** *Nucleic Acids Res* 1997, **25:**3389-3402.

65. Wistrand M, Sonnhammer EL: **Improved profile HMM performance by assessment of critical algorithmic features in SAM and HMMER.** *BMC Bioinformatics* 2005, **6:**99.

66. Wistrand M, Sonnhammer EL: **Improving profile HMM discrimination by adapting transition probabilities.** *J Mol Biol* 2004, **338:**847-854.

67. Burkard TR: *Gene expression analysis of 3T3-L1 cell lines during differentiation.* 2003.

68. Brown GC: **Total cell protein concentration as an evolutionary constraint on the metabolic control distribution in cells.** *J Theor Biol* 1991, **153:**195-203.

69. **IUPAC Compendium of Chemical Terminology, Electronic version, http://goldbook.iupac.org/R05140.html.** 2007.

70. Maglott D, Ostell J, Pruitt KD, Tatusova T: **Entrez Gene: gene-centered information at NCBI.** *Nucleic Acids Res* 2005, **33:**D54-D58.

71. Maglott D, Ostell J, Pruitt KD, Tatusova T: **Entrez Gene: gene-centered information at NCBI.** *Nucleic Acids Res* 2007, **35:**D26-D31.

72. Eppig JT, Bult CJ, Kadin JA, Richardson JE, Blake JA, Anagnostopoulos A, Baldarelli RM, Baya M, Beal JS, Bello SM et al.: **The Mouse Genome Database (MGD): from genes to mice--a community resource for mouse biology.** *Nucleic Acids Res* 2005, **33:**D471-D475.

73. Rebhan M, Chalifa-Caspi V, Prilusky J, Lancet D: **GeneCards: a novel functional genomics compendium with automated data mining and query reformulation support.** *Bioinformatics* 1998, **14:**656-664.

74. Rebhan M, Chalifa-Caspi V, Prilusky J, Lancet D: **GeneCards: integrating information about genes, proteins and diseases.** *Trends Genet* 1997, **13:**163.

75. Bairoch A, Boeckmann B, Ferro S, Gasteiger E: **Swiss-Prot: juggling between evolution and stability.** *Brief Bioinform* 2004, **5:**39-55.

76. Su AI, Cooke MP, Ching KA, Hakak Y, Walker JR, Wiltshire T, Orth AP, Vega RG, Sapinoso LM, Moqrich A et al.: **Large-scale analysis of the human and mouse transcriptomes.** *Proc Natl Acad Sci U S A* 2002, **99:**4465-4470.

77. Edgar R, Domrachev M, Lash AE: **Gene Expression Omnibus: NCBI gene expression and hybridization array data repository.** *Nucleic Acids Res* 2002, **30:**207-210.

78. Barrett T, Troup DB, Wilhite SE, Ledoux P, Rudnev D, Evangelista C, Kim IF, Soboleva A, Tomashevsky M, Edgar R: **NCBI GEO: mining tens of millions of expression profiles--database and tools update.** *Nucleic Acids Res* 2007, **35:**D760-D765.

79. Shmueli O, Horn-Saban S, Chalifa-Caspi V, Shmoish M, Ophir R, Benjamin-Rodrig H, Safran M, Domany E, Lancet D: **GeneNote: whole genome expression profiles in normal human tissues.** *C R Biol* 2003, **326:**1067-1072.

80. Schneider G, Wildpaner M, Kozlovszky M, Kubina W, Leitner F, Novatchkova M, Schleiffer A, Sun T, Eisenhaber F: **The ANNOTATOR software suite [abstract].** *[http://www iscb org/ismb2005/demos/15 pdf]* 2005,

81. Su AI, Wiltshire T, Batalov S, Lapp H, Ching KA, Block D, Zhang J, Soden R, Hayakawa M, Kreiman G: **A gene atlas of the mouse and human protein-encoding transcriptomes.** *Proc Natl Acad Sci U S A* 2004, **101:**6062-6067.

82. Soukas A, Socci ND, Saatkamp BD, Novelli S, Friedman JM: **Distinct transcriptional profiles of adipogenesis in vivo and in vitro.** *J Biol Chem* 2001, **276:**34167-34174.

83. Soukas A, Socci ND, Saatkamp BD, Novelli S, Friedman JM: **Distinct transcriptional profiles of adipogenesis in vivo and in vitro.** *J Biol Chem* 2001, **276:**34167-34174.

84. Zimmermann R, Strauss JG, Haemmerle G, Schoiswohl G, Birner-Gruenberger R, Riederer M, Lass A, Neuberger G, Eisenhaber F, Hermetter A et al.: **Fat mobilization in adipose tissue is promoted by adipose triglyceride lipase.** *Science* 2004, **306:**1383-1386.

85. Fukuhara A, Matsuda M, Nishizawa M, Segawa K, Tanaka M, Kishimoto K, Matsuki Y, Murakami M, Ichisaka T, Murakami H: **Visfatin: a protein secreted by visceral fat that mimics the effects of insulin.** *Science* 2005, **307:**426-430.

86. Kitani T, Okuno S, Fujisawa H: **Growth phase-dependent changes in the subcellular localization of pre-B-cell colony-enhancing factor.** *FEBS Lett* 2003, **544:**74-78.

87. Revollo JR, Grimm AA, Imai S: **The NAD biosynthesis pathway mediated by nicotinamide phosphoribosyltransferase regulates Sir2 activity in mammalian cells.** *J Biol Chem* 2004, **279:**50754-50763.

88. Jessen BA, Stevens GJ: **Expression profiling during adipocyte differentiation of 3T3-L1 fibroblasts.** *Gene* 2002, **299:**95-100.

89. Oishi Y, Manabe I, Tobe K, Tsushima K, Shindo T, Fujiu K, Nishimura G, Maemura K, Yamauchi T, Kubota N et al.: **Kruppel-like transcription factor KLF5 is a key regulator of adipocyte differentiation.** *Cell Metab* 2005, **1:**27-39.

90. Tang QQ, Otto TC, Lane MD: **Mitotic clonal expansion: A synchronous process required for adipogenesis.** *Proc Natl Acad Sci U S A* 2003, **100:**44-49.

91. Yabuta N, Kajimura N, Mayanagi K, Sato M, Gotow T, Uchiyama Y, Ishimi Y, Nojima H: **Mammalian Mcm2/4/6/7 complex forms a toroidal structure.** *Genes Cells* 2003, **8:**413-421.

92. Li X, Rosenfeld MG: **Transcription: origins of licensing control.** *Nature* 2004, **427:**687-688.

93. Vassin VM, Wold MS, Borowiec JA: **Replication protein A (RPA) phosphorylation prevents RPA association with replication centers.** *Mol Cell Biol* 2004, **24:**1930-1943.

94. Kim HS, Brill SJ: **Rfc4 interacts with Rpa1 and is required for both DNA replication and DNA damage checkpoints in Saccharomyces cerevisiae.** *Mol Cell Biol* 2001, **21:**3725-3737.

95. Larsen E, Gran C, Saether BE, Seeberg E, Klungland A: **Proliferation failure and gamma radiation sensitivity of Fen1 null mutant mice at the blastocyst stage.** *Mol Cell Biol* 2003, **23:**5346-5353.

96. Waga S, Bauer G, Stillman B: **Reconstitution of complete SV40 DNA replication with purified replication factors.** *J Biol Chem* 1994, **269:**10923-10934.

97. Stark JM, Hu P, Pierce AJ, Moynahan ME, Ellis N, Jasin M: **ATP hydrolysis by mammalian RAD51 has a key role during homology-directed DNA repair.** *J Biol Chem* 2002, **277:**20185-20194.

98. Kunitoku N, Sasayama T, Marumoto T, Zhang D, Honda S, Kobayashi O, Hatakeyama K, Ushio Y, Saya H, Hirota T: **CENP-A phosphorylation by Aurora-A in prophase is required for enrichment of Aurora-B at inner centromeres and for kinetochore function.** *Dev Cell* 2003, **5:**853-864.

99. Weis K: **Regulating access to the genome: nucleocytoplasmic transport throughout the cell cycle.** *Cell* 2003, **112:**441-451.

100. Trieselmann N, Armstrong S, Rauw J, Wilde A: **Ran modulates spindle assembly by regulating a subset of TPX2 and Kid activities including Aurora A activation.** *J Cell Sci* 2003, **116:**4791-4798.

101. Hirota T, Kunitoku N, Sasayama T, Marumoto T, Zhang D, Nitta M, Hatakeyama K, Saya H: **Aurora-A and an interacting activator, the LIM protein Ajuba, are required for mitotic commitment in human cells.** *Cell* 2003, **114:**585-598.

102. Wansa KD, Harris JM, Muscat GE: **The activation function-1 domain of Nur77/NR4A1 mediates trans-activation, cell specificity, and coactivator recruitment.** *J Biol Chem* 2002, **277:**33001-33011.

103. Lupas A: **Predicting coiled-coil regions in proteins.** *Curr Opin Struct Biol* 1997, **7:**388-393.

104. Aoki K, Sun YJ, Aoki S, Wada K, Wada E: **Cloning, expression, and mapping of a gene that is upregulated in adipose tissue of mice deficient in bombesin receptor subtype-3.** *Biochem Biophys Res Commun* 2002, **290:**1282-1288.

105. King T, Bland Y, Webb S, Barton S, Brown NA: **Expression of Peg1 (Mest) in the developing mouse heart: involvement in trabeculation.** *Dev Dyn* 2002, **225:**212-215.

106. Kamei Y, Suganami T, Kohda T, Ishino F, Yasuda K, Miura S, Ezaki O, Ogawa Y: **Peg1/Mest in obese adipose tissue is expressed from the paternal allele in an isoform-specific manner.** *FEBS Lett* 2007, **581:**91-96.

107. Takahashi M, Kamei Y, Ezaki O: **Mest/Peg1 imprinted gene enlarges adipocytes and is a marker of adipocyte size.** *Am J Physiol Endocrinol Metab* 2005, **288:**E117-E124.

108. Pogge vS, Senkel S, Ryffel GU: **ERH (enhancer of rudimentary homologue), a conserved factor identical between frog and human, is a transcriptional repressor.** *Biol Chem* 2001, **382:**1379-1385.

109. Scott JE: **Proteodermatan and proteokeratan sulfate (decorin, lumican/fibromodulin) proteins are horseshoe shaped. Implications for their interactions with collagen.** *Biochemistry* 1996, **35:**8795-8799.

110. Hildebrand A, Romaris M, Rasmussen LM, Heinegard D, Twardzik DR, Border WA, Ruoslahti E: **Interaction of the small interstitial proteoglycans biglycan, decorin and fibromodulin with transforming growth factor beta.** *Biochem J* 1994, **302 (Pt 2):**527-534.

111. Riquelme C, Larrain J, Schonherr E, Henriquez JP, Kresse H, Brandan E: **Antisense inhibition of decorin expression in myoblasts decreases cell responsiveness to transforming growth factor beta and accelerates skeletal muscle differentiation.** *J Biol Chem* 2001, **276:**3589-3596.

112. Comalada M, Cardo M, Xaus J, Valledor AF, Lloberas J, Ventura F, Celada A: **Decorin reverses the repressive effect of autocrine-produced TGF-beta on mouse macrophage activation.** *J Immunol* 2003, **170:**4450-4456.

113. Gurniak CB, Berg LJ: **A new member of the Eph family of receptors that lacks protein tyrosine kinase activity.** *Oncogene* 1996, **13:**777-786.

114. Luo H, Yu G, Tremblay J, Wu J: **EphB6-null mutation results in compromised T cell function.** *J Clin Invest* 2004, **114:**1762-1773.

115. Boudeau J, Miranda-Saavedra D, Barton GJ, Alessi DR: **Emerging roles of pseudokinases.** *Trends Cell Biol* 2006, **16:**443-452.

116. Hafner C, Schmitz G, Meyer S, Bataille F, Hau P, Langmann T, Dietmaier W, Landthaler M, Vogt T: **Differential gene expression of Eph receptors and ephrins in benign human tissues and cancers.** *Clin Chem* 2004, **50:**490-499.

117. Kim JB, Spotts GD, Halvorsen YD, Shih HM, Ellenberger T, Towle HC, Spiegelman BM: **Dual DNA binding specificity of ADD1/SREBP1 controlled by a single amino acid in the basic helix-loop-helix domain.** *Mol Cell Biol* 1995, **15:**2582-2588.

118. Klipp E, Heinrich R, Holzhutter HG: **Prediction of temporal gene expression. Metabolic opimization by re-distribution of enzyme activities.** *Eur J Biochem* 2002, **269:**5406-5413.

119. McKusick VA: **Mendelian Inheritance in Man and Its Online Version, OMIM.** *Am J Hum Genet* 2007, **80:**588-604.

120. Schomburg I, Chang A, Schomburg D: **BRENDA, enzyme data and metabolic information.** *Nucleic Acids Res* 2002, **30:**47-49.

121. Schomburg I, Chang A, Hofmann O, Ebeling C, Ehrentreich F, Schomburg D: **BRENDA: a resource for enzyme data and metabolic information.** *Trends Biochem Sci* 2002, **27:**54-56.

122. Kanehisa M, Goto S, Hattori M, Aoki-Kinoshita KF, Itoh M, Kawashima S, Katayama T, Araki M, Hirakawa M: **From genomics to chemical genomics: new developments in KEGG.** *Nucleic Acids Res* 2006, **34:**D354-D357.

123. Voet D, Voet JG: *Biochemie.* Weinheim (Germany): VHC Verlagsgesellschaft; 1994.

124. Haemmerle G, Lass A, Zimmermann R, Gorkiewicz G, Meyer C, Rozman J, Heldmaier G, Maier R, Theussl C, Eder S et al.: **Defective lipolysis and altered energy metabolism in mice lacking adipose triglyceride lipase.** *Science* 2006, **312:**734-737.

125. Tomczak KK, Marinescu VD, Ramoni MF, Sanoudou D, Montanaro F, Han M, Kunkel LM, Kohane IS, Beggs AH: **Expression profiling and identification of novel genes involved in myogenic differentiation.** *FASEB J* 2004, **18:**403-405.

126. Ader T, Norel R, Levoci L, Rogler LE: **Transcriptional profiling implicates TGFbeta/BMP and Notch signaling pathways in ductular differentiation of fetal murine hepatoblasts.** *Mech Dev* 2006, **123:**177-194.

127. Spin JM, Nallamshetty S, Tabibiazar R, Ashley EA, King JY, Chen M, Tsao PS, Quertermous T: **Transcriptional profiling of in vitro smooth muscle cell differentiation identifies specific patterns of gene and pathway activation.** *Physiol Genomics* 2004, **19:**292-302.

128. Soukas A, Socci ND, Saatkamp BD, Novelli S, Friedman JM: **Distinct transcriptional profiles of adipogenesis in vivo and in vitro.** *J Biol Chem* 2001, **276:**34167-34174.

129. Soukas A, Socci ND, Saatkamp BD, Novelli S, Friedman JM: **Distinct transcriptional profiles of adipogenesis in vivo and in vitro.** *J Biol Chem* 2001, **276:**34167-34174.

130. Novatchkova M, Eisenhaber F: **Can molecular mechanisms of biological processes be extracted from expression profiles? Case study: endothelial contribution to tumor-induced angiogenesis.** *Bioessays* 2001, **23:**1159-1175.

131. Yokoyama C, Wang X, Briggs MR, Admon A, Wu J, Hua X, Goldstein JL, Brown MS: **SREBP-1, a basic-helix-loop-helix-leucine zipper protein that controls transcription of the low density lipoprotein receptor gene.** *Cell* 1993, **75:**187-197.

132. Brown GC: **Total cell protein concentration as an evolutionary constraint on the metabolic control distribution in cells.** *J Theor Biol* 1991, **153:**195-203.

133. Zhang Z, Schwartz S, Wagner L, Miller W: **A greedy algorithm for aligning DNA sequences.** *J Comput Biol* 2000, **7:**203-214.

134. Pruitt KD, Katz KS, Sicotte H, Maglott DR: **Introducing RefSeq and LocusLink: curated human genome resources at the NCBI.** *Trends Genet* 2000, **16:**44-47.

135. Pruitt KD, Tatusova T, Maglott DR: **NCBI Reference Sequence (RefSeq): a curated non-redundant sequence database of genomes, transcripts and proteins.** *Nucleic Acids Res* 2005, **33 Database Issue:**D501-D504.

136. Okazaki Y, Furuno M, Kasukawa T, Adachi J, Bono H, Kondo S, Nikaido I, Osato N, Saito R, Suzuki H et al.: **Analysis of the mouse transcriptome based on functional annotation of 60,770 full-length cDNAs.** *Nature* 2002, **420:**563-573.

137. Schuler GD: **Pieces of the puzzle: expressed sequence tags and the catalog of human genes.** *J Mol Med* 1997, **75:**694-698.

138. Altschul SF, Gish W, Miller W, Myers EW, Lipman DJ: **Basic local alignment search tool.** *J Mol Biol* 1990, **215:**403-410.

139. Hubbard T, Barker D, Birney E, Cameron G, Chen Y, Clark L, Cox T, Cuff J, Curwen V, Down T et al.: **The Ensembl genome database project.** *Nucleic Acids Res* 2002, **30:**38-41.

140. **Large Scale Sequence Annotation System, Research Institute of Molecular Pathology (IMP), Bioinformatics Group, Vienna** [http://annotator.imp.univie.ac.at/]

141. Brendel V, Bucher P, Nourbakhsh IR, Blaisdell BE, Karlin S: **Methods and algorithms for statistical analysis of protein sequences.** *Proc Natl Acad Sci U S A* 1992, **89:**2002-2006.

142. Promponas VJ, Enright AJ, Tsoka S, Kreil DP, Leroy C, Hamodrakas S, Sander C, Ouzounis CA: **CAST: an iterative algorithm for the complexity analysis of sequence tracts. Complexity analysis of sequence tracts.** *Bioinformatics* 2000, **16:**915-922.

143. Wootton JC, Federhen S: **Analysis of compositionally biased regions in sequence databases.** *Methods Enzymol* 1996, **266:**554-571.

144. Sonnhammer EL, Eddy SR, Birney E, Bateman A, Durbin R: **Pfam: multiple sequence alignments and HMM-profiles of protein domains.** *Nucleic Acids Res* 1998, **26:**320-322.

145. Letunic I, Copley RR, Schmidt S, Ciccarelli FD, Doerks T, Schultz J, Ponting CP, Bork P: **SMART 4.0: towards genomic data integration.** *Nucleic Acids Res* 2004, **32:**D142-D144.

146. Sigrist CJ, Cerutti L, Hulo N, Gattiker A, Falquet L, Pagni M, Bairoch A, Bucher P: **PROSITE: a documented database using patterns and profiles as motif descriptors.** *Brief Bioinform* 2002, **3:**265-274.

147. Sigrist CJ, Cerutti L, Hulo N, Gattiker A, Falquet L, Pagni M, Bairoch A, Bucher P: **PROSITE: a documented database using patterns and profiles as motif descriptors.** *Brief Bioinform* 2002, **3:**265-274.

148. Marchler-Bauer A, Panchenko AR, Shoemaker BA, Thiessen PA, Geer LY, Bryant SH: **CDD: a database of conserved domain alignments with links to domain three-dimensional structure.** *Nucleic Acids Res* 2002, **30:**281-283.

149. Schaffer AA, Wolf YI, Ponting CP, Koonin EV, Aravind L, Altschul SF: **IMPALA: matching a protein sequence against a collection of PSI-BLAST-constructed position-specific score matrices.** *Bioinformatics* 1999, **15:**1000-1011.

150. Sigrist CJ, Cerutti L, Hulo N, Gattiker A, Falquet L, Pagni M, Bairoch A, Bucher P: **PROSITE: a documented database using patterns and profiles as motif descriptors.** *Brief Bioinform* 2002, **3:**265-274.

151. Tusnady GE, Simon I: **Principles governing amino acid composition of integral membrane proteins: application to topology prediction.** *J Mol Biol* 1998, **283:**489-506.

152. von Heijne G: **Membrane protein structure prediction. Hydrophobicity analysis and the positive-inside rule.** *J Mol Biol* 1992, **225:**487-494.

153. Cserzo M, Eisenhaber F, Eisenhaber B, Simon I: **On filtering false positive transmembrane protein predictions.** *Protein Eng* 2002, **15:**745-752.

154. Brendel V, Bucher P, Nourbakhsh IR, Blaisdell BE, Karlin S: **Methods and algorithms for statistical analysis of protein sequences.** *Proc Natl Acad Sci U S A* 1992, **89:**2002-2006.

155. Lupas A, Van Dyke M, Stock J: **Predicting coiled coils from protein sequences.** *Science* 1991, **252:**1162-1164.

156. Frishman D, Argos P: **Incorporation of non-local interactions in protein secondary structure prediction from the amino acid sequence.** *Protein Eng* 1996, **9:**133-142.

157. Eisenhaber F, Imperiale F, Argos P, Frommel C: **Prediction of secondary structural content of proteins from their amino acid composition alone. I. New analytic vector decomposition methods.** *Proteins* 1996, **25:**157-168.

158. Eisenhaber F, Frommel C, Argos P: **Prediction of secondary structural content of proteins from their amino acid composition alone. II. The paradox with secondary structural class.** *Proteins* 1996, **25:**169-179.

159. von Heijne G: **A new method for predicting signal sequence cleavage sites.** *Nucleic Acids Res* 1986, **14:**4683-4690.

160. Bendtsen JD, Nielsen H, von Heijne G, Brunak S: **Improved prediction of signal peptides: SignalP 3.0.** *J Mol Biol* 2004, **340:**783-795.

161. Eisenhaber B, Eisenhaber F, Maurer-Stroh S, Neuberger G: **Prediction of sequence signals for lipid post-translational modifications: insights from case studies.** *Proteomics* 2004, **4:**1614-1625.

162. Eisenhaber B, Bork P, Eisenhaber F: **Prediction of potential GPI-modification sites in proprotein sequences.** *J Mol Biol* 1999, **292:**741-758.

163. Maurer-Stroh S, Eisenhaber B, Eisenhaber F: **N-terminal N-myristoylation of proteins: prediction of substrate proteins from amino acid sequence.** *J Mol Biol* 2002, **317:**541-557.

164. Sigrist CJ, Cerutti L, Hulo N, Gattiker A, Falquet L, Pagni M, Bairoch A, Bucher P: **PROSITE: a documented database using patterns and profiles as motif descriptors.** *Brief Bioinform* 2002, **3:**265-274.

165. **http://www.postgresql.org/.** 2007.

166. Sonnhammer EL, Eddy SR, Birney E, Bateman A, Durbin R: **Pfam: multiple sequence alignments and HMM-profiles of protein domains.** *Nucleic Acids Res* 1998, **26:**320-322.

167. Mlecnik B, Scheideler M, Hackl H, Hartler J, Sanchez-Cabo F, Trajanoski Z: **PathwayExplorer: web service for visualizing high-throughput expression data on biological pathways.** *Nucleic Acids Res* 2005, **33:**W633-W637.

6. Glossary

3T3-L1	A sub-cell line of 3T3
Abhydrolase_3	Alpha/beta hydrolase fold
Acad	Acyl-CoA dehydrogenases
ACP	Anaphase promoting complex
Adfp	Adipose differentiation related protein
adh_short	Short chain dehydrogenase
AKA	Alpha-keto acids
aminotran_1_2	Aminotransferase class I and II
Apex1	Apurinic/apyrimidinic endonuclease 1
ApoD	Apolipoprotein D
ApoE	Apolipoprotein E
ATGL	Adipose triglyceride lipase
Aurka	Aurora A
BAT	Brown adipose tissue
BLAST	Basic Local Alignment Search Tool
BRENDA	BRaunschweig ENzyme Database
Bub1	Budding uninhibited by benzimidazoles 1 homolog (S. cerevisiae)
CAST	Complexity Analysis of Sequence Tracts
CAP	c-Cbl-associated proteins
Ccdc80	Coiled-coil domain containing 80
Cdc20	Cell division cycle 20 homolog (S. cerevisiae)
Cdca1	Cell division cycle associated 1
cDNA	Complementary deoxyribonucleic Acid
Cenpa	Centromere autoantigen A
C/EBP	CCAAT/enhancer binding protein
Chek1	Checkpoint kinases
CoA	Coenzyme A
CPT II	Carnitine palmitoyltransferase II
Cy3/Cy5	Cyanine fluorescence dyes
DAO	FAD dependent oxidoreductase
DBMS	Dtabase management system

Dcn	Decorin
Dhcr7	7-dehydrocholesterol reductase
Dut	Deoxyuridine triphosphatase
EC	Enzymatic commission
Elovl6	ELOVL family member 6, elongation of long chain fatty acids
Ephb6	Ephrin receptor B6
EST	Expressed Sequence Tag
FAD	Flavin adenine dinucleotide
FA_desaturase	Fatty acid desaturase
FANTOM	Functional Annotation of Mouse
Fasn	Fatty acid synthase
Fen1	Flap structure specific endonuclease 1
GNF	Genomics Institute of the Novartis Research Foundation
GO	Gene Ontology
GPI	Glucosylphosphatidylinositol
Hist1h1c	Histone 1, H1C
Hist1h4m	Histone 1, H4M
H2afz	H2A histone family, member Z
HMM	Hidden Markov model
ID	Identification number
IGB	Institute for Genomics and Bioinformatics, TUGraz
IMP	Research Institute of Molecular Pathology, Vienna
IPI	International protein index
IR	Iternal repeats
IUPAC	International Union for Pure and Applied Chemistry
Jub	ajuba
KEGG	Kyoto Encyclopedia of Genes and Genomes
Kif22	Kinase family member 22
Kntc2	Kinetochore associated 2
Kpna2	Karyopherin (importin) alpha 2
Lcat	Lecithin cholesterol acyltransferase
Lig1	Ligase I, DNA, ATP-dependent
LPL	Lipoprotein lipase

LRR	Leucin rich repeats
Mad2l1	MAD2 (mitotic arrest deficient, homolog)-like 1 (yeast)
Mcm	Minichromosome maintainance
MEF	Mouse embryonic fibroblasts
Mer	Enhancer of rudimentary homolog
Mest	mesoderm-specific transcript
MGI	Mouse Genome Informatics
MIM	Mendelian Inheritance in Man
Mod1	malic enzyme, supernatant
NAD	Nicotinamide adenine dinucleotide
NADP	Nicotinamide adenine dinucleotide phosphate
NCBI	National Center for Biotechnology Information
NLS	nuclear localization signal
nr	non-redundant
Nr4a1	Nuclear receptor subfamily 4 group A
OMIM	Online Mendelian Inheritance in Man
p450	Cytochrome P450
PBEF	pre-B cell colony-enhancing factor
Pcna	Proliferating cell nuclear antigen
Pcr1	protein regulator of cytokinesis
Peg1	paternally expressed gene 1
PEX5	Peroxisomal biogenesis factor 5
PPAR	Peroxisome proliferator-activated receptor
Pribosyltran	Phosphoribosyl transferase domain
PSI-BLAST	Position Specific Iterative BLAST
PTS1	Peroxisomal Targeting Sequence 1
Pyr_redox	Pyridine nucleotide-disulphide oxidoreductase
Pyridoxal_dec	Pyridoxal -dependent decarboxylase conserved domain
Rad51	Radiation sensitive 51
Ran	Ras-like, family 2 locus 9
RefSeq	NCBI Reference Sequence
Rfc4	replication factor C 4
Ris2	Retroviral integration site 2

RL	rate-limiting
RNA	Ribonucleic Acid
RPA	Replication protein A
RPS-BLAST	Reverse Position Specific BLAST
RT-PCR	Reverse Transcription Polymerase Chain Reaction
SAM	Significance Analysis for Microarray
SAPS	Statistical Analysis of Protein Sequences
Scd1	stearoyl-CoA desaturase 1
SCOP	Structural Classification of Proteins
Slc2a4	Solute carrier family 2 (facilitated glucose transporter), member 4
Slc2a8	Solute carrier family 2, (facilitated glucose transporter), member 8
Slc5a11	Solute carrier family 5 (sodium/glucose cotransporter), member 11
SMART	Simple Modular Architecture Research Tool
SMC	Smooth muscle cell
SREBP-1	Sterol regulatory element binding protein-1
ssDNA	Single stranded DNA
Suv39h1	Suppressor of variegation 3-9 homolog 1
Tacc3	Transforming acidic coiled-coil containing 3
TG	Triglyceride
TGF-beta	Transforming growth factor, beta
TIGR	The Institute for Genomic Research
Tpx2	Tpx2, microtubule-associated protein homolog
Tuba4	Tubulin, alpha 4
Tubb5	Tubulin, beta 5
Tubb6	Tubulin, beta 6
Tubg1	Tubulin, gamma 1
Uhrf1	Ubiquitine-like, containing PHD and RING finger domains, 1

7. Acknowledgment

This work was supported by GENAU: Bioinformatics Integration Network (BIN) and Genomics of Lipid-Associated Disorders (GOLD), bm:bwk. I would like to express my deepest gratitude to my mentors, Frank Eisenhaber and Zlatko Trajanoski, for their encouragement, vision, and belief in me.

Further thanks go to members of the Eisenhaber Group at the IMP Vienna and to the colleges of the Institute for Genomics and Bioinformatics at the University of Technology Graz for their fruitful discussions, support and friendship. A special thank is owed to all those people who have actively contributed to this work in alphabetical order: Hubert Hackl, Anne-Margarethe Krogsdam, Maria Novatchkova, Montserrat Pinent Armengol, Fátima Sánchez Cabo, Alexander Schleiffer, Georg Schneider, Juliane Strauss and Alexander Sturn. Special thanks goes also to Pidder Jansen-Duerr and the colleagues of the national research network FSP S93, who introduced me to the interesting field of aging and financed part of my studies.

I am indebted to my parents for their unfailing support, and to my wife, Beatrix, for being with me and for her love, encouragement and understanding.

8. Appendix A – Rate-limiting genes in mouse

The following table lists mouse genes/proteins, which are selected from more than 15,000 Pubmed abstracts. Additional information about reliability (e.g. also found in a curated curated database), information sources and sequences are stored in a relational database.

Official gene symbols	Nucleotide and protein RefSeq ID	Official gene name
Gch1	NM_008102.2→NP_032128.1	GTP cyclohydrolase 1
Dck	NM_007832.3→NP_031858.1	Deoxycytidine kinase
Th	NM_009377.1→NP_033403.1	tyrosine hydroxylase
Abca1	NM_013454.3→NP_038482.3	ATP-binding cassette, sub-family A (ABC1), member 1
Acaca	NM_133360.1→NP_579938.1	acetyl-Coenzyme A carboxylase alpha
Cyp27b1	NM_010009.1→NP_034139.1	cytochrome P450, family 27, subfamily b, polypeptide 1
Ren1	NM_031192.2→NP_112469.1	renin 1 structural
Gclc	NM_010295.1→NP_034425.1	glutamate-cysteine ligase, catalytic subunit
Gclm	NM_008129.2→NP_032155.1	glutamate-cysteine ligase , modifier subunit
Cyp11a1	NM_019779.2→NP_062753.2	cytochrome P450, family 11, subfamily a, polypeptide 1
Gsto1	NM_010362.1→NP_034492.1	glutathione S-transferase omega 1
Hmgcr	NM_008255.1→NP_032281.1	3-hydroxy-3-methylglutaryl-Coenzyme A reductase
Hmox1	NM_010442.1→NP_034572.1	heme oxygenase (decycling) 1
Ptgs1	NM_008969.2→NP_032995.1	Prostaglandin-endoperoxide synthase 1
Cyp19a1	NM_007810.1→NP_031836.1	cytochrome P450, family 19, subfamily a, polypeptide 1
Tyr	NM_011661.1→NP_035791.1	Tyrosinase
Tpmt	NM_016785.1→NP_058065.1	thiopurine methyltransferase
Impdh1	NM_011829.2→NP_035959.2	inosine 5'-phosphate dehydrogenase 1
H6pd	NM_173371.2→NP_775547.2	hexose-6-phosphate dehydrogenase (glucose 1-dehydrogenase)
Cpt1a	NM_013495.1→NP_038523.1	carnitine palmitoyltransferase 1a, liver
Cyp7a1	NM_007824.2→NP_031850.2	cytochrome P450, family 7, subfamily a, polypeptide 1
Trpv6	NM_022413.2→NP_071858.2	transient receptor potential cation channel, subfamily V, member 6
Tph1	NM_009414.2→NP_033440.1	tryptophan hydroxylase 1
Pank1	NM_023792.1→NP_076281.1	pantothenate kinase 1
Cps1	XM_129769.8→XP_129769.6	carbamoyl-phosphate synthetase 1
Star	NM_011485.3→NP_035615.2	steroidogenic acute regulatory protein
Aanat	NM_009591.1→NP_033721.1	arylalkylamine N-acetyltransferase

Odc1	NM_013614.1→NP_038642.1	ornithine decarboxylase, structural 1
Pnpla2	NM_025802.1→NP_080078.1	patatin-like phospholipase domain containing 2
Slc5a7	NM_022025.3→NP_071308.2	solute carrier family 5 (choline transporter), member 7
Gulo	NM_178747.2→NP_848862.1	gulonolactone (L-) oxidase
Fads2	NM_019699.1→NP_062673.1	fatty acid desaturase 2
Indo	NM_008324.1→NP_032350.1	indoleamine-pyrrole 2,3 dioxygenase
Tyms	NM_021288.2→NP_067263.1	thymidylate synthase
Bckdha	NM_007533.2→NP_031559.2	branched chain ketoacid dehydrogenase E1, alpha polypeptide
Dbt	NM_010022.1→NP_034152.1	dihydrolipoamide branched chain transacylase E2
Dld	NM_007861.2→NP_031887.2	dihydrolipoamide dehydrogenase
Oxct2a	NM_022033.1→NP_071316.1	3-oxoacid CoA transferase 2A
Pcyt1a	NM_009981.2→NP_034111.1	phosphate cytidylyltransferase 1, choline, alpha isoform
Xylt1	NM_175645.2→NP_783576.1	xylosyltransferase 1
Dpyd	NM_170778.1→NP_740748.1	dihydropyrimidine dehydrogenase
Gne	NM_015828.2→NP_056643.2	glucosamine
Gyk	NM_008194.3→NP_032220.1	glycerol kinase
Smurf1	NM_001038627.1→NP_001033716.1	SMAD specific E3 ubiquitin protein ligase 1
Lpl	NM_008509.1→NP_032535.1	lipoprotein lipase
Rrm1	NM_009103.2→NP_033129.2	ribonucleotide reductase M1
Rrm2	NM_009104.1→NP_033130.1	ribonucleotide reductase M2
Srm	NM_009272.2→NP_033298.1	spermidine synthase
Eif4e	NM_007917.3→NP_031943.3	eukaryotic translation initiation factor 4E
Tert	NM_009354.1→NP_033380.1	telomerase reverse transcriptase
P4ha1	NM_011030.1→NP_035160.1	procollagen-proline, 2-oxoglutarate 4-dioxygenase (proline 4-hydroxylase), alpha 1 polypeptide
Dhodh	NM_020046.3→NP_064430.1	dihydroorotate dehydrogenase
Pck1	NM_011044.1→NP_035174.1	phosphoenolpyruvate carboxykinase 1, cytosolic
Isyna1	NM_023627.1→NP_076116.1	myo-inositol 1-phosphate synthase A1
Pla2g4a	NM_008869.2→NP_032895.1	phospholipase A2, group IVA (cytosolic, calcium-dependent)
Pah	NM_008777.1→NP_032803.1	phenylalanine hydroxylase
Alox5	NM_009662.1→NP_033792.1	arachidonate 5-lipoxygenase
Tdo2	NM_019911.2→NP_064295.2	tryptophan 2,3-dioxygenase
Mat1a	NM_133653.1→NP_598414.1	methionine adenosyltransferase I, alpha
Sat1	NM_009121.3→NP_033147.1	spermidine/spermine N1-acetyl transferase 1
Mme	NM_008604.2→NP_032630.2	membrane metallo endopeptidase
Gfpt1	NM_013528.2→NP_038556.1	glutamine fructose-6-phosphate transaminase 1
Pam	NM_013626.1→NP_038654.1	peptidylglycine alpha-amidating monooxygenase
Lipe	NM_001039507.1→NP_001034596.1	Lipase, hormone sensitive
Bace1	NM_011792.3→NP_035922.3	beta-site APP cleaving enzyme 1
Pfkm	NM_021514.2→NP_067489.2	phosphofructokinase, muscle
Agt	NM_007428.3→NP_031454.3	angiotensinogen (serpin peptidase inhibitor, clade A, member 8)

Ptges	NM_022415.2→NP_071860.1	prostaglandin E synthase
Nos1	NM_008712.1→NP_032738.1	nitric oxide synthase 1, neuronal
Csad	NM_144942.1→NP_659191.1	cysteine sulfinic acid decarboxylase
Scd1	NM_009127.2→NP_033153.2	stearoyl-Coenzyme A desaturase 1
Alas1	NM_020559.1→NP_065584.1	aminolevulinic acid synthase 1
Sptlc1	NM_009269.2→NP_033295.2	serine palmitoyltransferase, long chain base subunit 1
Sptlc2	NM_011479.2→NP_035609.1	serine palmitoyltransferase, long chain base subunit 2
Ddc	NM_016672.2→NP_057881.1	dopa decarboxylase
Apex1	NM_009687.1→NP_033817.1	apurinic/apyrimidinic endonuclease 1
Gys1	NM_030678.2→NP_109603.2	glycogen synthase 1, muscle
Dicer1	NM_148948.1→NP_683750.1	Dicer1, Dcr-1 homolog (Drosophila)
2610203E10Rik	NM_183220.1→NP_899043.1	RIKEN cDNA 2610203E10 gene
Ass1	NM_007494.2→NP_031520.1	argininosuccinate synthetase 1
Akr1b3	NM_009658.2→NP_033788.2	aldo-keto reductase family 1, member B3 (aldose reductase)
Cyp1a2	NM_009993.2→NP_034123.1	cytochrome P450, family 1, subfamily a, polypeptide 2
Scnn1a	NM_011324.1→NP_035454.1	sodium channel, nonvoltage-gated, type I, alpha
Cs	NM_026444.2→NP_080720.1	citrate synthase
Gad1	NM_008077.3→NP_032103.2	glutamic acid decarboxylase 1
Ogdh	NM_010956.3→NP_035086.2	oxoglutarate dehydrogenase (lipoamide)
Pygm	NM_011224.1→NP_035354.1	muscle glycogen phosphorylase
Itpk1	NM_172584.1→NP_766172.1	inositol 1,3,4-triphosphate 5/6 kinase
Amd1	NM_009665.2→NP_033795.1	S-adenosylmethionine decarboxylase 1
Hdc	NM_008230.4→NP_032256.3	histidine decarboxylase
Acox1	NM_015729.2→NP_056544.2	acyl-Coenzyme A oxidase 1, palmitoyl
Uck2	NM_030724.1→NP_109649.1	uridine-cytidine kinase 2
Adc	NM_172875.1→NP_766463.1	arginine decarboxylase
Kdr	NM_010612.2→NP_034742.2	kinase insert domain protein receptor
Gpam	NM_008149.2→NP_032175.2	glycerol-3-phosphate acyltransferase, mitochondrial
Amy1	NM_007446.1→NP_031472.1	amylase 1, salivary
Msra	NM_026322.3→NP_080598.2	methionine sulfoxide reductase A
Coasy	NM_027896.2→NP_082172.2	Coenzyme A synthase
Cbs	NM_144855.1→NP_659104.1	cystathionine beta-synthase
Vkorc1	NM_178600.2→NP_848715.1	vitamin K epoxide reductase complex, subunit 1
Nrip1	NM_173440.1→NP_775616.1	nuclear receptor interacting protein 1
Asf1a	NM_025541.3→NP_079817.1	ASF1 anti-silencing function 1 homolog A (S. cerevisiae)
Cyp2e1	NM_021282.2→NP_067257.1	cytochrome P450, family 2, subfamily e, polypeptide 1
Ppat	XM_896000.2→XP_901093.1	phosphoribosyl pyrophosphate amidotransferase
Ubr1	NM_009461.1→NP_033487.1	ubiquitin protein ligase E3 component n-recognin 1
Mttp	NM_008642.1→NP_032668.1	microsomal triglyceride transfer protein
Hadha	NM_178878.1→NP_849209.1	hydroxyacyl-Coenzyme A dehydrogenase/3-ketoacyl-Coenzyme A thiolase/enoyl-Coenzyme A hydratase (trifunctional protein), alpha subunit
Ampd1	NM_001033303.2→NP_0010284	adenosine monophosphate deaminase 1 (isoform M)

	75.2	
Mgat5	NM_145128.2→NP_660110.2	mannoside acetylglucosaminyltransferase 5
Kif11	NM_010615.1→NP_034745.1	kinesin family member 11
Sphk1	NM_011451.1→NP_035581.1	sphingosine kinase 1
Pbef1	NM_021524.1→NP_067499.1	pre-B-cell colony-enhancing factor 1
Ppia	NM_008907.1→NP_032933.1	peptidylprolyl isomerase A
Cad	NM_023525.1→NP_076014.1	carbamoyl-phosphate synthetase 2, aspartate transcarbamylase, and dihydroorotase
Pip5k1a	NM_008846.2→NP_032872.1	phosphatidylinositol-4-phosphate 5-kinase, type 1 alpha
Cyp11b2	NM_009991.2→NP_034121.1	cytochrome P450, family 11, subfamily b, polypeptide 2
Rpe65		retinal pigment epithelium 65
Corin	NM_016869.1→NP_058565.1	corin
Pdpk1	NM_011062.1→NP_035192.1	3-phosphoinositide dependent protein kinase-1
Hk1	NM_010438.1→NP_034568.1	hexokinase 1
Apoa1	NM_009692.1→NP_033822.1	apolipoprotein A-I
Degs2	NM_027299.2→NP_081575.2	degenerative spermatocyte homolog 2 (Drosophila), lipid desaturase
Glud1	NM_008133.2→NP_032159.1	glutamate dehydrogenase 1
Gpd1	NM_010271.2→NP_034401.1	glycerol-3-phosphate dehydrogenase 1 (soluble)
Abcb11	NM_021022.2→NP_066302.1	ATP-binding cassette, sub-family B (MDR/TAP), member 11
Akp3	NM_007432.2→NP_031458.2	alkaline phosphatase 3, intestine, not Mn requiring
Alad	NM_008525.3→NP_032551.3	aminolevulinate, delta-, dehydratase
Hmbs	NM_013551.1→NP_038579.1	hydroxymethylbilane synthase
Hs3st1	NM_010474.1→NP_034604.1	heparan sulfate (glucosamine) 3-O-sulfotransferase 1
Gck	NM_010292.3→NP_034422.2	glucokinase
Il12a	NM_008351.1→NP_032377.1	interleukin 12a
Slc2a1	NM_011400.1→NP_035530.1	solute carrier family 2 (facilitated glucose transporter), member 1
Hsd17b1	NM_010475.1→NP_034605.1	hydroxysteroid (17-beta) dehydrogenase 1
Cat	NM_009804.1→NP_033934.1	catalase
Hsd3b1	NM_008293.2→NP_032319.1	hydroxy-delta-5-steroid dehydrogenase, 3 beta- and steroid delta-isomerase 1
Ccbl1	NM_172404.2→NP_765992.2	cysteine conjugate-beta lyase 1
Mogat2	NM_177448.3→NP_803231.1	monoacylglycerol O-acyltransferase 2
Pld1	NM_008875.3→NP_032901.2	phospholipase D1
Gatm	NM_025961.2→NP_080237.1	glycine amidinotransferase (L-arginine:glycine amidinotransferase)
Slc1a1	NM_009199.1→NP_033225.1	solute carrier family 1 (neuronal/epithelial high affinity glutamate transporter, system Xag), member 1
Prodh	NM_011172.1→NP_035302.1	proline dehydrogenase
G6pc	NM_008061.2→NP_032087.2	glucose-6-phosphatase, catalytic
Xdh	NM_011723.2→NP_035853.2	xanthine dehydrogenase
Dcp1a	NM_133761.2→NP_598522.2	decapping enzyme

Hmgcs1	NM_145942.2→NP_666054.2	3-hydroxy-3-methylglutaryl-Coenzyme A synthase 1
F2	NM_010168.1→NP_034298.1	coagulation factor II
Acads	NM_007383.2→NP_031409.2	acyl-Coenzyme A dehydrogenase, short chain
Taldo1	NM_011528.1→NP_035658.1	transaldolase 1
Cel	NM_009885.1→NP_034015.1	carboxyl ester lipase
Adk	NM_134079.1→NP_598840.1	adenosine kinase
Acmsd	NM_001033041.1→NP_001028213.1	amino carboxymuconate semialdehyde decarboxylase
Gsr	NM_010344.3→NP_034474.3	glutathione reductase 1
Ece1	NM_199307.1→NP_955011.1	endothelin converting enzyme 1
Slc5a5	NM_053248.1→NP_444478.1	solute carrier family 5 (sodium iodide symporter), member 5
Lta4h	NM_008517.1→NP_032543.1	leukotriene A4 hydrolase
Fasn	NM_007988.3→NP_032014.3	fatty acid synthase
Cds1	NM_173370.3→NP_775546.2	CDP-diacylglycerol synthase 1
Cds2	NM_138651.3→NP_619592.1	CDP-diacylglycerol synthase (phosphatidate cytidylyltransferase) 2
Nmnat1	NM_133435.1→NP_597679.1	nicotinamide nucleotide adenylyltransferase 1
Ctsd	NM_009983.2→NP_034113.1	cathepsin D
Mdh1	NM_008618.2→NP_032644.2	malate dehydrogenase 1, NAD (soluble)
Pts	NM_011220.2→NP_035350.1	6-pyruvoyl-tetrahydropterin synthase
Ecgf1	NM_138302.1→NP_612175.1	endothelial cell growth factor 1 (platelet-derived)
Elovl6	NM_130450.2→NP_569717.1	ELOVL family member 6, elongation of long chain fatty acids (yeast)
Sdha	NM_023281.1→NP_075770.1	succinate dehydrogenase complex, subunit A, flavoprotein (Fp)
Sdhb	NM_023374.3→NP_075863.2	succinate dehydrogenase complex, subunit B, iron sulfur (Ip)
Sdhc	NM_025321.1→NP_079597.1	succinate dehydrogenase complex, subunit C, integral membrane protein
Sdhd	NM_025848.1→NP_080124.1	succinate dehydrogenase complex, subunit D, integral membrane protein
Sqle	NM_009270.2→NP_033296.1	squalene epoxidase
Slc34a2	NM_011402.2→NP_035532.2	solute carrier family 34 (sodium phosphate), member 2
Cdo1	NM_033037.2→NP_149026.1	cysteine dioxygenase 1, cytosolic
Rdh5	NM_134006.4→NP_598767.1	retinol dehydrogenase 5
Tdh	NM_021480.4→NP_067455.4	L-threonine dehydrogenase
Hal	NM_010401.3→NP_034531.1	histidine ammonia lyase
Plat	NM_008872.1→NP_032898.1	plasminogen activator, tissue
Ugt8a	NM_011674.3→NP_035804.2	UDP galactosyltransferase 8A
Ltc4s	NM_008521.1→NP_032547.1	leukotriene C4 synthase
Xylb	NM_001033209.1→NP_001028381.1	xylulokinase homolog (H. influenzae)
Mmp2	NM_008610.2→NP_032636.1	matrix metallopeptidase 2
Gapdh	NM_001001303.1→NP_001001303.1	glyceraldehyde-3-phosphate dehydrogenase

Aass	NM_013930.3→NP_038958.2	aminoadipate-semialdehyde synthase
Fbp1	NM_019395.1→NP_062268.1	fructose bisphosphatase 1
Pcyt2	NM_024229.2→NP_077191.2	phosphate cytidylyltransferase 2, ethanolamine
Idh3b	NM_130884.1→NP_570954.1	isocitrate dehydrogenase 3 (NAD+) beta
Ace	NM_009598.1→NP_033728.1	angiotensin I converting enzyme (peptidyl-dipeptidase A) 1
Fads1	NM_146094.1→NP_666206.1	fatty acid desaturase 1
Tspo	NM_009775.2→NP_033905.2	translocator protein
Aqp2	NM_009699.2→NP_033829.2	aquaporin 2
Pgd	XM_001003312.1→XP_001003312.1	phosphogluconate dehydrogenase
Papss1	NM_011863.1→NP_035993.1	3'-phosphoadenosine 5'-phosphosulfate synthase 1
Mpg	NM_010822.2→NP_034952.1	N-methylpurine-DNA glycosylase
Chat	NM_009891.1→NP_034021.1	choline acetyltransferase
Rdh8	NM_001030290.1→NP_001025461.1	retinol dehydrogenase 8
Pnpo	NM_134021.1→NP_598782.1	pyridoxine 5'-phosphate oxidase
Pgs1	NM_133757.1→NP_598518.1	phosphatidylglycerophosphate synthase 1
Mod1	NM_008615.1→NP_032641.1	malic enzyme, supernatant
P4hb	NM_011032.1→NP_035162.1	prolyl 4-hydroxylase, beta polypeptide
Pnmt	NM_008890.1→NP_032916.1	phenylethanolamine-N-methyltransferase
Ube1x	NM_009457.2→NP_033483.1	ubiquitin-activating enzyme E1, Chr X
Elovl5	NM_134255.2→NP_599016.2	ELOVL family member 5, elongation of long chain fatty acids (yeast)
Psph	NM_133900.2→NP_598661.1	phosphoserine phosphatase
Apobec1	NM_031159.2→NP_112436.1	apolipoprotein B editing complex 1
Soat2	NM_146064.1→NP_666176.1	sterol O-acyltransferase 2
Srd5a1	NM_175283.3→NP_780492.2	steroid 5 alpha-reductase 1
Acly	NM_134037.2→NP_598798.1	ATP citrate lyase
Aco2	NM_080633.2→NP_542364.1	aconitase 2, mitochondrial
Gaa	NM_008064.2→NP_032090.2	glucosidase, alpha, acid
Cd79a	NM_007655.2→NP_031681.2	CD79A antigen (immunoglobulin-associated alpha)
F3	NM_010171.2→NP_034301.2	coagulation factor III
Lsr	NM_017405.1→NP_059101.1	lipolysis stimulated lipoprotein receptor
Mgll	NM_011844.3→NP_035974.1	monoglyceride lipase
Ide	NM_031156.1→NP_112419.1	insulin degrading enzyme
Dtymk	NM_023136.1→NP_075625.1	deoxythymidylate kinase
Chka	NM_001025566.1→NP_001020737.1	choline kinase alpha
Cmah	NM_007717.2→NP_031743.2	cytidine monophospho-N-acetylneuraminic acid hydroxylase
Etnk1	XM_908334.2→XP_913427.2	ethanolamine kinase 1
Ak1	NM_021515.1→NP_067490.1	adenylate kinase 1
Ela1	NM_033612.1→NP_291090.1	elastase 1, pancreatic
Ucp1	NM_009463.2→NP_033489.1	uncoupling protein 1 (mitochondrial, proton carrier)
Cyp8b1	NM_010012.2→NP_034142.2	cytochrome P450, family 8, subfamily b, polypeptide 1

Cyp51	NM_020010.2→NP_064394.2	cytochrome P450, family 51
Ugdh	NM_009466.2→NP_033492.1	UDP-glucose dehydrogenase
Tat	NM_146214.1→NP_666326.1	tyrosine aminotransferase
Hprt1	NM_013556.2→NP_038584.2	hypoxanthine guanine phosphoribosyl transferase 1
Bche	NM_009738.2→NP_033868.2	butyrylcholinesterase
Ache	NM_009599.3→NP_033729.1	acetylcholinesterase
Folh1	NM_016770.2→NP_058050.2	folate hydrolase
Bcat1	NM_001024468.1→NP_001019639.1	branched chain aminotransferase 1, cytosolic
Fdps	NM_134469.2→NP_608219.1	farnesyl diphosphate synthetase
Miox	NM_019977.2→NP_064361.2	myo-inositol oxygenase
Dhfr	NM_010049.3→NP_034179.1	dihydrofolate reductase
Mpi1	NM_025837.1→NP_080113.1	mannose phosphate isomerase 1
Fech	NM_007998.3→NP_032024.2	ferrochelatase
Nadk	NM_138671.1→NP_619612.1	NAD kinase
Acat1	NM_144784.2→NP_659033.1	acetyl-Coenzyme A acetyltransferase 1
Pemt	NM_008819.2→NP_032845.2	phosphatidylethanolamine N-methyltransferase
Ctps	NM_016748.1→NP_058028.1	cytidine 5'-triphosphate synthase
Dbh	NM_138942.3→NP_620392.2	dopamine beta hydroxylase
Rfk	NM_019437.1→NP_062310.1	riboflavin kinase
Tk1	NM_009387.1→NP_033413.1	thymidine kinase 1
Hpd	NM_008277.1→NP_032303.1	4-hydroxyphenylpyruvic acid dioxygenase
Aprt	NM_009698.1→NP_033828.1	adenine phosphoribosyl transferase
Kmo	NM_133809.1→NP_598570.1	kynurenine 3-monooxygenase (kynurenine 3-hydroxylase)
Ctsb	NM_007798.1→NP_031824.1	cathepsin B
Adss	NM_007422.2→NP_031448.2	adenylosuccinate synthetase, non muscle
Pgk1	NM_008828.2→NP_032854.2	phosphoglycerate kinase 1
Phgdh	NM_016966.3→NP_058662.2	3-phosphoglycerate dehydrogenase
Casp3	NM_009810.1→NP_033940.1	caspase 3
Ugt1a1	NM_201645.1→NP_964007.1	UDP glucuronosyltransferase 1 family, polypeptide A1
Aldh18a1	NM_153554.1→NP_705782.1	aldehyde dehydrogenase 18 family, member A1
Parn	NM_028761.1→NP_083037.1	poly(A)-specific ribonuclease (deadenylation nuclease)
Slc34a1	NM_011392.1→NP_035522.1	solute carrier family 34 (sodium phosphate), member 1
Polb	NM_017141.1→NP_058837.1	polymerase (DNA directed), beta
Tmem15	NM_177648.3→NP_808316.1	transmembrane protein 15
Lalba	NM_010679.1→NP_034809.1	lactalbumin, alpha
B4galt1	NM_022305.2→NP_071641.1	UDP-Gal:betaGlcNAc beta 1,4-galactosyltransferase, polypeptide 1
Lcat	NM_008490.1→NP_032516.1	lecithin cholesterol acyltransferase
Umps	NM_009471.1→NP_033497.1	uridine monophosphate synthetase
Dgat1	NM_010046.2→NP_034176.1	diacylglycerol O-acyltransferase 1

Abp1	NM_029638.1→NP_083914.1	amiloride binding protein 1 (amine oxidase, copper-containing)
Cyp2c29	NM_007815.2→NP_031841.2	cytochrome P450, family 2, subfamily c, polypeptide 29
Prps1	NM_021463.2→NP_067438.1	phosphoribosyl pyrophosphate synthetase 1
Suclg1	NM_019879.1→NP_063932.1	succinate-CoA ligase, GDP-forming, alpha subunit
Suclg2	NM_011507.1→NP_035637.1	succinate-Coenzyme A ligase, GDP-forming, beta subunit
Npl	NM_028749.1→NP_083025.1	N-acetylneuraminate pyruvate lyase
Aldh1l1	NM_027406.1→NP_081682.1	aldehyde dehydrogenase 1 family, member L1
Hpgd	NM_008278.1→NP_032304.1	hydroxyprostaglandin dehydrogenase 15 (NAD)
Hsd17b3	NM_008291.1→NP_032317.1	hydroxysteroid (17-beta) dehydrogenase 3
Lss	NM_146006.1→NP_666118.1	lanosterol synthase
Pik3cg	NM_020272.1→NP_064668.1	phosphoinositide-3-kinase, catalytic, gamma polypeptide
Ampd1	NM_001033303.2→NP_001028475.2	adenosine monophosphate deaminase 1 (isoform M)
Cyp27a1	NM_024264.3→NP_077226.2	cytochrome P450, family 27, subfamily a, polypeptide 1
Acss2	NM_019811.2→NP_062785.2	acyl-CoA synthetase short-chain family member 2
Cyp2j11	NM_001004141.1→NP_001004141.1	cytochrome P450, family 2, subfamily j, polypeptide 11
Acacb	NM_133904.1→NP_598665.1	acetyl-Coenzyme A carboxylase beta
Ren2	NM_031193.1→NP_112470.1	renin 2 tandem duplication of Ren1
Hmox2	NM_010443.1→NP_034573.1	heme oxygenase (decycling) 2
Ptgs2	NM_011198.2→NP_035328.2	prostaglandin-endoperoxide synthase 2
Impdh2	NM_011830.2→NP_035960.2	inosine 5'-phosphate dehydrogenase 2
G6pd2	NM_019468.1→NP_062341.1	glucose-6-phosphate dehydrogenase 2
G6pdx	NM_008062.2→NP_032088.1	glucose-6-phosphate dehydrogenase X-linked
Cpt1b	NM_009948.1→NP_034078.1	carnitine palmitoyltransferase 1b, muscle
Cpt1c	NM_153679.1→NP_710146.1	carnitine palmitoyltransferase 1c
Tph2	NM_173391.1→NP_775567.1	tryptophan hydroxylase 2
Pank2	NM_153501.1→NP_705721.2	pantothenate kinase 2
Pank3	NM_145962.1→NP_666074.1	pantothenate kinase 3
Pank4	NM_172990.1→NP_766578.1	pantothenate kinase 4
Hacu		high affinity choline uptake
Gsto2	NM_026619.1→NP_080895.1	glutathione S-transferase omega 2
Bckdhb	NM_199195.1→NP_954665.1	branched chain ketoacid dehydrogenase E1, beta polypeptide
Oxct2b	NM_181859.1→NP_862907.1	3-oxoacid CoA transferase 2B
Pcyt1b	NM_177546.2→NP_808214.1	phosphate cytidylyltransferase 1, choline, beta isoform
Trpv5	NM_001007572.2→NP_001007573.1	transient receptor potential cation channel, subfamily V, member 5
Xylt2	NM_145828.1→NP_665827.1	xylosyltransferase II
Gk2	NM_010294.1→NP_034424.1	glycerol kinase 2
Smurf2	NM_025481.1→NP_079757.1	SMAD specific E3 ubiquitin protein ligase 2

Rrm2b	NM_199476.1→NP_955770.1	ribonucleotide reductase M2 B (TP53 inducible)
Pck2	NM_028994.1→NP_083270.1	phosphoenolpyruvate carboxykinase 2 (mitochondrial)
Mat2a	NM_145569.2→NP_663544.1	methionine adenosyltransferase II, alpha
Mat2b	NM_134017.1→NP_598778.1	methionine adenosyltransferase II, beta
Sat2	XM_181304.5→XP_181304.1	spermidine/spermine N1-acetyl transferase 2
Gfpt2	NM_013529.1→NP_038557.1	glutamine fructose-6-phosphate transaminase 2
Bace2	NM_019517.2→NP_062390.2	beta-site APP-cleaving enzyme 2
Pfkl	NM_008826.2→NP_032852.2	phosphofructokinase, liver, B-type
Pfkp	NM_019703.2→NP_062677.1	phosphofructokinase, platelet
Pfkx		phosphofructokinase, polypeptide X
Ptges2	NM_133783.1→NP_598544.1	prostaglandin E synthase 2
Nos2	NM_010927.1→NP_035057.1	nitric oxide synthase 2, inducible, macrophage
Nos3	NM_008713.2→NP_032739.2	nitric oxide synthase 3, endothelial cell
Scd2	NM_009128.1→NP_033154.1	stearoyl-Coenzyme A desaturase 2
Scd3	NM_024450.2→NP_077770.1	stearoyl-coenzyme A desaturase 3
Scd4	NM_183216.2→NP_899039.2	stearoyl-coenzyme A desaturase 4
Alas2	NM_009653.1→NP_033783.1	aminolevulinic acid synthase 2, erythroid
Apex2	NM_029943.1→NP_084219.1	apurinic/apyrimidinic endonuclease 2
Gys2	NM_145572.1→NP_663547.1	glycogen synthase 2
Scnn1b	NM_011325.1→NP_035455.1	sodium channel, nonvoltage-gated 1 beta
Scnn1g	NM_011326.1→NP_035456.1	sodium channel, nonvoltage-gated 1 gamma
Gad2	NM_008078.1→NP_032104.1	glutamic acid decarboxylase 2
Pygl	NM_133198.1→NP_573461.1	liver glycogen phosphorylase
Pygb	NM_153781.1→NP_722476.1	brain glycogen phosphorylase
Amd2	NM_007444.2→NP_031470.2	S-adenosylmethionine decarboxylase 2
Uck1	NM_011675.1→NP_035805.1	uridine-cytidine kinase 1
Amy2	NM_009669.1→NP_033799.1	amylase 2, pancreatic
Amy2-1	NM_001042712.1→NP_001036177.1	amylase 2-1, pancreatic
Amy2-2	NM_001042711.1→NP_001036176.1	amylase 2-2, pancreatic
Sepx1	NM_013759.2→NP_038787.1	selenoprotein X 1
Msrb2	NM_029619.2→NP_083895.1	methionine sulfoxide reductase B2
Msrb3	NM_177092.3→NP_796066.1	methionine sulfoxide reductase B3
Ubr2	NM_146078.2→NP_666190.2	ubiquitin protein ligase E3 component n-recognin 2
Ampd2	NM_028779.3→NP_083055.1	adenosine monophosphate deaminase 2 (isoform L)
Ampd3	NM_009667.2→NP_033797.2	AMP deaminase 3
Sphk2	NM_020011.3→NP_064395.2	sphingosine kinase 2
Pip5k1b	NM_008847.2→NP_032873.2	phosphatidylinositol-4-phosphate 5-kinase, type 1 beta
Pip5k1c	NM_008844.1→NP_032870.1	phosphatidylinositol-4-phosphate 5-kinase, type 1 gamma
Hk2	NM_013820.1→NP_038848.1	hexokinase 2
Hk3	NM_001033245.1→NP_001028417.1	hexokinase 3
Glud2		glutamate dehydrogenase 2
Gpd2	NM_010274.2→NP_034404.2	glycerol phosphate dehydrogenase 2, mitochondrial

Slc2a4	NM_009204.1→NP_033230.1	solute carrier family 2 (facilitated glucose transporter), member 4
Ccbl2	NM_173763.2→NP_776124.1	cysteine conjugate-beta lyase 2
Mogat1	NM_026713.1→NP_080989.1	monoacylglycerol O-acyltransferase 1
Slc1a2	NM_011393.1→NP_035523.1	solute carrier family 1 (glial high affinity glutamate transporter), member 2
Prodh2	NM_019546.4→NP_062419.2	proline dehydrogenase (oxidase) 2
G6pc2	NM_021331.2→NP_067306.1	glucose-6-phosphatase, catalytic, 2
G6pc3	NM_175935.3→NP_787949.2	glucose 6 phosphatase, catalytic, 3
Dcp1b	NM_001033379.1→NP_001028551.1	DCP1 decapping enzyme homolog b (S. cerevisiae)
Hmgcs2	NM_008256.2→NP_032282.2	3-hydroxy-3-methylglutaryl-Coenzyme A synthase 2
Acad9	NM_172678.3→NP_766266.3	acyl-Coenzyme A dehydrogenase family, member 9
Acadm	NM_007382.1→NP_031408.1	acyl-Coenzyme A dehydrogenase, medium chain
Acadl	NM_007381.2→NP_031407.2	acyl-Coenzyme A dehydrogenase, long-chain
Acadsb	NM_025826.1→NP_080102.1	acyl-Coenzyme A dehydrogenase, short/branched chain
Acad11	NM_175324.2→NP_780533.2	acyl-Coenzyme A dehydrogenase family, member 11
Acadvl	NM_017366.1→NP_059062.1	acyl-Coenzyme A dehydrogenase, very long chain
Acad8	NM_025862.1→NP_080138.1	acyl-Coenzyme A dehydrogenase family, member 8
Acad10	NM_028037.1→NP_082313.1	acyl-Coenzyme A dehydrogenase family, member 10
Ece2	NM_139293.1→NP_647454.1	endothelin converting enzyme 2
Nmnat2	NM_175460.3→NP_780669.1	nicotinamide nucleotide adenylyltransferase 2
Nmnat3	NM_144533.1→NP_653116.1	nicotinamide nucleotide adenylyltransferase 3
Mdh1b	NM_029696.2→NP_083972.2	malate dehydrogenase 1B, NAD (soluble)
Mdh2	NM_008617.2→NP_032643.2	malate dehydrogenase 2, NAD (mitochondrial)
Fbp2	NM_007994.1→NP_032020.1	fructose bisphosphatase 2
Idh3a	NM_029573.2→NP_083849.1	isocitrate dehydrogenase 3 (NAD+) alpha
Idh3g	NM_008323.1→NP_032349.1	isocitrate dehydrogenase 3 (NAD+), gamma
Idh1	NM_010497.2→NP_034627.2	isocitrate dehydrogenase 1 (NADP+), soluble
Idh2	NM_173011.1→NP_766599.1	isocitrate dehydrogenase 2 (NADP+), mitochondrial
Papss2	NM_011864.2→NP_035994.2	3'-phosphoadenosine 5'-phosphosulfate synthase 2
Mod2		malic enzyme complex, mitochondrial
Me2	NM_145494.1→NP_663469.1	malic enzyme 2, NAD(+)-dependent, mitochondrial
Me3	NM_181407.2→NP_852072.1	malic enzyme 3, NADP(+)-dependent, mitochondrial
Soat1	NM_009230.3→NP_033256.2	sterol O-acyltransferase 1
Srd5a2	NM_053188.1→NP_444418.1	steroid 5 alpha-reductase 2
Chkb	NM_007692.4→NP_031718.1	choline kinase beta
Etnk2	NM_175443.2→NP_780652.1	ethanolamine kinase 2
Ela2	NM_015779.2→NP_056594.2	elastase 2, neutrophil
Ela2a	NM_007919.1→NP_031945.1	elastase 2A
Ela3	NM_026419.1→NP_080695.1	elastase 3, pancreatic
Ucp2	NM_011671.2→NP_035801.2	uncoupling protein 2 (mitochondrial, proton carrier)
Ucp3	NM_009464.2→NP_033490.1	uncoupling protein 3 (mitochondrial, proton carrier)
Bcat2	NM_009737.1→NP_033867.1	branched chain aminotransferase 2, mitochondrial
Acat2	NM_009338.1→NP_033364.1	acetyl-Coenzyme A acetyltransferase 2
Ctps2	NM_018737.2→NP_061207.1	cytidine 5'-triphosphate synthase 2

Tk2	NM_021028.2→NP_066356.2	thymidine kinase 2, mitochondrial
Pgk2	NM_031190.1→NP_112467.1	phosphoglycerate kinase 2
Ugt1a5	NM_201643.1→NP_964005.1	UDP glucuronosyltransferase 1 family, polypeptide A5
B4galt2	NM_017377.4→NP_059073.1	UDP-Gal:betaGlcNAc beta 1,4-galactosyltransferase, polypeptide 2
Dgat2	NM_026384.2→NP_080660.1	diacylglycerol O-acyltransferase 2
Prps2	NM_026662.2→NP_080938.1	phosphoribosyl pyrophosphate synthetase 2
Sucla2	NM_011506.1→NP_035636.1	succinate-Coenzyme A ligase, ADP-forming, beta subunit
Ampd2	NM_028779.3→NP_083055.1	adenosine monophosphate deaminase 2 (isoform L)
Ampd3	NM_009667.2→NP_033797.2	AMP deaminase 3
Acsl5	NM_027976.2→NP_082252.1	acyl-CoA synthetase long-chain family member 5

9. Appendix B - Publications

1. Hackl* H, Burkard* TR, Sturn A, Rubio R, Schleiffer A, Tian S, Quackenbush J, Eisenhaber F and Trajanoski Z (*contributed equally): **Molecular processes during fat cell development revealed by gene expression profiling and functional annotation.** *Genome Biol.* 2005; 6(13):R108

2. Burkard T, Trajanoski Z, Novatchkova M, Hackl H, Eisenhaber F: **Identification of New Targets Using Expression Profiles.** In: Antiangiogenic Cancer Therapy, Editors: Abbruzzese JL, Davis DW, Herbst RS; *CRC Press (in press)*

3. Hartler J, Thallinger GG, Stocker G, Sturn A, Burkard TR, Körner E, Scheucher A, Rader R, Schmidt A, Mechtler K, Trajanoski Z: **MASPECTRAS: a platform for management and analysis of proteomic LC-MS/MS data.** *BMC Bioinformatics.* (submitted)

Research

Open Access

Molecular processes during fat cell development revealed by gene expression profiling and functional annotation

Hubert Hackl[¤*], Thomas Rainer Burkard[¤*†], Alexander Sturn[*], Renee Rubio[‡], Alexander Schleiffer[†], Sun Tian[†], John Quackenbush[‡], Frank Eisenhaber[†] and Zlatko Trajanoski[*]

Addresses: [*]Institute for Genomics and Bioinformatics and Christian Doppler Laboratory for Genomics and Bioinformatics, Graz University of Technology, Petersgasse 14, 8010 Graz, Austria. [†]Research Institute of Molecular Pathology, Dr Bohr-Gasse 7, 1030 Vienna, Austria. [‡]Dana-Farber Cancer Institute, Department of Biostatistics and Computational Biology, 44 Binney Street, Boston, MA 02115.

¤ These authors contributed equally to this work.

Correspondence: Zlatko Trajanoski. E-mail: zlatko.trajanoski@tugraz.at

Published: 19 December 2005

Genome ***Biology*** 2005, **6:**R108 (doi:10.1186/gb-2005-6-13-r108)

The electronic version of this article is the complete one and can be found online at http://genomebiology.com/2005/6/13/R108

Received: 21 July 2005
Revised: 23 August 2005
Accepted: 8 November 2005

Abstract

Background: Large-scale transcription profiling of cell models and model organisms can identify novel molecular components involved in fat cell development. Detailed characterization of the sequences of identified gene products has not been done and global mechanisms have not been investigated. We evaluated the extent to which molecular processes can be revealed by expression profiling and functional annotation of genes that are differentially expressed during fat cell development.

Results: Mouse microarrays with more than 27,000 elements were developed, and transcriptional profiles of 3T3-L1 cells (pre-adipocyte cells) were monitored during differentiation. In total, 780 differentially expressed expressed sequence tags (ESTs) were subjected to in-depth bioinformatics analyses. The analysis of 3'-untranslated region sequences from 395 ESTs showed that 71% of the differentially expressed genes could be regulated by microRNAs. A molecular atlas of fat cell development was then constructed by *de novo* functional annotation on a sequence segment/domain-wise basis of 659 protein sequences, and subsequent mapping onto known pathways, possible cellular roles, and subcellular localizations. Key enzymes in 27 out of 36 investigated metabolic pathways were regulated at the transcriptional level, typically at the rate-limiting steps in these pathways. Also, coexpressed genes rarely shared consensus transcription-factor binding sites, and were typically not clustered in adjacent chromosomal regions, but were instead widely dispersed throughout the genome.

Conclusions: Large-scale transcription profiling in conjunction with sophisticated bioinformatics analyses can provide not only a list of novel players in a particular setting but also a global view on biological processes and molecular networks.

Background

Obesity, the excess deposition of adipose tissue, is among the most pressing health problems both in the Western world and in developing countries. Growth of adipose tissue is the result of the development of new fat cells from precursor cells. This process of fat cell development, known as adipogenesis, leads to the accumulation of lipids and an increase in the number and size of fat cells. Adipogenesis has been extensively studied *in vitro* for more than 30 years using the 3T3-L1 preadipocyte cell line as a model. This cell line was derived from disaggregated mouse embryos and selected based on the propensity of these cells to differentiate into adipocytes in culture [1]. When exposed to the appropriate adipogenic cocktail containing dexamethasone, isobutylmethylxanthine, insulin, and fetal bovine serum, 3T3-L1 preadipocytes differentiate into adipocytes [2].

Experimental studies on adipogenesis have revealed many important molecular mechanisms. For example, two of the CCAAT/enhancer binding proteins (C/EBPs; specifically C/EBPβ and C/EBPδ) are induced in the early phase of differentiation. These factors mediate transcriptional activity of C/EBPα and peroxisome proliferator-activated receptor (PPAR)-gamma (PPARγ) [3,4]. Another factor, the basic helix-loop-helix (bHLH) transcription factor adipocyte determination and differentiation dependent factor 1/sterol regulatory element binding protein 1 (ADD1/SREBP1c), could potentially be involved in a mechanism that links lipogenesis and adipogenesis. ADD1/SREBP1c can activate a broad program of genes that are involved in fatty acid and triglyceride metabolism in both fat and liver, and can also accelerate adipogenesis [5]. Activation of the adipogenesis process by ADD1/SREBP1c could be effected via direct activation of PPARγ [6] or through generation of endogenous ligands for PPARγ [7].

Knowledge of the transcriptional network is far from complete. In order to identify new components involved in fat cell development, several studies using microarrays have been initiated. These studies have used early Affymetrix technology [8-14] or filters [15], and might have missed many genes that are important to the development of a fat cell. The problem of achieving broad coverage of the developmental transcriptome became evident in a mouse embryo expressed sequence tag (EST) project, which revealed that a significant fraction of the genes are not represented in the collections of genes previously available [16]. Moreover, earlier studies on adipogenesis [8-14] focused on gene discovery for further functional analyses and did not address global mechanisms.

We conducted the present study to evaluate the extent to which molecular processes underlying fat cell development can be revealed by expression profiling. To this end, we used a recently developed cDNA microarray with 27,648 ESTs [17], of which 15,000 are developmental ESTs representing 78% novel and 22% known genes [18]. We then assayed expression profiles from 3T3-L1 cells during differentiation using biological and technical replicates. Finally, we performed comprehensive bioinformatics analyses, including *de novo* functional annotation and curation of the generated data within the context of biological pathways. Using these methods we were able to develop a molecular atlas of fat cell development. We demonstrate the power of the atlas by highlighting selected genes and molecular processes. With this comprehensive approach, we show that key loci of transcriptional regulation are often enzymes that control the rate-limiting steps of metabolic pathways, and that coexpressed genes often do not share consensus promoter sequences or adjacent locations on the chromosome.

Results

Expression profiles during adipocyte differentiation

The 3T3-L1 cell line treated with a differentiation cocktail was used as a model to study gene expression profiles during adipogenesis. Three independent time series differentiation experiments were performed. RNA was isolated at the preconfluent stage (reference) and at eight time points after confluence (0, 6, 12, 24, 48 and 72 hours, and 7 and 14 days). Gene expression levels relative to the preconfluent state were determined using custom-designed microarrays with spotted polymerase chain reaction (PCR) products. The microarray developed here contains 27,648 spots with mouse cDNA clones representing 16,016 different genes (UniGene clusters). These include 15,000 developmental clones (the NIA cDNA clone set from the US National Institute of Aging of the National Institutes of Health NIH), 11,000 clones from different brain regions in the mouse (Brain Molecular Anatomy Project [BMAP]), and 627 clones for genes which were selected using the TIGR Mouse Gene Index, Build 5.0 [19].

All hybridizations were repeated with reversed dye assignment. The data were filtered, normalized, and averaged over biological replicates. Data processing and normalization are described in detail under Materials and methods (see below). Signals at all time points could be detected from 14,368 elements. From these microarray data, we identified 5205 ESTs that exhibited significant differential expression between time points and had a complete profile ($P < 0.05$, one-way analysis of variance [ANOVA]). Because ANOVA filters out ESTs with flat expression profiles, we used a fold change criteria to select the ESTs for further analysis. We focused on 780 ESTs that had a complete profile over all time points, and that were more than twofold upregulated or downregulated in at least four of those time points. These stringent criteria were necessary to select a subset of the ESTs for in-depth sequence analysis and for examination of the dynamics of the molecular processes. The overlap between the ANOVA and twofold filtered ESTs was 414. All of the data, together with annotations and other files used in the analyses, are available as Additional data files and on our website [20]. The analyses

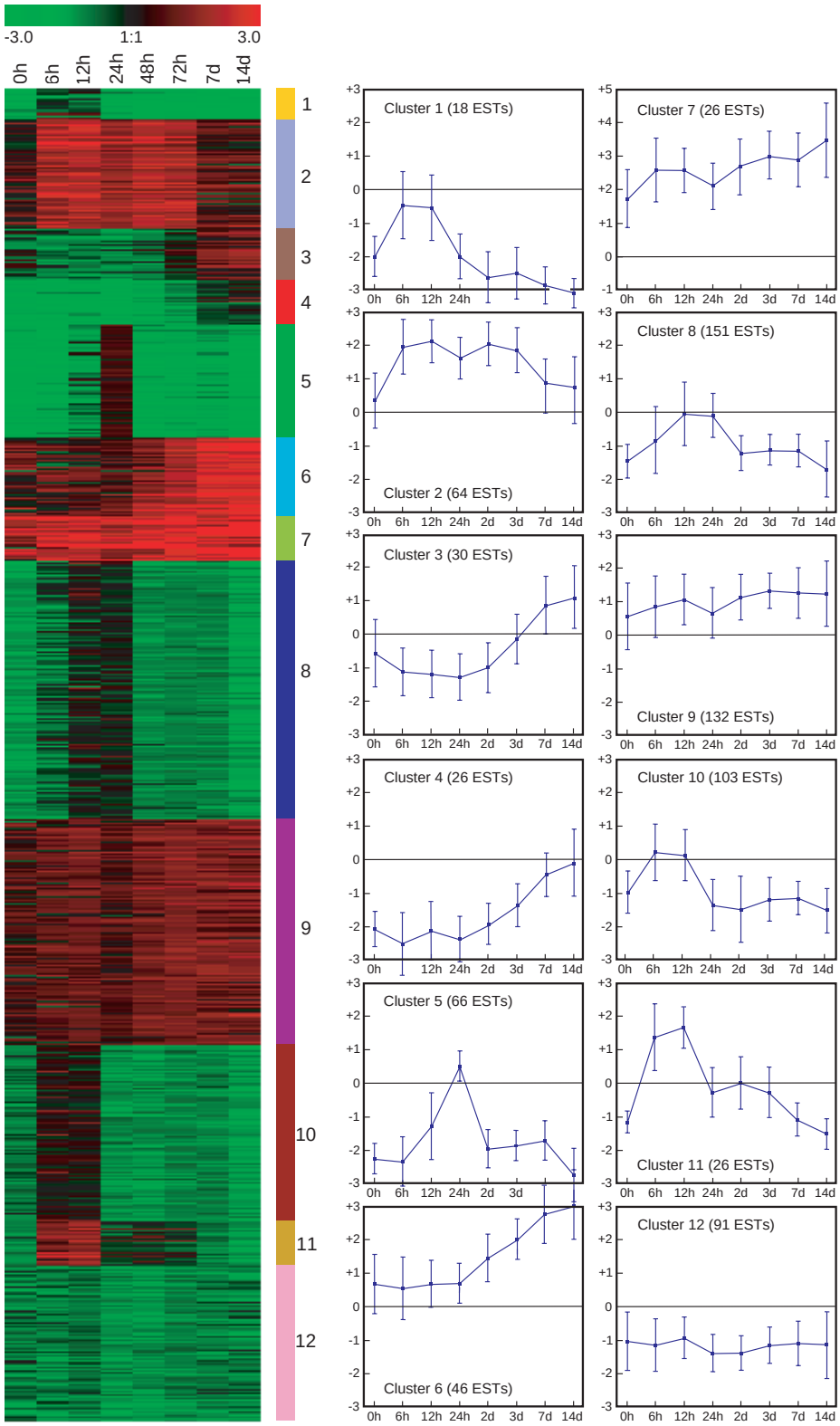

Figure 1 *(see legend on next page)*

Figure 1 *(see previous page)*
Clustering of ESTs found to be differentially expressed during fat cell differentiation. Shown is k-means clustering of 780 ESTs found to be more than twofold upregulated or downregulated at a minimum of four time points during fat cell differentiation. ESTs were grouped into 12 clusters with distinct expression profiles. Relative expression levels (log_2 ratios) for EST gene at different time points are shown and color coded according to the legend at the top (left) and expression profile (mean ± standard deviation) for each cluster (right). EST, expressed sequence tag.

described in the following text were conducted in the set of 780 ESTs.

Validation of expression data

Four lines of evidence support the quality of our data and its consistency with existing knowledge of fat cell biology. First, our array data are consistent with reverse transcriptase (RT)-PCR analysis. We compared the microarray data with quantitative RT-PCR for six different genes (*Pparg* [number 592, cluster 6], *Lpl* [number 14, cluster 6], *Myc* [number 224, cluster 11], *Dcn* [number 137, cluster 7], *Ccna2* [number 26, cluster 5/8], and *Klf9* [number 6, cluster 9]) at different time points (Additional data file 9 and on our website [20]). A high degree of correlation was found ($r^2 = 0.87$), confirming the validity of the microarray data.

Second, statistical analyses of the independent experiments showed that the reproducibility of the generated data is very high. The Pearson correlation coefficient between the replicates was between 0.73 and 0.97 at different time points. The mean coefficient of variation across all genes at each time point was between 0.11 and 0.27. The row data and the details of the statistical analyses can be found in Additional data file 10 and on our website [20].

Third, comparison between our data and the Gene Atlas V2 mouse data for adipose tissue [21] shows that the consistency of the two data sets increases with differentiation state (Additional data files 11 and 12, and our on website [20]). Therefore, this analysis supports the relevance of the chosen cell model to *in vivo* adipogenesis. Among the 382 transcriptionally modulated genes common in both data sets, 67% are regulated in the same direction at time point zero (confluent preadipocyte cell culture). At the final stage of differentiation, the correlation increases up to 72%. If the Gene Atlas expression data are restricted to strongly regulated genes (at least twofold and fourfold change respectively), then the consistency in mature adipocytes rises to 82% (135 genes) and 93% (42 genes), respectively. Out of all 60 tissues in the Gene Atlas V2 mouse, the adipose tissue describes the differentiated state of the 3T3-L1 cells best. Brown fat tissue is the second best match to the differentiated adipocytes (69% of the 382 genes), followed by adrenal gland (66%), kidney (65%), and heart (64%). At each time point in which cell cycle genes were not repressed (12 hours and 24 hours), all tissues had similar correlation to the data set (44-55% for 382 genes).

The fourth line of evidence supporting the quality of our data is that there is clear correspondence between our data and a previously published data set [8]. For a group of 153 genes shared among the two studies, the same upregulation or downregulation was found for 72-89% (depending on time point) of all genes (see Additional data file 13 and our website [20]). The highest identity (89%) was found for the stage terminally differentiated 3T3-L1 cells, for which the profile is less dependent on the precise extraction time. If the comparison is restricted to expression values that are strongly regulated in both experiments (at least twofold change at day 14, 96 ESTs), then the coincidence at every time point is greater than 90%. Comparisons with this [8] and two additional data sets [9,12], and the data pre-processing steps are given in Additional data files 13, 14, 15 and on our website [20]. Note that, because of the differences in the used microarray platforms, availability of the data, normalization methods, and annotations, only 96 genes are shared between all four studies. Of the 780 ESTs monitored in our work, 326 were not detected in the previous studies [8,9,12]: 106 RefSeqs (with prefix NM), 43 automatically generated RefSeqs (with prefix XM), and 173 ESTs (Additional data file 16).

Correspondence between transcriptional coexpression and gene function

To examine the relationships between coexpression and gene functions, we first clustered 780 ESTs that were twofold differentially expressed into 12 temporally distinct patterns, containing between 23 and 143 ESTs (Figure 1). ESTs in four of the clusters are mostly upregulated during adipogenesis, whereas genes in the other eight clusters are mostly downregulated.

We then categorized ESTs with available RefSeq annotation and Gene Ontology (GO) term (486 out of 780) for molecular function, cellular component, and biological process (Figure 2). Genes in clusters 5 and 8 are downregulated through the whole differentiation process and upregulated at 12/24 hours. Many of the proteins encoded by these genes are involved in cell cycle processes and were residing in the nucleus (Figure 2). Re-entry into the cell cycle of growth arrested pre-adipocytes is known as the clonal expansion phase and considered to be a prerequisite for terminal differentiation in 3T3-L1 adipocytes [22]. Genes grouped in cluster 2 are highly expressed from 6 hours (onset of clonal expansion) to 3 days (start of the appearance of adipocyte morphology) but are only modestly expressed at the terminal adipocyte differentiation stage. These include a number of genes that encode signaling molecules. Genes increasingly expressed toward the terminal differentiation stage are in clusters 4, 6, and 7, although from different starting values.

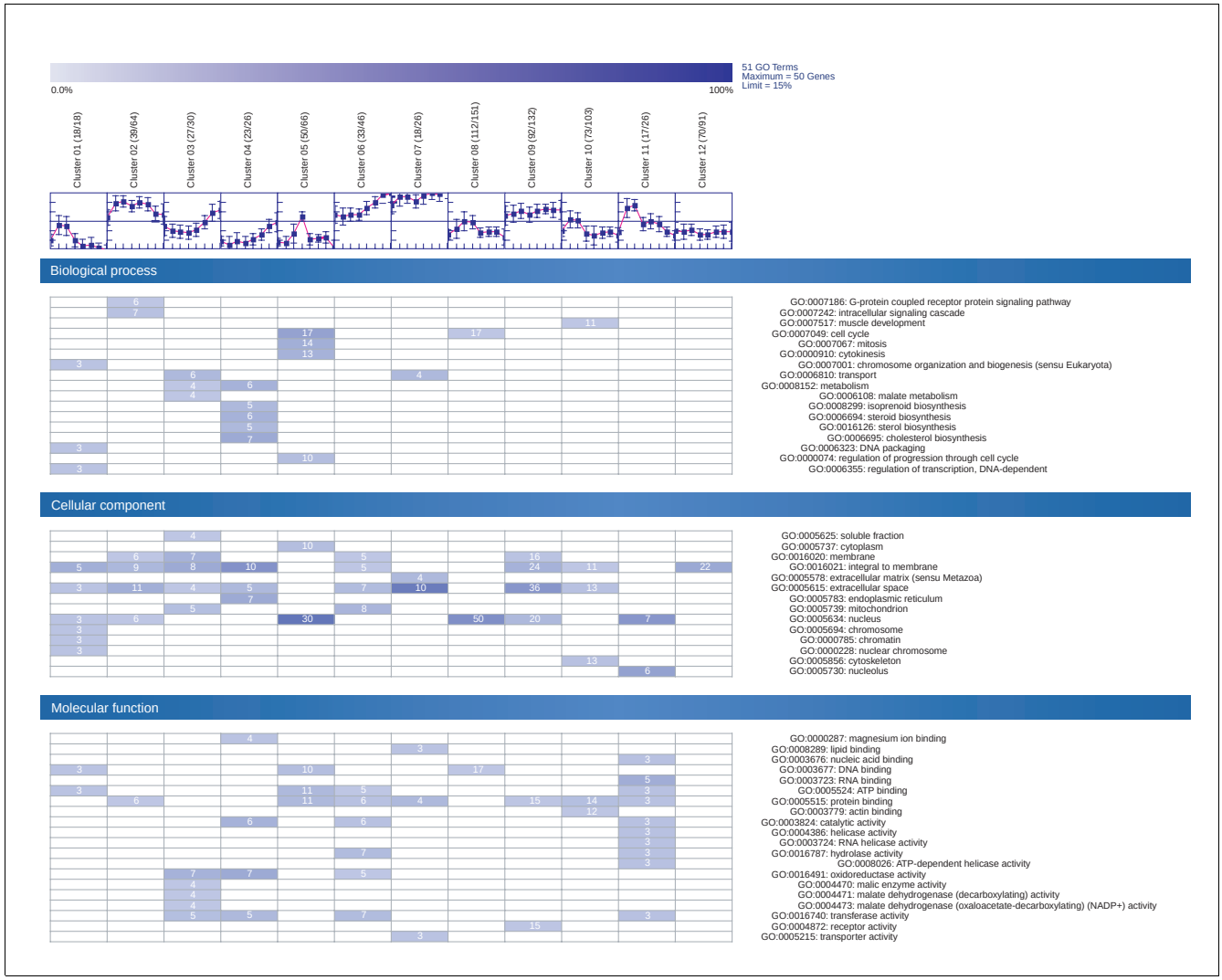

Figure 2
Distribution of GO terms for genes/ESTs in each cluster. The GO terms listed here are those present in at least 15% of the genes within the cluster. In brackets are the number of genes/ESTs with associated GO terms and the number of genes/ESTs within the cluster. EST, expressed sequence tag; GO, Gene Ontology.

Some genes in cluster 6 are known players in lipid metabolism and mitochondrial fatty acid metabolism, whereas some genes can be associated with cholesterol biosynthesis and related to extracellular space or matrix in clusters 4 and 7, respectively.

Correspondence between coexpression and targeting by microRNAs

Previous studies suggest that protein production for 10% or more of all human and mouse genes are regulated by microRNAs (miRNAs) [23,24]. miRNAs are short, noncoding, single-strand RNA species that are found in a wide variety of organisms. miRNAs cause the translational repression or cleavage of target messages [25]. Some miRNAs may behave like small interfering RNAs. It appears that the extent of base pairing between the small RNA and the mRNA determines the balance between cleavage and degradation [26]. Rules for matches between miRNA and target messages have been deduced from a range of experiments [24] and applied to the prediction and discovery of mammalian miRNA targets [23,27]. Moreover, it was shown that human miRNA-143 is involved in adipocyte differentiation [28].

Here we conducted an analysis to determine which of the 780 ESTs differentially expressed during adipocyte differentiation were potential targets of miRNAs and whether there is an over-representation of miRNA targets of coexpressed ESTs clustered in 12 distinct expression patterns. From the 780 ESTs, the 3'-untranslated region (UTR) could be derived for 539. Of these, 518 had at least one exact antisense match for

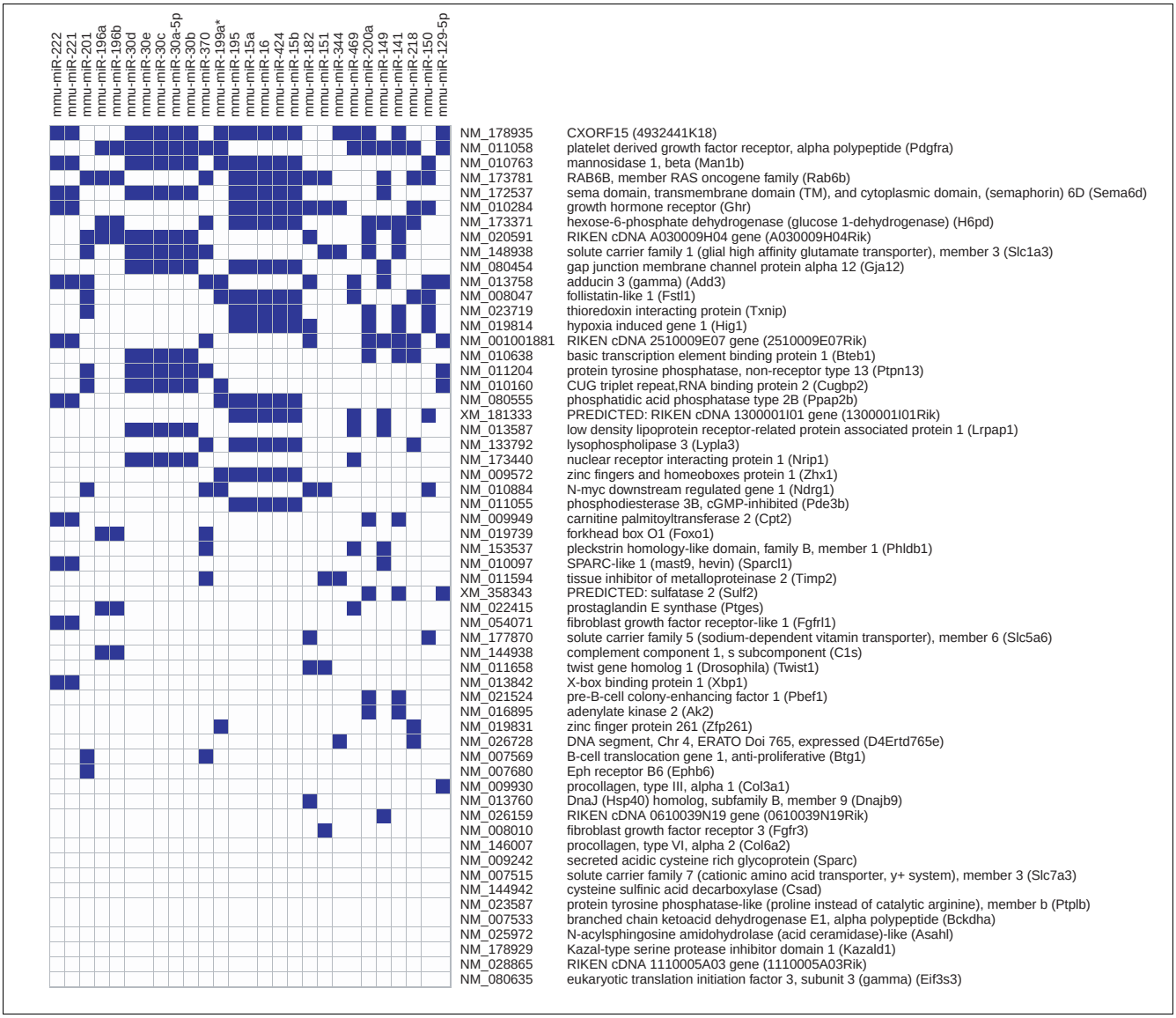

Figure 3
Genes in cluster 9 and significantly over-represented miRNA motifs (blue squares). miRNA, microRNA.

the seven-nucleotide miRNA seed (base 2-8 at the 5' end) from the 234 miRNA sequences (18-24 base pairs [bp]; Additional data file 14). From 395 ESTs with a unique 3'-UTR, 282 (71%) had at least one match over-represented compared with the whole 3'-UTR sequence set (21,396; $P < 0.05$, by one-sided Fisher's exact test). The distribution of statistically over-represented miRNA motifs in 3'-UTRs across the clusters was variable, with genes grouped in cluster 9 (including many transcriptional regulators) having the most statistically over-represented miRNA motifs and genes in cluster 5 having no detectable motifs (Additional data file 18). The results of the analysis of cluster 9 are given in Figure 3. One of the genes with the most significantly over-represented miRNA motifs in the 3'-UTR is related to the ras family (Figure 3). It was previously shown that human oncogene RAS is regulated by let-7 miRNA [29]. Further potential miRNA target genes from all clusters are given in Additional data files 9, 18, 19, 20, 21, 22, 23, 24, 25, 26, 27, 28, 29, 30.

Molecular atlas of fat cell development derived by *de novo* functional annotation of differentially expressed ESTs

In order to functionally characterize the molecular components underlying adipogenesis in detail, comprehensive bioinformatics analyses of 780 differentially expressed ESTs were performed. A total of 659 protein sequences could be derived, and these were subjected to in-depth sequence analytic procedures. The protein sequences have been annotated *de novo* using 40 academic prediction tools integrated in the ANNOTATOR sequence analysis system. The structure and

function was annotated on a sequence segment/domain-wise basis. After extensive literature search and curation using the sequence architecture, 345 gene products were mapped onto known pathways, possible cellular roles, and subcellular localizations (Figure 4) using the PathwayExplorer web service [30] as well as manual literature and domain-based assignment. The results of the sequence analyses and additional information is available in the supplementary material available on our website [20] and Additional data files 6, 7, 8.

This molecular atlas of fat cell development provides the first global view of the underlying biomolecular networks and represents a unique resource for deriving testable hypotheses for future studies on individual genes. Below we demonstrate the usefulness of the atlas by highlighting the following: established regulators of fat cell development, recently discovered fat cell gene products, and candidate transcription factors expressed during adipogenesis. The numbering of the genes is given according to the *de novo* functional annotation (Additional data file 7).

Established regulators of fat cell development

Key transcription factors SREBF1 (*Srebf1* [number 119, cluster 9]) and PPARγ (*Pparg* [number 592, cluster 6]) were highly expressed during the late phase of differentiation. PPARγ [31] (*Pparg* [number 592, cluster 6]) is increasing up to about 15-fold. *Srebf1* processing is inhibited by insulin-induced gene 1 (*Insig1* [number 62, cluster 3/4]) through binding of the SREBP cleavage-activation protein [32,33]. *Insig1* is regulated by *Srebf1* and *Pparg* at the transcriptional level [34] and the expression of known marker genes of the differentiated adipocyte was increased in parallel with these factors. These include genes from clusters 3, 6, and 9 that are targets of either of these factors: lipoprotein lipase (*Lpl* [number 14, cluster 6]), c-Cbl-associated protein (*Sorbs1* [number 92, cluster 6]), stearoyl-CoA desaturase 1 (*Scd1* [number 305, cluster 6]), carnitine palmitoyltransferase II (*Cpt2* [number 43, cluster 9]), and acyl-CoA dehydrogenase (*Acadm* [number 153, clusters 6 and 9]).

Recently discovered fat cell gene products

During the preparation of the manuscript, a number of factors shown to be important to adipocyte function were identified *in vivo*. All of these factors, which have a possible role in the pathogenesis of obesity and insulin resistance, were highly expressed in the present study. Adipose triglyceride lipase (*Pnpla2* [number 157, cluster 6]), a patatin domain-containing triglyceride lipase that catalyzes the initial step in triglyceride hydrolysis [35], was more than 20-fold upregulated at the terminal differentiation phase. Another example is Visfatin, which is identical to the pre-B cell colony-enhancing factor (*Pbef* [number 327, cluster 9]). This 52 kDa cytokine has enzymatic function in adipocytes, exerts insulin-mimetic effects in cultured cells, and lowers plasma glucose levels in mice by binding to the insulin receptor [36-38]. The imprinted gene mesoderm-specific transcript (*Mest* [number 17, cluster 6/9]), which appears to enlarge adipocytes and could be a novel marker of the size of adipocytes [12], is upregulated during the late stage of 3T3-L1 differentiation.

Members of the Krüppel-like factor (Klf) family, also known as basic transcription element binding proteins, are relevant within the context of adipocyte differentiation. Klf2 was shown to inhibit PPARγ expression and to be a negative regulator of adipocyte differentiation [39]; Klf5 [40], Klf6 [41], and Klf15 [42] have been demonstrated to induce adipocyte differentiation. Whereas Klf9 (*Bteb1* [number 6, cluster 9]) was upregulated in the intermediate phase in the present study, Klf4 (number 100, cluster 12), which was shown to exert effects on cell proliferation opposing those of Klf5 [43], was downregulated. Another twofold upregulated player is Forkhead box O1 (*Foxo1* [number 53, cluster 9]), which mediates effects of insulin on the cell. Activation occurs before the onset of terminal differentiation, when Foxo1 becomes dephosphorylated and localizes to the nucleus [44,45]. The glucocorticoid-induced leucine zipper (*Tsc22d3*/*Gilz* [number 173, cluster 2]) functions as a transcriptional repressor of PPARγ and can antagonize glucocorticoid-induced adipogenesis [46,47]. This is consistent with our observation that Gilz is highly upregulated during the first two days, when dexamethasone is present in the medium, and downregulated at the end of differentiation, when PPARγ is highly induced. C/EBP homologous protein 10 (*Ddit3* [number 498, cluster 3]), another type of transcriptional repressor that forms nonfunctional heterodimers with members of the C/EBP family, was early induced and then downregulated. This might be sufficient to restore the transcriptional activity of C/EBPβ and C/EBPδ [42]. The transcription factor insulinoma-associated 1 (*Insm1* [number 238, cluster 8]) is associated with differentiation into insulin-positive cells and is expressed during embryo development, where it can bind the PPARγ target Cbl-associated protein (*Sorbs1* [number 92, cluster 6]; upregulated after induction) [48,49].

Candidate transcription factors expressed during adipogenesis

Because knowledge of the transcriptional network during adipogenesis is far from complete, expression profiles have been generated and screened for candidate transcription factors [8,9,12]. Here, we identified a number of transcription factors

Figure 4 *(see following page)*
Cellular localization of gene products. Shown are the cellular localizations of gene products involved in (**a**) metabolism and (**b**) other biological processes during fat cell differentiation. Gene products are color coded for each of the 12 clusters (key given to the left of the figure). The numbering is given according to the *de novo* functional annotation (Additional data files 6, 7, 8).

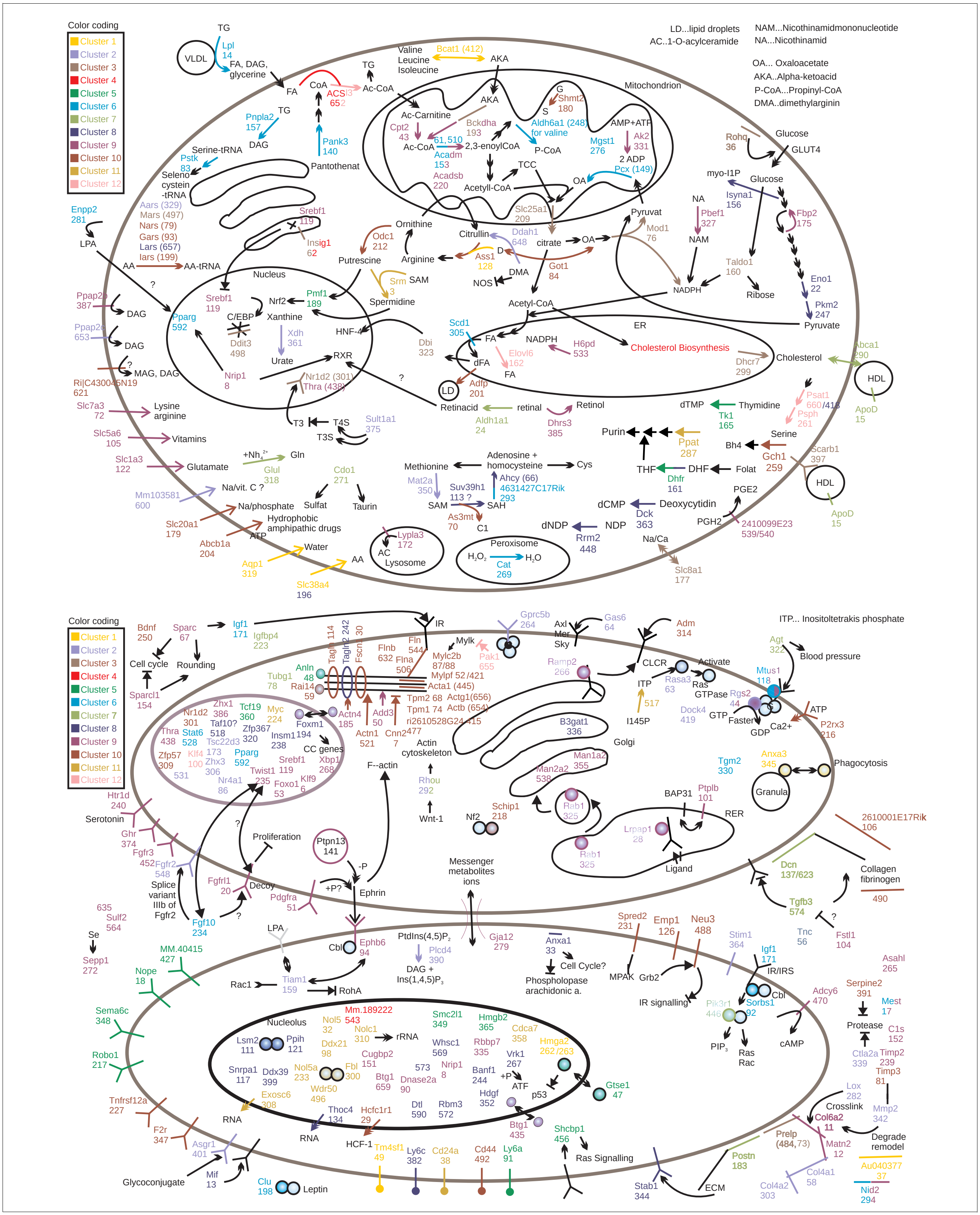

Figure 4 (see legend on previous page)

the exhibit distinct kinetic profiles during adipocyte differentiation that were previously not functionally associated with adipogenesis. Two transcription factors were unique to the present study (Zhx3 and Zfp367), and three more were confirmed (Zhx1, Twist1 and Tcf19) and annotated in the pathway context.

We found evidence for a role of the zinc finger and homeobox protein 3 (*Zhx3* [number 306, cluster 2]). Zhx3 as well as Zinc finger and homeobox protein 1 (*Zhx1* [number 386, cluster 9]) might attach to nuclear factor Y, which in turn binds many CCAAT and Y-box elements [50]. We also provide data regarding the expression of zinc finger protein 367 (*Zfp367* [number 320, cluster 8]) during adipogenesis. The molecular function of Zfp367 is as yet uncharacterized.

Additionally, we provide further experimental evidence and pathway context for candidate transcription factors previously identified in microarray screens [9,12], namely Twist1 and Tcf19. The Twist gene homolog 1 (*Twist1* [number 235, cluster 9]) was about two- to threefold upregulated at 0 hours, 72 hours, 7 days, and 14 days. Twist1 is a reversible inhibitor of muscle differentiation [51]. Heterozygous double mutants (*Twist1*$^{-/+}$, *Twist2*$^{-/+}$) exhibit loss of subcutaneous adipose tissue and severe fat deficiency in internal organs [52]. Twist1 is a downstream target of nuclear factor-κB and can repress transcription of tumor necrosis factor-α, which is a potent repressor of adipogenesis [52,53]. The differential expression during adipogenesis of Tcf19 was also confirmed in the present study. Tcf19 is a transcription regulator that is involved in cell cycle processes at later stages in cell cycle progression [54]. Expression of other regulators that are involved in the same process support this observation. Forkhead box M1 (*Foxm1* [number 194, cluster 8]) stimulates the expression of cell cycle genes (for instance the genes encoding cyclin B1 and cyclin B2, and *Cdc25B* and *Cdk1*). In addition, TAF10 RNA polymerase II, also known as TATA box binding protein-associated factor (*Taf10* [number 518, cluster 8]), is involved in G_1/S progression and cyclin E expression [55].

Correspondence between phenotypic changes and gene expression

In addition to the metabolic networks, the molecular atlas also provides a bird's eye view of other molecular processes, including signaling, the cell cycle, remodeling of the extracellular matrix, and cytoskeletal changes. Changes that occur during adipogenesis (phenotypically seen as rounding of densely packed cells) have aspects in common with other tissue differentiation processes such as endothelial angiogenesis (protease, collagen, and noncollagen molecule secretion) [56] and specific features. Here we show that phenotypic changes that occur in maturing adipocytes are paralleled by expression of the respective genes.

Extracellular matrix remodeling

Matrix metalloproteinase-2 (*MMP-2* [number 342, cluster 2]) was strongly upregulated during the entire process of adipocyte differentiation. Matrix metalloproteinase-2 can cleave various collagen structures and its inhibition can block adipogenesis [57]. Tissue inhibitor of metalloproteinase-2 (*Timp2* [number 239, cluster 9]), a known partner of matrix metalloproteinase-2, which balances the activity of the proprotease/protease [58], was mainly upregulated. Decreased levels of tissue inhibitor of metalloproteinase-3 (number 81, cluster 10; upregulated at 6 hours and repressed after 12 hours) are associated with obese mice [59]. New collagen structures of overexpressed *Col6a2* (number 11, cluster 9), *Col4a1* (number 58, cluster 2) and *Col4a2* (number 303, cluster 2) [60] are cross-linked by the lysyl oxidase (*Lox* [number 282, cluster 2]; upregulated during adipogenesis, which is contrary to findings reported by Dimaculangan and coworkers [61]). Strongly upregulated decorin (*Dcn* [number 137/623, cluster 7]) and osteoblast specific factor 2 (*Postn*/*Osf-2* [number 183, cluster 7]), as well as proline arginine-rich end leucine-rich repeats (*Prelp* [number 73/484, cluster 3]; upregulated in the final stages of adipogenesis), attach the matrix to the cell. Matrillin-2 (*Matn2* [number 12, cluster 9]; upregulated during adipogenesis) functions as adaptor for noncollagen structures [62], as does nidogen 2 (*Nid2* [number 294, clusters 6 and 9]; increasingly upregulated). Secreted protein acidic and rich in cysteine/osteonectin (*SPARC* [number 67, cluster 9]; mainly upregulated) and SPARC-like 1 (*Sparcl1* [number 154, cluster 9]; upregulated at 0 hours, 72 hours, 7days, and 14 days) can organize extracellular matrix remodeling, inhibit cell cycle progression, and induce cell rounding in cultured cells [63,64].

Reorganization of the cytoskeleton

Most cytoskeletal proteins are coexpressed in cluster 10 (not repressed from 6 to 12 hours) and might have a common regulatory mechanism. Transcription of actin α (*Acta1* [number 445, cluster 10]) and actin γ (*Actg1* [number 656, cluster 10]), tubulin α (*Tuba4* [number 377, cluster 8]), and tubulin β (*Tubb5* [number 110, cluster 8]) were found to diminish during differentiation, which is in agreement with other reports [65]. Myosin light chain 2 (*Mylc2b*/*Mylpf* [number 87/88/52/421, cluster 10]), and tropomyosin 1 and 2 (*Tpm1*/*Tpm2* [number 74/68, cluster 10]) are members of the mainly repressed cluster 10. The downregulated transgelin 1 and 2 (*Tagln*/*Tagln2* [number 114/242, cluster 10/8]) as well as fascin homolog 1 (*Fscn1* [number 30, cluster 10]) are known actin-bundling proteins [66,67]. Apparently, their absence decreases the cross-linking of microfilaments in compact parallel bundles. Calponin 2 (*Cnn2* [number 7, cluster 10]), a regulator of cytokinesis, is downregulated [68]. The insulin receptor and actin binding proteins filamin α and β (*Flna*/*Flnb* [number 506/632, cluster 10]) can selectively inhibit the mitogen-activated protein kinase signaling cascade of the insulin receptor [69]. Finally, the maintenance protein ankycorbin (*Rai14* [number 59, cluster 10]) and the cross-

Table 1

Activated metabolic pathways during adipocyte differentiation and their key enzymes (rate limiting steps)

Pathway	Enzyme/Protein name	Accession number	Number	Cluster
Urea cycle and arginine-citrulline cycles	Arginine succinate synthase	NP_031520	128	1/10
Phosphatidylinositol	Phosphatidylinositol 3-kinase, regulatory subunit, polypeptide 1	XP_127550	446	7
	Myoinositol 1-phosphate synthase A1	NP_076116	156	8
Cholesterol biosynthesis/keto-body synthesis	3-hydroxy-3-methylglutaryl-CoA synthase 1	NP_666054	178	4
	3-hydroxy-3-methylglutaryl-CoA reductase	XP_127496	619	12
Triglyceride hydrolysis (fatty acid assimilation)	Lipoprotein lipase (LPL)	NP_032535	14	6
β-Oxidation	Acetyl-CoA dehydrogenase (Acad)	NP_780533	61	6
	Acetyl-CoA dehydrogenase, medium chain (Acadm)	NP_031408	153	6/9
	Isovaleryl-CoA dehydrogenase (Acad)	Mm.6635	510	6
	Acyl-CoA dehydrogenase, short/branched chain (Acadsb)	NP_080102	220	9
Triglyceride metabolism	Adipose triglyceride lipase (Pnpla2/Atgl)	NP_080078	157	6
CoA biosynthesis	Pantothenate kinase 3	NP_666074	140	6
Anaplerotic processes	Pyruvate carboxylase	NP_032823	149	6
Branched chain amino acid metabolism (AKA metabolism)	Branched chain ketoacid dehydrogenase E1, α polypeptide	NP_031559	193	3/9
Methylation	S-adenosylhomocysteine hydrolase	NP_057870	66	8
	Methionine adenosyltransferase II, α	NP_663544	350	2
Unsaturated fatty acid biosynthesis	Stearoyl-CoA desaturase 1	NP_033153	305	6
Nucleotide metabolism	Xanthine dehydrogenase	NP_035853	361	2
Taurin biosynthesis	Cysteine dioxygenase	NP_149026	271	7
NH_4^+ metabolism/glutamate	Glutamate-ammonia ligase (glutamine synthase)	NP_032157	318	7
Glycolysis	Pyruvate kinase 3	NP_035229	247	8
Substrate cycle (glycolysis/gluconeogenesis)	Fructose bisphosphatase 2	NP_032020	175	9
Nucleotide biosynthesis	Deoxycytidine kinase	NP_031858	363	8
	Ribonucleotide reductase M2	NP_033130	448	8
Pentose phophate shunt	Hexose-6-phosphate dehydrogenase (AI785303)	XP_181411	533	9
NAD(P) biosynthesis	Pre-B-cell colony-enhancing factor	NP_067499	327	9
Polyamine biosynthesis	Ornithine decarboxylase, structural	NP_038642	212	10
Tetrahydrobiopterin biosynthesis	GTP cyclohydrolase 1	NP_032128	259	10
Purin biosynthesis	Phosphoribosyl pyrophosphate amidotransferase	NP_742158	287	11
Asparagine biosynthesis	Asparagine synthetase	NP_036185	109	12
Long chain fatty acids	ELOVL family member 6, elongation of long chain fatty acids	NP_569717	162	12
Serine biosynthesis	Phosphoserine phosphatase	NP_598661	261	12
Gluconeogenesis	PEPCK 2 (Riken 9130022B02)	NP_083270	393	12
Prostaglandin E biosynthesis	Prostaglandin E synthase (ri|2410099E23; ri|9230102G02)	ri|2410099E23 ri|9230102G02	539 540	9

CoA, coenzyme A.

linking protein actinin 1 (*Actn1* [number 521, cluster 10]) share the mainly repressed expression profile. Tubulin γ 1 (*Tubg1* [number 78, cluster 7]; upregulated during adipogenesis, about 42-fold at 6 hours) is not a component of the microtubules like *Tuba*/*Tubb*, but it plays a role in organizing their assembly and in establishing cell polarity [70]. Actinin 4 (*Actn4* [number 185, cluster 9]; upregulated throughout adipogenesis) differs from *Actn1* in its localization. Its expression leads to higher cell motility, and it can be translocated into the nucleus upon phosphatidylinositol 3-kinase inhibition [71]. Adducin 3γ (*Add3* [number 50, cluster 9]; permanently upregulated) has different actin-associated cytoskeletal roles.

T-lymphoma invasion and metastasis 1 (*Tiam1* [number 159, cluster 2]) is a guanine nucleotide exchange factor of the small GTPase Rac1, which regulates actin cytoskeleton, morphology and adhesion, and antagonizes RhoA signaling [72,73]. Additionally, the putative constitutive active Rho GTPase ras homolog gene family, member U/Wnt1 responsive Cdc42 homolog (*Rhou/Wrch-1* [number 292, clusters 2 and 7]), which has no detectable intrinsic GTPase activity and very high nucleotide exchange capacity, leads to an phenotype of mature adipocyte [74,75]. Interplay between *Rhou* and *Tiam1*, which might reverse *Rhou* activity through Rac1 signaling [74], could be a mechanism for regulating cell morphology in adipogenesis.

In summary, the evidence presented above suggests that reduced replenishment of the cytoskeleton with building blocks and the strong transcriptional upregulation of modulating proteins, together with the extracellular remodeling, are responsible for the morphological changes that occur during differentiation of 3T3-L1 cells.

Regulation of metabolic networks at the transcriptional level via key points of pathways

We next used the molecular atlas to derive novel biological insights from the global view of molecular processes. We analyzed transcriptionally regulated genes that are members of 36 different metabolic pathways. Within each pathway, we considered whether these transcriptionally regulated genes occupy key positions, such as a position at the pathway start, which is the typical rate-limiting step where the amount of enzyme is critical [76], or at some other point of regulation. We found that such key positions are occupied by transcriptionally regulated targets in 27 pathways (an overview is provided in Table 1). Those pathways that are strongly transcriptionally regulated at key points are illustrated in Figure 5 at the time points 0, 24 and 48 hours, and 14 days. For additional time points and images with more detailed information from all investigated pathways, see our website [20] and Additional data files Additional data file 31 and Additional data file 32.

In the following discussion we present the evidence for transcriptional regulation at key points for five selected metabolic pathways. Further information on other pathways can be found in Additional data files 31, 32, 33, 34, 35, 36, 37, 38 and on our website [20].

Biosynthesis of the important lipogenic cofactors CoA and NAD(P)+ are transcriptionally regulated at their key enzymes

Coenzyme A (CoA) is the carrier of the fatty acid precursor acetate/malonate [77,78]. Panthotenate kinase 3 (*Pank3* [number 140, cluster 6]; about eightfold upregulated) is responsible for the first and rate-limiting step in converting panthotenate to CoA [79]. Nicotinamide adenine dinucleotide phosphate (reduced form; NADPH) is necessary in reductive reactions for fatty acid synthesis. Pre-B-cell colony-enhancing factor (*Visfatin/Pbef1* [number 327, cluster 9]; strongest upregulated in the last three points of the time course in parallel with the emergence of fat droplets) is the rate-limiting enzyme in NAD(P)+ biosynthesis [38,80]. For reduction of NADP+ to NADPH, two major mechanisms are responsible: the pentose phosphate shunt and the tricarboxylate transport system. Hexose-6P dehydrogenase (*H6pd* [number 533, cluster 9]; upregulated throughout adipogenesis) is the rate limiting enzyme of the pentose phosphate shunt in the endoplasmic reticulum and provides NADPH to its lumen [81]. In the cytosolic pendant in the pentose phosphate shunt, the transaldolase (*Taldo1* [number 160, cluster 3]) is repressed at early stages and is about threefold upregulated at the end of 3T3-L1 differentiation. This expression change appears to switch the shunt between ribose-5-phosphate (for nucleic acid synthesis) and NADPH (for fatty acid production) synthesis at early and late time points, respectively. A similar expression profile is observed for the cytosolic NADP-dependent malic enzyme (*Mod1* [number 76, cluster 3]) and the citrate transporter (*Slc25a1/Ctp1* [number 209, cluster 3]). Both are part of the tricarboxylate transport system through the mitochondrial membrane. Transcription of the anaplerotic pyruvate carboxylase (*Pcx* [number 149, cluster 6]; activated by acetyl-CoA) is increasingly upregulated up to 16-fold toward the final two time points.

Fatty acid modification and assimilation is transcriptionally regulated at the rate-limiting steps

The transcriptional expression of stearoyl-CoA desaturase 1 (*Scd1* [number 305, cluster 6]), which catalyzes the rate-limiting reaction of monounsaturated fatty acid synthesis and which is an important marker gene of adipogenesis [82,83], is downregulated at induction but increases up to 60-fold with advancing adipogenesis. In contrast to previous reports [82], we found that the gene for elongation of long-chain fatty acid (*Elovl6* [number 162, cluster 12]) protein, which may be the rate-limiting enzyme of long chain elongation to stearate [84], is not overexpressed in differentiated 3T3-L1 cells as in adipose tissue. *Elovl6* appears repressed during the entire process of adipogenesis in 3T3-L1 cells. Expression of lipoprotein lipase (*Lpl* [number 14, cluster 6]), the rate-limiting enzyme of extracellular triglyceride-rich lipoprotein hydrolyzation and triglyceride assimilation [85-87], increases with time up to 21-fold in differentiated adipocytes.

Transcriptional regulation of triglyceride and fatty acid degradation is performed at key points

Adipose triglyceride lipase (*Pnpla2/Atgl* [number 157, cluster 6]) executes the initial step in triglyceride metabolism [35]. Its expression increases strongly with differentiation progression. Acyl-CoA dehydrogenases (*Acadm/Acadsb* [number 153/220, clusters 6 and 9]) [88], the rate-limiting enzymes of medium, short and branched chain β-oxidation, are strongly upregulated in the final four time points. In contrast, the acyl-CoA dehydrogenase (*Acadvl*) of very long chain fatty acids is not in the set of distinctly differentially regulated genes, and

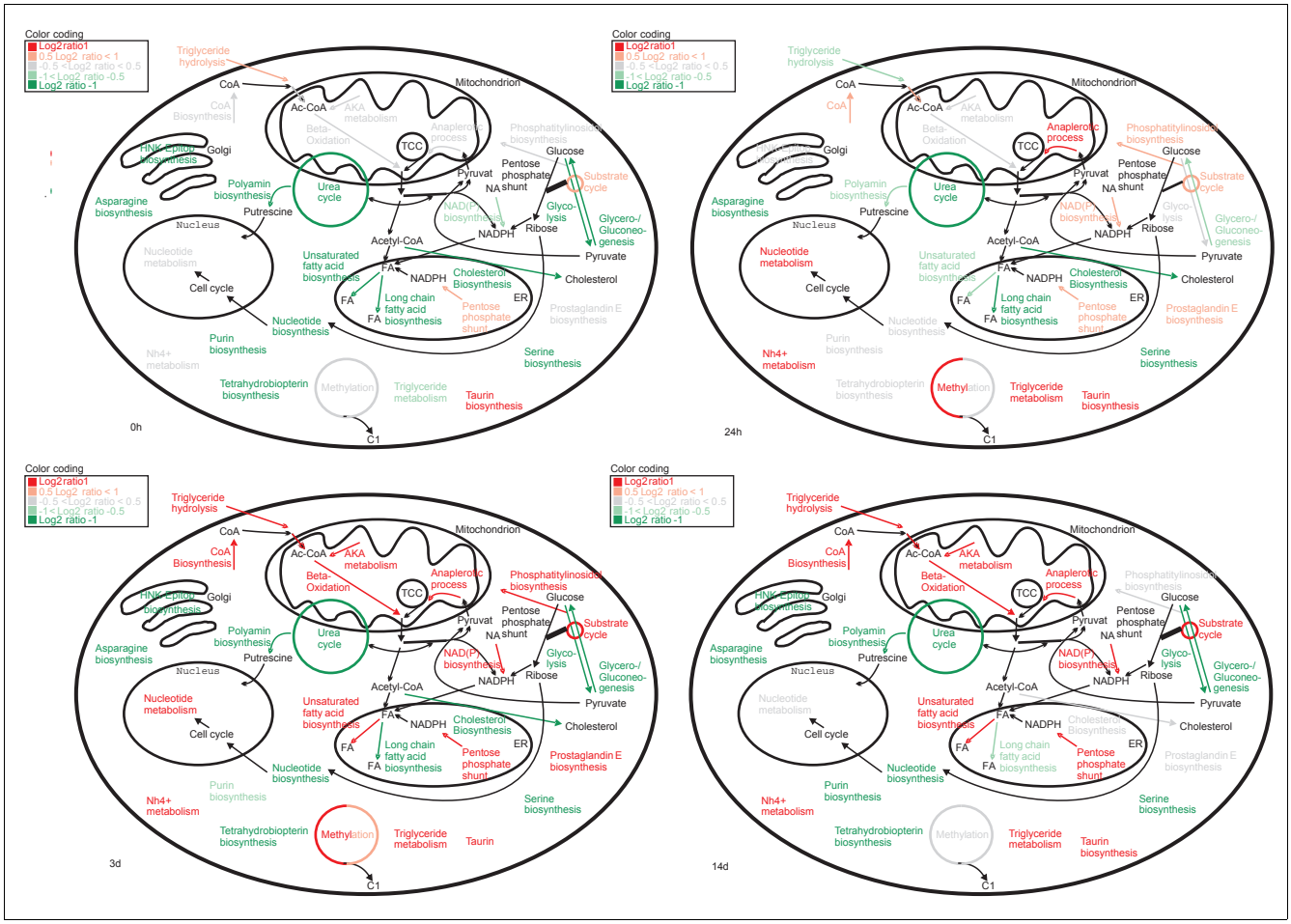

Figure 5
Temporal activation of metabolic pathways. Summarized is the activation of metabolic pathways at different time points (0 hours, 24 hours, 3 days, and 14 days) during fat cell differentiation. Color codes are selected according to expression levels of key enzymes in these pathways at distinct time points (red = upregulated; green = downregulated).

exhibits some upregulation at the final two time points. This difference in expression might shift the enrichment from short and medium to long chain fatty acids during adipogenesis. Branched chain ketoacid dehydrogenase E1 (*Bckdha* [number 193, clusters 3 and 9]) is the rate-limiting enzyme of leucine, valine, and isoleucine catabolism and is known to be inhibited by phosphorylation [89]. Its gene shares a similar expression profile with the *Acad* genes. The elevated degradation of amino acids allows conversion to fatty acids through acetyl-CoA.

Several important nucleotide biosynthetic pathway enzymes follow a cell cycle specific expression profile (strongly repressed except between 12 and 24 hours)

Phosphoribosylpyrophosphate amidotransferse (*Ppat* [number 287, cluster 11]) [90] is rate-limiting for purin production. Deoxycytidine kinase (*Dck* [number 363, cluster 8]) is the rate-limiting enzyme of deoxycytidine (dC), deoxyguanosine (dG) and deoxyadenosine (dA) phosphorylation [91-93]. Ribonucleotide reductase M2 (*Rrm2* [number 448, cluster 8]) converts ribonucleotides to desoxyribonucleotides [94,95]. Additionally, thymidine kinase 1 (*Tk1* [number 165, cluster 5]) and dihydrofolate reductase (*Dhfr* [number 161, cluster 5/8]) play important roles in dT and purin biosynthesis during the cell cycle. In contrast, purin degradation is about sixfold upregulated between 6 and 72 hours by the rate-limiting xanthine dehydrogenase (*Xdh* [number 361, cluster 2]) [96,97]. These findings are in concordance with those of a previous study [22], which showed that mitotic clonal expansion is a prerequisite for differentiation of 3T3-L1 preadipocytes into adipocytes. After induction of differentiation, the growth-arrested cells synchronously re-enter the cell cycle and undergo mitotic clonal expansion, as monitored by changes in cellular DNA content [22]. In accord with this experimental evidence, we observed changes in cell cycle genes, most of which were in clusters 5 and 8 (see our website [20] and Additional data file 37).

Table 2

Transcription factors that could regulate co-expressed genes in each cluster

Binding factors	Over-represented cluster	CS	FE	Putative target genes	Genes in cluster with promoter in PromoSer database	Putative target genes of all clusters
RORα1	Cluster 1	0.0322	0.0203	10	10	240
ATF	Cluster 2	0.0466	0.0481	15	27	133
CRE-BP1	Cluster 2	0.0050	0.0050	19	27	153
HLF	Cluster 2	0.0436	0.0452	15	27	132
XBP-1	Cluster 2	0.0378	0.0476	4	27	17
AhR	Cluster 2	0.0287	0.0446	3	27	9
Tal-1β/E47	Cluster 3	0.0400	0.0427	9	15	123
v-Maf	Cluster 4	0.0432	0.0308	2	12	11
SREBP-1	Cluster 4	0.0494	0.0484	9	12	166
Tal-1β/ITF-2	Cluster 5	0.0145	0.0169	19	46	89
Pbx-1	Cluster 5	0.0323	0.0206	45	46	312
NRF-2	Cluster 5	0.0310	0.0252	41	46	270
Sox-5	Cluster 5	-	0.0490	40	46	268
VBP	Cluster 5	0.0345	0.0276	42	46	281
NF-κB (p65)	Cluster 6	0.0354	0.0333	13	17	182
CCAAT box	Cluster 6	0.0458	0.0287	17	17	288
AP-2	Cluster 6	0.0330	0.0268	15	17	226
E4BP4	Cluster 8	0.0230	0.0243	31	69	113
CCAAT	Cluster 8	0.0211	0.0304	5	69	7
VBP	Cluster 8	0.0242	0.196	62	69	281
GC box	Cluster 9	-	0.0450	44	48	289
RREB-1	Cluster 10	0.0388	0.0435	13	42	65
SRF	Cluster 10	0.0221	0.0255	16	42	81
GC box	Cluster 10	0.0450	0.0366	39	42	289
Poly A downstream element	Cluster 11	0.0335	0.0431	5	13	55
E2	Cluster 12	0.0459	-	14	47	65

Probabilities for over-representation (<0.05) of genes having a predicted transcription factor binding site relative to the total of all clusters. CS, one-sided χ^2 test; FE, one-sided Fisher's exact test.

Cholesterol biosynthesis is regulated by expression of key steps and whole pathway segments

The synthesis of the early precursor molecule 3-hydroxy-3-methylglutaryl (HMG)-CoA, which might be also used in other metabolic pathways, is transcriptionally controlled at the key enzymes HMG-CoA synthase (*Hmgcs1* [number 178, cluster 4]; repressed except in terminal stages) and HMG-CoA reductase (*Hmgcr* [number 619, cluster 12]; always repressed), which is the rate-limiting enzyme of the cholesterol and mevalonate pathway [98,99]. After the step of isopentenylpyrophosphate synthesis, cholesterol biosynthesis genes are coexpressed in cluster 4.

Correspondence between coexpression and coregulation

To determine whether coexpressed genes are also coregulated, we analyzed the available promoter sequences of the 780 ESTs. Promoter sequences could be retrieved for 357 genes. Most ESTs are sequenced from the 3' end, and hence it is easier to retrieve the 3'-UTR. Retrieval of promoters is more difficult than retrieval of the 3'-UTR because of experimental problems in extracting full-length cDNAs (and hence transcription start sites) and insufficient computational methods for identifying beginning of the 5'-UTR. We analyzed the occurrences of the binding sites of all transcription factors in vertebrates from the TRANSFAC database. Based on statistical analyses, among transcription factors with binding site motifs described in TRANSFAC [100] those listed in

Table 3

Significance of occurrence of predicted SREBP-1 binding sites in the promoters of co-expressed genes identified by clustering

SREBP-1	Putative target genes	Genes in cluster	Against total PromoSer database		Against total of all clusters	
			CS	FE	CS	FE
Cluster 1	4	10	0.5000	0.7051	0.5339	0.7644
Cluster 2	11	27	0.5448	0.6892	0.6475	0.7812
Cluster 3	5	16	0.7076	0.8575	0.7697	0.8987
Cluster 4	9	12	0.0290	0.0289	0.0494	0.0484
Cluster 5	16	45	0.7787	0.8570	0.8568	0.9171
Cluster 6	10	20	0.1553	0.1554	0.2278	0.2277
Cluster 7	5	10	0.5000	0.5677	0.5000	0.6423
Cluster 8	31	66	0.2837	0.2827	0.4719	0.4711
Cluster 9	12	42	0.9025	0.9454	0.9414	0.9708
Cluster 10	22	41	0.1635	0.1635	0.2881	0.2877
Cluster 11	8	15	0.3230	0.3204	0.4057	0.4041
Cluster 12	25	45	0.0398	0.0404	0.1014	0.1014
PromoSer	5,456	12,493				

Probabilities for over-representation (<0.05) of genes having a predicted SREBP-1 site relative to all unique regulated genes of PromoSer and to the total of all clusters. Cluster 4 is the only one with significantly increased occurrence of predicted SREBP-1 binding sites. CS, one-sided χ^2 test; FE, one-sided Fisher's exact test; SREBP, sterol-regulatory element binding protein.

Table 2 are the most promising candidates for further functional studies on transcriptional regulation.

One example of a functional transcription factor binding site is SREBP-1 in cluster 4. A comparison among clusters showed that cluster 4 has significantly more genes with a SREBP-1 (SRE and E-box motifs [101]) binding site than all other clusters (P = 0.0484, Fisher's exact test; Table 3). Similarly, a putative SREBP-1 regulatory region is significantly more frequent in the promoters of the genes in cluster 4 compared with all unique sequences in the PromoSer database (P < 0.0289; PromoSer contains 22,549 promoters of 12,493 unique sequences). For a subset of the genes in cluster 4 with predicted SREBP-1 binding site (most genes of the cholesterol biosynthesis pathway), transcriptional regulation with SREBP-1 has been experimentally proven [102].

Surprisingly, binding sites for the key regulators of adipogenesis, namely PPAR and C/EBP, are not significantly over-represented in any of the promoters of the coexpressed genes. We generated a novel matrix for PPAR using 22 experimentally verified binding sites from the literature and analyzed the promoters of the coexpressed genes and all PromoSer promoters. Again, using this matrix the PPAR binding sites were not significantly over-represented.

Genomic position of coexpressed genes

Finally, we considered whether coexpressed genes also colocalize on the chromosomes. In a broad genomic interval (5 megabases [Mb]) on each mouse chromosome we mapped the ESTs from each cluster. Unexpectedly, our data do not support the observation of the highly significant correlation in the expression and genomic positioning of the genes. A typical example of mapped ESTs to chromosome 10 is illustrated in Figure 6, showing that expression levels of colocalized ESTs are divergent because only two mapped ESTs are members of the same cluster.

Additionally, we analyzed the genomic position of 5,205 ESTs that exhibited significant differentially expression between time points (P < 0.05; one-way ANOVA). These ESTs were grouped in 12 clusters, and we then searched for regions with three or more members in a genomic interval of 500 kilobases (kb). On average, 7 ± 5% of the ESTs from one cluster were colocalized. Comprehensive results of this analysis are accessible within the supplementary website [20] and Additional data files 42, 43, 44, 45.

In summary, these data do not provide evidence that colocalized genes in the genomic sequence are subject to the same transcriptional regulation (coexpression), as indicated by examples for different processes in other studies [103].

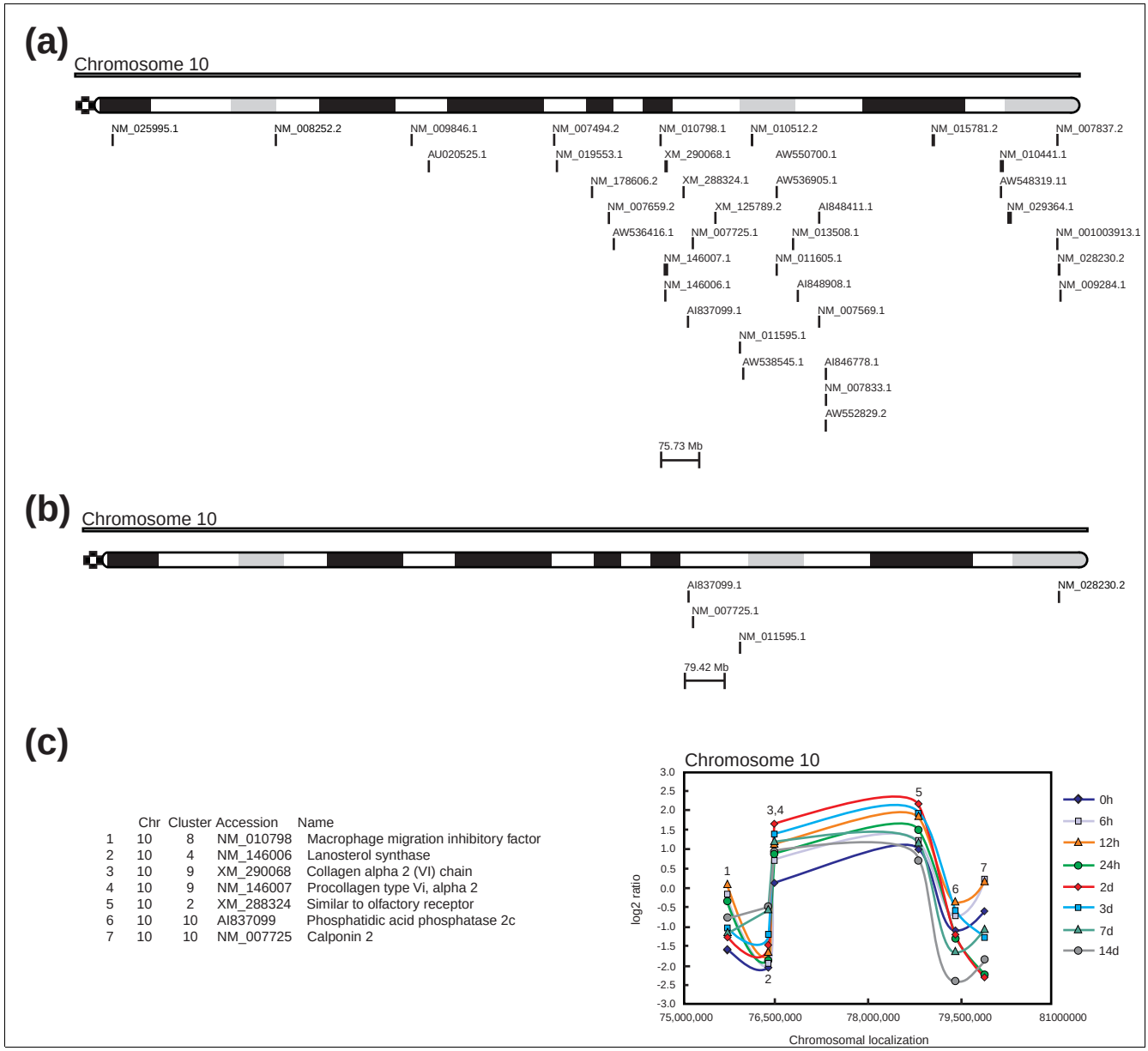

	Chr	Cluster	Accession	Name
1	10	8	NM_010798	Macrophage migration inhibitory factor
2	10	4	NM_146006	Lanosterol synthase
3	10	9	XM_290068	Collagen alpha 2 (VI) chain
4	10	9	NM_146007	Procollagen type Vi, alpha 2
5	10	2	XM_288324	Similar to olfactory receptor
6	10	10	AI837099	Phosphatidic acid phosphatase 2c
7	10	10	NM_007725	Calponin 2

Figure 6
Chromosomal localization analysis for ESTs found to be differentially expressed during fat cell differentiation. Chromosomal localization analysis for chromosome 10 from 780 ESTs shown to be more than two times upregulated or downregulated in a minimum of four time points during adipocyte differentiation. (**a**) Mapped ESTs to chromosome 10. (**b**) ESTs from cluster 10 mapped to chromosome 10. (**c**) Relative gene expression levels (log_2 ratios) at different time points for seven ESTs mapped within a genomic interval of 5 Mb from chromosome 10. EST, expressed sequence tag.

Discussion

The data presented here and the functional annotation considerably extend upon previous microarray analyses of gene expression in fat cells [8-14] and demonstrate the extent to which molecular processes can be revealed by global expression profiling in mammalian cells. Our strategy resulted in a molecular atlas of fat cell development and provided the first global view of the underlying biomolecular networks. The molecular atlas and the dissection of molecular processes suggest several important biological conclusions.

First, the data support the notion that there are hundreds of mouse genes involved in adipogenesis that were not previously linked to this process. Out of the 780 selected genes, 326 were not shared with previous studies [8,9,12], suggesting that our view of this process is far from complete. Using microarrays enriched with developmental ESTs, we were able

not only to identify new components of the transcriptional network but also to map the gene products onto molecular pathways. The molecular atlas we developed is a unique resource for deriving testable hypothesis. For example, we have identified several differentially expressed genes, including recently discovered gene products (Pnpla2, Pbef1, Mest) and transcription factors not previously detected in microarray screens (Zhx3 and Zfp367).

Second, from our global analysis of the potential role of miRNAs in fat cell differentiation, we were able to predict potential target genes for miRNAs in 71% of the 395 genes with a unique 3'-UTR that were differentially expressed during adipocyte differentiation. The distribution of predicted miRNA targets indicated that one miRNA may regulate many genes and that one gene can be regulated by a number of miRNAs. The function of the potential target genes was diverse and included transcription factors, enzymes, transmembrane proteins, and signaling molecules. Genes with the lowest number of over-represented miRNA motifs were cell cycle genes (clusters 5 and 8), whereas genes grouped in cluster 9 exhibited the most over-represented miRNA motifs in relation to the matches in the control set of all available 3'-UTR sequences. Genes in cluster 9 exhibited high expression values at time point 0 and may include genes relevant to the transition from pre-confluent to confluent cells. Genes in cluster 9 also represent molecular components that are involved in other cell processes, including extracellular matrix remodeling, transport, metabolism, and fat cell development (for example, *Foxo1* [44,45]). Genes in other clusters exhibited varying percentages of over-represented miRNA motifs and can be associated with diverse biological processes (Additional data file 6). As an example of functional miRNA targets, we showed that one signaling molecule of the ras family is a potential target of miRNAs, which is consistent with a previous observation in humans, in whom it was shown that the human RAS oncogene is regulated by the let-7 miRNA. This example indicates that the present analysis provides promising candidates ranked according to their significance of over-representation and the number of different miRNAs that might regulate these targets in the specific context of adipocyte differentiation. It should be noted that our analysis included only known miRNAs, suggesting that the number of target sites can be even higher. This striking observation could have implications for post-transcriptional regulation of other developmental processes. Microarrays for the analysis of miRNA expression are becoming available and future studies will shed light on the role of miRNAs in the context of cell differentiation.

Third, we were also able to characterize the mechanisms and gene products involved in the phenotypic changes of pre-adipocytes into mature adipocytes. Although the number of selected genes in this study was limited, we characterized gene products for extracellular matrix remodeling and cytoskeletal changes during adipogenesis. Other molecular components involved in these processes can be identified by mapping the characterized gene products onto curated pathways [30] and selecting missing candidates for further focused studies. Notably, most of the cytoskeletal proteins are coexpressed in cluster 10 and might have a common regulatory mechanism. Further computational and experimental analyses are needed to verify this hypothesis.

In addition to new information about fat cell development, our comprehensive analysis has provided new general biological insights that could only be derived from such a global analysis. First, we were able to examine at what points metabolic pathways were regulated. The global view of biological processes and networks derived from expression profiles showed that the metabolic networks are transcriptionally regulated at key points, usually the rate-limiting steps. This was the case in 27 out of the 36 metabolic pathways analyzed in this study. During the development of mature adipocytes from pre-adipocytes, distinct metabolic pathways are activated and deactivated by this molecular control mechanism. For example, at the beginning nucleotide metabolism is activated because the cells undergo clonal expansion and one round of the cell cycle (see out website [20] and Additional data file 37). At the end of development, major metabolic pathways for lipid metabolism are upregulated, including β-cell oxidation and fatty acid synthesis (Figure 5). Cell development is a dramatic process in which the cell undergoes biochemical and morphological changes. In our study signals at every time point could be detected from more than 14,000 ESTs. Thus, regulating metabolic networks at key points represents an energy efficient way to control cellular processes. Metabolic networks might be activated/inactivated in a similar manner in other types of cellular differentiation, such as myogenesis or osteogenesis. It is intriguing to speculate that signaling networks are also transcriptionally regulated at key points. However, as opposed to the metabolic networks, it is difficult to verify this hypothesis because the key points are not clearly identifiable due to both the interwoven nature and the partial incompleteness of the signaling pathways.

A second general biological insight derived from our global analysis is that we found that many genes were upregulated by well known transcription factors that nevertheless lacked anything resembling the established upstream promoter consensus sites. Over-represented binding sites for key regulators such as PPAR and C/EBP were not detectable with the TRANSFAC matrices. Even the use of a matrix based on all currently available experimentally validated sequences, such as PPAR, did not result in a significant hit. Hence, only few sequences contain this motif in their promoters. These results demonstrate either that much more sophisticated methods must be developed or that there are many cases where the current methods do not perform well because other aspects such as chromatin determine the recognition site.

A third general piece of information derived from our global analysis is the finding that coexpressed genes in fat cell development are not clustered in the genome. Previous studies identified a number of such cases in a range of organisms, including yeast [104], worms [105], and flies [106]. This observation of significant correlation in the expression and genomic position of genes was recently reported in the mouse [103]. In the present study we could not identify groups of genes with similar expression profiles, for instance within the same cluster within 5 Mb regions on the chromosomes. Our results suggest that such clustering may not be as widespread as may be presumed by extrapolating from previous studies. However, coexpressed genes could have distant locations and still be spatially colocalized due to DNA looping and banding, as was recently shown in a microscopy study [107]. A higher order chromatin structure of the mammalian transcriptome is an emerging concept [108], and new methods are required to examine the correlation between gene activity and spatial positioning.

The biological insights gained in this study were only possible with in-depth bioinformatics analyses based on segment and domain predictions. Distribution of GO terms permits a first view of the biological processes, molecular functions, and cellular components. However, in our work more than 40% of the ESTs could not be assigned to GO terms. Moreover, detailed information about the specific functions cannot be extracted. For example, the GO term 'DNA binding' could be specified by 'zinc-finger domain binding protein' only by in-depth analyses. Hence, de novo functional annotation of ESTs using integrated prediction tools and subsequent curation of the results based on the available literature is not only necessary to complete the annotation process but also to reveal the actual biological processes and metabolic networks. Although the number of protein sequences to which a GO term can be assigned is steadily increasing, specific and detailed annotation is only possible with de novo functional annotation.

Conclusion

In the present study we demonstrate that, despite the limitations due to mRNA abundance (many thousands of genes are never transcribed above threshold) and insufficient sensitivity, large-scale gene expression profiling in conjunction with sophisticated bioinformatics analyses can provide not only a list of novel players in a particular setting but also a global view on biological processes and molecular networks.

Materials and methods

cDNA microarrays

The microarray developed here contains 27,648 spots with mouse cDNA clones representing 16,016 different genes (UniGene clusters). These include developmental clones (the 15 K NIA cDNA clone set from National Institute of Aging, US National Institutes of Health) and the 11 K clones from different brain regions in the mouse (Brain Molecular Anatomy Project [BMAP]). Moreover, 627 clones for adipose-related genes were selected using the TIGR Mouse Gene Index Build 5.0 [19]. These cDNA clones were obtained from the IMAGE consortium (Research Genetics, Huntsville, AL, USA). The inserts of the NIA and BMAP clones were sequence verified (insert size about 1-1.5 kb). All PCR products were purified using size exclusion vacuum filter plates (Millipore, Billerica, MA, USA) and spotted onto amino-silanated glass slides (UltraGAPS II; Corning, Corning, NY, USA) in a 4 × 12 print tip group pattern. As spotting buffer 50% dimethyl sulfoxide was used. Negative controls (genomic DNA, genes from *Arabidopsis thaliana*, and dimethyl sulfoxide) and positive controls (Cot1-DNA and salmon sperm DNA) were included in each of the 48 blocks. Samples were bound to the slides by ultraviolet cross-linking at 200 mJ in a Stratalinker (Stratagene, La Jolla, CA, USA).

Cell culture

3T3-L1 cells (American Type Culture Collection number CL-173) were grown in 100 mm diameter dishes in Dulbecco's modified Eagle's medium supplemented with 10% fetal bovine serum, 100 units/ml penicillin, 100 μg/ml streptomycin, and 2 mmol/l L-glutamine in an atmosphere of 5% carbon dioxide at 37°C. Two days after reaching confluence (day 0), cells were induced to differentiate with a two-day incubation of a hormone cocktail [109,110] (100 μmol/l 3-iso-butyl-1-methylxanthine, 0.25 μmol/l dexamethasone, 1 μg/ml insulin, 0.16 μmol/l pantothenic acid, and 3.2 μmol/l biotin) added to the standard medium described above. After 48 hours (day 2), cells were cultured in the standard medium in the presence of 1 μg/ml insulin, 0.16 μmol/l pantothenic acid, and 3.2 μmol/l biotin until day 14. Nutrition media were changed every second day.

Three independent cell culture experiments were performed. Cells were harvested and total RNA was isolated at the preconfluent stage and at eight time points (0, 6, 12 and 24 hours, and 3, 4, 7 and 14 days) with TRIzol reagent (Invitrogen-Life Technologies; Carlsbad, CA, USA) [111]. For each independent experiment, RNA was pooled from three different culture dishes for each time point and from 24 dishes at the preconfluent stage used as reference. The quality of the RNA was checked using Agilent 2100 Bioanalyzer RNA assays (Agilent Technologies, Palo Alto, CA, USA) by inspection of the 28S and 18S ribosomal RNA intensity peaks.

Labeling and hybridization

The labeling and hybridization procedures used were based on those developed at the Institute for Genomic Research [112] and detailed protocols can be viewed on the supplementary website [20]. Briefly, 20 μg total RNA from each time point was reverse transcribed in cDNA and indirectly labeled with Cy5 and 20 μg RNA from the preconfluent stage (reference) was indirectly labeled with Cy3, respectively. This procedure was repeated with reversed dye assignment. Slides

were prehybridized with 1% bovine serum albumen. Then, 10 μg mouse Cot1 DNA and 10 μg poly(A) DNA was added to the labeled cDNA samples and pair-wise cohybridized onto the slide for 20 hours at 42°C. Following washing, slides were scanned with a GenePix 4000B microarray scanner (Axon Instruments, Sunnyvale, CA, USA) at 10 μm resolution. Identical photo multiplier voltage settings were used in the scanning of the corresponding dye-swapped hybridized slides. The resulting TIFF images were analyzed with GenePix Pro 4.1 software (Axon Instruments).

Data preprocessing and normalization

Data were filtered for low intensity, inhomogeneity, and saturated spots. To obtain expression values for the saturated spots, slides were scanned a second time with lower photomultiplier tube settings and reanalyzed. All spots of both channels were background corrected (by subtraction of the local background). Different sources of systematic (sample, array, dye, and gene effects) and random errors can be associated with microarray experiments [113]. Nonbiological variation must be removed from the measurement values and the random error can be minimized by normalization [114,115]. In the present study, gene-wise dye swap normalization was applied. Genes exhibiting substantial differences in intensity ratios between technical replicates were excluded from further analysis based on a two standard deviation cutoff. The resulting ratios were $\log_2$ transformed and averaged over three independent experiments. The expression profiles were not rescaled in order to identify genes with high expression values. All experimental parameters, images, and raw and transformed data were uploaded to the microarray database MARS [116] and submitted via MAGE-ML export to a public repository (ArrayExpress [117], accession numbers A-MARS-1 and E-MARS-2). Differentially expressed genes were first identified using one-way ANOVA ($P < 0.05$). They were then subjected to a more stringent criterion; specifically, we considered only those genes with a complete temporal profile that were more than twofold upregulated or downregulated at a minimum of four time points. The twofold cutoff for differentially expressed genes was estimated by applying the significance analyses of microarrays method [118] to the biological replicates and assuming false discovery rate of 5%. In order to capture the dynamics of various processes, only ESTs differentially expressed in at least half of the time points were selected. Data preprocessing was performed with ArrayNorm [119].

Real-time RT-PCR

Microarray expression results were confirmed with RT-PCR. cDNA was synthesized from 2.5 μg total RNA in 20 μl using random hexamers and SuperScript III reverse transcriptase (Invitrogen, Carlsbad, CA, USA). The design of LUX™ primers for *Pparg*, *Lpl*, *Myc*, *Dec*, *Ccna2*, and *Klf9* was done using the Invitrogen web service (for sequences, see Additional data file 9 and our website [20]). Quantitative RT-PCR analyses for these genes were performed starting with 50 ng reverse transcribed total RNA, with 0.5× Platinum Quantitative PCR SuperMix-UDG (Invitrogen, Carlsbad, CA, USA), with a ROX reference dye, and with a 200 nmol/l concentration of both LUX™ labeled sense and antisense primers (Invitrogen, Carlsbad, CA, USA) in a 25 μl reaction on an ABI PRISM 7000 sequence detection system (Applied Biosystems, Foster City, CA, USA). To measure PCR efficiency, serial dilutions of reverse transcribed RNA (0.24 pg to 23.8 ng) were amplified. Ribosomal 18S RNA amplifications were used to account for variability in the initial quantities of cDNA. The relative quantification for any given gene with respect to the calibrator (preconfluent stage) was determined using the $\Delta\Delta C_t$ method and compared with the normalized ratios resulting from microarray experiments.

Clustering and gene ontology classification

Common unsupervised clustering algorithms [120] were used for clustering expression profiling of 780 selected ESTs, according to the log ratios from all time points. Using hierarchical clustering the boundaries of the clusters were not clearly separable and required arbitrary determination of the branching point of the tree, whereas the results of the clustering using self-organized maps led to clusters with highly divergent number of ESTs (between 3 and 242). We have therefore used the k means algorithm [121] and Euclidean distance. The number of clusters was varied from k = 1 to k = 20, and predictive power was analyzed with the figure of merit [122]. Subsequently, k = 12 was found to be optimal. To evaluate the results of the k means clustering, principal component analysis [123] was applied and exhibited low intracluster distances and high intercluster dissimilarities. GO terms and GO numbers for molecular function, biological process, and cellular components were derived from the Gene Ontology database (Gene Ontology Consortium) using the GenPept/RefSeq accession numbers for annotated proteins encoded by selected genes (ESTs). All cluster analyses and visualizations were performed using Genesis [124].

De novo annotation of ESTs

For each of the 780 selected EST sequences, we attempted to find the corresponding protein sequence. Megablast [125] searches (word length w = 70, percentage identity $p = 95\%$) against nucleotide databases (in the succession of RefSeq [126,127], FANTOM [128], UniGene [129], nr GenBank, and TIGR Mouse Gene Index [19] until a gene hit was found) were carried out. For the ESTs still remaining without gene assignment, new Megablast searches were conducted with the largest compilation of RefSeq (including the provisional and automatically generated records [126,127]). If an EST remained unassigned, then the whole procedure was repeated with blastn [130]. In addition, a blastn search against the ENSEMBL mouse genome [131] was performed, and ESTs with long stretches (>100 base pairs) of unspecified nucleotides (N) were excluded.

All protein sequences were annotated *de novo* with academic prediction tools that are integrated into ANNOTATOR, a novel protein sequence analysis system [132]: compositional bias (SAPS [133], Xnu, Cast [134], GlobPlot 1.2 [135]); low complexity regions (SEG [136]); known sequence domains (Pfam [137], Smart [138], Prosite and Prosite pattern [139] with HMMER, RPS-BLAST [140], IMPALA [141], PROSITE-Profile [139]); transmembrane domains (HMMTOP 2.0 [142], TOPPRED [143], DAS-TMfilter [144], SAPS [133]); secondary structures (impCOIL [145], Predator [146], SSCP [147,148]); targeting signals (SIGCLEAVE [149], SignalP-3.0 [150], PTS1 [151]); post-translational modifications (big-PI [152], NMT [153], Prenylation); a series of small sequence motifs (ELM, Prosite patterns [139], BioMotif-IMPlibrary); and homology searches with NCBI blast [130]. Further information was retrieved from the databases of Mouse Genome Informatics [154] and LocusLink [126].

Promoter analysis

The promoters were retrieved from PromoSer database [155] through the gene accession number. PromoSer contains 22,549 promoters for 12,493 unique genes. Nucleotides from 2,000 upstream and 100 downstream of the transcription start site were obtained. With an implementation of the MatInspector algorithm [156], the Transfac matrices [100] were checked for binding sites in the promoter regions with a threshold for matrix similarity of 0.85. We counted the number of those gene sequences that were found to carry a predicted transcription factor binding site. As a reference set all unique genes of the PromoSer were reanalyzed. A one-sided χ^2 test and a one-sided Fisher's exact test (to improve the statistics for view counts) were performed with the statistical tool R [157] to determine the clusters with a higher affinity for a transcription factor.

Identification of miRNA target sites in 3'-UTR

All available 3'-UTR sequences (21,396) for mouse genes were derived with EnsMart [158], using Ensembl gene build for the NCBI m33 mouse assembly. 3'-UTRs for unique genes represented by the 780 selected ESTs were extracted using Ensembl transcript ID. A total of 234 mouse miRNA sequences were derived from the Rfam database [159]. The 3'-UTR sequences were searched for antisense matches to the designated seed region of each miRNA (bases 1-8, 2-8, 1-9, and 2-9 starting from the 5' end). Significantly over-represented miRNA motifs in each cluster in comparison with the remaining motifs in the whole 3'-UTR sequence set were determined using the one-sided Fisher's exact test (significance level: $P < 0.05$) and miRNA targets of all clusters were analyzed for significantly over-represented miRNAs.

Chromosomal localization analysis

RefSeq sequences for 780 selected ESTs, shown to be more than two times upregulated or downregulated in a minimum of four time points during adipocyte differentiation and clustered according their expression profiles, were mapped onto the chromosomes from the NCBI *Mus musculus* genome (build 33) using ChromoMapper 2.1.0 software [160] based on MegaBlast with the following parameters: 99% identity cutoff, word size 32, and E-value (0.001). Colocalized sequences of all selected ESTs and from each of the 12 clusters within a 5 Mb genomic interval were identified. Within the 5Mb genomic intervals of each chromosome with the highest density of mapped ESTs, relative gene expression levels (log2 ratios) of these ESTs at different time points were related to the genomic localization.

Additional data files

The following additional data are provided with the online version of this article: A spot map for the array design (Additional data file 1); a fasta file containing the EST sequences used for the array (Additional data file 2); an Excel file containing expression values for the 780 selected ESTs (Additional data file 3); an Excel file containing expression values for the 5205 ESTs filtered with ANOVA (Additional data file 4); GenePix result files containing raw data (Additional data file 5); images showing the distribution of gene ontology (Additional data file 6); a table listing relevant proteins (Additional data file 7); a fasta file containing sequences of the relevant proteins (Additional data file 8); a pdf file containing real-time RT-PCR data (Additional data file 9); a table including statistical analysis of independent experiments (Additional data file 10); figure showing a comparison with GeneAtlas (Additional data file 11); a table including expression levels from the present study and GeneAtlas (Additional data file 12); figure showing a comparison with the data set reported by Soukas and coworkers [8]Additional data file 13); figure showing a comparison with the data set reported by Ross and coworkers [9] (Additional data file 14); figure showing a comparison with the data set reported by Burton and coworkers [12] (Additional data file 15); a table including ESTs unique to the present study (Additional data file 16); a figure showing genes with miRNA motifs in 3'-UTR (Additional data file 17); a figure illustrating the significant over-representation of miRNA motifs in the 3'-UTR of genes in each cluster (Additional data file 18); figures showing the significant over-representation of miRNA motifs in the 3'-UTR from genes in each cluster (Additional data files 19, 20, 21, 22, 23, 24, 25, 26, 27, 28, 29); a table including over-represented miRNA motifs in the 3'-UTR from genes in the set of 780 selected ESTs (Additional data file 30); text describing regulation of metabolic pathways (Additional data file 31); figure showing regulation of metabolic pathways by key points (Additional data file 32); figure showing the cellular localization of gene products involved in metabolism and their gene expression at different time points (Additional data file 33); figure showing the cellular localization of gene products involved in other biological processes and their gene expression at different time points (Additional data file 30); text describing signaling networks (Additional data file 35); text file describing extracellular matrix remodeling and cytoskele-

ton reorganization (Additional data file 36); figure showing cell cycle processes (Additional data file 37); figure showing the cholesterol pathway (Additional data file 38); a list of experimental verified binding site for PPAR:RXR and the derived position weight matrix (Additional data file 39); text file containing TRANSFAC matrices for vertebrates (Additional data file 40); a file showing the promoter sequences in fasta format (Additional data file 41); figure showing cluster-wise mapping of 780 ESTs to all chromosomes (Additional data file 42); figure showing expression of colocalized ESTs for each cluster (Additional data file 43); an Excel file showing a statistical analysis of colocalized ESTs for 780 selected ESTs (Additional data file 44); and an Excel file showing a statistical analysis of colocalized ESTs for 5,502 ANOVA selected ESTs (Additional data file 45).

Acknowledgements

We thank Dr Fatima Sanchez-Cabo for assistance with the statistical analyses, Bernhard Mlecnik for assistance with the miRNA analysis, Dietmar Rieder for chromosomal mapping, Gernot Stocker for support with the computational infrastructure, Roman Fiedler for RT-PCR analysis, and Dr James McNally for discussions and comments on the manuscript. This work was supported by the Austrian Science Fund, Project SFB Biomembranes F718, the bm:bwk GEN-AU projects Bioinformatics Integration Network (BIN), and Genomics of Lipid-Associated Disorders (GOLD).

References

1. Green H, Meuth M: **An established pre-adipose cell line and its differentiation in culture.** *Cell* 1974, **3:**127-133.
2. Macdougald OA, Lane MD: **Transcriptional regulation of gene expression during adipocyte differentiation.** *Annu Rev Biochem* 1995, **64:**345-373.
3. Yeh WC, Cao Z, Classon M, McKnight SL: **Cascade regulation of terminal adipocyte differentiation by three members of the C/EBP family of leucine zipper proteins.** *Genes Dev* 1995, **9:**168-181.
4. Tanaka T, Yoshida N, Kishimoto T, Akira S: **Defective adipocyte differentiation in mice lacking the C/EBPbeta and/or C/EBP-delta gene.** *EMBO J* 1997, **16:**7432-7443.
5. Kim JB, Spiegelman BM: **ADD1/SREBP1 promotes adipocyte differentiation and gene expression linked to fatty acid metabolism.** *Genes Dev* 1996, **10:**1096-1107.
6. Fajas L, Schoonjans K, Gelman L, Kim JB, Najib J, Martin G, Fruchart JC, Briggs M, Spiegelman BM, Auwerx J: **Regulation of peroxisome proliferator-activated receptor gamma expression by adipocyte differentiation and determination factor 1/sterol regulatory element binding protein 1: implications for adipocyte differentiation and metabolism.** *Mol Cell Biol* 1999, **19:**5495-5503.
7. Kim JB, Wright HM, Wright M, Spiegelman BM: **ADD1/SREBP1 activates PPARgamma through the production of endogenous ligand.** *Proc Natl Acad Sci USA* 1998, **95:**4333-4337.
8. Soukas A, Socci ND, Saatkamp BD, Novelli S, Friedman JM: **Distinct transcriptional profiles of adipogenesis *in vivo* and *in vitro*.** *J Biol Chem* 2001, **276:**34167-34174.
9. Ross SE, Erickson RL, Gerin I, DeRose PM, Bajnok L, Longo KA, Misek DE, Kuick R, Hanash SM, Atkins KB, *et al.*: **Microarray analyses during adipogenesis: understanding the effects of Wnt signaling on adipogenesis and the roles of liver X receptor alpha in adipocyte metabolism.** *Mol Cell Biol* 2002, **22:**5989-5999.
10. Burton GR, Guan Y, Nagarajan R, McGehee RE: **Microarray analysis of gene expression during early adipocyte differentiation.** *Gene* 2002, **293:**21-31.
11. Burton GR, McGehee REJ: **Identification of candidate genes involved in the regulation of adipocyte differentiation using microarray-based gene expression profiling.** *Nutrition* 2004, **20:**109-114.
12. Burton GR, Nagarajan R, Peterson CA, McGehee REJ: **Microarray analysis of differentiation-specific gene expression during 3T3-L1 adipogenesis.** *Gene* 2004, **329:**167-185.
13. Jessen BA, Stevens GJ: **Expression profiling during adipocyte differentiation of 3T3-L1 fibroblasts.** *Gene* 2002, **299:**95-100.
14. Gerhold DL, Liu F, Jiang G, Li Z, Xu J, Lu M, Sachs JR, Bagchi A, Fridman A, Holder DJ, *et al.*: **Gene expression profile of adipocyte differentiation and its regulation by peroxisome proliferator-activated receptor-gamma agonists.** *Endocrinology* 2002, **143:**2106-2118.
15. Guo X, Liao K: **Analysis of gene expression profile during 3T3-L1 preadipocyte differentiation.** *Gene* 2000, **251:**45-53.
16. Ko MS, Kitchen JR, Wang X, Threat TA, Wang X, Hasegawa A, Sun T, Grahovac MJ, Kargul GJ, Lim MK, *et al.*: **Large-scale cDNA analysis reveals phased gene expression patterns during preimplantation mouse development.** *Development* 2000, **127:**1737-1749.
17. Larkin JE, Frank BC, Gaspard RM, Duka I, Gavras H, Quackenbush J: **Cardiac transcriptional response to acute and chronic angiotensin II treatments.** *Physiol Genomics* 2004, **18:**152-166.
18. Tanaka TS, Jaradat SA, Lim MK, Kargul GJ, Wang X, Grahovac MJ, Pantano S, Sano Y, Piao Y, Nagaraja R, *et al.*: **Genome-wide expression profiling of mid-gestation placenta and embryo using a 15,000 mouse developmental cDNA microarray.** *Proc Natl Acad Sci USA* 2000, **97:**9127-9132.
19. Quackenbush J, Liang F, Holt I, Pertea G, Upton J: **The TIGR gene indices: reconstruction and representation of expressed gene sequences.** *Nucleic Acids Res* 2000, **28:**141-145.
20. **Molecular processes during fat cell development revealed by gene expression profiling and functional annotation** [http://genome.tugraz.at/fatcell]
21. Su AI, Wiltshire T, Batalov S, Lapp H, Ching KA, Block D, Zhang J, Soden R, Hayakawa M, Kreiman G, *et al.*: **A gene atlas of the mouse and human protein-encoding transcriptomes.** *Proc Natl Acad Sci U S A* 2004, **101:**6062-6067.
22. Tang QQ, Otto TC, Lane MD: **Mitotic clonal expansion: A synchronous process required for adipogenesis.** *Proc Natl Acad Sci U S A* 2003, **100:**44-49.
23. Xie X, Lu J, Kulbokas EJ, Golub TR, Mootha V, Lindblad-Toh K, Lander ES, Kellis M: **Systematic discovery of regulatory motifs in human promoters and 3' UTRs by comparison of several mammals.** *Nature* 2005, **434:**338-345.
24. John B, Enright AJ, Aravin A, Tuschl T, Sander C, Marks DS: **Human MicroRNA targets.** *PLoS Biol* 2004, **2:**e363.
25. Doench JG, Sharp PA: **Specificity of microRNA target selection in translational repression.** *Genes Dev* 2004, **18:**504-511.
26. Hutvagner G, Simard MJ, Mello CC, Zamore PD: **Sequence-specific inhibition of small RNA function.** *PLoS Biol* 2004, **2:**E98.
27. Lewis BP, Shih IH, Jones-Rhoades MW, Bartel DP, Burge CB: **Prediction of mammalian microRNA targets.** *Cell* 2003, **115:**787-798.
28. Esau C, Kang X, Peralta E, Hanson E, Marcusson EG, Ravichandran LV, Sun Y, Koo S, Perera RJ, Jain R, *et al.*: **MicroRNA-143 regulates adipocyte differentiation.** *J Biol Chem* 2004, **279:**52361-52365.
29. Johnson SM, Grosshans H, Shingara J, Byrom M, Jarvis R, Cheng A, Labourier E, Reinert KL, Brown D, Slack FJ: **RAS is regulated by the let-7 microRNA family.** *Cell* 2005, **120:**635-647.
30. Mlecnik B, Scheideler M, Hackl H, Hartler J, Sanchez-Cabo F, Trajanoski Z: **PathwayExplorer: web service for visualizing high-throughput expression data on biological pathways.** *Nucleic Acids Res* 2005, **33:**W633-W637.
31. Tontonoz P, Hu E, Spiegelman BM: **Stimulation of adipogenesis in fibroblasts by PPAR gamma 2, a lipid-activated transcription factor.** *Cell* 1994, **79:**1147-1156.
32. Inoue J, Kumagai H, Terada T, Maeda M, Shimizu M, Sato R: **Proteolytic activation of SREBPs during adipocyte differentiation.** *Biochem Biophys Res Commun* 2001, **283:**1157-1161.
33. Yang T, Espenshade PJ, Wright ME, Yabe D, Gong Y, Aebersold R, Goldstein JL, Brown MS: **Crucial step in cholesterol homeostasis: sterols promote binding of SCAP to INSIG-1, a membrane protein that facilitates retention of SREBPs in ER.** *Cell* 2002, **110:**489-500.
34. Kast-Woelbern HR, Dana SL, Cesario RM, Sun L, de Grandpre LY, Brooks ME, Osburn DL, Reifel-Miller A, Klausing K, Leibowitz MD: **Rosiglitazone induction of Insig-1 in white adipose tissue reveals a novel interplay of peroxisome proliferator-activated receptor gamma and sterol regulatory element-binding protein in the regulation of adipogenesis.** *J Biol Chem* 2004, **279:**23908-23915.
35. Zimmermann R, Strauss JG, Haemmerle G, Schoiswohl G, Birner-

Gruenberger R, Riederer M, Lass A, Neuberger G, Eisenhaber F, Hermetter A, Zechner R: **Fat mobilization in adipose tissue is promoted by adipose triglyceride lipase.** *Science* 2004, **306:**1383-1386.
36. Fukuhara A, Matsuda M, Nishizawa M, Segawa K, Tanaka M, Kishimoto K, Matsuki Y, Murakami M, Ichisaka T, Murakami H, *et al.*: **Visfatin: a protein secreted by visceral fat that mimics the effects of insulin.** *Science* 2005, **307:**426-430.
37. Kitani T, Okuno S, Fujisawa H: **Growth phase-dependent changes in the subcellular localization of pre-B-cell colony-enhancing factor.** *FEBS Lett* 2003, **544:**74-78.
38. Revollo JR, Grimm AA, Imai S: **The NAD biosynthesis pathway mediated by nicotinamide phosphoribosyltransferase regulates Sir2 activity in mammalian cells.** *J Biol Chem* 2004, **279:**50754-50763.
39. Banerjee SS, Feinberg MW, Watanabe M, Gray S, Haspel RL, Denkinger DJ, Kawahara R, Hauner H, Jain MK: **The Kruppel-like factor KLF2 inhibits peroxisome proliferator-activated receptor-gamma expression and adipogenesis.** *J Biol Chem* 2003, **278:**2581-2584.
40. Oishi Y, Manabe I, Tobe K, Tsushima K, Shindo T, Fujiu K, Nishimura G, Maemura K, Yamauchi T, Kubota N, *et al.*: **Krüppel-like transcription factor KLF5 is a key regulator of adipocyte differentiation.** *Cell Metab* 2005, **1:**27-39.
41. Li D, Yea S, Li S, Chen Z, Narla G, Banck M, Laborda J, Tan S, Friedman JM, Friedman SL, Walsh MJ: **Kruppel-like factor-6 promotes preadipocyte differentiation through histone deacetylase 3-dependent repression of DLK1.** *J Biol Chem* 2005, **280:**26941-26952.
42. Mori T, Sakaue H, Iguchi H, Gomi H, Okada Y, Takashima Y, Nakamura K, Nakamura T, Yamauchi T, Kubota N, *et al.*: **Role of Kruppel-like factor 15 (KLF15) in transcriptional regulation of adipogenesis.** *J Biol Chem* 2005, **280:**12867-12875.
43. Ghaleb AM, Nandan MO, Chanchevalap S, Dalton WB, Hisamuddin IM, Yang VW: **Kruppel-like factors 4 and 5: the yin and yang regulators of cellular proliferation.** *Cell Res* 2005, **15:**92-96.
44. Nakae J, Kitamura T, Kitamura Y, Biggs WH, Arden KC, Accili D: **The forkhead transcription factor foxo1 regulates adipocyte differentiation.** *Dev Cell* 2003, **4:**119-129.
45. Farmer SR: **The forkhead transcription factor Foxo1: a possible link between obesity and insulin resistance.** *Mol Cell* 2003, **11:**6-8.
46. D'Adamio F, Zollo O, Moraca R, Ayroldi E, Bruscoli S, Bartoli A, Cannarile L, Migliorati G, Riccardi C: **A new dexamethasone-induced gene of the leucine zipper family protects T lymphocytes from TCR/CD3-activated cell death.** *Immunity* 1997, **7:**803-812.
47. Shi X, Shi W, Li Q, Song B, Wan M, Bai S, Cao X: **A glucocorticoid-induced leucine-zipper protein, GILZ, inhibits adipogenesis of mesenchymal cells.** *EMBO Rep* 2003, **4:**374-380.
48. Xie J, Cai T, Zhang H, Lan MS, Notkins AL: **The zinc-finger transcription factor INSM1 is expressed during embryo development and interacts with the Cbl-associated protein.** *Genomics* 2002, **80:**54-61.
49. Zhu M, Breslin MB, Lan MS: **Expression of a novel zinc-finger cDNA, IA-1, is associated with rat AR42J cells differentiation into insulin-positive cells.** *Pancreas* 2002, **24:**139-145.
50. Yamada K, Printz RL, Osawa H, Granner DK: **Human ZHX1: cloning, chromosomal location, and interaction with transcription factor NF-Y.** *Biochem Biophys Res Commun* 1999, **261:**614-621.
51. Hebrok M, Wertz K, Fuchtbauer EM: **M-twist is an inhibitor of muscle differentiation.** *Dev Biol* 1994, **165:**537-544.
52. Sosic D, Richardson JA, Yu K, Ornitz DM, Olson EN: **Twist regulates cytokine gene expression through a negative feedback loop that represses NF-kappaB activity.** *Cell* 2003, **112:**169-180.
53. Chae GN, Kwak SJ: **NF-kappaB is involved in the TNF-alpha induced inhibition of the differentiation of 3T3-L1 cells by reducing PPARgamma expression.** *Exp Mol Med* 2003, **35:**431-437.
54. Ku DH, Chang CD, Koniecki J, Cannizzaro LA, Boghosian-Sell L, Alder H, Baserga R: **A new growth-regulated complementary DNA with the sequence of a putative trans-activating factor.** *Cell Growth Differ* 1991, **2:**179-186.
55. Metzger D, Scheer E, Soldatov A, Tora L: **Mammalian TAF(II)30 is required for cell cycle progression and specific cellular differentiation programmes.** *EMBO J* 1999, **18:**4823-4834.
56. Novatchkova M, Eisenhaber F: **Can molecular mechanisms of biological processes be extracted from expression profiles? Case study: endothelial contribution to tumor-induced angiogenesis.** *Bioessays* 2001, **23:**1159-1175.
57. Croissandeau G, Chretien M, Mbikay M: **Involvement of matrix metalloproteinases in the adipose conversion of 3T3-L1 preadipocytes.** *Biochem J* 2002, **364:**739-746.
58. Karagiannis ED, Popel AS: **A theoretical model of type I collagen proteolysis by matrix metalloproteinase (MMP) 2 and membrane type 1 MMP in the presence of tissue inhibitor of metalloproteinase 2.** *J Biol Chem* 2004, **279:**39105-39114.
59. Chavey C, Mari B, Monthouel MN, Bonnafous S, Anglard P, Van Obberghen E, Tartare-Deckert S: **Matrix metalloproteinases are differentially expressed in adipose tissue during obesity and modulate adipocyte differentiation.** *J Biol Chem* 2003, **278:**11888-11896.
60. Weiner FR, Shah A, Smith PJ, Rubin CS, Zern MA: **Regulation of collagen gene expression in 3T3-L1 cells. Effects of adipocyte differentiation and tumor necrosis factor alpha.** *Biochemistry* 1989, **28:**4094-4099.
61. Dimaculangan DD, Chawla A, Boak A, Kagan HM, Lazar MA: **Retinoic acid prevents downregulation of ras recision gene/lysyl oxidase early in adipocyte differentiation.** *Differentiation* 1994, **58:**47-52.
62. Piecha D, Wiberg C, Morgelin M, Reinhardt DP, Deak F, Maurer P, Paulsson M: **Matrilin-2 interacts with itself and with other extracellular matrix proteins.** *Biochem J* 2002, **367:**715-721.
63. Brekken RA, Sage EH: **SPARC, a matricellular protein: at the crossroads of cell-matrix.** *Matrix Biol* 2000, **19:**569-580.
64. Bradshaw AD, Sage EH: **SPARC, a matricellular protein that functions in cellular differentiation and tissue response to injury.** *J Clin Invest* 2001, **107:**1049-1054.
65. Spiegelman BM, Farmer SR: **Decreases in tubulin and actin gene expression prior to morphological differentiation of 3T3 adipocytes.** *Cell* 1982, **29:**53-60.
66. Edwards RA, Herrera-Sosa H, Otto J, Bryan J: **Cloning and expression of a murine fascin homolog from mouse brain.** *J Biol Chem* 1995, **270:**10764-10770.
67. Winder SJ, Jess T, Ayscough KR: **SCP1 encodes an actin-bundling protein in yeast.** *Biochem J* 2003, **375:**287-295.
68. Hossain MM, Hwang DY, Huang QQ, Sasaki Y, Jin JP: **Developmentally regulated expression of calponin isoforms and the effect of h2-calponin on cell proliferation.** *Am J Physiol Cell Physiol* 2003, **284:**C156-C167.
69. He HJ, Kole S, Kwon YK, Crow MT, Bernier M: **Interaction of filamin A with the insulin receptor alters insulin-dependent activation of the mitogen-activated protein kinase pathway.** *J Biol Chem* 2003, **278:**27096-27104.
70. Oakley BR: **Gamma-tubulin: the microtubule organizer?** *Trends Cell Biol* 1992, **2:**1-5.
71. Honda K, Yamada T, Endo R, Ino Y, Gotoh M, Tsuda H, Yamada Y, Chiba H, Hirohashi S: **Actinin-4, a novel actin-bundling protein associated with cell motility and cancer invasion.** *J Cell Biol* 1998, **140:**1383-1393.
72. Leeuwen FN, Kain HE, Kammen RA, Michiels F, Kranenburg OW, Collard JG: **The guanine nucleotide exchange factor Tiam1 affects neuronal morphology; opposing roles for the small GTPases Rac and Rho.** *J Cell Biol* 1997, **139:**797-807.
73. Sander EE, ten Klooster JP, van Delft S, van der Kammen RA, Collard JG: **Rac downregulates Rho activity: reciprocal balance between both GTPases determines cellular morphology and migratory behavior.** *J Cell Biol* 1999, **147:**1009-1022.
74. Saras J, Wollberg P, Aspenstrom P: **Wrch1 is a GTPase-deficient Cdc42-like protein with unusual binding characteristics and cellular effects.** *Exp Cell Res* 2004, **299:**356-369.
75. Shutes A, Berzat AC, Cox AD, Der CJ: **Atypical mechanism of regulation of the Wrch-1 Rho family small GTPase.** *Curr Biol* 2004, **14:**2052-2056.
76. Klipp E, Heinrich R, Holzhutter HG: **Prediction of temporal gene expression. Metabolic opimization by re-distribution of enzyme activities.** *Eur J Biochem* 2002, **269:**5406-5413.
77. Lynen F: **Acetyl coenzyme A and the fatty acid cycle.** *Harvey Lect* 1952, **48:**210-244.
78. Ganguly J: **Studies on the mechanism of fatty acid synthesis. VII. Biosynthesis of fatty acids from malonyl CoA.** *Biochim Biophys Acta* 1960, **40:**110-118.
79. Song WJ, Jackowski S: **Kinetics and regulation of pantothenate kinase from Escherichia coli.** *J Biol Chem* 1994, **269:**27051-27058.
80. Rongvaux A, Shea RJ, Mulks MH, Gigot D, Urbain J, Leo O, Andris F: **Pre-B-cell colony-enhancing factor, whose expression is up-**

regulated in activated lymphocytes, is a nicotinamide phosphoribosyltransferase, a cytosolic enzyme involved in NAD biosynthesis. *Eur J Immunol* 2002, **32:**3225-3234.
81. Clarke JL, Mason PJ: **Murine hexose-6-phosphate dehydrogenase: a bifunctional enzyme with broad substrate specificity and 6-phosphogluconolactonase activity.** *Arch Biochem Biophys* 2003, **415:**229-234.
82. Enoch HG, Catala A, Strittmatter P: **Mechanism of rat liver microsomal stearyl-CoA desaturase. Studies of the substrate specificity, enzyme-substrate interactions, and the function of lipid.** *J Biol Chem* 1976, **251:**5095-5103.
83. Ntambi JM: **Regulation of stearoyl-CoA desaturase by polyunsaturated fatty acids and cholesterol.** *J Lipid Res* 1999, **40:**1549-1558.
84. Moon YA, Shah NA, Mohapatra S, Warrington JA, Horton JD: **Identification of a mammalian long chain fatty acyl elongase regulated by sterol regulatory element-binding proteins.** *J Biol Chem* 2001, **276:**45358-45366.
85. Nilsson-Ehle P: **Impaired regulation of adipose tissue lipoprotein lipase in obesity.** *Int J Obes* 1981, **5:**695-699.
86. Semenkovich CF, Wims M, Noe L, Etienne J, Chan L: **Insulin regulation of lipoprotein lipase activity in 3T3-L1 adipocytes is mediated at posttranscriptional and posttranslational levels.** *J Biol Chem* 1989, **264:**9030-9038.
87. Koike T, Liang J, Wang X, Ichikawa T, Shiomi M, Liu G, Sun H, Kitajima S, Morimoto M, Watanabe T, *et al.*: **Overexpression of lipoprotein lipase in transgenic Watanabe heritable hyperlipidemic rabbits improves hyperlipidemia and obesity.** *J Biol Chem* 2004, **279:**7521-7529.
88. Zhang J, Zhang W, Zou D, Chen G, Wan T, Zhang M, Cao X: **Cloning and functional characterization of ACAD-9, a novel member of human acyl-CoA dehydrogenase family.** *Biochem Biophys Res Commun* 2002, **297:**1033-1042.
89. Harris RA, Hawes JW, Popov KM, Zhao Y, Shimomura Y, Sato J, Jaskiewicz J, Hurley TD: **Studies on the regulation of the mitochondrial alpha-ketoacid dehydrogenase complexes and their kinases.** *Adv Enzyme Regul* 1997, **37:**271-293.
90. Clark DV, MacAfee N: **The purine biosynthesis enzyme PRAT detected in proenzyme and mature forms during development of *Drosophila melanogaster*.** *Insect Biochem Mol Biol* 2000, **30:**315-323.
91. Bohman C, Eriksson S: **Deoxycytidine kinase from human leukemic spleen: preparation and characteristics of homogeneous enzyme.** *Biochemistry* 1988, **27:**4258-4265.
92. Hatzis P, Al Madhoon AS, Jullig M, Petrakis TG, Eriksson S, Talianidis I: **The intracellular localization of deoxycytidine kinase.** *J Biol Chem* 1998, **273:**30239-30243.
93. Sabini E, Ort S, Monnerjahn C, Konrad M, Lavie A: **Structure of human dCK suggests strategies to improve anticancer and antiviral therapy.** *Nat Struct Biol* 2003, **10:**513-519.
94. Wright JA, Chan AK, Choy BK, Hurta RA, McClarty GA, Tagger AY: **Regulation and drug resistance mechanisms of mammalian ribonucleotide reductase, and the significance to DNA synthesis.** *Biochem Cell Biol* 1990, **68:**1364-1371.
95. Dong Z, Liu LH, Han B, Pincheira R, Zhang JT: **Role of eIF3 p170 in controlling synthesis of ribonucleotide reductase M2 and cell growth.** *Oncogene* 2004, **23:**3790-3801.
96. Xu P, Hueckstedt TP, Harrison R, Hoidal JR: **Molecular cloning, tissue expression of human xanthine dehydrogenase.** *Biochem Biophys Res Commun* 1994, **199:**998-1004.
97. Xu P, Hueckstedt TP, Hoidal JR: **Molecular cloning and characterization of the human xanthine dehydrogenase gene (XDH).** *Genomics* 1996, **34:**173-180.
98. Popplewell PY, Azhar S: **Effects of aging on cholesterol content and cholesterol-metabolizing enzymes in the rat adrenal gland.** *Endocrinology* 1987, **121:**64-73.
99. Sato R, Takano T: **Regulation of intracellular cholesterol metabolism.** *Cell Struct Funct* 1995, **20:**421-427.
100. Matys V, Fricke E, Geffers R, Gossling E, Haubrock M, Hehl R, Hornischer K, Karas D, Kel AE, Kel-Margoulis OV, *et al.*: **TRANSFAC: transcriptional regulation, from patterns to profiles.** *Nucleic Acids Res* 2003, **31:**374-378.
101. Kim JB, Spotts GD, Halvorsen YD, Shih HM, Ellenberger T, Towle HC, Spiegelman BM: **Dual DNA binding specificity of ADD1/SREBP1 controlled by a single amino acid in the basic helix-loop-helix domain.** *Mol Cell Biol* 1995, **15:**2582-2588.
102. Yokoyama C, Wang X, Briggs MR, Admon A, Wu J, Hua X, Goldstein JL, Brown MS: **SREBP-1, a basic-helix-loop-helix-leucine zipper protein that controls transcription of the low density lipoprotein receptor gene.** *Cell* 1993, **75:**187-197.
103. Salomonis N, Cotte N, Zambon AC, Pollard KS, Vranizan K, Doniger SW, Dolganov G, Conklin BR: **Identifying genetic networks underlying myometrial transition to labor.** *Genome Biol* 2005, **6:**R12.
104. Cohen BA, Mitra RD, Hughes JD, Church GM: **A computational analysis of whole-genome expression data reveals chromosomal domains of gene expression.** *Nat Genet* 2000, **26:**183-186.
105. Roy PJ, Stuart JM, Lund J, Kim SK: **Chromosomal clustering of muscle-expressed genes in *Caenorhabditis elegans*.** *Nature* 2002, **418:**975-979.
106. Spellman PT, Rubin GM: **Evidence for large domains of similarly expressed genes in the *Drosophila genome*.** *J Biol* 2002, **1:**5.
107. Osborne CS, Chakalova L, Brown KE, Carter D, Horton A, Debrand E, Goyenechea B, Mitchell JA, Lopes S, Reik W, Fraser P: **Active genes dynamically colocalize to shared sites of ongoing transcription.** *Nat Genet* 2004, **36:**1065-1071.
108. Oliver B, Misteli T: **A non-random walk through the genome.** *Genome Biol* 2005, **6:**214.
109. Student AK, Hsu RY, Lane MD: **Induction of fatty acid synthetase synthesis in differentiating 3T3-L1 preadipocytes.** *J Biol Chem* 1980, **255:**4745-4750.
110. Le Lay S, Lefrere I, Trautwein C, Dugail I, Krief S: **Insulin and sterol-regulatory element-binding protein-1c (SREBP-1C) regulation of gene expression in 3T3-L1 adipocytes. Identification of CCAAT/enhancer-binding protein beta as an SREBP-1C target.** *J Biol Chem* 2002, **277:**35625-35634.
111. Chomczynski P, Sacchi N: **Single-step method of RNA isolation by acid guanidinium thiocyanate-phenol-chloroform extraction.** *Anal Biochem* 1987, **162:**156-159.
112. Hegde P, Qi R, Abernathy K, Gay C, Dharap S, Gaspard R, Hughes JE, Snesrud E, Lee N, Quackenbush J: **A concise guide to cDNA microarray analysis.** *Biotechniques* 2000, **29:**548-556.
113. Kerr MK, Martin M, Churchill GA: **Analysis of variance for gene expression microarray data.** *J Comput Biol* 2000, **7:**819-837.
114. Quackenbush J: **Microarray data normalization and transformation.** *Nat Genet* 2002, **32(Suppl):**496-501.
115. Yang YH, Dudoit S, Luu P, Lin DM, Peng V, Ngai J, Speed TP: **Normalization for cDNA microarray data: a robust composite method addressing single and multiple slide systematic variation.** *Nucleic Acids Res* 2002, **30:**e15.
116. Maurer M, Molidor R, Sturn A, Hartler J, Hackl H, Stocker G, Prokesch A, Scheideler M, Trajanoski Z: **MARS: Microarray analysis, retrieval and storage system.** *BMC Bioinformatics* 2005, **6:**101.
117. Brazma A, Parkinson H, Sarkans U, Shojatalab M, Vilo J, Abeygunawardena N, Holloway E, Kapushesky M, Kemmeren P, Lara GG, *et al.*: **ArrayExpress--a public repository for microarray gene expression data at the EBI.** *Nucleic Acids Res* 2003, **31:**68-71.
118. Tusher VG, Tibshirani R, Chu G: **Significance analysis of microarrays applied to the ionizing radiation response.** *Proc Natl Acad Sci USA* 2001, **98:**5116-5121.
119. Pieler R, Sanchez-Cabo F, Hackl H, Thallinger GG, Trajanoski Z: **ArrayNorm: comprehensive normalization and analysis of microarray data.** *Bioinformatics* 2004.
120. Quackenbush J: **Computational analysis of microarray data.** *Nat Rev Genet* 2001, **2:**418-427.
121. Hartigan JA: *Clustering Algorithms* New York: Wiley & Sons; 1975.
122. Yeung KY, Haynor DR, Ruzzo WL: **Validating clustering for gene expression data.** *Bioinformatics* 2001, **17:**309-318.
123. Raychaudhuri S, Stuart JM, Altman RB: **Principal components analysis to summarize microarray experiments: application to sporulation time series.** *Pac Symp Biocomput.* 2000, **2000:**455-466.
124. Sturn A, Quackenbush J, Trajanoski Z: **Genesis: cluster analysis of microarray data.** *Bioinformatics* 2002, **18:**207-208.
125. Zhang Z, Schwartz S, Wagner L, Miller W: **A greedy algorithm for aligning DNA sequences.** *J Comput Biol* 2000, **7:**203-214.
126. Pruitt KD, Katz KS, Sicotte H, Maglott DR: **Introducing RefSeq and LocusLink: curated human genome resources at the NCBI.** *Trends Genet* 2000, **16:**44-47.
127. Pruitt KD, Tatusova T, Maglott DR: **NCBI Reference Sequence (RefSeq): a curated non-redundant sequence database of genomes, transcripts and proteins.** *Nucleic Acids Res* 2005:D501-D504.
128. Okazaki Y, Furuno M, Kasukawa T, Adachi J, Bono H, Kondo S, Nikaido I, Osato N, Saito R, Suzuki H, *et al.*: **Analysis of the mouse transcriptome based on functional annotation of 60,770 full-**

length cDNAs. *Nature* 2002, **420:**563-573.
129. Schuler GD: **Pieces of the puzzle: expressed sequence tags and the catalog of human genes.** *J Mol Med* 1997, **75:**694-698.
130. Altschul SF, Gish W, Miller W, Myers EW, Lipman DJ: **Basic local alignment search tool.** *J Mol Biol* 1990, **215:**403-410.
131. Hubbard T, Barker D, Birney E, Cameron G, Chen Y, Clark L, Cox T, Cuff J, Curwen V, Down T, *et al.*: **The Ensembl genome database project.** *Nucleic Acids Res* 2002, **30:**38-41.
132. **Large Scale Sequence Annotation System** [http://annotator.imp.univie.ac.at/]
133. Brendel V, Bucher P, Nourbakhsh IR, Blaisdell BE, Karlin S: **Methods and algorithms for statistical analysis of protein sequences.** *Proc Natl Acad Sci USA* 1992, **89:**2002-2006.
134. Promponas VJ, Enright AJ, Tsoka S, Kreil DP, Leroy C, Hamodrakas S, Sander C, Ouzounis CA: **CAST: an iterative algorithm for the complexity analysis of sequence tracts. Complexity analysis of sequence tracts.** *Bioinformatics* 2000, **16:**915-922.
135. Linding R, Russell RB, Neduva V, Gibson TJ: **GlobPlot: Exploring protein sequences for globularity and disorder.** *Nucleic Acids Res* 2003, **31:**3701-3708.
136. Wootton JC, Federhen S: **Analysis of compositionally biased regions in sequence databases.** *Methods Enzymol* 1996, **266:**554-571.
137. Sonnhammer EL, Eddy SR, Birney E, Bateman A, Durbin R: **Pfam: multiple sequence alignments and HMM-profiles of protein domains.** *Nucleic Acids Res* 1998, **26:**320-322.
138. Letunic I, Copley RR, Schmidt S, Ciccarelli FD, Doerks T, Schultz J, Ponting CP, Bork P: **SMART 4.0: towards genomic data integration.** *Nucleic Acids Res* 2004, **32:**D142-D144.
139. Sigrist CJ, Cerutti L, Hulo N, Gattiker A, Falquet L, Pagni M, Bairoch A, Bucher P: **PROSITE: a documented database using patterns and profiles as motif descriptors.** *Brief Bioinform* 2002, **3:**265-274.
140. Marchler-Bauer A, Panchenko AR, Shoemaker BA, Thiessen PA, Geer LY, Bryant SH: **CDD: a database of conserved domain alignments with links to domain three-dimensional structure.** *Nucleic Acids Res* 2002, **30:**281-283.
141. Schaffer AA, Wolf YI, Ponting CP, Koonin EV, Aravind L, Altschul SF: **IMPALA: matching a protein sequence against a collection of PSI-BLAST-constructed position-specific score matrices.** *Bioinformatics* 1999, **15:**1000-1011.
142. Tusnady GE, Simon I: **Principles governing amino acid composition of integral membrane proteins: application to topology prediction.** *J Mol Biol* 1998, **283:**489-506.
143. von Heijne G: **Membrane protein structure prediction. Hydrophobicity analysis and the positive-inside rule.** *J Mol Biol* 1992, **225:**487-494.
144. Cserzo M, Eisenhaber F, Eisenhaber B, Simon I: **On filtering false positive transmembrane protein predictions.** *Protein Eng* 2002, **15:**745-752.
145. Lupas A, Van Dyke M, Stock J: **Predicting coiled coils from protein sequences.** *Science* 1991, **252:**1162-1164.
146. Frishman D, Argos P: **Incorporation of non-local interactions in protein secondary structure prediction from the amino acid sequence.** *Protein Eng* 1996, **9:**133-142.
147. Eisenhaber F, Imperiale F, Argos P, Frommel C: **Prediction of secondary structural content of proteins from their amino acid composition alone. I. New analytic vector decomposition methods.** *Proteins* 1996, **25:**157-168.
148. Eisenhaber F, Frommel C, Argos P: **Prediction of secondary structural content of proteins from their amino acid composition alone. II. The paradox with secondary structural class.** *Proteins* 1996, **25:**169-179.
149. von Heijne G: **A new method for predicting signal sequence cleavage sites.** *Nucleic Acids Res* 1986, **14:**4683-4690.
150. Bendtsen JD, Nielsen H, von Heijne G, Brunak S: **Improved prediction of signal peptides: SignalP 3.0.** *J Mol Biol* 2004, **340:**783-795.
151. Eisenhaber B, Eisenhaber F, Maurer-Stroh S, Neuberger G: **Prediction of sequence signals for lipid post-translational modifications: insights from case studies.** *Proteomics* 2004, **4:**1614-1625.
152. Eisenhaber B, Bork P, Eisenhaber F: **Prediction of potential GPI-modification sites in proprotein sequences.** *J Mol Biol* 1999, **292:**741-758.
153. Maurer-Stroh S, Eisenhaber B, Eisenhaber F: **N-terminal N-myristoylation of proteins: prediction of substrate proteins from amino acid sequence.** *J Mol Biol* 2002, **317:**541-557.
154. Blake JA, Richardson JE, Bult CJ, Kadin JA, Eppig JT: **MGD: the Mouse Genome Database.** *Nucleic Acids Res* 2003, **31:**193-195.
155. Halees AS, Leyfer D, Weng Z: **PromoSer: A large-scale mammalian promoter and transcription start site identification service.** *Nucleic Acids Res* 2003, **31:**3554-3559.
156. Quandt K, Frech K, Karas H, Wingender E, Werner T: **MatInd and MatInspector: new fast and versatile tools for detection of consensus matches in nucleotide sequence data.** *Nucleic Acids Res* 1995, **23:**4878-4884.
157. **R Project** [http://www.r-project.org]
158. Kasprzyk A, Keefe D, Smedley D, London D, Spooner W, Melsopp C, Hammond M, Rocca-Serra P, Cox T, Birney E: **EnsMart: a generic system for fast and flexible access to biological data.** *Genome Res* 2004, **14:**160-169.
159. Griffiths-Jones S: **The microRNA registry.** *Nucleic Acids Res* 2004, **32:**D109-D111.
160. **ChromoMapper** [http://mcluster.tu-graz.ac.at/clustercontrol/modules/ChromoMapper/]

Identification of New Targets Using Expression Profiles

Thomas R. Burkard[1,2], Zlatko Trajanoski[1], Maria Novatchkova[2], Hubert Hackl[1], Frank Eisenhaber[2*]

[1]Institute for Genomics and Bioinformatics and Christian Doppler Laboratory for Genomics and Bioinformatics, Graz University of Technology, Petersgasse 14, 8010 Graz, Austria; [2]Research Institute of Molecular Pathology, Dr Bohr-Gasse 7, 1030 Vienna, Austria

*correspondence address
Research Institute of Molecular Pathology, Dr Bohr-Gasse 7, 1030 Vienna, Austria, Tel. +43-1-79730557, E-mail: Frank.Eisenhaber@imp.univie.ac.at

In: *Antiangiogenic Cancer Therapy* (in press)
Editors: Abbruzzese JL, Davis DW, Herbst RS
CRC Press

Abstract

When large-scale expression profiling methods were first published about a decade ago, their introduction into the lab praxis was accompanied with high expectations of getting system-wide understanding of gene interactions. Although this hope has not yet materialized, expression profiling tools have become an indispensable part of the methodical arsenal in biological laboratories. In this review, we describe the experimental variants of gene expression profiling. The computational methods for post-experimental expression profile analysis, both for expression value treatment and gene/protein function prediction from sequence, are considered in detail since they do not receive the necessary attention in many practical applications. Finally, biologically significant results from expression profiling studies with special emphasis on angiogenic systems including the identification of new targets are assessed.

1 Introduction

The end of the 20th century has seen life sciences entering a qualitatively new era of their development. The major change is connected with progress in research technologies, the introduction of high-throughput methods for the generation of large amounts of uniform, quantitative data describing the status and the development of biological systems. This trend is associated with a new, essential and creative role of computational biology for handling this data and for interpreting it in terms of biological functions. DNA sequencing was in the first wave and the complete sequencing of genomes of all major model organisms and human (beginning with that of *H. influencae* in 1995) was the major highlight of this development.

In the late nineties, expression profiling was seen as a continuation of this process with the promise of simultaneous, large-scale and high-throughput characterization of the transcriptional status of all genes, especially in contrast to the, at that time, usual single-gene Northern blot technology. The euphoria that systematic understanding of networks and pathway interactions is just in reach has vanished due to several reasons. First, high-throughput expression profiling methods did not reach the necessary level of sensitivity to monitor simultaneously frequently occurring and low-abundant mRNAs with sufficient accuracy. The hope of mathematical network modeling has often moved away instead of a semi-quantitative evaluation of expression data (up to a distinction of only ‘high’ and ‘low’ expression) and the determination of sets of genes that are markedly transcriptionally regulated. I.e., expression profiling is used just as one type of screen for target identification. Second, the transcriptional status is only a facet of a complex biological reality that has many additional regulation mechanisms at the translational, proteome, physiological or population level. After the euphoria has settled, expression profiling tools have become an important part of the laboratory repertoire that complements other techniques and approaches.

Application of expression profiling in the angiogenic context is an especially demanding task since angiogenesis is a process that involves many cell types, tissues and both local and

organism-level regulation mechanisms. Most often, the focus is on the transcriptional status of endothelial cells, a material that is not easy to collect from sample organism and where isolated *in vitro* culturing substantially influences intracellular processes [1,2].

In the first part of this chapter, we present an overview of experimental methods applicable for monitoring gene expression profiles as well as a review of computational approaches used for the analysis and the biological interpretation of the resulting complex data. The second part of this treatise summarizes achievements of these techniques with an emphasis on angiogenesis research but also a few other cases that appear especially methodically significant.

2 Methods

2.1 Expression profiling methods – The data creation

A variety of expression profiling methods are available which take a snapshot of the currently expressed genes at a given time, state, environment, genetic background and treatment in one or numerous cells. The older and simpler methods, differential display and subtractive hybridization, are methods which lack the sensitivity to detect relative differences in the transcript abundance between two samples. Compared with other technologies, these two methods belong to the group of low-throughput processes together with differential hybridization. On the other hand, they have the advantage not to require specialized equipment and, therefore, can be applied in a standard biological laboratory. The state of the art for large-scale gene expression profiling is represented by Serial Analysis of Gene Expression (SAGE) [3], Massive Parallel Signature Sequencing (MPSS) [4], oligo- and cDNA-microarrays [5,6] and Real Time Polymerase Chain Reaction (RT-PCR). With these approaches, it is possible to determine the absolute or relative abundance of RNA in a medium- or high-throughput manner. Any of these methods has their own advantages and limitations. SAGE and MPSS profit from the possibility to quantify transcript numbers in absolute terms without prior knowledge of the transcriptome. Oligo- and cDNA-microarray are the most commonly used technology. Arrays are able to measure the expression level

from several hundreds or thousands of entities on one single glass slide. Since the scientific community in this field is large, a variety of analytical tools is available. Finally, RT-PCR has an outstandingly low detection limit of only 1 transcript in 1000 cells and is often applied for validation of array measurements.

If sufficiently complete, the transcript abundance data generated by gene expression profiling methods described above are very useful for the determination of transcriptional networks. Nevertheless, it should be noted that the transcriptional status is only one aspect of the cellular physiology. Although an essentially linear relationship between the amount of transcripts and protein abundance is assumed in most studies for the extraction of biological conclusions, this preposition is not true in many cases, for example in instances of posttranscriptional regulation or translational control.
In addition to the problem of the protein/transcript ratio, the diversity of proteins originating from a single transcript must be taken into account. Post-translational modifications (intein exclusion, proteolytic processing, phosphorylation, acetylation, myristylation, glycosylaton, etc.) have a great influence on the functional properties of proteins but their occurrence cannot be measured with gene expression profiling methods. Therefore, transcription profiling results would need to be complemented with proteome analysis methods such as LC/MS/MS and protein arrays.

Several efforts using genomic and proteomic methods have tried to shed light in the assumption of protein/transcript correlation. Gygi *et. al*. [7] showed that for a set of 106 *S.cerevisiae* genes the Pearson product moment correlation coefficient between the SAGE transcript expression and protein expression was 0.935. This high level was biased by few highly abundant species. For transcripts represented by less than 10 copies per cell (69% of the 106 gene set), the coefficient dropped to 0.356. This effect might be a general observation or a problem of higher inaccuracies in measuring low abundances. Another study by Ideker *et. al.* [8] compared the protein and transcript ratios of *S.cerevisiae wt+gal* and *wt-gal*. A moderate correlation (r=0.61) was observed for 289 expression pairs. Interestingly, the change of ribosomal-proteins on the transcript level was not passed on to the protein level. On the other hand, Kern *et al.* [9] observed that there is a significant correlation between protein and gene expression in acute myeloid leukemia for several

markers.

For a final conclusion, the accuracy of the quantitative measuring methods of transcripts and especially of proteins has to improve considerably. The limits of all involved methods have to be considered exhaustively for an appropriate comparison to avoid influences of all kind of biases on the comparison. Most likely, a general correlation is not possible and the proteins have to be divided into two groups of highly transcript-sensitive and -insensitive ones. The insensitive proteins might be further separated into subgroups depending on different regulatory mechanisms (e.g. codon bias) probably associated with cellular localization or functional groups/processes (metabolism, transcription factor, transport, etc.). The expression level might be an additional but important parameter.

2.1.1 Differential Display is a simple but limited method

Differential display is one of the simplest expression profiling methods. It determines the abundance of a RNA species through comparison of two probes. Extracted total RNA of the sample and the control are separately reverse transcribed to cDNA and, thereafter, are amplified by PCR using arbitrary primers. Control and sample RNA are separated on a denaturing polyacryl gel by electrophoresis and, after visualization, the discrete bands are compared side by side. Quantitative differences can be estimated by the intensities of the bands in the gel. cDNA that is abundant in only one part is extracted, further amplified with PCR and sequenced [10,11]. The classical differential display uses radioactive nucleotides to detect mRNAs but this disadvantage can be overcome by fluorescence techniques [12].

A more advanced variation allows a separation of the RNA fraction into smaller ones. Therefore, the reverse transcription uses an oligo-dT primer with two additional nucleotides. Due to one more hydrogen bond, primers with G and C are more efficient than those containing A and T [13,14]. Depending on the nucleotide variations, many different RNA subjects can be separated.

The advantage of differential display lies in the simplicity by using only standard procedures. It allows simultaneous determination of up- and down-regulated genes in two or

more samples of about 5-10ng of total RNA. Its main purpose is to identify uncharacterized and not yet sequenced mRNA species easily. On the other side, the classical differential display often generates false-negative results during PCR amplification and cloning [15]. The workload can grow considerably with the number of different nucleotide variations in the primers. Finally, differential display is more or less only a qualitative method.

2.1.2 cDNA libraries and Differential Hybridization

cDNA libraries are constructed from reverse transcribed mRNA of a tissue of interest typically with oligo-dT primers. The resulting cDNAs are cloned into bacteria and, therefore, each bacterial colony represents one gene of a tissue [16]. Non-normalized libraries preserve the relative abundance of the mRNA levels [16]. An expression profile can be determined by randomly picking out clones and sequencing an expressed sequence tag (EST) of approximately 300bp. This method is biased towards strongly abundant expressed transcripts; it is labour intensive and expensive. To identify rare mRNA species, methods to construct normalized libraries exist, which contains each mRNA species at a similar level [17].

Differential hybridization relies on the hybridization of cDNA of a tissue of interest to a cDNA library with fixed colony positions. The cDNA library is transferred to filter membranes and is treated with alkali to release the cDNA and to denature it. mRNAs of different tissues of interest are subjected to reverse transcription with radioactive nucleotides and hybridized to fixed cDNAs on the filters. Comparison of the X-ray films reveals the relative abundance of a gene in the tissues [18].

2.1.3 Subtractive Hybridization

The principle of this method is based on the fact that single-stranded cDNA (ss-cDNA) can be separated from double-stranded cDNA (ds-cDNA) with a hydroxylapatite column or the avidin-biotin method [19]. After reverse transcription, cDNA obtained from the sample mRNA is hybridized to the mRNA of the control fraction. A part of the sample cDNA finds no complementary RNA in the control and remains as ss-cDNA, which can be separated by

chromatography with hydroxylapatite columns. To increase the purity, further rounds of hybridization with control mRNA and chromatography remove the slower hybridizing sequences. A sample-overrepresented cDNA library is constructed from the ss-cDNA fraction and specific clones are sequenced. In typical cases of successful application of this technique, less than 5% of the initial cDNA sequences will be isolated as single-stranded [20].

Similarly to differential display, this technique is mainly used to identify the abundance of a mRNA species in one tissue compared to another. It is an inexpensive method, which can be carried out in a basic molecular biology laboratory. Compared to differential display, it has a lower rate of false-negatives [15] but determines only the abundance of a mRNA species in one sample. RNAs with only slight differences in expression are hard to identify (for reliability, a 5-10-fold difference in abundance is required) [20]. The fact that high abundant transcripts are easier to hybridize than low abundant ones represents another problem. Due to the subtractive nature of the procedure, relative expression values cannot be measured.

2.1.4 Serial Analysis of Gene Expression is a good choice for acquiring transcript counts

Serial Analysis of Gene Expression (SAGE) [3] is a method based on sequencing concatemer clones of 9-10 bp sequence tags instead of whole expressed sequence tag (EST) libraries. The tags have a unique position within the mRNA species and, typically, contain enough information to describe the whole mRNA [1]. Many variations of SAGE are now available that can work with a reduced amount of necessary raw material [21] or that generate sequence tags with increased length [22].

Shortly, RNA of purified cells is captured by hybridization of the poly-A tail to oligo-T magnetic beads. Double-stranded cDNA is constructed and cleaved with the endonuclease *Nla*III. The bead-bound part is processed further [21]. In another approach, cDNA with biotinylated primers is synthesized. The cDNAs are cleaved and attached to streptavidin beads [3]. The tags are divided in two parts and are ligated each to two types of adaptors. The adapters contain sites for the restriction enzyme *Bsm*F1, which produces an overhang of 14-base pairs (bp) composed of 10 tag-specific and 4 non-specific bp. The blunt-ended

fragments are pooled and ligated to form di-tags. PCR is used to amplify the resulting di-tags with primers for the adapters. Finally, the di-tags are released by the restriction enzyme *Nla*III, concatenated, cloned and sequenced. To create a typical library of 100.000 tags, preparation, screening and sequencing of approximately 3000 concatemer clones is needed [21]. The frequency distribution is calculated by dividing the count of a tag by the total of sequenced tags. In the typical case, each 9-10bp long tag entity has enough information to describe sufficiently a unique transcript in the analyzed cells.

The transcript numbers generated by SAGE are measured effectively in absolute terms and, thus, are easy to compare to different datasets [23]. It should be noted that sensitivity of transcript detection and accuracy of transcript occurrence measurements depend greatly on mRNA abundance in the sample and the number of sequenced tags. For example, there is a 37% chance to miss a transcript that occurs in the sample with the fraction of p=1:100000 in the mRNA pool if 100000 tags are sequenced [1]. If the transcript is ten times more abundant (p=1:10000), there is still a 22% chance that the tag is found not more than 7 times or a 14% chance that the tag occurs at least 15 times. Thus, the systematic measurement error ranges at least between the 0.7- and 1.5-fold of the final number for rare transcripts. Statistical estimates show that SAGE yields good quantitative measures of transcript occurrences for p=1:1000, qualitative estimates (high/low expression) for transcript occurrences with p=1:10000 and no reliable results for more rare transcripts [1].

SAGE needs no prior knowledge about the expressed transcripts. This is especially interesting for organisms without a sequenced genome. On the contrary, SAGE is an expensive and labor-intensive method (a large number of clones must be purified and sequenced). It is biased as a result of possible sampling and sequencing errors, non-uniqueness and non-randomness of tag sequences [1,24]. Further, a link to a gene or genomic entry is needed for each tag in a sequence database. SAGE can results in a different distribution of expression values than microarray experiments. Therefore, the clustering methods based on Pearson correlation and Euclidean distance, used in microarray analysis, are not appropriate for SAGE profiles. Cai *et. al* considered that Poisson-based distances are more suitable, which have been incorporated into a clustering algorithm for SAGE analysis [25].

2.1.5 Massive Parallel Signature Sequencing arrays transcript tags on microbeads

Massive Parallel Signature Sequencing (MPSS) [4] is a combination of arraying sequences fixed on a bead and sequencing 16-20 bp long signatures. In the first step, transcripts are cloned on microbeads. Therefore, a complex conjugate mixture of transcripts and 32-oligomere microbead-specific tags are generated. The number of different tags has to be at least 100-fold higher than that of the transcript entities. A representative part is subjected to PCR and hybridized to tag-specific microbeads. Beads with sequences attached are sorted out with a fluorescence-activated cell sorter (FACS). These microbeads are arrayed in a fixed position within a flow cell. After cutting the sequence, it is ligated with an initiating adapter, which contains a type II restriction site for *Bbv1*. As in SAGE experiments, *Bbv1* cuts at a specific distance away from its recognition site with a 4 bp overhang. This overhang is sequenced by ligating it to an adapter which is specific for one nucleotide at a certain position. Each microbead is attached to 4 adapters which are specific for the 4bp sequence. In 16 cycles, phycoerythrin-labeled decoder probes are hybridized to the adapters, scanned with CCD detectors and washed off. The fluorescent images of the arrayed microbeads allow reconstructing the sequence. The cycle of *Bbv1* cutting, adaptor ligation and decoder hybridization and imaging is repeated until enough sequence information is achieved. Analyzing a statistical significant amount of microbeads enables the measurement of the expression profile of the transcripts.

Similar to SAGE, MPSS requires no prior knowledge of the transcripts. The measured absolute transcript counts allow direct comparison between experiments. Due to cloning on the microbeads and parallel sequencing, the workload is lower than in the case of SAGE. The disadvantage of the technology is the requirement of specialized equipment only available through Lynx Genetics [23].

2.1.6 Oligo- and cDNA-Microarrays are the most widely used gene expression profiling methods in genomic scale

Microarray technology [6,5] is the most widely used method to measure gene expression

profiles in a highly parallel manner. All different microarray platforms have in common that a nucleotide sequence is arrayed on a solid carrier, which is hybridized with a labeled nucleotide mixture of interest (with a radioactive marker or a fluorescent dye). The expression of each gene is measured by scanning each spot on the chip. Due to the fact that the gene position on the carrier is exactly known, the expression can be instantly assigned to a specific gene.

The fabrication of chips can be generally divided into spotted and *in situ* synthesized microarrays. Up to 780.000 oligonucleotides can be *in situ* synthesized on a single silicon wafer with photolithographic methods. The production of these high density chips remain in commercial hands like Affymetrix [5] and NimbleGen [26,27]. Further, an ink-jet system is developed by Rosetta Inpharmatics, which is licensed by Agilent [28]. These systems avoid handling of large cDNA and oligo-libraries as in the case of spotting methods. Contrary, the relative short length of *in situ* synthesized oligonucleotides (20-25mers) can result in a reduced selectivity and sensitivity [29]. Advances in this technology by NimbleGen use a Maskless Array Synteziser (MAS) method, which reduces costs and allow oligonucleotide lengths up to 70mers combined with higher flexibility in customized chip design [27,26].

Spotted chips [6] are based on arrayed cDNA clones of an expressed sequence tag library or on pre-synthesized oligonucleotides. Many resources of cDNA libraries, PCR primers and oligonucleotide (50-70mer) sets of various organisms are reviewed by Lyons [30]. A density of approximately ~30.000 genes per chip can be reached. Contrary to *in situ* synthesis, it is possible to use not yet sequenced clones, which enables the identification of completely uncharacterized mRNA species [29]. Due to the higher flexibility of spotted elements and the lower cost than *in situ* techniques, it is widely used in the academic research field. ESTs and oligos are printed with high-throughput robots on poly-lysin, amino silanes or amino-reactive silanes coated glass slide, which have a low inherent fluorescence. The surface coating enhances hydrophobicity and the adherence of the spotted probes [31]. The arrayed DNA is typically fixed by ultraviolet irradiation to the chip surface. A variety of currently available slides and printing systems are summarized by Affara [32]. To minimize the spot size and to improve the reproducibility the diameter of the pin tip, the hydrophobicity of the carrier surface, the humidity, the buffer types and the temperature must be optimized [32].

Total RNA is extracted from the samples of interest. The RNA must be purified from proteins, lipids and carbohydrate, which influence the hybridization negatively. If insufficient amounts of RNA are available, the signal can be amplified to continue the experiment with standard labeling and hybridization techniques. Different amplification methods are reviewed by Livesey [33]. One example of signal amplification consists in marking the reverse transcribed cDNA with specific tags. These are recognized by antibodies or proteins that are linked to an enzyme, which breaks down a tyramide-fluorophore dye that is added to the system. This technique has a 10-100 fold lower detection level with representative and reproducible results [34]. Sample amplification is divided in linear (T7) [35] and exponential (PCR) methods. Standardized linear T7 protocols allow amplification of nanogram quantities but are suffering from the transcript shortening resulting in a 3' bias [36,35].

Due to the high reproducibility of *in situ* syntheses of oligonucleotide chips, it is possible to compare accurately between chips hybridized only with one sample [29]. In contrast, spotted microarray techniques are relative methods and need hybridization of Cy3/Cy5 labeled sample and reference. During direct Cy3/Cy5 labeling, the two fluorescents are incorporated with a different rate. To resolve this issue, amino-allyl modified nucleotides are incorporated in the first reverse transcription step followed by a coupling of the dyes to the reactive amino groups of the cDNA [37]. Nevertheless, some dye-bias is persistent but it can be addressed by the dye-swapping technique, which is explained below. After labeling, the cDNA is denatured and hybridized to the chip in specific chambers. Unmatched cDNA is removed with stringent washing solutions. The last step in the experimental procedure consists of scanning of the slides in a chip reader. A variety of available scanners is summarized by Affara [32].

2.1.7 Real-time Reverse Transcription Polymerase Chain Reaction is the preferred method to detect expression of low abundant genes

Real-time Reverse Transcription Polymerase Chain Reaction (real-time RT-PCR) is a powerful method to identify the expression profile of low abundant transcripts (100-fold

more sensitive than microarrays). Real-time RT-PCR has a detection range of 0.001 to 100 transcripts per cell [38,39]. Detailed information about the sequences of interest is needed. For each transcript, two unique primers of 20-24 nucleotides in length with a melting temperature of 60 ± 2°C, a guanine-cysteine content of 45%-55% and a PCR amplicon length of 60-150 bp have to be designed. Splice variants can be assessed if the amplicon reaches over an exon-exon boundary. The polymerase chain reaction (with its cycling temperature profile for primer annealing, DNA synthesizing and denaturing) is performed in an optical 384-well plate using a fluorescence dye to monitor the dsDNA synthesis. A large RT-PCR profiling study measured the expression level of more than 1400 low abundant transcription factor (known and putative) [38].

2.1.8 Proteomic methods allow insights into posttranscriptional and posttranslational expression profiles

Transcripts are the blue prints for their corresponding proteins, which are the main players of cellular processes beside functional RNA. It is widely assumed that gene expression correlates with the translated products, but to ultimately derive the protein amounts, turn-over and post-translational modification, quantitative proteomic methods are needed. Due to the diverse physico-biological properties of proteins and the high dynamic range from one to millions of copies, it is with the state of the art nearly impossible to determine reliable and accurate amounts of proteins among others [40,41]. Nevertheless, ambitious technologies aim at solving these problems. Isotope-coded-affinity-tag (ICAT) uses a combination of liquid chromatography and mass spectrometry (LC/MS/MS) to measure protein levels quantitatively in a complex mixture [42]. Therefore, light and heavy ICATs are used as an internal standard. Relative expression values are obtained by binding the different ICATs to two different cell states. LC separates the proteins of the combined samples but the isotopes remain close together. Fragments of the co-eluted isotopes are separated by MS with an 8 Dalton mass difference, which can be used to obtain the relative abundance.

As the different ‘omic’ technologies and the bioinformatic tools for data integration evolve further, the most powerful approaches will be at the end an appropriate combination of genomic, transcriptomic, proteomic and metabolomic research which will lead to an

extensive understanding of the globular mechanism of cells and give complex insights into development and diseases.

2.1.9 To obtain meaningful results, a thoughtful experimental design is mandatory for large-scale expression profiling

Since large scale expression studies are labor-intensive and costly, a significant time should be spent for planning the experiments to maximize the informative results and minimize result bias. Randomization, replications and local control should be considered [43]. If differences in personnel, equipment, reagents and times, which can leave a signature on the gene expression profile, cannot be controlled by a good design, randomization and experiment repetitions are the best way to deal with them. Measurements of only one single sample do not allow the inference to the general behavior of the population of the respective biological systems. Therefore, biological (at least two samples for one set of measurements) and technical (one sample divided among at least two sets of measurement) replicates are needed [44]. Since biological variations are generally higher in any expression study than the technical noise, independent biological replicates are strongly preferred to generalize the results. Local control is used for arranging experimental material in relation to extraneous sources of variability. For example, if two different sample probes are to be compared (mice, tissues, …), the groups should be analyzed equally distributed over time to minimize a possible day-to-day difference (e.g. environmental influences, operator condition), which could otherwise bias the expression profile, if one group is investigated solely on one day and the other on a different.

Pooling biological samples might provide a form of “biological averaging” by achieving more accurate results with fewer measurements. A danger lies in a possible unrecognized camouflage of an outlier within the pool that cannot be identified but could influence the expression profile significantly in a wrong way. Therefore, pooling should be avoided, unless cost issues or material amounts do not allow it [43].

Ruijter et. al [45] investigated pair-wise comparisons of SAGE libraries and concluded that the most efficient way to set up a SAGE study without knowledge of transcript abundance is

to compile two SAGE libraries of equal size. A major drawback is that SAGE libraries represent only one experimental measurement lacking information of biological variation and experimental precision and, therefore, depend on simulations and assumptions of these parameters.

Two color microarray studies rely on appropriate labeling and hybridization strategies. Several reviews address these concerns [46,43,47]. Issues regarding the aim of the experiment, availability of RNA and chips as well as the experimental processes have to be considered. Two principal comparison routines are available: direct and indirect. If two samples are hybridized to the same chip, these can be compared directly. In contrast, indirect comparison between two slides needs a common reference (universal or biological relevant). Often a combination is the most practical way to go. Single-factor, loop or multifactorial design has to be chosen to address the biological question correctly [48,49]. For example, if treated or diseased tissues should be compared to healthy samples, the clear design choice is to compare all atypical once to a common reference (the healthy). To confront the systematic color bias of the two fluorescent dyes used in cDNA microarrays, dye-swapping should be used wherever possible. Therefore, two chips have to be hybridized with vice versa labeled samples.

2.2 Computational analysis of expression profiling data – Biological significance of the expressed genes

Designing the experiment and obtaining the expression values is the first part of an expression profiling study, resulting only in a plain list of differentially expressed tags/transcripts/proteins under specific conditions. Computational methods can help to correct the raw expression data from systematic and random bias, to determine the true expression status of genes, to derive new insights and hypotheses with regard to function of genes and biomolecular networks, processes and mechanisms. Due to the large scale of SAGE, MPSS and microarray experiments, these important analyses typically take a significant if not the largest time of the whole study. Since expression profiling studies are typically initiated in laboratories without tradition of computational biology research, human resources (with respect to number and qualification of researchers), time ranges and capital

investments in an appropriate computer and biological software environment dedicated to this effort are typically grossly underestimated.

Normalization of data minimizes biases of the expression values. There are general statistical considerations specialized for the different profiling applications [48]. Several tools integrate different normalization algorithms. ArrayNorm [50] is an academic, freely available, stand-alone software package; the Bioconductor project [51] is another alternative. Some normalization functions are also available as part of the Genesis suite [52]. Several public and commercial expression profile databases are available for sharing the measured profiles within the community. These function as a central repository to retrieve data for re-analyzes and comparisons. Clustering algorithms group genes or samples with similar expression profiles together. Co-expressed genes could share possibly a common regulatory mechanism. Groups of samples may identify specific cancer types. *De novo* prediction of functional domains can identify novel molecular and cellular functions of proteins. Especially for pharmacological treatment, transmembrane proteins, receptors and enzymes with small binding pockets are of enhanced interest. Finally, pathway mapping and network re-construction together with extensive literature enquiry might give an insight into the global interactions and the molecular atlas of the cell.

2.2.1 Repositories of expression data - Differences to other tissues and health states can be uncovered through comparison

Expression databases (Table 1) provide access to raw and sometimes also processed versions of a multitude of measured gene expression profiles. Such deposits allow to reanalyze and validate experiments as well as to compare data with other related topics. Data sharing in publicly available databases is, therefore, an important issue that is, especially in microarray studies, mandatory for submission in some journals. Since experimental design, treatment, tissue type, normalization and many other factors influence the expression profiles, these parameters have to be stored together with the measured and normalized data. *Minimal Information About a Microarray Experiment* (MIAME) is a standard proposed for describing chip datasets by the Microarray Gene Expression Data Society to ensure that data can be easily interpreted and results can be independently verified [53].

An analysis of the expression datasets in the database GEO reveals interesting trends. As shown in Figure 1, there are two techniques that are most popular in expression profiling – *in situ* hybridization microarrays (including Affymetrix chips) and cDNA spotted microarrays. Whereas the first type of arrays can be applied only in manufacturer-supplied customized forms, the second is technologically simpler and cheaper to produce and, therefore, the method of choice for researchers working on more esoteric model organisms then human, rat or mouse. Figure 2 illustrates that expression profiling is still far from reaching a saturation phase, the number of new datasets coming into public databases each quarter is still growing.

Comparison of absolute as well as relative expression values can be carried out between datasets of various sources. Often, it is an extremely difficult task due to differences in methods, experimental designs and systematic biases. Relative measurements already implicate comparisons intrinsically. For a 'counting' method like SAGE and for *in situ* oligo-microarrays, comparison to public data is easy. Such studies can reveal specific marker genes, differences in mechanisms between healthy and diseased states and show variations among sample groups (e.g., cancer subtypes). If similar sources are compared, hypotheses for upcoming new experiments can be derived and, hopefully, an expansion of the present mechanistic knowledge is achieved.

2.2.2 Clustering reveals distinct patterns in expression profiles

To find similarities and differences between biologically comparable datasets, algorithms clustering genes with similar expression status are used. Generally, it is possible to group genes by their co-expressed genes, samples by similar expression profiles or to combine both. Clusters of co-expressed genes can share similar cellular functions and are likely to be transcriptionally co-regulated. For example, groups of samples can identify cancer subclasses by their expression profiles [54,55].

Several public and commercial tools are available on the market that have implemented a large variety of clustering algorithms and distance measurements (e.g. Genesis [52], TM4 [56]). It should be noted that there are more than 30 papers that offer different mathematical

forms of clustering expression profiles but it is not really clear whether mathematical sophistication is always good for the application. None of the clustering algorithms can claim for itself that its special analytical form does reflect aspects of the biological system better than the others and, therefore, they should be similarly good for the purpose. Even more, cluster assignments of genes and experiments that change dramatically upon application of specific clustering algorithms are rather not informative from the biological point of view. It should also not be forgotten that some datasets contain considerable noise (error margins of ~100% are not rare) and clustering of such data can result in artifacts.

Typically, the clustered expression profiles are visualized by coloring them in accordance with their log2(*ratio*). This analytical form of the ratio between a sample and a reference state is used because of its simplicity for interpretation (a two-fold change increases or decreases the log2(*ratio*) by one unit). Mostly, repression of the genes in comparison to the reference is visualized by green (negative log2(*ratio*)) and over-expressed genes are colored red (positive log2(*ratio*)). The higher the expression or repression the brighter the colors are. Black represents equal amounts.

For measuring the similarity of expression profiles, each gene is characterized by a n-dimensional vector defining n as the number of samples/experiments. Various distance metrics (Euclidean distances, correlation distances, semi-metric distances, …) are proposed to identify a closely related group [57]. The correct choice of the appropriate distance metric between the vectors is a difficult question and might depend on the data preprocessing (e.g., normalization). For SAGE experiments it is shown that Poisson-based distances fit well [25]. Generally, the observed biological effects should be stable with regard to minor aspects of the distance metric.

Provided with a distance measurement, supervised and unsupervised clustering methods can group the genes by their similarities. Unsupervised approaches are used to find co-regulated genes or related samples. For supervised methods (e.g. supported vector machine), which can create classifiers to predict some behavior, additional knowledge for some profiles must be provided like functional classes or healthy and diseased states [58]. Three different unsupervised methods will be described shortly to give an insight into the mechanism behind the most important algorithms.

Hierarchical clustering [59], one of the most common unsupervised methods, joins consecutively the nearest clusters/genes together until all are combined in one large group. As a result, the clustered genes are placed into a dendrogram that visualizes the closeness of the transcriptional status among the genes. Single-, complete- and average-linkage clustering corresponds to joining of growing clusters regarding the minimum, maximum and average distances between them [57]. Comparing the minimum distances results in loose clusters, whereas with complete-linkage compact clusters are achieved. It is a drawback of the simple hierarchical clustering that an incorrect intermediate assignment cannot be reversed and, thus, the expression vector defining a cluster might no longer represent the genes in it.

K-means clustering [60] is an iterative method which requires the initial knowledge of the cluster number K. The genes are randomly assigned to the K clusters. Through iterative gene shuffling between the clusters, the within-cluster dispersion is minimized and the inter-cluster distances are maximized. It stops if no improvement can be achieved anymore or if a specified number of iterations is exceeded. The method is computing-intensive but some early incorrect assignment can be modified at later iterations. A hierarchical ordering of clusters is not achieved and, therefore, no dendrogram is generated.

Principal component analysis (PCA) [61] reduces the dimensionality of the expression data through eigenvector calculations and data projection into the space spanned by the most important eigenvectors. Therefore, redundant properties of the expression profile are filtered out and major distinct patterning that describes the data separation of genes best might become clear. PCA results are visualized in the 3D-space with small clouds of data points that correspond to clustered genes or experiments.

2.2.3 The molecular role of a gene product can be identified through sequence analysis

Essentially, the basic element of expression data has a composite structure: On the one hand, it comprises a vector of n real numbers describing the expression status for n conditions/experiments/time points. Quantitative and qualitative methods for analyzing the

real value part of the data have been considered in the previous chapters. On the other hand, a sequence tag is associated with the vector of expression values. Without the knowledge of the identity of the gene represented by the expressed sequence tag and the biological function of the respective gene, interpretation of the expression data in terms of biological mechanisms and processes is impossible. It should be noted that protein function requires a hierarchical description with molecular function, cellular function and phenotypic function [62].

The first step is to allocate the corresponding gene and protein if available. With the knowledge of complete genomes, sequence comparisons can identify genes from sufficiently long sequence tags. For instance rounds of Megablast searches [63] against various nucleotide databases of decreasing trust-levels (in the order of RefSeq [64,65], FANTOM [66], UniGene [67], nr GenBank, and TIGR Mouse Gene Index [68] or other organism-specific databases) can be initially applied. If not all nucleic sequences can be assigned, the routine should be repeated with blastn [69] and finally against the genome of the whole organism. Long stretches (>100) of non-specific nucleotides have to be excluded. For the obtained genes, the respective gene product can be retrieved: This is either a protein sequence if the expressed RNA is translated to a protein or a functional RNA species (microRNA, …).

The molecular and cellular role of novel protein targets derived from an expression study is of special interest. A first insight of the processes involved can be obtained from Gene Ontology (GO) terms [70]. With the GenPept/RefSeq accession numbers, GO numbers for molecular function, biological process, and cellular component can be derived from the gene ontology database (Gene Ontology Consortium). If considered in context with the expression cluster identity, it is possible to observe groups of co-regulated proteins which are part of an unique process or share a molecular function. Such groups of genes can be visualized with Genesis [52].

Detailed *de novo* function prediction for the target proteins can reveal new aspects of their molecular and cellular function. This analysis step is especially important for sequences that entered the databases after large-scale sequencing efforts and that have remained

experimentally uncharacterized. A large variety of different sequence analysis tools are available. Sometimes, a homology search with the blast tool [69] (with low e-value cut-off <e-10) finds an almost full-length homologue with a described function that can be transferred to the protein of interest.

In-depth sequence-analytic studies involve a three-step procedure. This approach is based on the assumption that proteins consist of linear sequence modules that have their own structural and functional characteristics. The function of the whole protein is a superposition of the segments' functions. The sequence modules can represent globular domains or non-globular segments such as fibrillar segments with secondary structure, transmembrane helical segments or polar, flexible regions without inherent structural preferences.

The first step involves the detection of the non-globular part of the protein sequence, which houses many membrane-embedded segments, localization and posttranslational modifications sequence signals. Typically, non-globular segments are characterized by some type of amino acid type compositional bias. Therefore, the principle procedure is to begin with analyses of compositional biases. They are found as low complexity regions with SEG [71] and compositional biased stretches with SAPS [72], Xnu, Cast [73] and GlobPlot 1.2 [74]. N-terminal localization signals can be studied with SignalP [75] and Sigcleave[76], the C-terminal PTS1 signal for peroxisomal targeting via the PEX5 mechanism is checked for with the predictor of Neuberger *et al*. [77,78,79]. A number of quite accurate predictors test the capacity of the query protein for lipid posttranslational modifications such as GPI lipid anchors [80,81,82], myristoyl [83] or prenyl (farnesyl or geranylgeranyl) [84] anchors. Membrane-embedded regions are recognized via the occurrence of strongly hydrophobic stretches. Standard predictors such as HMMTOP [85], TOPPRED, DAS-TMfilter [86] and SAPS [72] find transmembrane helical regions. Generally, several transmembrane prediction methods should map to the same loci to obtain reliable results. Secondary structure prediction methods (COILS [87], SSCP [88,89], Predator [90]) can generate information about secondary structural elements in non-globular parts of proteins.

The second step involves comparisons of the query sequence with libraries of known domains. Since domain definitions of even the same domain type do slightly differ among

authors, it is necessary to check all available for the given query sequence. Known sequence domains of the repositories PFAM and SMART [91] are characterized by hidden Markov models (HMM), which can be searched against a sequence with HMMER both in a global and local search mode. Further domain prediction method and databases are RPS-BLAST (CDD) [92], IMPALA [93] and PROSITE [94].

The third, the last step involves analysis of query protein segments (at least 50 amino acid residues long) that are not covered by hits produced by any of the prediction tools for non-globular regions and known domains. Most likely, these sequence segments represent not yet characterized globular domains. It is necessary to collect protein sequence segments that are significantly similar to the respective part of the query. This can be done with tools from the BLAST/PSI-BLAST suite [95,96,97], HMMsearch or SAM [98,99]. There are several strategies to collect as complete as possible sequence families; for example, each identified homologous protein can be resubmitted to an additional PSI-BLAST in an attempt to find more homologues. Through multiple alignments of the conserved residue stretches, sequence analysis of the found proteins and extensive literature search, a new functional domain can be characterized. Further, prediction of tertiary structure can sometimes help to answer additional questions (e.g. small pockets for therapeutics). PDBblast can identify the structure through homology to proteins with known tertiary structure. *De novo* structure prediction methods are evolving very fast. An excellent meta-server combining various structural prediction method can be found at bioinfo.pl [100].

Finally, the different sequence-analytic findings for the various query segments need to be synthesized for a description of the function of the whole protein. Overlaps of predicted features have to be resolved by assessing significances of hits, the amino acid compositional status of the respective segment and expected false-positive prediction rates of algorithms. With the entirety of the sequence-analytic methods, some functional conclusion at least in very general terms is possible for most sequences. All these academic prediction tools for *de novo* sequence prediction are integrated in the user-friendly ANNOTATOR/NAVIGATOR environment, a novel protein sequence analysis system which is in development at the IMP Bioinformatics group. A single experienced researcher can reasonably characterize ~100

sequence targets per day in this environment.

2.2.4 Network reconstruction gives insight into the transcriptional mechanisms of small genomes

Expression profiling is, due to the wealth of data, a good source for reconstruction of gene networks. Generally, these methods determine genes, which affect the activity of other ones. Genes are represented in the networks as a node and the impact on another gene is shown in a connective arc. The arcs can receive a label, like up- or down-regulation [101,102]. Networks can describe as diverse conditions as the influence of one gene expression on another expression [102] or the influence of a deletion mutant on other gene expressions [101] and even the mention of two genes in the same paper as in literature based networks [103,104]. The construction of these interactions relies among others on Boolean networks, Bayesian networks or biological-meaningful decision trees. Further, it is possible to integrate additional knowledge like transcription factor binding of chromatin-immunoprecipitation (ChIP) or computational prediction of transcription factor binding [105].

Unfortunately, most of these studies are limited to small genomes and dataset. Especially the well characterized yeast *Saccharomyces cerevisiae* is a preferred model system for network reconstruction. This is no surprise since the accuracy of the genome sequence, the established methodologies of measuring precise and reproducible expression profiles and the wealth of other biological data available invite for such analyses. It will take a while until methods will generate similar biologically reasonable insight for more complex organism.

Several procedures allow prediction of regulatory elements of genes important for the regulatory network, which is implicated in the expression profile. One way is to cluster the genes by their expression profile and search for transcription factor binding sites of public databases (e.g. TRANSFAC) that are specific for a cluster [106]. A different approach is a *de novo* prediction of regulatory oligonucleotides based on the genome-wide expression profiles and the promoter sequences. The web-based tool, Regulatory Element Detection Using Correlation with Expression (REDUCE), tries to explain the log-ratio of a gene expression by the number of occurrences of the motif in its promoter. The regression coefficient

associated with the motif occurrence can be directly interpreted as the change in concentration of the active transcription factor in the nucleus [107].

2.3 Validation of expression profiles – Testing the hypothesis

In large scale expression profiling, there are many sources of errors beginning from wrong sequencing, tag assignment, arraying, labeling biases, difficulties in managing large clone sets and datasets, over reagent, color, equipment, personal and day-by-day biases and sample specific errors. Therefore, an identified novel target gene of a large scale expression study must always be validated with a second different method to exclude a wrong measurement of a specific method and to be sure to address the right target. Especially Northern-Blotting and RT-PCR are the preferred methods to verify DNA microarray expression data [37]. Expression profile analysis-based hypotheses have to be investigated in further follow-up studies using appropriate techniques such as RNAi, overexpression or knock-out experiments.

3 Success stories with expression profiling in angiogenesis and other biological processes

The original idea of using large-scale gene expression profiling for the elucidation of systembiological properties (for example, gene networks) of cells has found its realization only in a few studies and these focused mainly on simple model organisms. At the beginning, the problems with accuracy and reproducibility of large-scale expression measurements favored two other types of applications, namely (i) the usage of microarrays for the identification of a handful or even a single target that are most up-regulated in certain physiological conditions and (ii) the numerical overall comparison of large sets of expression values between different physiological states for diagnostic purposes (for example, for the differentiation between cancer development stages). In both cases, even gross errors of expression values for a limited number of genes do not affect the outcome dramatically. With the technology improving, the original idea of understanding gene networks has

revived and it has become possible to delineate groups of genes in expression profiles that are together responsible for certain cellular processes and explain the molecular mechanism behind physiological phenomena.

The following sections highlight some selected recent expression profiling studies, which have led to the identification (i) of only a few but critical targets, (ii) of group of transcripts that are involved in common pathways and processes, and (iii) of genes that could be placed into a network construct. We put special emphasis on attempts to study expression profiles of cells/tissues with a role in angiogenic processes but, if appropriate, we will present also other examples.

3.1 Identification of targets with prominent expression regulation

Roca *et al.* [108] investigated the mechanisms underlying the inhibition of *in vitro* and *in vivo* angiogenesis during hyperthermia. This treatment often complements radiotherapy or chemotherapy of cancer [109,110]. First, an inhibition of angiogenesis was observed in *in vitro* endothelial cells on a three dimensional preparation, which were exposed to temperatures 41-45ºC. Culture medium treatment with the angiogenic factor VEGF-A_{165} could not neutralize this inhibition. The same observation was found in the *in vivo* chick embryo chorioallantoic membrane assay. To understand the molecular mechanism, a microarray experiment was performed. The results showed a marked up-regulation of the plasminogen activator inhibitor 1 (PAI-1) [108]. PAI-1 is responsible for the extracellular matrix homeostasis during angiogenesis [111]. Finally, the hypothesis of the PAI-1 involvement was further manifested by the indication that anti-PAI-1 antibodies antagonize the hypothermia effects on angiogenesis of *in vitro* and *in vivo* systems [108]. This study started with a phenotypic observation in *in vitro* and *in vivo* systems. The investigation has relevance for real therapy. Further, this led to the characterization of the effects at the transcriptional level with microarrays. The hypothesis of PAI-1 involvement in the process of angiogenic inhibition during hypothermia evolved from this experiment and it was proven with additional experiments.

Watanabe *et al.* [112] searched with cDNA microarrays for VEGF-inducible genes in human

umbilical vein endothelial cells (HUVECs). 97 genes were up-regulated more than two-fold by VEGF. This group contained 11 uncharacterized products. In their follow-up study, they concentrated on KIAA1036, which was named vasohibin. The recombinant protein inhibited VEGF- and FGF2-induced angiogenesis, which indicated that vasohibin secreted into the extracellular space acts on endothelial cells. Further, this endothelial cell specific transcript inhibited tumor angiogenesis *in vivo* in transfected Lewis lung carcinoma cells. Therefore, the first evidence of a feedback inhibitory factor involved in angiogenesis was found by large-scale microarray techniques combined with appropriate experiments to prove the hypothesis.

Tubulogenesis by epithelial cells regulates kidney, lung, and mammary development, whereas that by endothelial cells regulates vascular development. Albig and Schiemann [113] studied gene expression differences of endothelial tubulogenesis and of epithelial tubulogenesis with the microarray technology. The regulator of G protein signaling 4 (RGS4), which was not previously associated with tubulogenesis, was found to be up-regulated >8-fold in tubulating cells compared to the control samples, thereby implicating RGS4 as a potential regulator of tubulogenesis.

Zhang *et al.* [114] wanted to shed light into the molecular mechanism of the phenotypic observation that antithrombin is transformed to a potent angiogenic inhibitor by limited proteolysis or mild heating [115]. Treatment of bFGF-induced and control HUVECs with latent antiangiogenic antithrombin repressed the key proangiogenic heparan sulfate proteoglycan, perlecan, significantly compared to HUVECs treated with native antithrombin. This observation made with the cDNA microarray technology was confirmed on the mRNA and protein level with semi-quantitative reverse transcriptase-polymerase chain reaction (RT-PCR), Northern blotting, and immunoblotting analyses. Finally, it was shown, that the exposure to TGF-beta1, another stimulator of perlecan expression, overcomes the inhibitory effect of antiangiogenic antithrombin [114].

Yuan *et al.* [116] investigated the role of ephrinB2 and its receptor ephB4, which have to be localized in the membranes of adjacent cells for interaction, in inflammatory angiogenesis. cDNA membrane microarray experiments identified a group of 13 up-regulated genes after

ephrinB2 stimulation of HUVEC. Syntenin, which binds syndecan, is a member of this gene group. Subsequently, RT-PCR and Northern blotting confirmed the increased expression of syndecan-1. Further experiments showed that ephrin stimulated up-regulation of syndecan-1, which exhibited *in vitro* antiangiogenic and *in vivo* angiogenic effects. Due to the fact that the enzyme heparanase, which converts soluable syndecan-1 from an inhibitor into a potent activator of angiogenesis, is expressed in inflammatory environments, controversial effects were observed [116]. This study emphasizes that the observations of simplified *in vitro* studies cannot always be generalized for *in vivo* systems even if the same expression is measured. Due to additional, probably unmeasured signals and proteins, further rational inspiration and literature research can help to identify missing links of the original expression profiles. This is especially important if only a limited number of genes were profiled. Therefore, it is critical to keep in mind that a gene expression profile mirrors only a snapshot of the transcripts at a specific time in a specific environment, which might not be able to explain effects caused at higher levels of regulations, for example post-translation modifications. Further, genes that are not arrayed slip through the measurement in the case of DNA chips.

The Nanog story nicely illustrates the difficulties in proper interpretation of expression data. Microarray-based studies of expression profiles focused on embryonic stem cells have generated a long lists of putative important genes involved in the core stem cell properties [117]. Only a year later, Nanog was identified as a key gene with important roles in pluripotency and self-renewal of embryonic stem cells [118]. The vast amount of uncharacterized genes of the original experiment left this protein unrecognized until it was re-identified with cDNA library screening methods followed by the molecular characterization of the homeodomain containing transcriptional regulator, which proved to be a key player of self-renewal [118]. Yet another year later, a microarray study [119] revealed with hierarchical clustering that Nanog is also highly expressed in carcinoma *in situ* (CIS), the common precursor of testicular germ cell tumors, and might play an important role in malignant behavior. Comparison of the CIS expression profile showed common patterns with embryonic stem cells supporting the hypothesis of early fetal origin of CIS cells.

Expression analysis studies that focus only on the handful of top-regulated genes have received considerable support from large-scale expression profiling and lead to many research results with biological and medical significance. At the same time, it might be considered a waste of effort if the rest of the expression profile was not studied with appropriate scrutiny. Interestingly, most single factor identification experiments in angiogenesis research didn't use basic profile analyses methods such as normalization and clustering. Instead, they concentrated on a single differentially regulated factor and performed further experiments to verify the hypotheses. A higher success rate in identification of novel targets and mechanisms might be achieved if the profiles of large scale expression studies are analyzed rigorously with the goal of deriving hypothesis from these results. Naturally, this effort is combined with huge work of computational analysis (both with respect to expression value studies and gene function prediction with sequence-analytic methods together with literature research). We think that such a hypothesis-driven strategy might prevent some trial-and-error approaches and, therefore, redirects the sequel experiments into the right direction reducing time- and resource-consumption of follow-up studies.

3.2 Identification of groups of target genes responsible for cellular mechanisms

In the consideration of expression studies, quality aspects of sample preparation are often overlooked. This issue is especially important for angiogenesis-related investigations since endothelial cells form only single layers on the base membrane in vessels that intimately penetrate other tissues. The pure extraction of endothelial cell from human tissue samples in a form useful for expression profiling from in vivo material was first achieved by St. Croix *et al.* [2]. As an application, they examined differential gene expression in normal and tumor endothelial cells (ECs). Purified human ECs were subjected to SAGE profiling (with sequencing of ca. 100000 tags). On the one hand, 93 pan-endothelial markers were extracted with similarly high expression in normal and tumor ECs. On the other hand, 33 tags (named Normal Endothelial Markers; NEM) and 46 tags were identified to be specifically elevated in normal endothelium and in tumor endothelium respectively. Despite of the methodical progress, the work of St. Croix *et al*. left several issues open.

(i) Surprisingly, the second group of 46 tags was called Tumor Endothelial Markers

(TEMs), although the authors could not bring up any biological argument justifying specificity of the ECs extracted from tumor tissue for the tumor state. Not surprisingly, an in-depth sequence-analytic study of the TEMs [1] showed that they are generally highly expressed during angiogenesis of wound healing, corpus luteum formation, bone restructuring, etc. Thus, the TEMs are in fact markers of angiogenesis describing common features of the respective cellular processes.

(ii) Many tags were left without link to genes and many genes missed a functional characterization. Novatchkova and Eisenhaber [1] carried out a case study of the identification of molecular mechanism from gene expression profiles. A careful strategy of tag-to-gene mapping was applied, which led to only nine tags without a link to a gene. With a variety of different sequence analysis algorithms, putative non-globular domains and globular domains were assigned to the protein sequence. This information of the protein architecture together with homology searches and target-specific scientific literature links led to molecular and cellular function and mechanistic insights of the involved PEMs and TEMs.

Novatchkova and Eisenhaber found that most TEM targets identified are relatively downstream of the regulatory cascades leading to angiogenesis. They are involved in more general features such as extracellular matrix remodeling, migration, adhesion and cell-cell communication typical for migrating cells in restructuring tissues rather than specific for angiogenesis initiation and control. Therefore, these genes should be termed more correctly as angiogenic endothelial markers. Apparently, also the abundance of transcripts is important. The identification of genes that are mainly endpoints of regulation cascades mirrors the preferred registration of highly abundant transcripts in the original SAGE study. Further, it was shown that *in vitro* endothelial expression studies are very different from *in vivo* profiles and, therefore, hardly representative for the *in vivo* situation.

SP100 interacts with the proangiogenic transcription factor ETS1 and represses thereby the DNA-binding and transcriptional activity [120,121]. Since SP100 is also expressed in endothelial cells, Yordy et. al. [122] tested the hypothesis that SP100 alters the ETS1 response in endothelial cells. It was shown that the antiangiogenic interferons IFN-α, IFN-γ and TNF-γ induce SP100 in endothelial cells. To characterize the negative phenomenological

modulation of SP100 on ETS1 on the molecular level, gene expression profiles were generated with microarrays. With hierarchical clustering, 1000 expressed sequence tags (ESTs) were grouped and the complexity was further reduced with a self organizing tree algorithm. This resulted in 129 ESTs which are reciprocally regulated between the SP100 and ETS1 experiments. Gene ontology terms were assigned. This strategy led to the conclusion, that only a part of ETS1 regulated genes can be modulated by SP100 but genes that show reciprocal expression in response to ETS1 and SP100 have anti-migratory or anti-angiogenic properties.

Nagawaka *et al*. [123] investigated the influence of hematopoietically expressed homeobox (HEX), which is transiently up-regulated in endothelial cells during vascular formation in embryos [124]. Therefore, HUVECs were transfected with the transcription factor HEX and the effects on the transcriptome were compared relative to not transfected cells with cDNA microarray. The repression of several important factors including VEGFR-1, VEGFR-1, TIE-1, TIE-2, and neuropilin-1 was observed. In contrast, mRNA levels of endoglin, ephrin B2, urokinase-type plasminogen activator, tissue-type plasminogen activator, plasminogen activator inhibitor-1, TIMP-1, TIMP-2, and TIMP-3 were upregulated >2-fold [123]. This expression profile mirrors a repression of angiogenesis induced by HEX in an *in vitro* study and assigns, thereby, an antiangiogenic role to HEX in this environment.

Angiogenesis is an important process for tumor growth [125]. Nevertheless, it was reported that tumors can grow without new vessel formation by taking advantage of pre-existing ones [126]. Hu *et al.* [127] investigated the transcriptional differences between angiogenic and nonangiogenic non-small-cell lung cancer with cDNA microarrays. These two phenomenological characteristics could be distinguished by a group of 62 genes. It was found that non-angiogenic tumors have more up-regulated genes involved in mitochondrial metabolism. Thus, intracellular respiration appears more effective in non-angiogenic tumors.

Thijssen *et al.* [128] followed an interesting approach to profile the important communication and interaction between tumor and endothelial cells. Therefore, a xenograft tumor was constructed by inoculation of mice with human tumor cells. Quantitative real time RT-PCR (qRT-PCR) was used to measure the expression level of 16 angiogenesis-related

genes. To distinguish between the mRNA origins, primers specific for mouse and human were constructed in low homology regions. bFGF expression was for instance 300-fold higher in non-tumor cells. The real power of this method was shown by monitoring the changes in the two compartments in response to different antitumor treatments.

The combination of vascular endothelial growth factor (VEGF) and hepatocyte growth factor (HGF) induces a more robust angiogenesis than by each factor alone [129]. Gerritsen *et. al.* [130] investigated the underlying mechanisms of this additive affect by measuring the response of VEGF and HGF as well as the combination of both with Affymetrix microarrys. Relative log ratios were obtained by comparing the induced profile with the basal one. Only a small fraction of the enhanced genes were up-regulated in both datasets after VEGF or HGF stimulation. The synergistic interaction differentially regulated twice as many genes as for each growth factor alone, including many totally different genes. This study emphasizes the importance to investigate not only the response of a single factor but also the synergistic combination of two or more to identify the important targets for an efficient anti-angiogenic cancer therapy.

3.3 Identification of gene networks

The reconstruction of gene networks from expression profiles is the ultimate goal; although, it remains a matter of the future with respect to angiogenesis. In this section, we describe a few examples that highlight the principal possibilities. It should be noted that most network reconstruction studies were carried out on yeast and other model organisms with small gene numbers. Even under these conditions, the level of system understanding and the biological significance of results remain limited.

Ideker *et al.* [8] investigated the galactose utilization in yeast by an integrated approach of genomic and proteomic data. Therefore, the genome sequence and the identity genes, proteins and other players in pathways were known at the beginning and an initial qualitative (topology) model of the galactose related part of the network could be constructed *a priori*. The authors introduced several perturbations in yeast cultures and recorded the genomic and proteomic response. Analysis of the expression profiles allowed improving the model of the

network. This process of perturbation and integration of its resulting influences into the model was iteratively repeated. This approach led to a number of refinements of the galactose utilization model with regard to network interactions and new regulators.

Basso *et al.* [131] claim to have reconstructed a genetic network from large scale expression profiles in the mammalian cells. For a substantial range of absolute expression, a large set of 336 human B cell phenotypes were profiled with microarrays and an algorithm for the reconstruction of accurate cellular networks (ARACN) was applied. The network indicates a topology of few highly connected hubs and a high number of less connected nodes with a hierarchical control mechanism, which is already known for phylogenetically earlier organisms [131,132]. Further the gene named BYSL was biochemically identified to be part of the proto-oncogene MYC network, which might have important cellular roles. The interpretation approach might be especially interesting for investigation of tumor subtype differentiation [131].

Gao *et al.* [105] analyzed transcription networks by combining genome-wide expression data of ~750 expression pattern and the genome-wide promoter occupancies for 113 transcription factors. Surprisingly, roughly the half of the transcription factor targets, which were predicted by the ChIP analysis, was not regulated by them. Therefore, the regulatory coupling strength was calculated between all transcription factors and genes, which might enhance the specificity of target predictions. The importance of coupling was further manifested by enrichment of specific Gene Ontology categories and significant change in mRNA expression of transcription factor deletion mutants in the coupled test group compared the bound transcription factor but un-coupled group. This study highlights that binding of a transcription factor is not sufficient to predict the regulation of the gene.

4 Summary

This review has considered both experimental and computational biology methodologies used for gene expression profiling as well as applications of these techniques to angiogenesis. Although the expectations from expression profiling techniques within the

scientific community were initially high (especially with respect to the system-wide view and analysis), the additional insight produced by the respective research efforts are limited and our understanding of molecular processes remains fragmentary. Nobody has ever calculated the costs that were funneled into expression profiling in general and for angiogenesis and tumor analysis specifically and analyzed possible outcomes of alternative investment scenarios. It is widely accepted that expression profiling methods have become an indispensable part of the arsenal of modern research methods. In carefully selected cases, these techniques will generate the decisive data.

We think that, for some applications, currently gene expression profiling methods might be simply insufficiently mature. We expect their considerable technical sophistication in coming years with emerging solutions for improving accuracy, reproducibility, sensitivity and reduced requirements in sample size. Single cell expression profiling will certainly become a standard. In addition to technical improvements for expression measuring, the consequent application of available computational biology approaches (for the post-experimental treatment of data) can extract more value from available expression profiles already now. Normalization and clustering of expression vectors should become a standard as well as sequence-based function prediction for insufficiently characterized genes and their protein products. Most studies have not invested enough for these purposes and the respective principal investigators should be encouraged to look after appropriate collaborations.

Finally, expression profiling should be viewed in context of cellular hierarchies and the different methods that generate information about them. For proper biological interpretation, it will be important to integrate genome sequence data, gene and protein functional annotation, gene expression profiles and protein occurrence data from proteomics experiments.

TABLES

Table 1 Gene Expression Databases accessible through the internet

Database	**Database type**	**Internet location**
Gene Expression Omnibus (GEO) [133,134]	Repository for expression data	http://www.ncbi.nlm.nih.gov/projects/geo/
ArrayExpress [135,136]	Repository for microarrays	http://www.ebi.ac.uk/arrayexpress/
SAGEmap [137]	Repository for SAGE	http://www.ncbi.nlm.nih.gov/projects/SAGE/
GNF SymAtlas [138]	Normal tissues (Affymetrix)	http://symatlas.gnf.org/SymAtlas/
Riken Expression Array Database [139]	Normal tissues (cDNA microarray)	http://read.gsc.riken.go.jp/fantom2/
SAGE Genie [140]	Normal tissues and cancers (SAGE)	http://cgap.nci.nih.gov/SAGE

Gene Expression Omnibus (GEO) is a public repository of high-throughput molecular abundance data. GEO is dedicated mainly to gene expression data but can even store proteomic abundances. ~1300 platform entries and over 40000 public samples have been stored till June 2005: ~38500 cDNA-, ~1100 genomic- and ~600 SAGE-samples [133,134]. ArrayExpress is a public microarray repository of well annotated raw and normalized data which is stored in the Minimum Information About a Microarray Experiment (MIAME) standard [135,136]. SAGEmap is a repository for SAGE expression data which allows the mapping of the tags to the corresponding transcripts [137]. Tissue-specific transcript expression of a normal physiological status in mouse and human are extensively profiled with Affymetrix- and cDNA- microarrays and stored in databases. The expression profiles of normal tissues provide the base-line for identification of transcript candidates of diseased and cancerous states through comparison [141,138,139]. The SAGE Genie of the Cancer Genome Anatomy Project is helpful in comparing SAGE results with numerous non-pathological tissue and cancers [140].

FIGURES

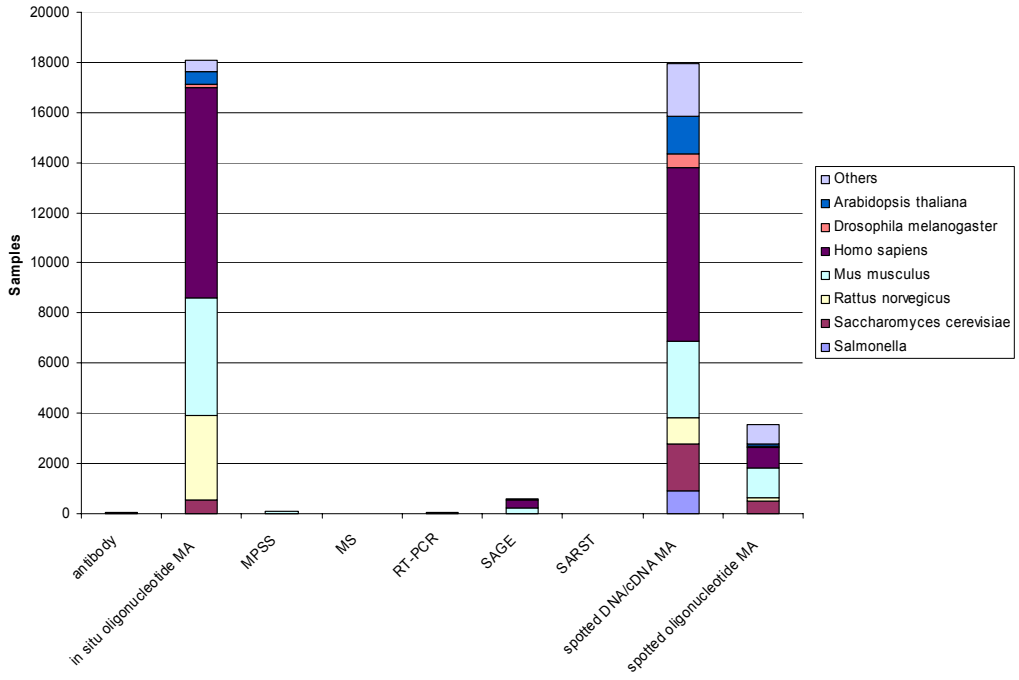

Figure 1 Gene Expression Omnibus sample distribution

The prevalent method for expression profiling stored in the largest expression database GEO (http://www.ncbi.nlm.nih.gov/projects/geo/) is the microarray (MA) technology. According to the sample number, *in situ* hybridized and cDNA spotted chips are approximately equally popular. The dedication of these two technologies differs in the sample origin. *In situ* hybridized chips are mainly used for the species *Homo sapiens, Mus musculus and Rattus norvegicus*. In contrast, the flexibility of cDNA microarrays allows a much broader range of ~70 different organism origins.

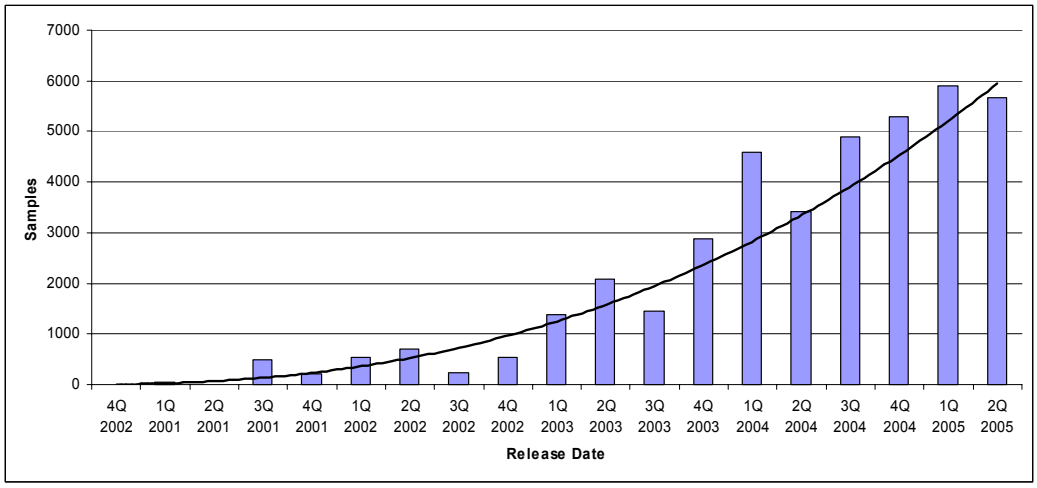

Figure 2 Incremental change of dataset numbers in GEO

This diagram illustrates the number of incoming datasets for GEO per quarter. Apparently, the stream of new expression profiles grows in accordance to a power law (with exponent of ~2.5).

Reference List

1. Novatchkova, M. and Eisenhaber, F., Can molecular mechanisms of biological processes be extracted from expression profiles? Case study: endothelial contribution to tumor-induced angiogenesis, *Bioessays*, 23, 1159, 2001

2. St Croix, B.et. al, Genes expressed in human tumor endothelium, *Science*, 289, 1197, 2000

3. Velculescu, V.E.et. al, Serial analysis of gene expression, *Science*, 270, 484, 1995

4. Brenner, S.et. al, Gene expression analysis by massively parallel signature sequencing (MPSS) on microbead arrays, *Nat. Biotechnol.*, 18, 630, 2000

5. Lipshutz, R.J.et. al, Using oligonucleotide probe arrays to access genetic diversity, *Biotechniques*, 19, 442, 1995

6. Schena, M.et. al, Quantitative monitoring of gene expression patterns with a complementary DNA microarray, *Science*, 270, 467, 1995

7. Gygi, S.P.et. al, Correlation between protein and mRNA abundance in yeast, *Mol. Cell Biol.*, 19, 1720, 1999

8. Ideker, T.et. al, Integrated genomic and proteomic analyses of a systematically perturbed metabolic network, *Science*, 292, 929, 2001

9. Kern, W.et. al, Correlation of protein expression and gene expression in acute leukemia, *Cytometry B Clin. Cytom.*, 55, 29, 2003

10. Liang, P. and Pardee, A.B., Differential display of eukaryotic messenger RNA by means of the polymerase chain reaction, *Science*, 257, 967, 1992

11. Welsh, J.et. al, Arbitrarily primed PCR fingerprinting of RNA, *Nucleic Acids Res*, 20, 4965, 1992

12. Ito, T.et. al, Fluorescent differential display: arbitrarily primed RT-PCR fingerprinting on an automated DNA sequencer, *FEBS Lett*, 351, 231, 1994

13. Liang, P.et. al, Differential display using one-base anchored oligo-dT primers, *Nucleic Acids Res*, 22, 5763, 1994

14. Mou, L.et. al, Improvements to the differential display method for gene analysis, *Biochem Biophys Res Commun*, 199, 564, 1994

15. Carulli, J.P.et. al, High throughput analysis of differential gene expression, *J Cell Biochem Suppl*, 30-31, 286, 1998

16. Sim, G.K.et. al, Use of a cDNA library for studies on evolution and developmental expression of the chorion multigene families, *Cell*, 18, 1303, 1979

17. Patanjali, S.R., Parimoo, S., and Weissman, S.M., Construction of a uniform-abundance (normalized) cDNA library, *Proc Natl Acad Sci U S A*, 88, 1943, 1991

18. Gergen, J.P., Stern, R.H., and Wensink, P.C., Filter replicas and permanent collections of recombinant DNA plasmids, *Nucleic Acids Res*, 7, 2115, 1979

19. Sive, H.L. and St John, T., A simple subtractive hybridization technique employing photoactivatable biotin and phenol extraction, *Nucleic Acids Res*, 16, 10937, 1988

20. Byers, R.J.et. al, Subtractive hybridization--genetic takeaways and the search for meaning, *Int. J. Exp. Pathol.*, 81, 391, 2000

21. Velculescu, V.E., Vogelstein, B., and Kinzler, K.W., Analysing uncharted transcriptomes with SAGE, *Trends Genet*, 16, 423, 2000

22. Saha, S.et. al, Using the transcriptome to annotate the genome, *Nat. Biotechnol.*, 20, 508, 2002

23. Pollock, J.D., Gene expression profiling: methodological challenges, results, and prospects for addiction research, *Chem Phys Lipids*, 121, 241, 2002

24. Tuteja, R. and Tuteja, N., Serial analysis of gene expression (SAGE): unraveling the

bioinformatics tools, *Bioessays*, 26, 916, 2004

25. Cai, L.et. al, Clustering analysis of SAGE data using a Poisson approach, *Genome Biol*, 5, R51, 2004

26. Singh-Gasson, S.et. al, Maskless fabrication of light-directed oligonucleotide microarrays using a digital micromirror array, *Nat. Biotechnol.*, 17, 974, 1999

27. Nuwaysir, E.F.et. al, Gene expression analysis using oligonucleotide arrays produced by maskless photolithography, *Genome Res.*, 12, 1749, 2002

28. Shoemaker, D.D.et. al, Experimental annotation of the human genome using microarray technology, *Nature*, 409, 922, 2001

29. Schulze, A. and Downward, J., Navigating gene expression using microarrays--a technology review, *Nat. Cell Biol.*, 3, E190, 2001

30. Lyons, P., Advances in spotted microarray resources for expression profiling, *Brief. Funct. Genomic. Proteomic.*, 2, 21, 2003

31. Duggan, D.J.et. al, Expression profiling using cDNA microarrays, *Nat. Genet.*, 21, 10, 1999

32. Affara, N.A., Resource and hardware options for microarray-based experimentation, *Brief Funct Genomic Proteomic*, 2, 7, 2003

33. Livesey, F.J., Strategies for microarray analysis of limiting amounts of RNA, *Brief. Funct. Genomic. Proteomic.*, 2, 31, 2003

34. Karsten, S.L.et. al, An evaluation of tyramide signal amplification and archived fixed and frozen tissue in microarray gene expression analysis, *Nucleic Acids Res.*, 30, E4, 2002

35. Eberwine, J.et. al, Analysis of gene expression in single live neurons, *Proc. Natl. Acad. Sci. U. S. A*, 89, 3010, 1992

36. Baugh, L.R.et. al, Quantitative analysis of mRNA amplification by in vitro

transcription, *Nucleic Acids Res.*, 29, E29, 2001

37. Richter, A.et. al, Comparison of fluorescent tag DNA labeling methods used for expression analysis by DNA microarrays, *Biotechniques*, 33, 620, 2002

38. Czechowski, T.et. al, Real-time RT-PCR profiling of over 1400 Arabidopsis transcription factors: unprecedented sensitivity reveals novel root- and shoot-specific genes, *Plant J*, 38, 366, 2004

39. Horak, C.E. and Snyder, M., Global analysis of gene expression in yeast, *Funct. Integr. Genomics*, 2, 171, 2002

40. Zhang, H., Yan, W., and Aebersold, R., Chemical probes and tandem mass spectrometry: a strategy for the quantitative analysis of proteomes and subproteomes, *Curr. Opin. Chem. Biol.*, 8, 66, 2004

41. Linscheid, M.W., Quantitative proteomics, *Anal. Bioanal. Chem.*, 381, 64, 2005

42. Gygi, S.P.et. al, Quantitative analysis of complex protein mixtures using isotope-coded affinity tags, *Nat. Biotechnol.*, 17, 994, 1999

43. Bolstad, B.M.et. al, Experimental design and low-level analysis of microarray data, *Int. Rev. Neurobiol.*, 60, 25, 2004

44. Churchill, G.A., Fundamentals of experimental design for cDNA microarrays, *Nat. Genet.*, 32 Suppl, 490, 2002

45. Ruijter, J.M., Van Kampen, A.H., and Baas, F., Statistical evaluation of SAGE libraries: consequences for experimental design, *Physiol Genomics*, 11, 37, 2002

46. Armstrong, N.J. and van de Wiel, M.A., Microarray data analysis: from hypotheses to conclusions using gene expression data, *Cell Oncol.*, 26, 279, 2004

47. Yang, Y.H. and Speed, T., Design issues for cDNA microarray experiments, *Nat. Rev. Genet.*, 3, 579, 2002

48. Quackenbush, J., Microarray data normalization and transformation, *Nat. Genet.*, 32

Suppl, 496, 2002

49. Yang, I.V.et. al, Within the fold: assessing differential expression measures and reproducibility in microarray assays, *Genome Biol.*, 3, research0062, 2002

50. Pieler, R.et. al, ArrayNorm: comprehensive normalization and analysis of microarray data, *Bioinformatics.*, 20, 1971, 2004

51. Gentleman, R.C.et. al, Bioconductor: open software development for computational biology and bioinformatics, *Genome Biol.*, 5, R80, 2004

52. Sturn, A., Quackenbush, J., and Trajanoski, Z., Genesis: cluster analysis of microarray data, *Bioinformatics.*, 18, 207, 2002

53. Brazma, A.et. al, Minimum information about a microarray experiment (MIAME)-toward standards for microarray data, *Nat. Genet.*, 29, 365, 2001

54. Wessels, L.F.et. al, A protocol for building and evaluating predictors of disease state based on microarray data, *Bioinformatics.*, 2005

55. 't Veer, L.J.et. al, Expression profiling predicts outcome in breast cancer, *Breast Cancer Res.*, 5, 57, 2003

56. Saeed, A.I.et. al, TM4: a free, open-source system for microarray data management and analysis, *Biotechniques*, 34, 374, 2003

57. Quackenbush, J., Computational analysis of microarray data, *Nat. Rev. Genet.*, 2, 418, 2001

58. Brazma, A. and Vilo, J., Gene expression data analysis, *FEBS Lett.*, 480, 17, 2000

59. Eisen, M.B.et. al, Cluster analysis and display of genome-wide expression patterns, *Proc. Natl. Acad. Sci. U. S. A*, 95, 14863, 1998

60. Tavazoie, S.et. al, Systematic determination of genetic network architecture, *Nat. Genet.*, 22, 281, 1999

61. Raychaudhuri, S., Stuart, J.M., and Altman, R.B., Principal components analysis to summarize microarray experiments: application to sporulation time series, *Pac. Symp. Biocomput.*, 455, 2000

62. Bork, P.et. al, Predicting function: from genes to genomes and back, *J. Mol. Biol.*, 283, 707, 1998

63. Zhang, Z.et. al, A greedy algorithm for aligning DNA sequences, *J Comput Biol*, 7, 203, 2000

64. Pruitt, K.D.et. al, Introducing RefSeq and LocusLink: curated human genome resources at the NCBI, *Trends Genet*, 16, 44, 2000

65. Pruitt, K.D., Tatusova, T., and Maglott, D.R., NCBI Reference Sequence (RefSeq): a curated non-redundant sequence database of genomes, transcripts and proteins, *Nucleic Acids Res*, 33 Database Issue, D501, 2005

66. Okazaki, Y.et. al, Analysis of the mouse transcriptome based on functional annotation of 60,770 full-length cDNAs, *Nature*, 420, 563, 2002

67. Schuler, G.D., Pieces of the puzzle: expressed sequence tags and the catalog of human genes, *J Mol Med*, 75, 694, 1997

68. Quackenbush, J.et. al, The TIGR gene indices: reconstruction and representation of expressed gene sequences, *Nucleic Acids Res*, 28, 141, 2000

69. Altschul, S.F.et. al, Basic local alignment search tool, *J Mol Biol*, 215, 403, 1990

70. Ashburner, M.et. al, Gene ontology: tool for the unification of biology. The Gene Ontology Consortium, *Nat. Genet.*, 25, 25, 2000

71. Wootton, J.C. and Federhen, S., Analysis of compositionally biased regions in sequence databases, *Methods Enzymol*, 266, 554, 1996

72. Brendel, V.et. al, Methods and algorithms for statistical analysis of protein sequences, *Proc Natl Acad Sci U S A*, 89, 2002, 1992

73. Promponas, V.J.et. al, CAST: an iterative algorithm for the complexity analysis of sequence tracts. Complexity analysis of sequence tracts, *Bioinformatics*, 16, 915, 2000

74. Linding, R.et. al, GlobPlot: Exploring protein sequences for globularity and disorder, *Nucleic Acids Res*, 31, 3701, 2003

75. Bendtsen, J.D.et. al, Improved prediction of signal peptides: SignalP 3.0, *J Mol Biol*, 340, 783, 2004

76. von Heijne, G., A new method for predicting signal sequence cleavage sites, *Nucleic Acids Res*, 14, 4683, 1986

77. Neuberger, G.et. al, Hidden localization motifs: naturally occurring peroxisomal targeting signals in non-peroxisomal proteins, *Genome Biol.*, 5, R97, 2004

78. Neuberger, G.et. al, Prediction of peroxisomal targeting signal 1 containing proteins from amino acid sequence, *J. Mol. Biol.*, 328, 581, 2003

79. Neuberger, G.et. al, Motif refinement of the peroxisomal targeting signal 1 and evaluation of taxon-specific differences, *J. Mol. Biol.*, 328, 567, 2003

80. Eisenhaber, B., Bork, P., and Eisenhaber, F., Prediction of potential GPI-modification sites in proprotein sequences, *J Mol Biol*, 292, 741, 1999

81. Eisenhaber, B.et. al, Glycosylphosphatidylinositol lipid anchoring of plant proteins. Sensitive prediction from sequence- and genome-wide studies for Arabidopsis and rice, *Plant Physiol*, 133, 1691, 2003

82. Eisenhaber, B.et. al, A sensitive predictor for potential GPI lipid modification sites in fungal protein sequences and its application to genome-wide studies for Aspergillus nidulans, Candida albicans, Neurospora crassa, Saccharomyces cerevisiae and Schizosaccharomyces pombe, *J. Mol. Biol.*, 337, 243, 2004

83. Maurer-Stroh, S., Eisenhaber, B., and Eisenhaber, F., N-terminal N-myristoylation of proteins: prediction of substrate proteins from amino acid sequence, *J Mol Biol*,

317, 541, 2002

84. Maurer-Stroh, S. and Eisenhaber, F., Refinement and prediction of protein prenylation motifs, *Genome Biology*, 6, R55, 2005

85. Tusnady, G.E. and Simon, I., Principles governing amino acid composition of integral membrane proteins: application to topology prediction, *J Mol Biol*, 283, 489, 1998

86. Cserzo, M.et. al, On filtering false positive transmembrane protein predictions, *Protein Eng*, 15, 745, 2002

87. Lupas, A., Van Dyke, M., and Stock, J., Predicting coiled coils from protein sequences, *Science*, 252, 1162, 1991

88. Eisenhaber, F.et. al, Prediction of secondary structural content of proteins from their amino acid composition alone. I. New analytic vector decomposition methods, *Proteins*, 25, 157, 1996

89. Eisenhaber, F., Frommel, C., and Argos, P., Prediction of secondary structural content of proteins from their amino acid composition alone. II. The paradox with secondary structural class, *Proteins*, 25, 169, 1996

90. Frishman, D. and Argos, P., Incorporation of non-local interactions in protein secondary structure prediction from the amino acid sequence, *Protein Eng*, 9, 133, 1996

91. Letunic, I.et. al, SMART 4.0: towards genomic data integration, *Nucleic Acids Res*, 32 Database issue, 142, 2004

92. Marchler-Bauer, A.et. al, CDD: a database of conserved domain alignments with links to domain three-dimensional structure, *Nucleic Acids Res*, 30, 281, 2002

93. Schaffer, A.A.et. al, IMPALA: matching a protein sequence against a collection of PSI-BLAST-constructed position-specific score matrices, *Bioinformatics*, 15, 1000, 1999

94. Sigrist, C.J.et. al, PROSITE: a documented database using patterns and profiles as motif descriptors, *Brief Bioinform*, 3, 265, 2002

95. Schaffer, A.A.et. al, Improving the accuracy of PSI-BLAST protein database searches with composition-based statistics and other refinements, *Nucleic Acids Res.*, 29, 2994, 2001

96. Altschul, S.F. and Koonin, E.V., Iterated profile searches with PSI-BLAST--a tool for discovery in protein databases, *Trends Biochem. Sci.*, 23, 444, 1998

97. Altschul, S.F.et. al, Gapped BLAST and PSI-BLAST: a new generation of protein database search programs, *Nucleic Acids Res.*, 25, 3389, 1997

98. Wistrand, M. and Sonnhammer, E.L., Improved profile HMM performance by assessment of critical algorithmic features in SAM and HMMER, *BMC. Bioinformatics.*, 6, 99, 2005

99. Wistrand, M. and Sonnhammer, E.L., Improving profile HMM discrimination by adapting transition probabilities, *J. Mol. Biol.*, 338, 847, 2004

100. Ginalski, K.et. al, 3D-Jury: a simple approach to improve protein structure predictions, *Bioinformatics*, 19, 1015, 2003

101. Rung, J.et. al, Building and analysing genome-wide gene disruption networks, *Bioinformatics*, 18 Suppl 2, 202, 2002

102. Soinov, L.A., Krestyaninova, M.A., and Brazma, A., Towards reconstruction of gene networks from expression data by supervised learning, *Genome Biol*, 4, R6, 2003

103. Jenssen, T.K.et. al, A literature network of human genes for high-throughput analysis of gene expression, *Nat. Genet.*, 28, 21, 2001

104. Stapley, B.J. and Benoit, G., Biobibliometrics: information retrieval and visualization from co-occurrences of gene names in Medline abstracts, *Pac. Symp. Biocomput.*, 529, 2000

105. Gao, F., Foat, B.C., and Bussemaker, H.J., Defining transcriptional networks through integrative modeling of mRNA expression and transcription factor binding data, *BMC. Bioinformatics.*, 5, 31, 2004

106. Matys, V.et. al, TRANSFAC: transcriptional regulation, from patterns to profiles, *Nucleic Acids Res.*, 31, 374, 2003

107. Roven, C. and Bussemaker, H.J., REDUCE: An online tool for inferring cis-regulatory elements and transcriptional module activities from microarray data, *Nucleic Acids Res.*, 31, 3487, 2003

108. Roca, C.et. al, Hyperthermia inhibits angiogenesis by a plasminogen activator inhibitor 1-dependent mechanism, *Cancer Res.*, 63, 1500, 2003

109. Overgaard, J.et. al, Randomised trial of hyperthermia as adjuvant to radiotherapy for recurrent or metastatic malignant melanoma. European Society for Hyperthermic Oncology, *Lancet*, 345, 540, 1995

110. Falk, M.H. and Issels, R.D., Hyperthermia in oncology, *Int. J. Hyperthermia*, 17, 1, 2001

111. Johnsen, M.et. al, Cancer invasion and tissue remodeling: common themes in proteolytic matrix degradation, *Curr. Opin. Cell Biol.*, 10, 667, 1998

112. Watanabe, K.et. al, Vasohibin as an endothelium-derived negative feedback regulator of angiogenesis, *J. Clin. Invest*, 114, 898, 2004

113. Albig, A.R. and Schiemann, W.P., Identification and characterization of regulator of G protein signaling 4 (RGS4) as a novel inhibitor of tubulogenesis: RGS4 inhibits mitogen-activated protein kinases and vascular endothelial growth factor signaling, *Mol. Biol. Cell*, 16, 609, 2005

114. Zhang, W.et. al, Antiangiogenic antithrombin down-regulates the expression of the proangiogenic heparan sulfate proteoglycan, perlecan, in endothelial cells, *Blood*, 103, 1185, 2004

115. O'Reilly, M.S.et. al, Antiangiogenic activity of the cleaved conformation of the serpin antithrombin, *Science*, 285, 1926, 1999

116. Yuan, K.et. al, Syndecan-1 up-regulated by ephrinB2/EphB4 plays dual roles in inflammatory angiogenesis, *Blood*, 104, 1025, 2004

117. Ramalho-Santos, M.et. al, "Stemness": transcriptional profiling of embryonic and adult stem cells, *Science*, 298, 597, 2002

118. Chambers, I.et. al, Functional expression cloning of Nanog, a pluripotency sustaining factor in embryonic stem cells, *Cell*, 113, 643, 2003

119. Almstrup, K.et. al, Embryonic stem cell-like features of testicular carcinoma in situ revealed by genome-wide gene expression profiling, *Cancer Res*, 64, 4736, 2004

120. Vandenbunder, B.et. al, Complementary patterns of expression of c-ets 1, c-myb and c-myc in the blood-forming system of the chick embryo, *Development*, 107, 265, 1989

121. Yordy, J.S.et. al, SP100 expression modulates ETS1 transcriptional activity and inhibits cell invasion, *Oncogene*, 23, 6654, 2004

122. Yordy, J.S.et. al, SP100 inhibits ETS1 activity in primary endothelial cells, *Oncogene*, 24, 916, 2005

123. Nakagawa, T.et. al, HEX acts as a negative regulator of angiogenesis by modulating the expression of angiogenesis-related gene in endothelial cells in vitro, *Arterioscler. Thromb. Vasc. Biol.*, 23, 231, 2003

124. Thomas, P.Q., Brown, A., and Beddington, R.S., Hex: a homeobox gene revealing peri-implantation asymmetry in the mouse embryo and an early transient marker of endothelial cell precursors, *Development*, 125, 85, 1998

125. Folkman, J., Angiogenesis in cancer, vascular, rheumatoid and other disease, *Nat. Med.*, 1, 27, 1995

126. Pezzella, F.et. al, Non-small-cell lung carcinoma tumor growth without morphological evidence of neo-angiogenesis, *Am. J. Pathol.*, 151, 1417, 1997

127. Hu, J.et. al, Gene expression signature for angiogenic and nonangiogenic non-small-cell lung cancer, *Oncogene*, 24, 1212, 2005

128. Thijssen, V.L.et. al, Angiogenesis gene expression profiling in xenograft models to study cellular interactions, *Exp. Cell Res.*, 299, 286, 2004

129. Xin, X.et. al, Hepatocyte growth factor enhances vascular endothelial growth factor-induced angiogenesis in vitro and in vivo, *Am. J. Pathol.*, 158, 1111, 2001

130. Gerritsen, M.E.et. al, Using gene expression profiling to identify the molecular basis of the synergistic actions of hepatocyte growth factor and vascular endothelial growth factor in human endothelial cells, *Br J Pharmacol*, 140, 595, 2003

131. Basso, K.et. al, Reverse engineering of regulatory networks in human B cells, *Nat. Genet.*, 37, 382, 2005

132. Jeong, H.et. al, The large-scale organization of metabolic networks, *Nature*, 407, 651, 2000

133. Barrett, T.et. al, NCBI GEO: mining millions of expression profiles--database and tools, *Nucleic Acids Res.*, 33, D562, 2005

134. Edgar, R., Domrachev, M., and Lash, A.E., Gene Expression Omnibus: NCBI gene expression and hybridization array data repository, *Nucleic Acids Res.*, 30, 207, 2002

135. Parkinson, H.et. al, ArrayExpress--a public repository for microarray gene expression data at the EBI, *Nucleic Acids Res.*, 33, D553, 2005

136. Brazma, A.et. al, ArrayExpress--a public repository for microarray gene expression data at the EBI, *Nucleic Acids Res.*, 31, 68, 2003

137. Lash, A.E.et. al, SAGEmap: a public gene expression resource, *Genome Res.*, 10, 1051, 2000

138. Su, A.I.et. al, Large-scale analysis of the human and mouse transcriptomes, *Proc. Natl. Acad. Sci. U. S. A*, 99, 4465, 2002

139. Bono, H.et. al, Systematic expression profiling of the mouse transcriptome using RIKEN cDNA microarrays, *Genome Res.*, 13, 1318, 2003

140. Liang, P., SAGE Genie: a suite with panoramic view of gene expression, *Proc. Natl. Acad. Sci. U. S. A*, 99, 11547, 2002

141. Shyamsundar, R.et. al, A DNA microarray survey of gene expression in normal human tissues, *Genome Biol.*, 6, R22, 2005

MASPECTRAS: a platform for management and analysis of proteomics LC-MS/MS data

Jürgen Hartler[*§], Gerhard G. Thallinger[*], Gernot Stocker[*], Alexander Sturn[*], Thomas R. Burkard[*], Erik Körner[†], Robert Rader[*], Andreas Schmidt[#], Karl Mechtler[‡], and Zlatko Trajanoski[*]

[*]Institute for Genomics and Bioinformatics and Christian-Doppler Laboratory for Genomics and Bioinformatics, Graz University of Technology, Petersgasse 14, 8010 Graz, Austria.

[§]Austrian Research Centers Gmbh –ARC, eHealth Systems, Reininghausstrasse 13/1, 8020 Graz, Austria

[†]FH Joanneum, Kapfenberg, Werk-VI-Sraße 46, 8605 Kapfenberg, Austria.

[‡]Research Institute for Molecular Pathology, Dr. Bohr-Gasse 7, 1030 Vienna, Austria.

Christian Doppler Laboratory for Proteome Analysis, Dr. Bohr-Gasse 3, 1030 Vienna, Austria

Correspondence: Zlatko Trajanoski

Institute for Genomics and Bioinformatics

Graz University of Technology

Phone: +43 316 873 5332

Fax: +43 316 873 5340

E-mail: zlatko.trajanoski@tugraz.at

Abstract

We have developed MAss SPECTRometry Analysis System (MASPECTRAS), a platform for management and analysis of proteomics LC-MS/MS data. MASPECTRAS is based on the Proteome Experimental Data Repository (PEDRo) relational database scheme and follows the guidelines of the Proteomics Standards Initiative (PSI). Analysis modules include: 1) import and parsing of the results form the search engines SEQUEST, Mascot, Spectrum Mill, X! Tandem, and OMSSA; 2) peptide validation, 3) clustering of proteins based on Markov Clustering and multiple alignments; and 4) quantification using the Automated Statistical Analysis of Protein Abundance Ratios algorithm (ASAPRatio). The system provides customizable data retrieval and visualization tools, as well as export to PRoteomics IDEntifications public repository (PRIDE). MASPECTRAS is freely available at http://genome.tugraz.at/MASPECTRAS.

BACKGROUND

The advancement of genomic technologies – including microarray, proteomic and metabolic approaches – have led to a rapid increase in the number, size and rate at which genomic datasets are generated. Managing and extracting valuable information from such datasets requires the use of data management platforms and computational approaches. In contrast to genome sequencing projects, there is a need to store much more complex ancillary data than would be necessary for genome sequences. Particularly the need to clearly describe an experiment and report the variables necessary for data analysis became a new challenge for the laboratories. Furthermore, the vast quantity of data associated with a single experiment can become problematic at the point of publishing and disseminating results. Fortunately, the communities have recognized and tackled the problem through the development of standards for the capturing and sharing of experimental data. The microarray community arranged to define the critical information necessary to effectively analyze a microarray experiment and developed the Minimal Information About a Microarray Experiment (MIAME)[1] . Subsequently, MIAME was adopted by scientific journals as a prerequisite for publications and several software platforms supporting MIAME were developed [2,3] .

The principles underlying MIAME have reasoned beyond the microarray community. The Proteomics Standard Initiative (PSI) [4] aims to define standards for data representation in proteomics analogues to that of MIAME and developed Minimum Information About a Proteomics Experiment (MIAPE) [5]. An implementation independent approach for defining the data structure of a Proteomics Experiment Data repository (PEDRo) [6] was developed using unified modeling language (UML) and a PSI compliant public repository was set up [7]. Hence, given the defined standards and available public repositories proteomics laboratories computational systems can now be developed to support proteomics laboratories and enhance data dissemination.

To meet the needs for high-throughput MS laboratories several tools and platforms covering various parts of the analytical pipeline were recently developed including the Trans Proteomics Pipeline [8],

The Global Proteome Machine [9], VEMS [10,11], CPAS [12], CHOMPER [13], ProDB [14], PROTEIOS [15], GAPP [16], PeptideAtlas [17], EPIR [18], STEM [19], and TOPP [20] (see table 1 for a comparison of the features). However, to the best of our knowledge there is currently no academic or commercial data management platform supporting MIAPE and enabling PRoteomics IDEntifications database (PRIDE) export. Moreover, it became evident that several search engines should be used to validate proteomics results [21]. Hence, a system enabling comparison of the results generated by the different search engines would be of great benefit. Additionally, integration of algorithms for peptide validation, protein clustering and protein quantification into a single analytical pipeline would considerably facilitate analyses of the experimental data.

We have therefore developed the MAss SPECTRometry Analysis System (MASPECTRAS), a web-based platform for management and analysis of proteomics liquid chromatography tandem mass spectrometry (LC-MS/MS) data supporting MIAPE. MASPECTRAS was developed using state-of-the-art software technology and enables data import from five common search engines. Analytical modules are provided along with visualization tools and PRIDE export as well as a module for distributing intensive calculations to a computing cluster.

ANALYSIS PIPELINE

MASPECTRAS extends the PEDRo relational database scheme and follows the guidelines of the PSI. It accepts the native file formats from SEQUEST [22], Mascot [23], Spectrum Mill [24], X! Tandem [25], and OMSSA [26]. The core of MASPECTRAS is formed by the MASPECTRAS analysis platform (Figure 1). The platform encompasses modules for the import and parsing data generated by the above mentioned search engines, peptide validation, protein clustering, protein quantification, and a set of visualization tools for post-processing and verification of the data, as well as PRIDE export.

Import and Parsing Data from Search Engines

There are several commercial and academic search engines for proteomics data. Based on known protein sequences stored in a database, these search engines perform *in silico* protein digestion to calculate theoretical spectra for the resulting peptides and compare them to the obtained ones. Based on the similarity of the two spectra, a probability score is assigned. The results (score, peptide sequence, etc.) are stored in a single or in multiple files, and often only an identification string for the protein is stored whereas the original sequence is discarded. However, the search engines are storing different identification strings for the proteins (e.g. X! Tandem: gi|231300|pdb|8GPB|; Spectrum Mill: 231300). Moreover, several databases are not using common identifiers (eg. National Center for Biotechnology Information non redundant (NCBI nr): gi|6323680; Mass Spectrometry protein sequence DataBase (MSDB) [27]: S39004). In order to compare the search results from different search engines additional information from the corresponding sequence databases is needed. The format of the accession string has to be known to retrieve the protein sequence and additional required information from the sequence database, like protein description, or the organism the protein belongs to. The only common basis within the different databases used by the search algorithms is the sequence information. In order to make results of different algorithms comparable and to find the corresponding proteins in the different result files the sequence information is taken as unique identification criteria.

We have developed parsers for the widely used search engines SEQUEST, Mascot, Spectrum Mill, X! Tandem, and OMSSA. MASPECTRAS manages the sequence databases used while searching with different modules internally. Any database available in FASTA format [28] can be uploaded to MASPECTRAS. Parsing rules are user definable and therefore easily adaptable to different types of sequence databases. When results of a search engine are imported into MASPECTRAS, the system first tries to determine whether the same accession string for the same database version exists. If that is not the case, the original sequence information is retrieved from the corresponding sequence database. Subsequently the system tries to match the sequence against the sequences already stored in the database. If an entry with the same sequence information but a different accession string is found, the new accession string is associated with the unique identifier of the already stored sequence. Otherwise a new unique identifier is created and the sequence is stored with the appropriate accession strings.

Peptide Validation

SEQUEST and Mascot provide custom probability scores. MASPECTRAS provides a probability score on its own for SEQUEST and Mascot which is based on the algorithm of PeptideProphet [22]. Data re-scoring adds a further layer, which improves the specificity of the highly sensitive SEQUEST and Mascot database searches. This procedure could be applied to other database search algorithms as well and can additionally offer a remap of the results from different database search algorithms onto one single probability scale [21]. The statistical model incorporates a linear discriminant score based on the database search scores (for SEQUEST: XCorr, dCn, Sp rank, and mass difference) as well as the tryptic termini and missed cleavages [22]. After scoring the data has to pass a user definable filter, which depends on the search programs specific score to discard the most unlikely data.

Protein Clustering

In peptide fragmentation fingerprinting (PFF) peptides are identified by search engines, which have to be mapped to proteins. A single peptide often corresponds to a group of proteins. Therefore, PFF identifies protein groups, each protein owning similar peptides. A grouped protein view represents the result more concisely and proteins with a small number of identified peptides can be recognized easier

in complex samples. The protein grouping implemented in MASPECTRAS is based on Markov clustering [29] using Basic Local Alignment Search Tool (BLAST) [30] and multiple alignments. A file in FASTA format is assembled containing all sequences to be clustered. Each sequence is then compared against each other. The all-against-all sequence similarities generated by this analysis are parsed and stored in an upper triangular matrix. This matrix represents sequence similarities as a connection graph. Nodes of the graph represent proteins, and edges represent sequence similarity that connects such proteins. A weight is assigned to each edge by taking the average pair wise $-\log_{10}$ of the BLAST E-value. These weights are transformed into probabilities associated with a transition from one protein to another within this graph. This matrix is parsed through iterative round of matrix multiplication and inflation until there is little or no net change in the matrix. The final matrix is then interpreted as the protein clustering and the number of the corresponding cluster is stored for every protein hit. The visualization of the protein grouping of a single search is performed by the integrated Jalview Alignment Editor [31]. If proteins from different searches are the same the two corresponding protein groups are combined into one protein group at the time the searches are compared.

Protein Quantification

For quantification of peptides the ASAPRatio algorithm described in [32] has been integrated and applied: To determine a peak area a single ion chromatogram is reconstructed for a given m/z range by summation of ion intensities. This chromatogram is then smoothed tenfold by repeated application of the Savitzky - Golay smooth filtering method [33]. For each isotopic peak center and width are determined. The peak width is primarily calculated by using the standard ASAPRatio algorithm and for further peak evaluation a new algorithm for recognizing peaks with saddle-points has been implemented. With this algorithm a valley (a local minimum of the smoothed signal) is recognized to be part of the peak and added to the area. The calculated peak area is determined as the average of the smoothed and the unsmoothed peak. From this value background noise is subtracted, which is estimated from the average signal amplitude of the peak's neighborhood (50 chromatogram value pairs above and below the respective peak's borders). The peak error is estimated as the difference of the smoothed and the unsmoothed peak. A calculated peak area is accepted in case the calculated peak

area is bigger than the estimated error and the peak value is at least twice the estimated background noise, otherwise the peak area is set to zero. The acceptance process is applied in automated peak area determination, only. In case of interactive peak determination this process is replaced by the operator's decision. In order to demonstrate the quantification capabilities of MASPECTRAS two samples where mixed at different ratios and quantified with MSQuant [34], PepQuan (provided with the Bioworks browser from SEQUEST), and MASPECTRAS. The results are described in "System Validation". For a detailed description of the experiment see "Experimental Procedures".

Visualization Tools

MASPECTRAS allows the storage and comparison of search results from the search engines SEQUEST, Mascot, Spectrum Mill, X! Tandem, and OMSSA matched to different sequence databases merged in a single user-definable view (Figure 2). MASPECTRAS provides customizable (clustered) protein, peptide, spectrum, and chromatogram views, as well as a view for the quantitative comparison.

The clustered protein view displays one representative for each protein cluster. In the peptide centric view the peptides with the same modifications are combined together and only the representative with the highest score is displayed. The spectrum viewer of MASPECTRAS enables manual inspection of the data by providing customizable zooming and printing features (Figure 3). The chromatogram viewer allows manual definition of the peak areas (Figure 4). The chromatograms of all charge states of the found peptide are displayed. The quantitative comparison view offers the possibility to compare peptides with two different post translational modifications (PTMs) or with one PTM and an unmodified version. The calculated peaks are displayed graphically together with a regression line.

PRIDE Export

MASPECTRAS has been designed to comply with the MIAPE requirements and provide researchers all the advantages of following standards: data can be easily exported to other file formats (Excel, Word, and plain text). MASPECTRAS features a module for the PRIDE export. The export to the

PRIDE XML format is possible directly from the protein and peptide views and the resulting file can be submitted to PRIDE.

SYSTEM VALIDATION

Analysis of large proteomics data set

To demonstrate the utility of the MASPECTRAS we used data from a large-scale study recently published by Kislinger et. al. [35]. We analyzed the data from the heart cytosol compartment which comprised 84 SEQUEST searches performed against a database obtained form the authors (see https://maspectras.genome.tugraz.at) containing the same amount of "decoy" proteins presented in inverted amino acid orientation. The files were imported, parsed, the data analyzed and the results exported in PRIDE format. In the study of Kislinger et. al. a protein was accepted with a minimum of two high scoring spectra with a likelihood value >95% (calculated by STATQUEST [36]), which resulted in 698 protein identifications in the cytosol compartment. Applying the same filter criteria and using the PeptideProphet algorithm implemented in MASPECTRAS resulted in 570 protein identifications (81.7%). The results of this analysis are shown in additional data file 1 and at https://maspectras.genome.tugraz.at.

Quantitative analysis

To evaluate the performance of the quantification tool we initiated a controlled experiment in triplicates using mixture of ICPL-labeled (Isotope Coded Protein Label) proteins (see Experimental Procedures). ICPL-labeled probes were mixed at 7 different ratios (1:1, 2:1, 5:1 10:1, 1:2, 1:5 and 1:10). To demonstrate the capabilities of MASPECTRAS, the quantitative analysis was performed with MSQuant [34], PepQuan, and ASAPRatio as implemented in MASPECTRAS. Due to the fact that MSQuant lacks the ability to quantify samples in centroid mode, the automatic quantification of MSQuant and MASPECTRAS has been performed on profile mode data. Additionally we compared the automatic quantification of MASPECTRAS in centroid mode and observed no significant deviation (data not shown).

Since in the centroid mode the data amount is smaller (~1/8) the manual review and correction of the automatically calculated results has been conducted with centroid mode data. The reasons for the

manual correction are: (i) there are additional peaks in a chromatogram in the m/z neighborhood; (ii) the found peptides are not in the main peak but in neighboring smaller peak. A ratio between each found light and heavily labeled peptide has been calculated, and from those ratios the mean value, the standard deviation, the relative error, and a regression line has been calculated as well (with the integrated PTM quantitative comparison tool described in the "Visualization tools" section). A filter for outlier removal has been applied to the automatically calculated ratios. For the manual evaluation, these automatically removed peptides were checked manually and the misquantification due to the above mentioned reasons could be corrected. Therefore the number of manually accepted peptides could be higher than the automatically accepted ones. The performance of the quantification with ASAPRatio integrated in MASPECTRAS was superior compared to both, MSQuant and PepQuan. Furthermore, for all ratios the relative error calculated was considerably lower than the relative error obtained with MSQuant and PepQuan (see table 2 and for more detailed information additional data file 2 for a direct comparison between MSQuant, PepQuan, and MASPECTRAS).

DISCUSSION

We have developed an integrated platform for the analysis and management of proteomics LC-MS/MS data using state-of-the-art software technology. The uniqueness of the platform lies in the MIAPE compliance, PRIDE export, and the scalability of the system for computationally intensive tasks, in combination of common features for data import from common search engines, integration of peptide validation, protein grouping and quantification tools.

MIAPE compliance and PRIDE export are necessary to disseminate data and effectively analyze a proteomics experiment. As more and more researchers are adopting the standards, public repositories will not only enhance data sharing but will also enable data mining within and across experiments. Surprisingly, although standards for data representation have been widely accepted, the necessary software tools are still missing. This can be partly explained by the volume and complexity of the generated data and by the heterogeneity of the used technologies. We have therefore positioned the beginning of the analytical pipeline of MASPECTRAS at the point at which the laboratory workflows converge, i.e. analysis of the data generated by the search engines.

The capability to import and parse data from five search engines makes the platform universal and independent of the workflow performed by the proteomics research group. The system was not designed to support a specific manufacturer and can therefore be used in labs equipped with different instruments. Moreover, MASPECTRAS is the first system that provides the basis for consensus scoring between MS/MS search algorithms. It was recently suggested that the interpretation of the results from proteomics studies should be based on the analysis of the data using several search engines [21]. Importing and parsing the results from search engines and side-by-side graphical representation of the results is a prerequisite for this type of analysis and would enhance correct identification of peptides. The results of the validation of our system using large proteomics data sets further support this observation. The differences in the results of the analyses are due to the different algorithms used for the likelihood calculation. In our system PeptideProphet [22] was used whereas in

the study by Kislinger et al. [35] STATQUEST [36] was applied. We have selected PeptideProphet algorithm based on the results of the benchmarking study [21] in which PeptideProphet was ranked first with respect to the number of correctly identified peptide spectra. The study by Kapp et al. [21] showed also that the concordance between MS/MS search algorithms can vary up to 55% (335 peptides were identified by all four algorithms out of possible 608 hits). Important considerations when carrying out MS/MS database searches is not only the chosen search engine, but also the specified search parameters, the search strategy, and the chosen protein sequence database. Evaluation of the performance of the used algorithms was beyond the scope of this study. Further work need to be carried out to determine the number of independent scoring functions necessary to allow automated validation of peptide identifications. It should be noted that inclusion of additional validation algorithms in MASPECTRAS is straightforward due to the flexibility of the platform and the use of standard software technology.

The integration of peptide validation, protein grouping and quantification algorithms in conjunction with visualization tools is important for the usability and acceptability of the system. Particularly the inclusion of a quantification algorithm in the pipeline is of interest since more and more quantitative studies are initiated. We have selected the ASAPRatio algorithm for automated statistical analysis of protein abundance ratios [32] and integrated it into our platform. The results of our validation experiment showed that the performance of ASAPRatio was superior to MSQuant and PepQuan. Again, the modularity of the platform allows future integration of other quantification algorithms. Moreover, the use of three-tier software architecture in which the presentation, the calculation and the database part are separated enables not only easier maintenance but also future changes like inclusion of additional algorithms as well as distribution of the load to several servers. We made use of the flexibility of this concept and developed a module for distributing the load to a computing cluster (JClusterService, see Software Architecture). Tests with the ASAPRatio algorithm showed that the computing time decreases linearly with the number of used processors.

In summary, given the unique features and the flexibility due to the use of standard software technology, our platform represents significant advance and could be of great interest to the proteomics community.

SOFTWARE ARCHITECTURE

The application is based on a three-tier architecture, which is separated into presentation-, middle-, and database layer. Each tier can run on an individual machine without affecting the other tiers. This makes every component easily exchangeable. A relational database (MySQL, PostgreSQL or Oracle) forms the database layer. MASPECTRAS follows and extends the PEDRo database scheme [6] (additional data file 3) to suit the guidelines of PSI [4]. The business layer consists of a Java 2 Enterprise Edition (J2EE) compliant application which is deployed to the open source application server JBoss [37]. Access to the data is provided by a user-friendly web-interface using Java Servlets and Java Server Pages [38] via the Struts framework [39]. Computational or disk space intensive tasks can be distributed to a separate server or to a computing cluster by using the in-house developed JClusterService interface. This web service based programming interface uses the Simple Object Access Protocol (SOAP) [40] to transfer data for the task execution between calculation server and MASPECTRAS server. The tasks can be executed on dedicated computation nodes and therefore do not slow down the MASPECTRAS web interface. This remote process execution system is used as a backend for the protein grouping analysis, for the mass quantification and for the management of the sequence databases and their sequence retrieval during import.

The current implementation of MASPECTRAS allows the comparison of search results from SEQUEST, Mascot, Spectrum Mill, X! Tandem [25], and OMSSA [26]. The following file formats are supported: SEQUEST: ZIP-compressed file of the *.dta, *.out and SEQUEST.params files; Mascot: *.dat; Spectrum Mill: ZIP-compressed file of the results folder including all subfolders; X! Tandem: the generated *.xml; OMSSA: the generated *.xml with included spectra and search params; Raw data: XCalibur raw format (*.raw) version 1.3, mzXML [41] and mzData [42] format. The data can be imported into MASPECTRAS database asynchronously in batch mode, without interfering with the analysis of already uploaded data. The spectrum viewer applet and the diagrams are implemented with the aid of JFreeChart [43] and Cewolf [44] graphics programming frameworks. The whole system is secured by a user management system which has the ability to manage the access rights for projects and offers data sharing and multiple user access roles in a multi-user environment.

EXPERIMENTAL PROCEDURES

In order to demonstrate the capabilities of MASPECTRAS the following experiments were performed.

Materials

Proteins were purchased from Sigma as lyophyllized, dry powder. Solvents (HPLC grade) and chemicals (highest available grade) were purchased from Sigma, TFA (trifluoroacetic acid) was from Pierce. The ICPL (isotope coded protein label) chemicals kit was from Serva Electrophoresis this kit contained reduction solution with TCEP (Tris (2-carboxy-ethyl) phosphine hydrochloride), cysteine blocking solution with IAA (Iodoacetamide), stop solutions I and II and the labeling reagent nicotinic acid N-hydroxysuccinimide ester as light (6 ^{12}C in the nicotinic acid) and heavy (6x ^{13} C) form as solutions. Trypsin was purchased from Sigma at proteomics grade.

ICPL labeling of proteins

Proteins bovine serum albumin [GenBank:AAA51411.1], human apotransferrin [ref:NP_001054.1] and rabbit phosphorylase b [PDB:8GPB] were dissolved with TEAB (Tetraammoniumbicarbonate) buffer (125 mM, pH 7.8) in three vials to a final concentration of 5 mg/ml each. A 40 µl aliquot was used for reduction of disulfide bonds between cysteine sidechains and blocking of free cysteines. For reduction of disulfide bonds 4 µl of reduction solution were added to the aliquot and the reaction was carried out for 35 min at 60 °C. After cooling samples to room temperature, 4 µl of cysteine blocking solution were added and the samples were sat in a dark cupboard for 35 min. To remove excess of blocking reagent 4 µl of stop solution I were added and samples were put on a shaker for 20 minutes. Protein aliquots were split to two samples which contained 20 µl each. First row of samples was labeled with the ^{12}C isotope by adding 3 µl of the nicotinic acid solution which contained the light reagent. Second row was labeled with the heavy reagent and labeling reaction was carried out for 2 h and 30 min while shaking at room temperature.

Proteolytic digest of Proteins

Protein solutions were diluted using 50 mM NH_4HCO_3 solution to a final volume of 90 µl. 10 µl of a fresh prepared trypsin solution (2.5 µg/µl) were added and the proteolysis was carried out at 37 °C over night in an incubator. The reaction was stopped by adding 10 µl of 10% TFA. The peptide solutions were diluted with 0.1 % TFA to give 1 nM final concentration. From these stock solutions samples for MS/MS analysis which contained defined ratios of heavy and light were made up by mixing the solutions of light and heavy labeled peptides.

HPLC and mass spectrometry

To separate peptide mixtures prior to MS analysis, nanoRP-HPLC was applied on the Ultimate 2 Dual Gradient HPLC system (Dionex, buffer A: 5% ACN, 0.1% TFA, buffer B: 80% ACN, 0.1% TFA) on a PepMap separation column (Dionex, C18, 150 mm x 75 µm x 3 µm, 300 A). 500 fMol of each mixture was separated three times using the same trapping and separation column to reduce the quantification error which comes from HPLC and mass spectrometry. A gradient from 0% B to 50% B in 48 min was applied for the separation; peptides were detected at 214 and 280 nm in the UV detector. The exit of the HPLC was online coupled to the electrospray source of the LTQ mass spectrometer (Thermo Electron). Samples were analyzed in centroid mode first to test digest and labeling quality. For the quantitative analysis the LTQ was operated in enhanced profile mode for survey scans to gain higher mass accuracy. Samples were mass spectrometrically analyzed using a top one method, in which the most abundant signal of the MS survey scan was fragmented in the subsequent MS/MS event in the ion trap. Although with this method a lower number of MS/MS spectra were acquired, the increased number of MS scans leads to a better determination of the eluting peaks and therefore provides improved quantification of peptides.

Data analysis was done with the Mascot Daemon [23] (Matrix Science), BioWorks 3.2 [22] (Thermo Electron) software packages using an in house database. To demonstrate the merging of results from all of the mentioned search engines the ICPL labeled probes at an ratio of 1:1 were searched with Spectrum Mill A.03.02 (Agilent Technologies) [24], X! Tandem [25] (The Global Proteome Machine

Organization) version 2006.04.01, and OMSSA 1.1.0 [26] (NCBI) The results were uploaded to MASPECTRAS and quantified automatically.

AUTHORS' CONTRIBUTIONS

JH designed the current version of MASPECTRAS. He was responsible for the implementation of the database, the development the presentation and many parts of the business logic. GS, AS[1], TRB and EK implemented most of the parts of the analysis pipeline. GS developed the JClusterService and the services provided for MASPECTRAS. TRB integrated the PeptideProphet, AS[1] the protein clustering pipeline, and EK the peptide quantification and the chromatogram viewer. RR implemented the PRIDE data export. AS[2] and KM conducted the proteomics experiments. JH and AS[2] analyzed the biological data. KM and GGT contributed to conception and design. ZT was responsible for the overall conception and project coordination. All authors gave final approval of the version to be published.

ACKNOWLEDGEMENTS

The authors thank the staff of the protein chemistriy facility at the Research Institute of Molecular Pathology Vienna, Sandra Morandell and Stefan Ascher, Biocenter Medical University Innsbruck, Manfred Kollroser, Institute of Forensic Medicine, Medical University of Graz, Gerald Rechberger, Institute of Molecular Biosciences, University of Graz, Andreas Scheucher, and Thomas Fuchs for valuable comments and contributions. We want to thank Andrew Emili and Vincent Fong from the Donnelly Centre for Cellular and Biomolecular Research (CCBR), University of Toronto for providing the data for our study. This work is supported by the Austrian Federal Ministry of Education, Science and Culture GEN-AU projects "Bioinformatics Integration Network II" (BIN) and "Austrian Proteomics Platform II" (APP). Jürgen Hartler was supported by a grant of the Austrian Academy of Sciences (OEAW).

REFERENCES

Reference List

1. Brazma A, Hingamp P, Quackenbush J, Sherlock G, Spellman P, Stoeckert C, Aach J, Ansorge W, Ball CA, Causton HC et al.: **Minimum information about a microarray experiment (MIAME)-toward standards for microarray data.** *Nat Genet* 2001, **29:**365-371.

2. Maurer M, Molidor R, Sturn A, Hartler J, Hackl H, Stocker G, Prokesch A, Scheideler M, Trajanoski Z: **MARS: microarray analysis, retrieval, and storage system.** *BMC Bioinformatics* 2005, **6:**101.

3. Saal LH, Troein C, Vallon-Christersson J, Gruvberger S, Borg A, Peterson C: **BioArray Software Environment (BASE): a platform for comprehensive management and analysis of microarray data.** *Genome Biol* 2002, **3:**SOFTWARE0003.

4. Orchard S, Hermjakob H, Apweiler R: **The proteomics standards initiative.** *Proteomics* 2003, **3:**1374-1376.

5. Orchard S, Hermjakob H, Julian RKJ, Runte K, Sherman D, Wojcik J, Zhu W, Apweiler R: **Common interchange standards for proteomics data: Public availability of tools and schema.** *Proteomics* 2004, **4:**490-491.

6. Taylor CF, Paton NW, Garwood KL, Kirby PD, Stead DA, Yin Z, Deutsch EW, Selway L, Walker J, Riba-Garcia I et al.: **A systematic approach to modeling, capturing, and disseminating proteomics experimental data.** *Nat Biotechnol* 2003, **21:**247-254.

7. Martens L, Hermjakob H, Jones P, Adamski M, Taylor C, States D, Gevaert K, Vandekerckhove J, Apweiler R: **PRIDE: The proteomics identifications database (vol. 5, Issue 13, pp. 3537-3545).** *Proteomics* 2005, **5:**4046.

8. Keller A, Eng J, Zhang N, Li XJ, Aebersold R: **A uniform proteomics MS/MS analysis platform utilizing open XML file formats.** *Mol Sys Biology* 2005, **4100024:**E1-E8.

9. Craig R, Cortens JP, Beavis RC: **Open source system for analyzing, validating, and storing protein identification data.** *J Proteome Res* 2004, **3:**1234-1242.

10. Matthiesen R, Trelle MB, Hojrup P, Bunkenborg J, Jensen ON: **VEMS 3.0: algorithms and computational tools for tandem mass spectrometry based identification of post-translational modifications in proteins.** *J Proteome Res* 2005, **4:**2338-2347.

11. Matthiesen R, Bunkenborg J, Stensballe A, Jensen ON, Welinder KG, Bauw G: **Database-independent, database-dependent, and extended interpretation of peptide mass spectra in VEMS V20.** *Proteomics* 2004, **4:**2583-2593.

12. Rauch A, Bellew M, Eng J, Fitzgibbon M, Holzman T, Hussey P, Igra M, Maclean B, Lin CW, Detter A et al.: **Computational Proteomics Analysis System (CPAS): an extensible, open-source analytic system for evaluating and publishing proteomic data and high throughput biological experiments.** *J Proteome Res* 2006, **5:**112-121.

13. Eddes JS, Kapp EA, Frecklington DF, Connolly LM, Layton MJ, Moritz RL, Simpson RJ: **CHOMPER: a bioinformatic tool for rapid validation of tandem mass spectrometry search results associated with high-throughput proteomic strategies.** *Proteomics* 2002, **2:**1097-1103.

14. Wilke A, Ruckert C, Bartels D, Dondrup M, Goesmann A, Huser AT, Kespohl S, Linke B, Mahne M, McHardy A et al.: **Bioinformatics support for high-throughput proteomics.** *J Biotechnol* 2003, **106:**147-156.

15. Garden P, Alm R, Hakkinen J: **PROTEIOS: an open source proteomics initiative.** *Bioinformatics* 2005, **21:**2085-2087.

16. Shadforth I, Xu W, Crowther D, Bessant C: **GAPP: a fully automated software for the confident identification of human peptides from tandem mass spectra.** *J Proteome Res* 2006, **5:**2849-2852.

17. Desiere F, Deutsch EW, King NL, Nesvizhskii AI, Mallick P, Eng J, Chen S, Eddes J, Loevenich SN, Aebersold R: **The PeptideAtlas project.** *Nucleic Acids Res* 2006, **34:**D655-D658.

18. Kristensen DB, Brond JC, Nielsen PA, Andersen JR, Sorensen OT, Jorgensen V, Budin K, Matthiesen J, Veno P, Jespersen HM et al.: **Experimental Peptide Identification Repository (EPIR): an integrated peptide-centric platform for validation and mining of tandem mass spectrometry data.** *Mol Cell Proteomics* 2004, **3:**1023-1038.

19. Shinkawa T, Taoka M, Yamauchi Y, Ichimura T, Kaji H, Takahashi N, Isobe T: **STEM: a software tool for large-scale proteomic data analyses.** *J Proteome Res* 2005, **4:**1826-1831.

20. Kohlbacher O, Reinert K, Gropl C, Lange E, Pfeifer N, Schulz-Trieglaff O, Sturm M: **TOPP--the OpenMS proteomics pipeline.** *Bioinformatics* 2007, **23:**e191-e197.

21. Kapp EA, Schutz F, Connolly LM, Chakel JA, Meza JE, Miller CA, Fenyo D, Eng JK, Adkins JN, Omenn GS et al.: **An evaluation, comparison, and accurate benchmarking of several publicly available MS/MS search algorithms: sensitivity and specificity analysis.** *Proteomics* 2005, **5:**3475-3490.

22. Keller A, Nesvizhskii AI, Kolker E, Aebersold R: **Empirical statistical model to estimate the accuracy of peptide identifications made by MS/MS and database search.** *Anal Chem* 2002, **74:**5383-5392.

23. Perkins DN, Pappin DJ, Creasy DM, Cottrell JS: **Probability-based protein identification by searching sequence databases using mass spectrometry data.** *Electrophoresis* 1999, **20:**3551-3567.

24. **Agilent Technologies** [http://cagchem.cos.agilent.com]

25. Craig R, Beavis RC: **TANDEM: matching proteins with tandem mass spectra.** *Bioinformatics* 2004, **20:**1466-1467.

26. Geer LY, Markey SP, Kowalak JA, Wagner L, Xu M, Maynard DM, Yang X, Shi W, Bryant SH: **Open mass spectrometry search algorithm.** *J Proteome Res* 2004, **3:**958-964.

27. **MSDB** [http://csc-fserve.hh.med.ic.ac.uk/msdb.html]

28. Pearson WR, Lipman DJ: **Improved tools for biological sequence comparison.** *Proc Natl Acad Sci U S A* 1988, **85:**2444-2448.

29. Enright AJ, Van Dongen S, Ouzounis CA: **An efficient algorithm for large-scale detection of protein families.** *Nucleic Acids Res* 2002, **30:**1575-1584.

30. Thompson JD, Higgins DG, Gibson TJ: **CLUSTAL W: improving the sensitivity of progressive multiple sequence alignment through sequence weighting, position-specific gap penalties and weight matrix choice.** *Nucleic Acids Res* 1994, **22:**4673-4680.

31. Clamp M, Cuff J, Searle SM, Barton GJ: **The Jalview Java alignment editor.** *Bioinformatics* 2004, **20:**426-427.

32. Li XJ, Zhang H, Ranish JA, Aebersold R: **Automated statistical analysis of protein abundance ratios from data generated by stable-isotope dilution and tandem mass spectrometry.** *Anal Chem* 2003, **75:**6648-6657.

33. Press WH, Teukolsky SA, Vetterling WT, Flannery BP: *Numerical recipes in C: the art of scientific computing.* Cambridge Press: New York; 1997.

34. **MSQuant** [http://msquant.sourceforge.net/]

35. Kislinger T, Cox B, Kannan A, Chung C, Hu P, Ignatchenko A, Scott MS, Gramolini AO, Morris Q, Hallett MT et al.: **Global survey of organ and organelle protein expression in mouse: combined proteomic and transcriptomic profiling.** *Cell* 2006, **125:**173-186.

36. Kislinger T, Rahman K, Radulovic D, Cox B, Rossant J, Emili A: **PRISM, a generic large scale proteomic investigation strategy for mammals.** *Mol Cell Proteomics* 2003, **2:**96-106.

37. **JBoss.com: The Professional Open Source Company** [http://www.jboss.org]

38. Hall M., Brown L.: *Core Servlets and Java Server Pages: Core Technologies.* A Sun Microsystems Press/Prentice Hall PTR Book; 2003.

39. **Struts** [http://struts.apache.org/]

40. **SOAP** [http://www.w3.org/TR/soap/]

41. Pedrioli PG, Eng JK, Hubley R, Vogelzang M, Deutsch EW, Raught B, Pratt B, Nilsson E, Angeletti RH, Apweiler R et al.: **A common open representation of mass spectrometry data and its application to proteomics research.** *Nat Biotechnol* 2004, **22:**1459-1466.

42. Orchard S, Hermjakob H, Taylor CF, Potthast F, Jones P, Zhu W, Julian RK, Jr., Apweiler R: **Further steps in standardisation. Report of the second annual Proteomics Standards Initiative Spring Workshop (Siena, Italy 17-20th April 2005).** *Proteomics* 2005, **5:**3552-3555.

43. **JFreeChart** [http://www.jfree.org/jfreechart/]

44. **Cewolf** [http://cewolf.sourceforge.net]

FIGURE LEGENDS

Figure 1

Schematic overview of the analysis pipeline of MASPECTRAS. Search results from SEQUEST, Mascot, Spectrum Mill, X! Tandem, and OMSSA are imported and parsed. In the next steps peptides are validated using PeptideProphet [22] and the corresponding proteins clustered using ClustalW [30]. Then the peptides are quantified using the ASAPRatio algorithm [32], the results stored in the database and exported to the public repository PRIDE [7].

Figure 2

Combined view of the results from the search engines. The combined result view shows the comparison from 5 different search engines (SEQUEST, Mascot, Spectrum Mill, X! Tandem, and OMSSA) for bovine serum albumin (see experimental procedures for details). The line on the top lists the search results displayed in color. Sequence segments found only in one of the searches have the corresponding color whereas sequence segments found in multiple searches are colored red. The possible peptide modifications are shown under the protein sequence box. Three types of peptide modifications were defined: ICPL-light (K%), ICPL-heavy (K*), and oxidized methionine (MX$). X! Tandem generates additional modifications at the N-terminus (N-term@, N-term&, and N-term"). X! Tandem does not provide the possibility to search variable modification states on one amino acid. Therefore, for the X! Tandem search a fixed modification at K(+105.02) and a variable modification (K§+6.02) has been applied. In the last table the peptides are listed and only one representative for the peptide at this modification state is shown.

Figure 3

Spectrum viewer of MASPECTRAS. The spectrum viewer offers the selection of different ion series, the change to other peptide hits, zooming- and printing possibilities.

Figure 4

Chromatogram viewer for the quantification. The raw data is filtered with the m/z of the peptide found. The calculated chromatogram and the chromatograms of the neighborhood are displayed in the first view. The second view shows the selected chromatogram (the yellow colored one in the first view). Additional peaks can be added and stored peaks (colored red) can be removed. The manually selected peaks are displayed in green. The chromatogram viewer allows changing the m/z step-size, the number of displayed neighborhood chromatograms, and the charge state.

TABLES

	TPP [8]	GPM [9]	VEMS [10,11]	CPAS [12]	CHOMPER [13]	ProDB [14]	PROTEIOS [15]	GAPP [16]	PeptideAtlas [17]	EPIR [18]	STEM [19]	TOPP [20]	MASPECTRAS
Compliance													
MIAPE MSI compliant	–	*	–	–	–	–	✓	–	–	–	–	–	✓
MIAPE MS compliant	–	–	–	–	–	–	–	–	–	–	–	–	✓
MIAPE GE compliant	–	–	–	–	–	–	✓	–	–	–	–	–	✓
MIAPE GI compliant	–	–	–	–	–	–	✓	–	–	–	–	–	✓
MIAPE LC compliant	–	–	–	–	–	–	✓	–	–	–	–	–	✓
PRIDE export	–	–	–	–	–	–	–	plan.	–	–	–	–	✓
Data Import													
mzXML	✓	✓	conv.	✓	–	–	✓	–	✓	–	–	✓	✓
mzData	–	–	conv.	–	–	–	✓	✓	–	–	–	✓	✓
SEQUEST	pepX	–	–	pepX	✓	✓	–	–	✓	–	–	✓	✓
Mascot	pepX	–	✓	pepX	–	✓	✓	✓	–	✓	✓	✓	✓
SpectrumMill	–	–	–	–	–	–	–	–	–	–	–	–	✓
X!Tandem	–	✓	✓	✓	–	–	✓	✓	–	–	–	–	✓
OMSSA	–	–	–	–	–	–	–	–	–	–	–	–	✓
Data validation and visualization													
Search engine included	–	✓	✓	✓	–	?	–	✓	–	–	–	–	–
Additional validation algorithms	✓	✓	✓	–	✓	–	✓	✓	✓	✓	✓	✓	✓
Protein grouping - clustering	–	✓	✓	–	–	–	–	–	–	✓	–	–	✓
Merging of results from different search engines	–	–	?	✓	–	✓	✓	✓	–	–	–	–	✓
Customizable filtering	?	✓	–	part.	–	✓	?	SQL	–	✓	✓	?	✓
Spectrum viewer	✓	✓	?	✓	✓	?	?	–	–	–	✓	?	✓
Quantification:													
Relative peptide quantification	✓	–	✓	–	–	–	–	plan.	–	✓	✓	✓	✓
Adjustable m/z width for quantification	–	–	–	–	–	–	–	–	–	–	–	–	✓
Visualization of chromatograms	✓	–	✓	–	–	–	–	–	–	?	–	✓	✓
Visualization of surrounding chromatograms	–	–	?	–	–	–	–	–	–	–	–	✓	✓
Scalability:													
Parallel computing	–	–	–	–	–	–	–	?	–	–	–	–	✓

Table 1

Comparison of MASPECTRAS to other proteomics tools. ✓ fulfills criteria; ─ does not fulfill criteria; ? not enough information to answer this question; part. partially fulfills criteria; plan. planned; pepX fulfills via pepXML; n.a. not applicable; conv. after conversion; * fulfills parts of MIAPE called XIAPE; MSI Mass Spectrometry Informatics; MS Mass Spectrometry; GE Gel Electrophoresis; GI Gel Informatics; LC Liquid Chromatography; SQL filtering over SQL only;

10 heavy to 1 light

	MSQuant	PepQuan	MASPECTRAS	
	auto	manual	auto	manual
# peptides	22	33	27	40
mean	4.64	8.94	8.31	9.85
stdev	4.83	4.9	2.85	2.99
relative error	104.09%	54.81%	34.30%	30.36%

ratio: heavy/light

1 heavy to 10 light

	MSQuant	PepQuan	MASPECTRAS	
	auto	manual	auto	manual
# peptides	20	82	28	39
mean	7.54	7	9.77	9.29
stdev	4.94	2.51	3.96	1.92
relative error	65.52%	35.86%	40.53%	20.67%

ratio: light/heavy

5 heavy to 1 light

	MSQuant	PepQuan	MASPECTRAS	
	auto	manual	auto	manual
# peptides	14	43	50	53
mean	2.94	4.27	4.16	4.67
stdev	2.3	1.69	1.56	1.12
relative error	78.23%	39.58%	37.50%	23.98%

ratio: heavy/light

1 heavy to 5 light

	MSQuant	PepQuan	MASPECTRAS	
	auto	manual	auto	manual
# peptides	16	67	41	40
mean	13.36	3.74	4.25	4.84
stdev	5.18	1.36	1.15	0.93
relative error	38.77%	36.36%	27.06%	19.21%

ratio: light/heavy

2 heavy to 1 light

	MSQuant	PepQuan	MASPECTRAS	
	auto	manual	auto	manual
# peptides	25	50	48	72
mean	1.048	2.17	2.07	2.03
stdev	1.15	0.7	0.71	0.54
relative error	109.73%	32.26%	34.30%	26.60%

ratio: heavy/light

1 heavy to 2 light

	MSQuant	PepQuan	MASPECTRAS	
	auto	manual	auto	manual
# peptides	16	74	42	47
mean	4.24	2.07	2.11	1.94
stdev	4.97	3.04	0.63	0.3
relative error	117.22%	146.86%	29.86%	15.46%

ratio: light/heavy

1 heavy to 1 light

	MSQuant	PepQuan	MASPECTRAS	
	auto	manual	auto	manual
# peptides	15	67	98	77
mean	0.92	1.28	0.97	0.99
stdev	0.46	0.48	0.24	0.19
relative error	49.30%	37.50%	24.74%	19.10%

Table 2

Summary of quantitative analysis with MASPECTRAS, MSQuant and PepQuan. A filter for outlier removal has been applied to the automatically calculated ratios in MASPECTRAS. For the manual evaluation, these automatically removed peptides were checked manually and the misquantification due to wrong peak detection could be corrected. Therefore the amount of manually accepted peptides could higher than the automatically accepted ones. The quantification with ASAPRatio integrated in MASPECTRAS performed superior compared to both, MSQuant and PepQuan. Furthermore, for all ratios the relative error calculated was considerably lower than the relative error obtained with MSQuant and PepQuan

ADDITIONAL DATA FILES

The following additional data files are included with the online version of this article: the evaluation of the heart cytosol data for the study by Kislinger et al. (additional data file 1); quantification results and comparision with MSquant and PepQuan (additional data file 2); and a tiff image of the database scheme of MASPECTRAS (additional data file 3). The original data files are downloadable directly at the MASPECTRAS application at https://maspectras.genome.tugraz.at.

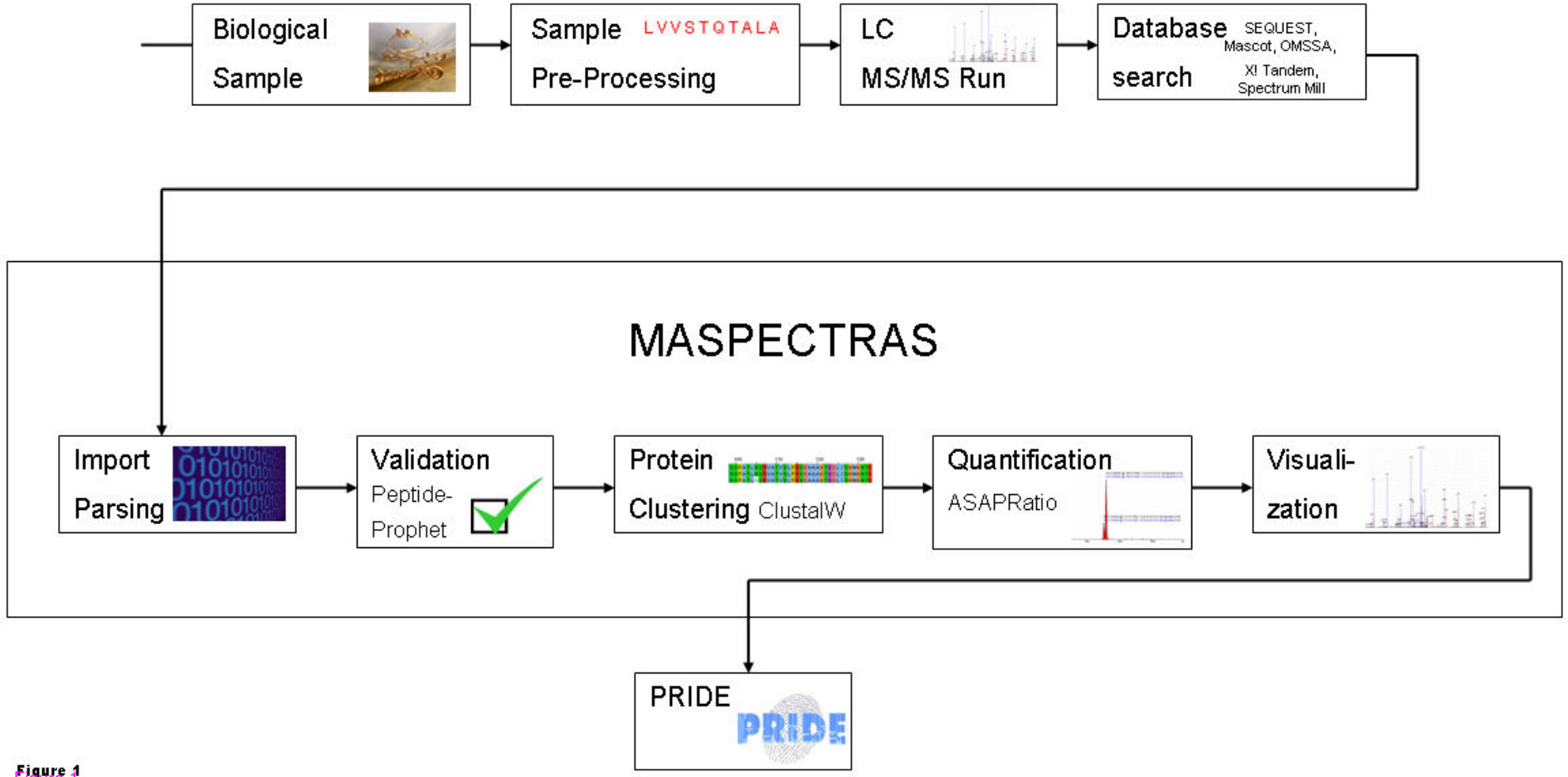

Figure 1

Figure 1

albumin [Bos taurus]; albumin [Bos taurus]

Query | Edit Display Settings | Show Sequence

1 = 060606FTc2_phosphb_bsa_1hzu1lMascot 2 = 060606FTc2_phosphb_bsa_1hzu1lOmssa 3 = 1hzu1lSpectrumMill
4 = 060606FTc2_phosphb_bsa_1hzu1lSequest 5 = 060606FTc2_phosphb_bsa_1hzu1lXTandem
sequence segments found in multiple searches are colored in red

Sequence

MKWVTFISLLLLFSSAYSRGVFRRDTHKSEIAHRFKDLGEEHFKGLVLIAFSQYLQQCPFDEHVKLVNE
LTEFAKTCVADESHAGCEKSLHTLFGDELCKVASLRETYGDMADCCEKQEPERNECFLSHKDDSPDLPKL
KPDPNTLCDEFKADEKKFWGKYLYEIARRHPYFYAPELLYYANKYNGVFQECCQAEDKGACLLPKIETMR
EKVLASSARQRLRCASIQKFGERALKAWSVARLSQKFPKAEFVEVTKLVTDLTKVHKECCHGDLLECADD
RADLAKYICDNQDTISSKLKECCDKPLLEKSHCIAEVEKDAIPENLPPLTADFAEDKDVCKNYQEAKDAF
LGSFLYEYSRRHPEYAVSVLLRLAKEYEATLEECCAKDDPHACYSTVFDKLKHLVDEPQNLIKQNCDQFE
KLGEYGFQNALIVRYTRKVPQVSTPTLVEVSRSLGKVGTRCCTKPESERMPCTEDYLSLILNRLCVLHEK
TPVSEKVTKCCTESLVNRRPCFSALTPDETYVPKAFDEKLFTFHADICTLPDTEKQIKKQTALVELLKHK
PKATEEQLKTVMENFVAFVDKCCAADDKEACFAVEGPKLVVSTQTALA

☐ All found in Red

	fixed modifications
060606FTc2_phosphb_bsa_1hzu1lMascot:	Carbamidomethyl (C)
060606FTc2_phosphb_bsa_1hzu1lOmssa:	carbamidomethyl C(C)
1hzu1lSpectrumMill:	Carbamidomethylation(C)
060606FTc2_phosphb_bsa_1hzu1lSequest:	(C)
060606FTc2_phosphb_bsa_1hzu1lXTandem:	(K),(C)

K*: 111.04 N-term@: 42.01 K%: 105.02 MX$: 15.99 K§: 6.02 N-term&: -18.02 N-term": -17.03

Peptidehits per page: 15 [25] 50 100

72 Peptidehits found | Page 1 of 3 | Next >> go to page go

	Search	Score	Sequence	
☑	1 2 3	2931.6749108729373	.ALK%AWSVAR.	
☑	1 2 3 5	2931.5490195998573	.HPEYAVSVLLR.	
☑	1 2 3 5	2929.586073148418	.M$PCTEDYLSLILNR.	

Figure 2

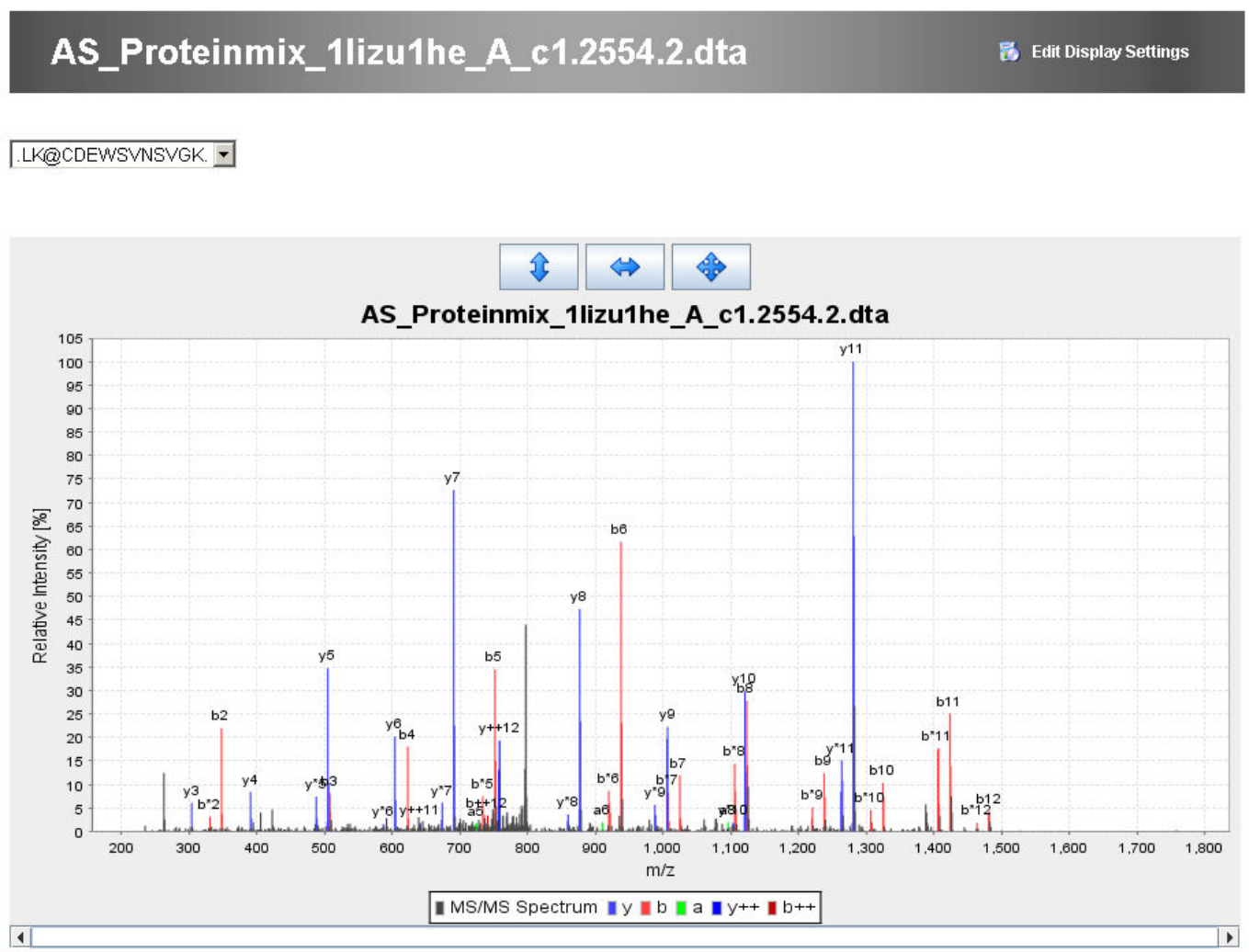

	a	b	b*	b0	b++		y	y*	y0	y++	
1	86.09	114.09	97.06	96.08	57.54	L					13
2	319.21	347.2	330.18	329.19	174.1	K	1513.67	1496.64	1495.66	757.34	12
3	479.24	507.23	490.21	489.22	254.12	C	1280.55	1263.53	1262.54	640.78	11
4	594.27	622.26	605.23	604.25	311.63	D	1120.52	1103.5	1102.51	560.76	10
5	723.31	751.3	734.28	733.29	376.15	E	1005.5	988.47	987.48	503.25	9
6	909.39	937.38	920.36	919.37	469.19	W	876.45	859.43	858.44	438.73	8
7	996.42	1024.41	1007.39	1006.4	512.71	S	690.37	673.35	672.36	345.69	7
8	1095.49	1123.48	1106.46	1105.47	562.24	V	603.34	586.32	585.33	302.17	6
9	1209.53	1237.53	1220.5	1219.52	619.26	N	504.27	487.25	486.26	252.64	5
10	1296.56	1324.56	1307.53	1306.55	662.78	S	390.23	373.2	372.22	195.62	4
11	1395.63	1423.63	1406.6	1405.62	712.31	V	303.2	286.17	285.19	152.1	3
12	1452.65	1480.65	1463.62	1462.64	740.83	G	204.13	187.1	186.12	102.57	2
13						K	147.11	130.08	129.1	74.06	1

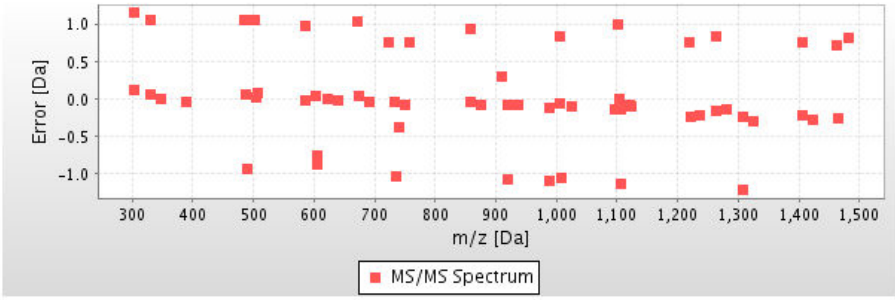

Figure 3

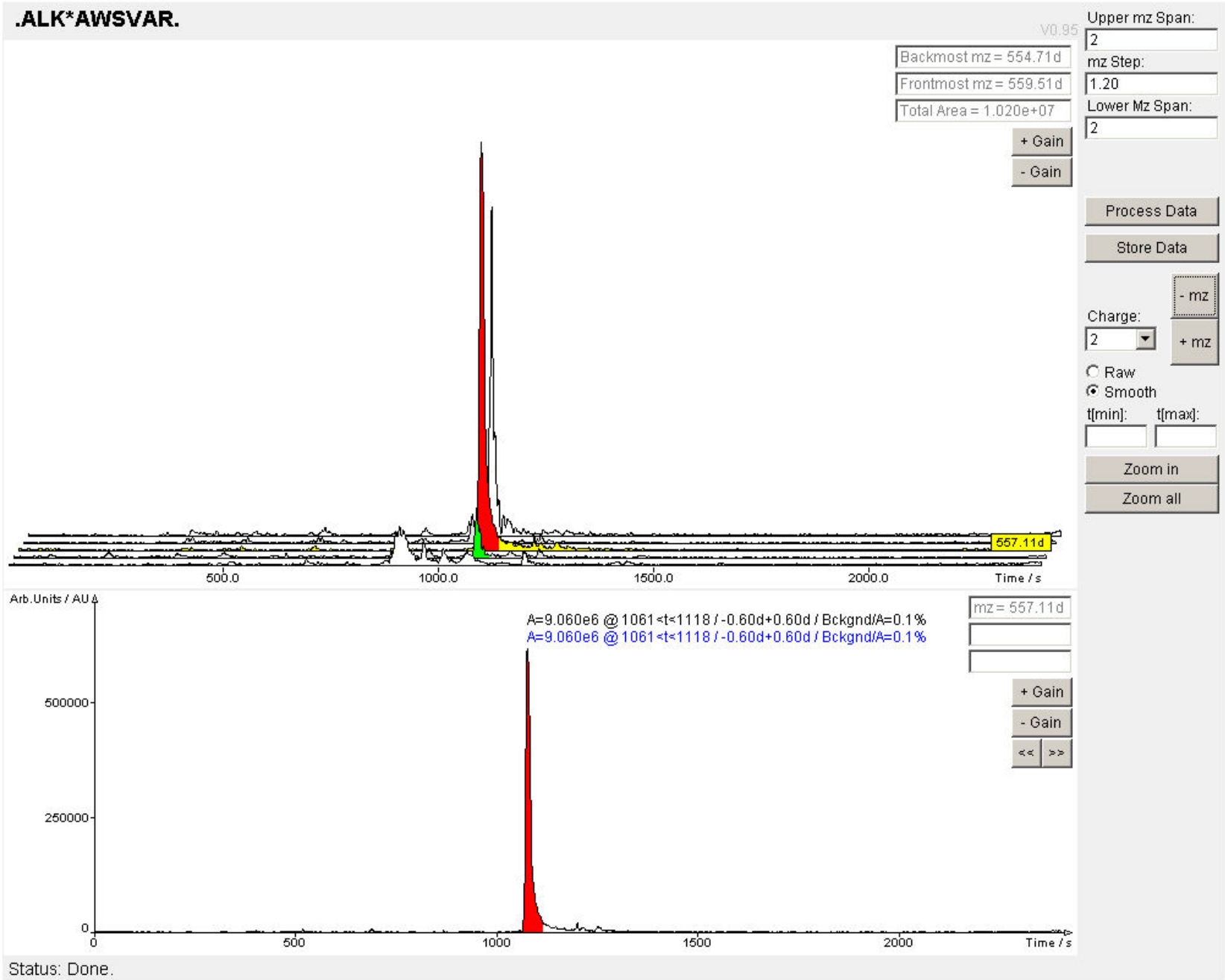

Figure 4

Figure 4

Additional files provided with this submission:

Additional file 1: adddata1.txt, 27K
http://www.biomedcentral.com/imedia/9498783881405709/supp1.txt
Additional file 2: adddata2.zip, 357K
http://www.biomedcentral.com/imedia/7722822914057092/supp2.zip
Additional file 3: adddata3.tif, 1010K
http://www.biomedcentral.com/imedia/1479938682140570/supp3.tiff